



# PROGRESS REPORT

## ON THE ACTIVITIES AT THE BUDAPEST RESEARCH REACTOR



**BUDAPEST NEUTRON CENTRE**  
2010 – 2012

## **Budapest Neutron Centre Progress report 2010-2012**

Edited by R. Baranyai, M. Makai  
H. Pálffy, L. Rosta  
Budapest, September, 2013

### ***Postal address and contact persons:***

Centre for Energy Research,  
Hungarian Academy of Sciences  
1121 Budapest, Konkoly Thege u. 29-33.  
Hungary  
Dr. Rózsa F. BARANYAI  
Phone: 36-1-392-2799  
Fax: 36-1-395-9293  
e-mail: baranyai.rozsa@energia.mta.hu

Wigner Research Centre for Physics  
Hungarian Academy of Sciences  
1121 Budapest, Konkoly Thege u. 29-33.  
Dr. László ROSTA  
Phone: 36-1-392-2789  
Fax: 36-1-392-2501  
e-mail: rosta.laszlo@wigner.mta.hu

### ***Location:***

Budapest Research Reactor  
1121 Budapest, Konkoly Thege út 29-33  
KFKI, Bld, 10.

### ***Cover page:***

Years 2010-12 were marked with numerous international events in BNC's life – also thanks to the Hungarian EU presidency in the first half of 2011. For example, the upper picture shows the participants of the CHARISMA EU FP7 project meeting held in Budapest in March 2011. In the middle, pictures show some moments of the inauguration of the bronz bust of Frederic Joliot-Curie by Catherine Cesarsky, High Commissioner for CEA and József Pálincás, President of HAS, in the presence of the Ambassador of France, in front of the Reactor building in June 2010. In the lower part, young scientists are performing experiment in the neutron guide hall on the occasion of the 5th Central European Training School in May 2010.

---

***The publishing of this Progress Report was sponsored by the ANTE and MIRROTRON industrial companies, BNC partners in neutron instrumentation development projects.***

# *Progress Report*



# CONTENTS

<b>PREFACE</b>	<b>7</b>
<b>1. BUDAPEST RESEARCH REACTOR</b>	<b>8</b>
<b>2. INTERNATIONAL SCIENTIFIC ADVISORY COUNCIL</b>	<b>13</b>
<b>3. USER SELECTION PANEL</b>	<b>14</b>
<b>4. RESEARCH HIGHLIGHTS</b>	<b>16</b>
4.1. STRUCTURE ANALYSES OF AMORPHOUS AND CRYSTALLINE MATERIALS BY NEUTRON DIFFRACTION	16
4.2. NEUTRON RADIOGRAPHY AND ANCARA (A SUPERCRITICAL WATER TEST FACILITY)	19
4.3. PROMPT-GAMMA ACTIVATION ANALYSIS	22
4.3.1. STUDY OF THE DEACON REACTION WITH IN-SITU PGAA	25
4.4. CHARISMA FIXLAB HIGHLIGHT QUANTITATIVE ANALYSIS AND DISTRIBUTION OF CHLORIDE IN ARCHAEOLOGICAL IRON	27
4.5. FE SELF-DIFFUSION IN FEPD REVEALED BY REFLECTOMETRY	29
4.6. CONDENSED MATTER RESEARCH BY NEUTRON SPECTROSCOPY	30
4.7. TIME-OF-FLIGHT NEUTRON DIFFRACTION FOR LONG PULSE NEUTRON SOURCES – BUDAPEST EXPERIMENTS	37
<b>5. DETAILED RESULTS</b>	<b>40</b>
<b>6. INSTRUMENTS</b>	<b>194</b>
6.1. PSD – NEUTRON POWDER DIFFRACTOMETER WITH POSITION SENSITIVE DETECTORS	194
6.2. MTEST DIFFRACTOMETER	196
6.3. TOF – HIGH RESOLUTION TIME-OF-FLIGHT POWDER DIFFRACTOMETER	198
6.4. YS-SANS – SMALL ANGLE NEUTRON SCATTERING INSTRUMENT YELLOW SUBMARINE	200
6.5. REF – COLD NEUTRON REFLECTOMETER	202
6.6. GINA - NEUTRON REFLECTOMETER WITH POLARIZATION OPTION	204
6.7. ATHOS - COLD NEUTRON TREE-AXIS SPECTROMETER	206
6.8. TAST/HOLO - THERMAL NEUTRON TREE-AXIS SPECTROMETER AND NEUTRON HOLOGRAPHIC INSTRUMENT	208
6.9. DYNAMIC RADIOGRAPHY STATION	210
6.10. NORMA - NEUTRON OPTICS AND RADIOGRAPHY FOR MATERIAL ANALYSIS	212
6.11. BIO – BIOLOGICAL IRRADIATION CHANNEL	214
6.12. PGAA – PROMPT GAMMA ACTIVATION ANALYSIS	216
6.13. NIPS - NEUTRON-INDUCED PROMPT GAMMA-RAY SPECTROSCOPY	218
6.14. BAGIRA3 – REACTOR IRRADIATION LOOP	220
6.15. RNAA – REACTOR-NEUTRON ACTIVATION ANALYSIS	222
<b>7. EDUCATION</b>	<b>225</b>
<b>8. EVENTS</b>	<b>228</b>
<b>9. PUBLICATIONS</b>	<b>232</b>
<b>APPENDIX</b>	<b>242</b>



# PREFACE

One of the key and largest research infrastructures in Hungary is the 10 MW Budapest Research Reactor (BRR) with its experimental stations. This is the base for domestic and international user community to serve for exploratory and applied research in many fields of science and technology as well as for methodical developments in neutron beam and irradiation techniques. In 2010, 2011 and 2012 the Reactor was operated according to its usual regime in ten-day cycles, resuming 2574, 3510 and 32600 hours of yearly operation, respectively. During the first two years of the mentioned period the reactor was running with a "mixed fuel core" having started the core conversion procedure according to the Russian Research Reactor Fuel Return (RRRFR) programme, which aimed to convert gradually the BRR's core from high enriched uranium (HEU 36%) to low enriched uranium (LEU). From early 2012 only 20% enriched fuel has been used. Following this core conversion no significant loss in neutron flux was detected.

BNC is an open access facility for the domestic and international user community – a suit of reactor irradiation equipment, thermal neutron beam instruments and cold neutron spectrometers in the neutron guide hall are available and assisted by a professional team of scientists and engineers for experimental services. Research proposals can be submitted twice a year, an international selection panel takes care of the review of the proposals, even "fast-track" processing of proposals is possible thanks to the electronic communication. BNC has been involved in several EU Framework Programmes (FP5, FP6 and FP7). The second Neutron and Muon Integrated Infrastructure Initiative (NMI3-II) access programme was approved by the Commission in 2011, so EU partner users can again profit this project for performing experiments at BNC. The CHARISMA project started in 2009 is another FP7 transnational access project for the investigation of objects of cultural heritage. In 2010-11 many

interesting experiments were brought to BNC in this frame, just to mention one of them: The meteoritic origin and hammering fabrication of the "mankind's earliest iron pieces" (5300 years old beds from Egypt) was proved by neutron and X-ray techniques. Several projects sponsored by the International Atomic Energy Agency were also performed.

The instrument development programme was progressed, mostly thanks to a domestic project (named Large International Projects, with Hungarian acronym NAP) financed by the Hungarian Innovation Fund. Within this NAP project the installation of a new reflectometer GINA was completed and entered in the user programme. The extension of the PGAA stations with neutron tomography option is a major advancement for a wider use of this successful technique.

This Progress Report contains most of the relevant experiments performed at BNC during the past 3 years. This booklet serves also as information for the users: A table of experimental stations is given in the Appendix. The call for proposals including the conditions how one can make use of the EC travel support is regularly advertised in the journal *Neutron News* and on the web ([www.bnc.hu](http://www.bnc.hu)). The web site of BNC offers also the possibility of reading reports on BNC activities, e.g. the present Report. This booklet gives also the description of our experimental stations. A list of publications concerning this three years activity is also attached. On the occasion of 20 years of its international user operation the Budapest Research Reactor was presented in a review article of *Neutron News*, the most widely read journal of the neutron community (Vol. **22**, 31-36, 2011).

Budapest, September 2013

Ákos Horváth  
Chairman of the BNC  
Board of Directors

# 1. BUDAPEST RESEARCH REACTOR

The Budapest Research Reactor is one of the leading research infrastructures in Hungary and in Central-Europe. The basic scientific activity at BRR is the use of neutron beam lines for neutron scattering investigations. We have more than 50 years of tradition in this field. BRR is a VVR-type (water-cooled, water-moderated reactor) Soviet designed and built reactor: it went critical on March 25, 1959 – with its construction starting in summer 1957 (I). Originally, the reactor power was 2 MW, but it was upgraded to 5 MW in 1967. A second full-scale reactor refurbishment was started in 1986, fully designed and performed by Hungarian companies. The project was supported by the International Atomic Energy Agency (IAEA) and the European Union. The reconstruction was completed by the end of 1990, but due to the political changes in the country, the license for reactor start-up was issued only in 1992. The reactor has been operated by the KFKI Atomic Energy Research Institute (AEKI – one of the research units of the Hungarian Academy of Sciences). In 1992, a consortium, named Budapest Neutron Centre (BNC), was formed as an association of the neutron-research based laboratories of AEKI and three other academic institutes (RISP – Research Institute for Solid State Physics, IKI – Institute of

Isotopes and RMKI – Research Institute for Nuclear and Particle Physics) on the so called KFKI campus site.

The role of BNC is to coordinate the reactor utilization and to provide scientific infrastructure for managing access for the international user community.

BRR is a tank type reactor, moderated and cooled by light water. Until 2009 the reactor was fuelled with Russian type VVR-SM fuel with 36% uranium enrichment and later due to the program of the core conversion, 20% enriched VVR-M2 type will be used. The core is surrounded by a solid beryllium reflector. The main technical data of the reactor are: thermal power 10 MW; mean power density: 39.7 kW/litre; approx. maximal thermal flux:  $2.1 \times 10^{14}$  n/cm<sup>2</sup>s, maximum cooling water outlet temperature: 60°C.

The reactor cycle is about 10 effective days, which is followed by a short break for a weekend. The Budapest Research Reactor is known for its reliable operation. About a 160 operational days per year are foreseen for the next years. However, the timetable will be flexible accommodating the various requirements of the instrument developments.



▲ KFKI Campus (reactor building is in middle)



▲ Panorama view of the Reactor Hall



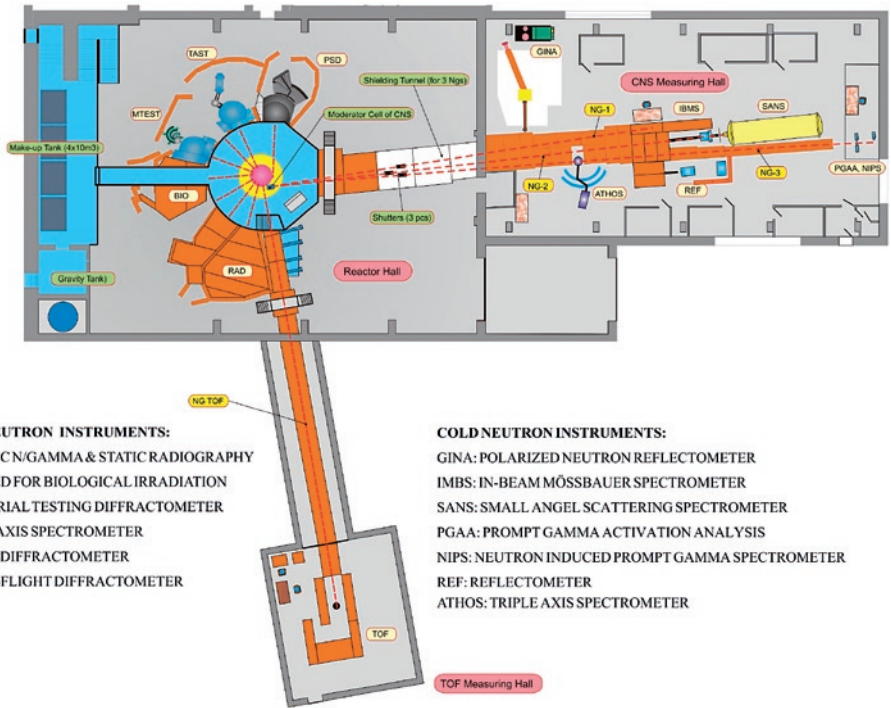
▲ Control Room



**Core conversion**

Following the commitment to join the Russian Research Reactor Fuel Return (RRFR) programme, BRR was prepared to change from HEU to LEU. The preparation for the core conversion has been running since 2007. The selected type of LEU was the Russian made VVR-M2 fuel: the geometric and thermo-hydraulic parameters are identical, whilst its nuclear features are similar to the previously used VVR-M and -M2 HEU fuel elements. In this way

the core conversion scenario was including HEU and LEU fuels with gradually decreasing HEU fuel assembly numbers. During the core conversion 4 cycles with mixed HEU-LEU cores will take place (over 8 months), then the utilisation of HEU fuel will be finished in 2012 and later on only 20% enriched fuel will be used. According to neutronic calculations no more than a 10% loss in neutron flux is expected due to the core conversion.



◀ Lay-out of the horizontal neutron beam-lines at the Budapest Research Reactor.

**Mission of the Reactor – multipurpose utilisation**

The Budapest Research Reactor has been utilized as a neutron source for basic and applied research or direct applications in various fields of industry, healthcare as well as in exploration and conservation for objects of cultural heritage. The major fields of the reactor utilization are as follows:

I) BRR is a research and development base for the energy sector. In Hungary 40% of electric energy is produced by the Paks Nuclear Power Plant (4 blocks of 500 MW electric power). The expertise and knowledge accumulated at BRR during the past decades is a solid basis for scientific and safety support for the Paks NPP as well as for the national nuclear regulatory body. BBR also serves as a scientific

and development tool in other fields of energy research, both in energy saving and production (e.g. development of new materials for energy production and storage, research of materials and structural components for fusion energy or reactors of new generation, development of new energy saving technologies such as superconductors).

II) This reactor is also a complex source of irradiations for materials testing and modification, diagnostics in nanotechnologies, engineering, healthcare and similar. The radioisotope production – using vertical irradiation channels of the core – is crucial for society. For example, in our country 60 hospitals are supplied by isotopes produced at BRR. A fast rabbit system

serves as a pneumatic irradiation facility, situated in the reactor core; it provides convenient production of short-lived isotopes as well as neutron activation analysis for environmental chemistry, geochemistry, biological and medical research. BAGIRA is the name of a gas-cooled irradiation rig in a dry channel inside the core. This serves basically for irradiation of nuclear reactor vessel and fusion equipment materials to investigate irradiation ageing. This is complemented by a laboratory equipped for hot sample studies.

III) The most extended utilization of BRR is neutron beam research. This activity results in a significant number of experiments (including PhD and contract-based works). For example in 2008, nearly 120 experiments were completed by local staff and in collaboration with national or foreign users coming from university, industrial or other research laboratories. The number of publications (typically quoted in annual reports) is 100–120 a year. BNC is a recognized component of the European network of neutron centres and a partner in the EU Framework Programme projects. It was a great honour at the closing meeting of last framework programme's NMI3 in 2009 that, out of nearly 1,000 experiments performed under the umbrella of the programme,

32 highlights were presented by four European experts and 11 of these highlights were coming from BNC. This shows that our users, coming mostly from developing regions, produce many exciting ideas and experiments although the quality of our facilities can do with further development.

IV) University education as well as postgraduate and professional training in the nuclear field has always been an important task at BNC. The first international neutron scattering school was organised in 1999 together with the 2<sup>nd</sup> European Conference on Neutron Scattering in Budapest (this was an occasion for several hundreds of neutron scientists to visit BRR). It has developed into a series of regional events. These schools provide an introduction to neutron scattering with special emphasis to hands-on-training at BRR facilities. For example, the 5th Central European Training School (CETS) was held in June 2010. We consider that CETS 2010 was a highly successful event, we organize CETS since 10 years and it has really taken its shape to serve the regional neutron community. Most of the attendees (including Hungarians) came from our neighbour countries, indeed; although we had students from Russia, Germany and even China.



► The photo was taken on the 5th CETS

### East European Research Reactor Initiative (EERRI)

While the reactor has been fulfilling its traditional mission since its first criticality, the operating environment, the user and public demands have significantly changed in recent years. Thus, perceiving these changing demands a research reactor coalition was launched under the name of EERRI (East European Research Reactor Initiative) by the initiation of BRR. The exploratory meeting was held in Budapest, Hungary on January 28-29, 2008 at the invitation of the KFKI Atomic Energy Research Institute (AEKI).

The purpose of the reactor coalitions is the potential to offer complex services in wide range of activities which a single reactor cannot offer. The Eastern European Research Reactor Initiative is the oldest one among the research reactor coalitions and it is considered as an excellent example how a coalition can work.

EERRI has a big potential of hosting nine reactors from seven countries. The wide power range and various reactor utilization programs allow to offer and to solve any type of experimental work usually performed at research reactors from beam experiments through various types of neutron activation analysis, fuel investigation, material science, radioisotope production to education and training. All EERRI activities are focused on four main areas:

- neutron beam applications,
- radioisotope production,
- fuel and material testing,
- education and training.

Significant results have been achieved on the field of education and training and beam applications: EERRI developed a six week training course for IAEA called Group Fellowship Training Programme on Research Reactors. The program focuses on participants from non-nuclear countries, whose aim is to develop national nuclear competence. The third EERRI course for the IAEA was held on February and March 2011 and the fourth on March and April 2011. 8 participants from Sudan and Peru were trained in the 3<sup>rd</sup> program at the Budapest Research Reactor and at the Institute of Nuclear Techniques of the Budapest University of Technology and Economics.

Workshop called “Concerted Actions in Research and Applications with Neutron Beams in Europe” was organized by MTA KFKI AEKI with collaboration of IAEA. The workshop aimed to strengthen the cooperation of the member institutions in the field of neutron beam research and applications. The meeting covered the main neutron beam methods, examine the current status of neutron beam facilities and discuss the future trends in neutron science and applications in Europe.

◀ List of EERRI reactors:

Country	Reactor name	Licensee	Power	Reactor type
Austria	TRIGA	VUT/ATI Vienna	250 kW	TRIGA Mark II
Czech Republic	VR-1	CTU in Prague	1 kW	Training reactor
Czech Republic	LWR-15	NRI Rez	10 MW	MTR
Hungary	BME-TR	BUTE Budapest	100 kW	Training reactor
Hungary	BRR	KFKI AEKI Budapest	10 MW	MTR
Poland	MARIA	IAE Otwock	30 MW	MTR
Romania	TRIGA	ICN Pitesti	14 MW	TRIGA-SSR
Serbia	RB	Vinca Belgrade	0 W	Critical assembly
Slovenia	TRIGA	IJS Ljubljana	250 kW	TRIGA Mark II

*Progress  
Report*

## 2. INTERNATIONAL SCIENTIFIC ADVISORY COUNCIL

Victor L. Aksenov	PNPI "Kurchatov Institute"	Russia
A. Yu. Rumyantsev	Foreign Ministry	Russia
Alexander Ioffe	Jülich Centre for Neutrons	Germany
<b>Béla Faragó (chair)</b>	Institute-Laue-Langevin	France
Ferenc Mezei	Wigner RCP/ESS Lund	Hungary/Sweden
Gérard Pépy	LLB Saclay	France
Gerhard Krexner	Univeritat Wien	Austria
Helmuth Schober	Institute-Laue-Langevin	France
László Cser	Wigner RCP/ELTE	Hungary
László Rosta	Wigner RCP	Hungary
Margarita Russina	Helmholz Zentrum Berlin	Germany
Massimo Rogante	Rogante Engineering	Italy
Matthias Rossbach	FZ-Jülich	Germany
Michael Jentschel	Institute-Laue-Langevin	France
Mihail Avdeev	FLNP Dubna	Russia
Pavol Mikula	INP Rez	Czech Republic
Thomas Geue	Paul-Scherer Institute	Switzerland
<b>Present ex-officio</b>		
Rózsa Baranyai	MTA EK	Hungary
Tamás Belgya	MTA EK	Hungary
Ákos Horváth	MTA EK	Hungary
János Major	MPI, Stuttgart	Germany
Mihály Makai	MTA EK	Hungary
Péter Lévai	Wigner RCP	Hungary

### 3. USER SELECTION PANEL

Gerard Pepy	Laboratoire Leon Brillouin,	France
Gerhard Krexner	Institute of Experimental Physics, Austria	Austria
János Major (Chair)	Max-Planck Institute für Metallforschung	Germany
Jyrki Raisanen	University of Helsinki	Finland
Ivan Krakovszky	Charles University	Czech Republic
Katalin T. Bíró	Hungarian National Museum	Hungary
Matthias Rossbach	Forschungszentrum Juelich GmbH	Germany
Michael Jentschel	Institute Laue-Langevin,	France
Mihály Makai	Budapest Technical University	Hungary
Tamás Grósz	Chemical Research Centre	Hungary
Thomas Geue	Paul-Scherer Institute	Switzerland

*Research  
Highlights* | **4.**

## 4.1. STRUCTURE ANALYSES OF AMORPHOUS AND CRYSTALLINE MATERIALS BY NEUTRON DIFFRACTION

*Erzsébet Sváb<sup>1</sup>, Margit Fábrián<sup>1,2</sup>, György Mészáros<sup>1</sup>*

<sup>1</sup> Institute for Solid State Physics and Optics, Wigner Research Centre for Physics, Hungarian Academy of Sciences, H-1525 Budapest P.O.B. 49, Hungary

<sup>2</sup> Centre for Energy Research, Hungarian Academy of Sciences, H-1525 Budapest P.O.B. 49, Hungary

**Sodium borosilicate glasses** - The special interest of this ternary system lies in the different glass forming mechanisms of  $\text{SiO}_2$  and  $\text{B}_2\text{O}_3$ . One of the main questions is the structural changes of boron-oxygen network and the coordination around B atom induced by the increasing  $\text{B}_2\text{O}_3$  content. Samples of composition  $(75-x)\text{SiO}_2 \cdot x\text{B}_2\text{O}_3 \cdot 25\text{Na}_2\text{O}$  with  $x=5, 10, 15, 20\text{mol}\%$  have been prepared by rapid-quench method. Neutron- and high energy X-ray diffraction experiments have been performed and for data evaluation the reverse Monte Carlo (RMC) simulation technique [1] was applied (see Fig. 1 for one composition). A possible 3-dimensional structure model has been obtained which is consistent with the experimental data. The

partial atomic correlation functions, coordination number distributions and three-atom bond angle distributions have been revealed. We have established that the basic network is formed by 4-fold coordinated (tetrahedral)  $\text{SiO}_4$  units with a first neighbour distance of  $1.60 \text{ \AA}$ . The boron surrounding is more complicated, both 3- and 4-fold coordinated oxygen atoms are present. In the  $\text{BO}_3$  units the first neighbour distance is at  $1.40 \text{ \AA}$ , while in the  $\text{BO}_4$  units at  $1.60 \text{ \AA}$ . One of the main questions is the relative number of  $\text{BO}_3$  and  $\text{BO}_4$  units in the glassy network. We have established that the ratio of  $\text{BO}_3/(\text{BO}_3+\text{BO}_4)$  numbers is increasing from 20% up to 60% with increasing the  $\text{B}_2\text{O}_3$  content, as it is illustrated in Fig. 2.

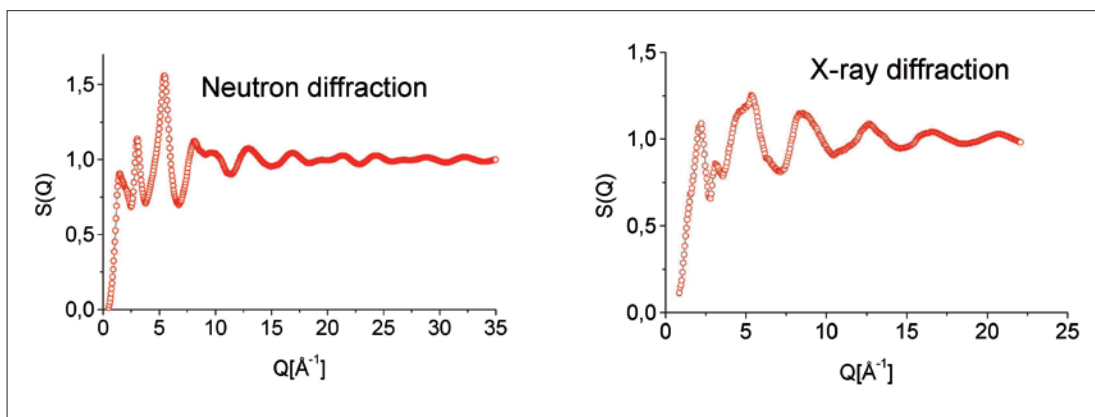


**Figure 1.** Experimental (circle) and RMC (solid line) total structure factors for the  $60\text{SiO}_2 \cdot 15\text{B}_2\text{O}_3 \cdot 25\text{Na}_2\text{O}$  glass

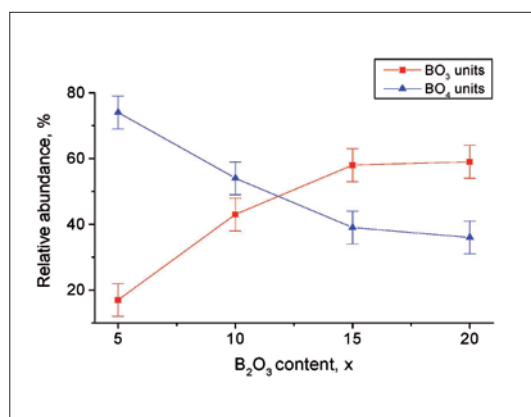


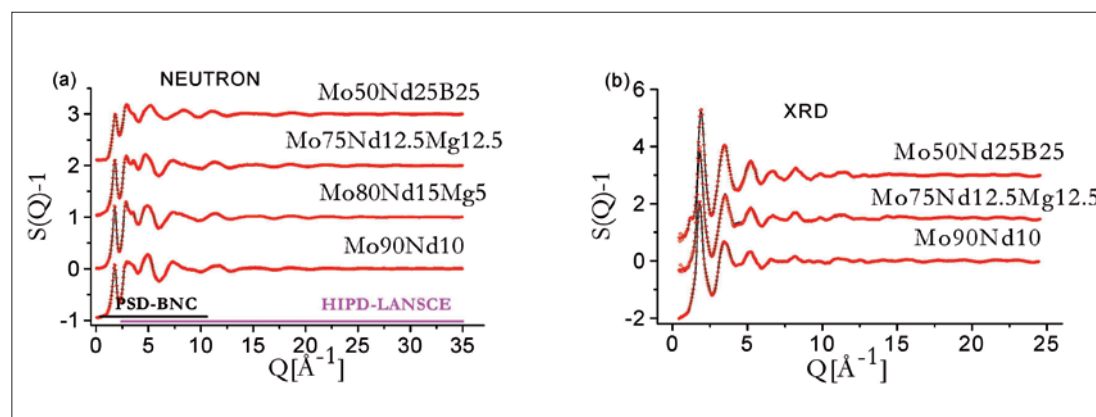
**Figure 2.** Relative abundance of  $\text{BO}_3$  (red square) and  $\text{BO}_4$  (blue triangle) units in the  $(75-x)\text{SiO}_2 \cdot x\text{B}_2\text{O}_3 \cdot 25\text{Na}_2\text{O}$  glasses,  $x=5, 10, 15$  and  $20 \text{ mol}\%$ .



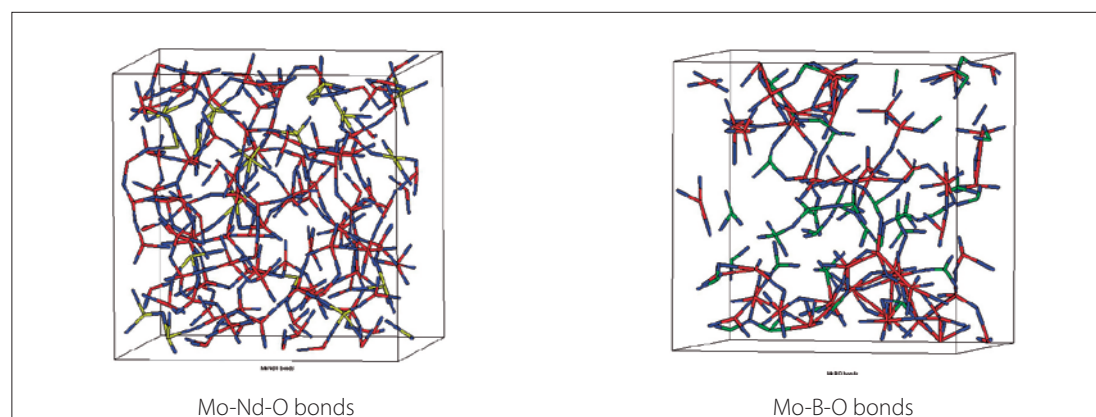
**Amorphous Mo-oxide glasses** - The Mo-rare earth oxides are widely used, due to physical and chemical properties, i.e. large ion- and electron conductivity, catalytic activity, non-linear optical properties and good mechanical resistance.  $\text{MoO}_3$  is well-known as a conditional network former and it is not able to form a glass itself at slow cooling rates. Therefore, in contrast to the most crystalline molybdates with relatively well characterised crystalline and magnetic structures, the structural information on amorphous molybdate systems is not ample and relies mainly on optical experiments and X-ray diffraction data. The aim of our work is to characterise selected new molybdate glasses [2-5] containing  $\text{Nd}_2\text{O}_3$  and  $\text{B}_2\text{O}_3$  and to verify their effect on the molybdate glass network. The  $\text{Nd}_2\text{O}_3$  is appropriate component due to its specific optical properties but it increases the melting temperature. By introducing of  $\text{B}_2\text{O}_3$  it is possible to obtain low melting materials in wider concentration range.

For this study the following amorphous samples have been prepared by rapid quench technique:  $90\text{MoO}_3\text{-}10\text{Nd}_2\text{O}_3$  (Mo90Nd10),  $80\text{MoO}_3\text{-}15\text{Nd}_2\text{O}_3\text{-}5\text{MgO}$  (Mo80Nd15Mg5),  $75\text{MoO}_3\text{-}12.5\text{Nd}_2\text{O}_3\text{-}12.5\text{MgO}$  (Mo75Nd12.5Mg12.5) and  $50\text{MoO}_3\text{-}25\text{Nd}_2\text{O}_3\text{-}25\text{B}_2\text{O}_3$  (Mo50Nd25B25). The boron

containing sample was prepared from  $^{11}\text{B}$ -isotope enriched to 99.6%. Both neutron (ND) and high energy X-ray diffraction (XRD) experiments have been performed. For data evaluation the RMC simulation was applied to obtain a possible 3-dimensional network configuration, which is consistent with the experimental data. The RMC simulation box did contain 10000 atoms and the usual constraints were applied, i.e. atomic density, cut-off distances (nearest neighbour distances for all atom pairs) and connectivity. The final RMC run gave an excellent fit for both the ND and XRD experiments, as it is illustrated in Fig. 3. From the RMC modelling the partial atomic correlation functions  $g_{ij}(r)$ , the coordination number distributions  $\text{CN}_{ij}$ , and the three-atom bond angle distributions have been revealed. For the Mo-O network the first neighbour distance at  $1.8 \text{ \AA}$  was obtained with 4-fold oxygen coordination. For the B-O network former two characteristic first neighbour distances were obtained at  $1.40 \text{ \AA}$  and  $1.60 \text{ \AA}$ , corresponding to the 3-fold and 4-fold oxygen coordination. It can be concluded that the basic network is formed by mixed  $\text{MoO}_4\text{-BO}_4$  tetrahedral and  $\text{MoO}_4\text{-BO}_3$  trigonal units, a schematic illustration of the atomic network bond structure is shown in Fig. 3.



◀ **Figure 3.** Experimental data (circle) and RMC simulation (solid line): a) Neutron b) X-ray diffraction



◀ **Figure 4.** Schematic illustration of the atomic network bond structure: Mo-red, Nd-yellow, B-green and O-blue.

**Yttrium aluminium borate** -  $YAl_3(BO_3)_4$  (YAB) single crystals have excellent non-linear optical properties, and doped YAB crystals have important applications in laser engineering. YAB crystals have suitable sites for some rare-earth elements at the  $Y^{3+}$  site ( $Er^{3+}$ ,  $Nd^{3+}$ ,  $Yb^{3+}$ ,  $La^{3+}$ ) or other doping ions at  $Al^{3+}$  site ( $Cr^{3+}$ ,  $Ga^{3+}$ ). The aim of our study was to investigate the crystallographic effect of the substitution of  $Er^{3+}$  and  $Yb^{3+}$  into  $YAl_3(BO_3)_4$ . Neutron powder diffraction measurements have been performed on  $YAl_3(BO_3)_4$  (YAB), on doped  $Y_{0.88}Er_{0.12}Al_3(BO_3)_4$ ,  $Y_{0.5}Er_{0.5}Al_3(BO_3)_4$ ,  $Y_{0.5}Yb_{0.5}Al_3(BO_3)_4$  and on co-doped  $Y_{0.84}Er_{0.01}Yb_{0.15}Al_3(BO_3)_4$  compositions.

The crystal system of  $YAl_3(BO_3)_4$  is trigonal with space group s.g. R32 (No. 155) ([6] and references therein). For the description of the compounds under investigation the triple hexagonal unit cell has been applied, the number of formula units in the unit cell is  $Z=3$ . The Y, Al and B atoms are coordinated

by oxygen ions in the respective trigonal-prismatic, octahedral and planar-triangle geometry. Following the Wyckoff notation, the unit cell contains 12 B atoms in two different sites B(1) in (3b) and B(2) in (9e) positions, 9 Al atoms in three differently oriented but energetically equivalent (9d) positions, 3 Y atoms in (3a) positions and 36 O atoms in three different sites O(1) in (9e), O(2) in (9e) and O(3) in (18f) positions. The neutron diffraction pattern and the Rietveld refinement are illustrated in Fig. 5. For more details of the refined parameters see ref. [6]. It was established that both  $Er^{3+}$  and  $Yb^{3+}$  ions occupy the  $Y^{3+}$  (3a) sites and not the possible  $Al^{3+}$  (9d) sites. The lattice parameters are decreasing with increasing amount of the dopant elements. Slight changes are revealed in the positional parameters and interatomic distances with increasing concentration of the dopant ions. For the co-doped  $Y_{0.84}Er_{0.01}Yb_{0.15}Al_3(BO_3)_4$  the changes are more significant than for the doped YAB compounds with only one type of dopant element, Er or Yb.

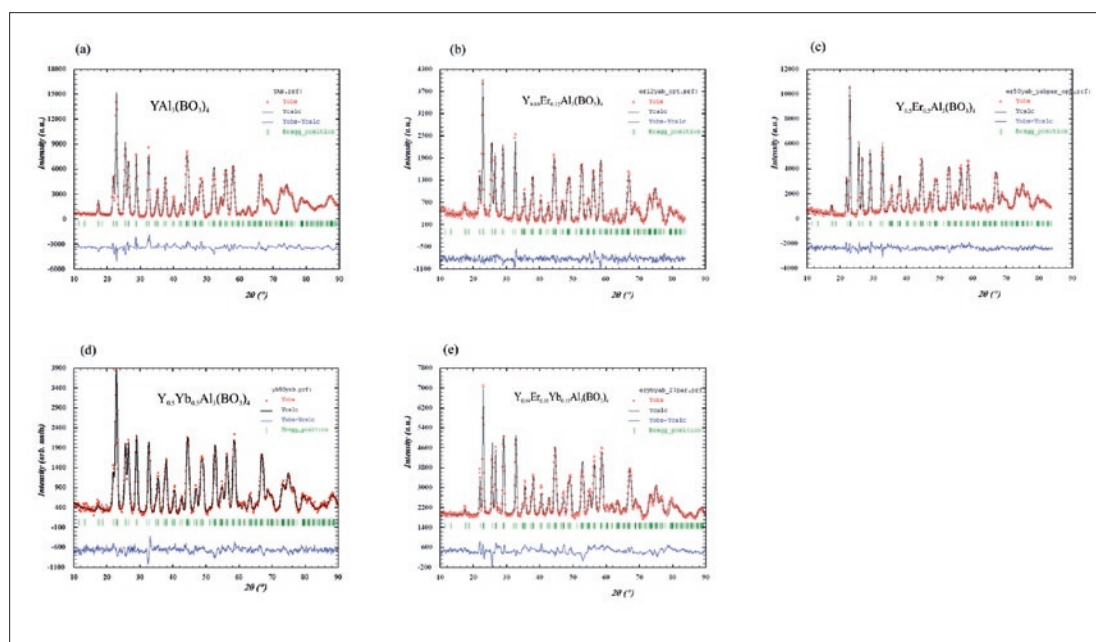


**Figure 5.** Neutron diffraction pattern ( $\lambda=1.0577 \text{ \AA}$ ) and Rietveld refinement in space group R32 of doped YAB compounds: (a)  $YAl_3(BO_3)_4$  ( $R_B=4.7\%$ ); (b)  $Y_{0.88}Er_{0.12}Al_3(BO_3)_4$  ( $R_B=3.7\%$ ); (c)  $Y_{0.5}Er_{0.5}Al_3(BO_3)_4$  ( $R_B=5.9\%$ ); (d)  $Y_{0.5}Yb_{0.5}Al_3(BO_3)_4$  ( $R_B=4.4\%$ ); (e)  $Y_{0.84}Er_{0.01}Yb_{0.15}Al_3(BO_3)_4$  ( $R_B=11.7\%$ ).

### References:

1. R.L. McGreevy, L. Pusztai: Mol. Simul. 1988, 1, 359
2. A. Bachvarova, Y. Dimitriev and R. Iordanova, *Journal of Non-Crystalline Solids*, 2005, 351(12-13) 998-1002;
3. Y. Dimitriev, A. Bachvarova-Nedelcheva, R. Iordanova, *Materials Research Bulletin*, 2008, 43, 1905-1910;
4. R. Iordanova, L. Aleksandrov, A. Stoyanova, Y. Dimitriev, In: *Glass – The Challenge for the 21st Century, Advanced Materials Research*, 2008, 39 – 40, 73-76;
5. R. Iordanova, L. Aleksandrov, Y. Dimitriev, *Physics and Chemistry of Glasses: Eur.J.Glass Sci&Technology B*, 2009 50(3), 212-218
6. E. Sváb, E. Beregi, M. Fábíán, Gy. Mészáros, Neutron diffraction structure study of Er and Yb doped  $YAl_3(BO_3)_4$ , *Optical Materials* 34 (2012) 1473–1476

## 4.2. NEUTRON RADIOGRAPHY AND ANCARA (A SUPERCRITICAL WATER TEST FACILITY)

*Márton Balaskó<sup>1</sup>, Attila Kiss<sup>2</sup>, László Horváth<sup>1</sup>*

<sup>1</sup> Centre for Energy Research

<sup>2</sup> Institute of Nuclear Techniques (INT) of the Budapest University of Technology and Economics

Since the beginning of 1990's the interest in **S**upercritical pressure **W**ater Cooled **R**eactor (SCWR) has revived, and has initiated extensive research worldwide. SCWR is one of the six Generation IV nuclear reactor concepts under development. The specialty of the SCWR concept is in the 25 MPa pressure of the light water coolant surmounting its critical value (22.1 MPa). Furthermore, the outlet water temperature of the reactor is well above (500°C) the critical temperature (374°C). The concept is based partly on the design of the present Light Water Reactors (LWRs), partly on the commercial supercritical – ultra supercritical boilers. Whereas the two above mentioned technical bases currently are in daily use, there are unresolved challenges and questions about the SCWR concept. We mention first the need for new, high temperature resistant structural materials, but the role of hyper-compressibility at supercritical conditions is also questionable, and the three specific heat transfer regimes: normal, enhanced, deteriorated are hard to separate, and regenerated heat transfer may occur under certain supercritical conditions. Our ongoing research aims to study the different heat transfer regimes by supplementary measurement of temperature, pressure, mass flow rate by conventional technique and dynamic neutron radiography for simultaneous visualization.

Since the 1930's more than 500 experiments studied supercritical fluids, mainly supercritical pressure water (SCW). A major disadvantage of these experiments has been that a rather limited amount of data has been recorded on the distributions of thermal-hydraulic variables. There is no structural material which would be both transparent and resistant to high pressure and temperature. That makes the experiment a

challenge. The above mentioned high pressure and temperature conditions of SCW have also made these experiments more complicated. In the last two decades, the computational fluid dynamic (CFD) technique has undergone a significant development.

Nowadays, CFD has made it possible to model the thermal-hydraulics of the SCR in 3D. Results are very promising, but validation is still required. The application of DNR supplemented by conventional measurements seems a very powerful tool for both to validate the CFD calculations and discover more details of the thermal-hydraulics of SCW. In the first step, an SCW cooled natural circulation loop has been designed relying on the successful previous experiments. The experiment is abbreviated as ANCARA (MTA KFKI **A**EKI-BME **N**TI Budapest Super**C**ritical **w**Ate**R** test **f**Acility).

The loop is essentially a bended closed pipe. The structure of the loop can be seen on Fig. 1. The vertical leg is heated. That is the reason why a big density difference occurs between the hot and cold leg. This density difference drives the natural circulation flow. The loop includes various measuring equipment, mounted on an aluminium alloy frame.

The inner diameter (ID) of the stainless steel pipe is 5 mm, its outer diameter (OD) is 8 mm. This ID is of the same order of magnitude as the equivalent diameters in an individual cooling channel of a fuel assembly in a current SCWR design. The loop consists of more pipe parts with a total length of 5.2 m. The hot leg consists of the heated and investigated straight part which height is approximately 1 m. The total volume of the closed loop is 102.1 cm<sup>3</sup>.

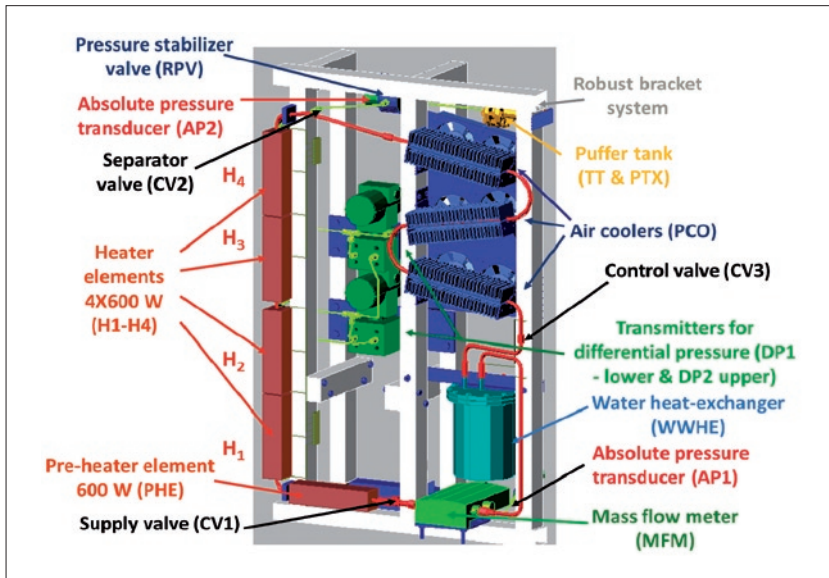


**Figure 1.**  
Construction of the ANCARA loop

Below description of each part will be presented starting from the lower right corner of the loop. An absolute pressure transducer measures the absolute pressure in the loop (AP1). A mass flow meter measures simultaneously the density and temperature of the fluid as well as the mass flow rate (or the volume flow rate).

The last equipment in the lower horizontal part is a pre-heater. This is an individually manufactured heater, which is identical with the four heaters in the vertical hot leg. Its total heating power is 600 W per unit (the total power is 3000 W).

The temperature distribution on the outer wall of the hot leg is measured by ten thermocouples.

### Measurement

The goal of the DNR investigation is to supply visual information on the behavior of the SCW in the loop. Before commencing the DNR investigation, a cleaning and a filling-up procedures have to be carried out. The first period of the heating procedure (0 – 10 minutes) is applied for the verification of the upper limit of the temperature and the pressure (450 °C and 30 MPa). Visual observation has confirmed that the target temperature and pressure have been reached, see Fig. 2, which is a simplified version of the original registered parameters. The running time of the measurement is written on the horizontal coordinate in minutes. The temperature and the pressure are written by the vertical coordinate in °C and bars with nominally same values. The highest curve (1) is described by the temperature of  $H_4$  on the middle part, the next (2) is in downstream the temperature of  $H_3$  on the middle part,

The length of the hot leg is approximately 1 m. Pressure drops are measured by two differential pressure transducers. The first one (DP1) measures the differential pressure between the start and middle point of the hot leg. The second one (DP2) measures the differential pressure between the middle and the end point of the hot leg.

To reach the SCW state, the high purity water has been heated from room temperature to above the critical temperature. In the meantime the fluid expands and its pressure increases. This is how the pressure is controlled but if the heating power is not sufficient (higher than needed) then fast blow-down would be needed. To accomplish this function, an electricity controlled blow-down valve has been connected to the beginning of the upper horizontal part. The water blown down through this valve is collected in a tiny tank (TT) of 33 cm<sup>3</sup> total volume. This tank has its own heating capability which enables water feed back to the loop. There is an active air-cooled pre-cooler (PCO) at the cold leg. Downstream from the pre-coolers there is a cross-current water-water heat exchanger (WWHE) contained in a stainless steel tank. The next equipment is an electric circuit controlled valve to control the mass flow rate.

For the necessary vacuum and high purity water charge processes two manually operated valves (CV1 and CV2) have been installed in the loop at the bottom and upper horizontal parts.

the next (3) is in downstream the temperature of  $H_2$  on the middle part, the next (4) is in downstream the pressure on the AP2. The further curves are negligible now. Ilyen nincsi!

The heating power can be varied between 1,1 and 1,9 kW. The SCW state is stabilized in between 58 and 63 minutes.

It should be noted that the sensors of the pressure measurements are covered by a high thickness complex, sandwich style biological shielding (boron-carbide, cadmium and lead) against the damage of the high level scattered radiation. In accordance with the goal of the experiment, the hot leg is only a vertical tube, and the neutron beam is reduced by an additive complex shielding.

Simultaneously the temperatures, absolute and differential pressure values, the mass flow rate, heating powers were registered together in an in-house developed data acquisition software.

The measurements on the ANCARA loop has just been started. That is why some preliminary results can only be seen in Fig. 3. – Fig. 4. Fig. 3. shows the dynamic neutron radiography (DNR) snapshot of the middle part of the hot leg at the upper part of the heating element  $H_2$  and the lower part of element  $H_3$ . The light intensity on the line between the two

yellow crosses (shown on Fig. 3.) can be seen on Fig. 4. The light intensity was analysed by a QUANTEL CRYSTAL SAPPHIRE type picture analyzer.

When the temperature of the water is 25 °C, a little valley is observed between the two parts of the tube wall of the hot leg. Later, when the temperature and the pressure increased above the critical values (374 °C and 22,1 MPa, respectively), the depth of the valley has reduced because the SCW density is lower than that of the water at room temperature.

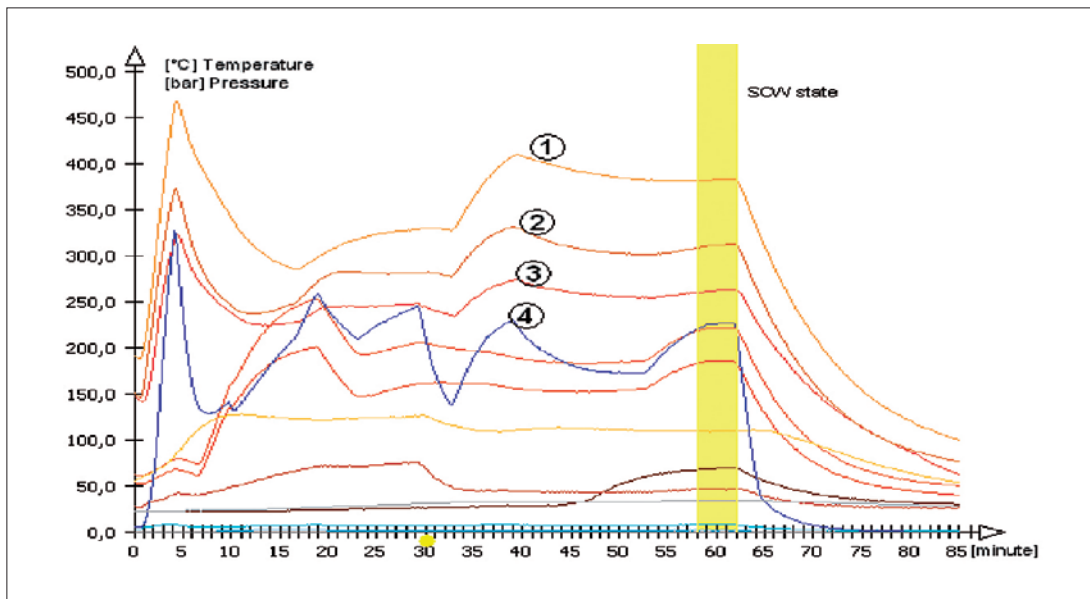


Figure 2. Simplified parameters of the measurement process

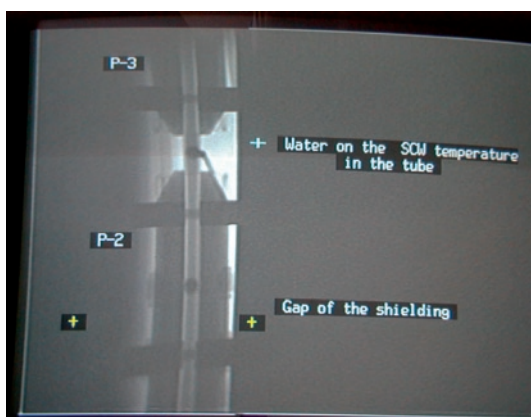


Figure 3. DNR picture of the middle part of the hot leg ( $H_2$  and  $H_3$  heating elements)

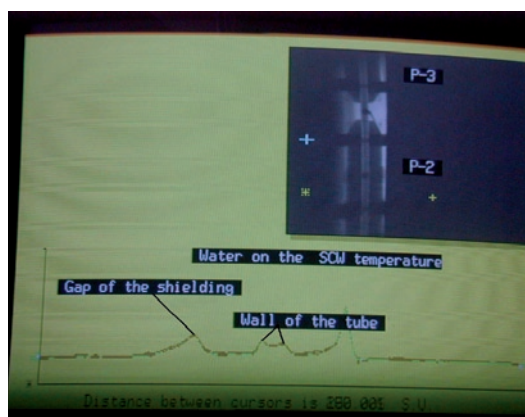


Figure 4. The light intensity between the yellow crosses shown in Fig. 3. for SCW state

### Conclusions

The present work has reported on the first, preliminary observations and measurements with the ANCARA natural circulation loop. ANCARA has proved to be applicable to study

the natural circulation flow of SCW and to study the applicability of the CFD codes to supercritical water flows. Further details will be given in the follow-up publications.

## 4.3. PROMPT-GAMMA ACTIVATION ANALYSIS

L. Szentmiklósi, Zs. Kasztovszky, B. Maróti, Z. Kis

BNC – Centre for Energy Research, Department of Nuclear Analysis and Radiography

Thanks to the progress in instrumentation and methodology of prompt gamma activation analysis achieved since the establishment of our laboratory in 1995, PGAA evolved to a well-established and broadly-utilized non-destructive element analysis technique. In addition to routine element analysis of powders, liquids and small metallic samples, it became practical to analyze more challenging samples, such as oversized objects, time-dependent samples, nuclear/radioactive materials and heterogeneous samples. In the following sections, we present two case studies, one from material science and one from archaeometry.

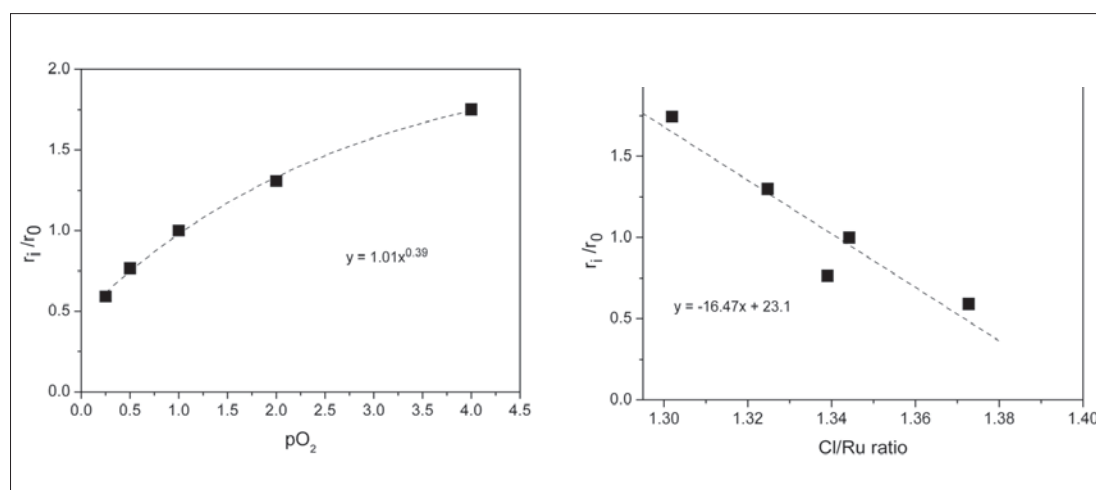
**In-situ Prompt Gamma Activation Analysis** - In an international collaboration coordinated by *Detre Teschner of the Fritz-Haber Institute, Max Planck Society, Berlin*, we investigated the so-called Deacon reaction with *in-situ* PGAA. In the course of the past few years we demonstrated the high relevance of PGAA in studying the mechanism of heterogeneous catalytic processes. Efforts to understand the reaction mechanism and design a proper catalyst for selective hydrogenation resulted in a low-cost alternative for palladium in heterogeneous hydrogenation reactions [M. Armbrüster, K. Kovnir, M. Friedrich, D. Teschner, G. Wowsnick, M. Hahne, P. Gille, L. Szentmiklósi, M. Feuerbacher, M. Heggen, F. Girgsdies, D. Rosenthal, R. Schlögl, Yu. Grin, *The Intermetallic Compound Al<sub>13</sub>Fe<sub>4</sub> Outperforms Expensive Noble-Metal Catalysts in Selective Hydrogenation, Nature Materials* **11** (2012) 690].

Chlorine is nowadays used as reactive intermediate in many processes to create thousands of often indispensable products of the chemical industry. On the large scale, it is produced using the electrolysis of NaCl (or HCl) water solution, however, these are very strongly energy demanding processes. The catalytic oxidation of (waste) HCl to Cl<sub>2</sub>, the Deacon process (2 HCl + 1/2 O<sub>2</sub> → Cl<sub>2</sub> + H<sub>2</sub>O), is an energetically efficient yet environmentally friendly solution to recycle chlorine. The current state-of-the-art system is based on RuO<sub>2</sub> catalyst, which is highly competitive to the electrochemical process: However, ruthenium is a very expensive noble metal; therefore a cheaper alternative catalyst would be highly desirable.

We adopted the same methodology to study the chlorination of differently dispersed RuO<sub>2</sub> samples under the Deacon reaction. The quartz reactor (internal diameter=8 mm) was placed into the neutron beam and surrounded by a specially designed oven having openings for the incoming and outgoing neutrons and for the emitted gamma rays. These openings were covered by thin aluminum foils to minimize heat losses. The reaction feed, at constant total flow, was supplied by mass flow controllers, and used gases of HCl (4.5), O<sub>2</sub> (5.0) N<sub>2</sub> (5.0) and Cl<sub>2</sub> (4.0). The Cl<sub>2</sub> production was monitored by iodometric titration.

Based on the results from several techniques we revisited the mechanism of the reaction. We find

**Figure 1.** Influence of p(O<sub>2</sub>) (a) and the chlorine uptake (Cl/Ru ratio) (b) on the normalized reaction rate (r<sub>t</sub>/r<sub>0</sub>) over the RuO<sub>2</sub>/SnO<sub>2</sub>-Al<sub>2</sub>O<sub>3</sub> catalyst during *in situ* PGAA experiment carried out at atmospheric pressure. pO<sub>2</sub> is expressed in pHCl units. HCl flow was constant at 33.3 cm<sup>3</sup> min<sup>-1</sup> and the total flow was kept constant at 166.6 cm<sup>3</sup> min<sup>-1</sup> with the addition of inert N<sub>2</sub>. Rate is normalized to activity at O<sub>2</sub>:HCl:N<sub>2</sub> = 1:1:3.



[D. Teschner, R. Farra, L. Yao, R. Schlögl, H. Soerijanto, R. Schomäcker, T. Schmidt, L. Szentmiklósi, A. P. Amrute, C. Mondelli, J. Pérez-Ramírez, G. Novell-Leruth, N. López, *An integrated approach to Deacon chemistry on RuO<sub>2</sub>-based catalysts*, *J. Catalysis*, 285 (2012) 273] that the practically-relevant RuO<sub>2</sub>/SnO<sub>2</sub> Bayer catalyst consists of two major RuO<sub>2</sub> morphologies, namely 2-4 nm sized particles and 1-3 ML thick epitaxial RuO<sub>2</sub> films attached to the SnO<sub>2</sub> support particles.

Steady-state Deacon kinetics indicates a weak-to-medium positive effect of the partial pressures of reactants and deep inhibition by both water and chlorine products. Temporal Analysis of Products and in situ Prompt Gamma Activation Analysis strongly suggest a Langmuir-Hinshelwood mechanism and that adsorbed Cl poisons the surface. Under relevant operation conditions the reactivity is proportional to the coverage of a specific atomic oxygen species. On the extensively chlorinated surface, oxygen activation is the rate-determining step and not the energetically demanding recombination of Cl atoms.

Additionally, based on the in situ PGAA experiments, we find that the chlorine production over RuO<sub>2</sub> can be expressed in a very simple form [D. Teschner, G. Novell-Leruth, R. Farra, A. Knop-Gericke, R. Schlögl, L. Szentmiklósi, M. González Hevia, H. Soerijanto, R. Schomäcker, J. Pérez-Ramírez, and N. López: *In situ surface coverage analysis of the RuO<sub>2</sub>-catalyzed HCl oxidation reveals the entropic origin of compensation in heterogeneous catalysis*, *Nature Chemistry* 4 (2012) 739] as the product of a rate coefficient and the coverage of non-Cl (O) species:

$$r = k \theta(T, p)$$

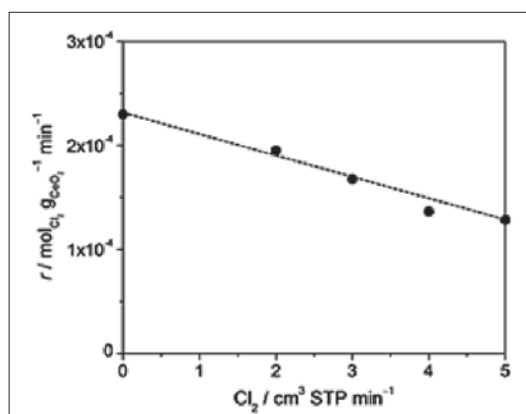
The rate coefficient is independent of temperature and this is related to the so-called compensation effect. Our results based on experiments and DFT calculations show that compensation effects are essentially linked to the balance between free sites and pressures and temperatures, thus giving a molecular level understanding to the compensation phenomenon.

After evaluating the mechanism of Deacon-reaction over ruthenium-oxide based catalysts with success, a new generation of alternative catalysts, based on cerium-oxide and CuAlO<sub>2</sub> were designed and prepared. These catalysts are still capable of withstanding the corrosive Deacon condition, thus

showing long-term stability, as well as reasonable activity at a much lower material cost level.

In the next step these materials were studied using PGAA under Deacon condition. In the latest experiments, much more experimental conditions (such as feed compositions,  $p(\text{O}_2)$ ,  $p(\text{HCl})$  and  $p(\text{Cl}_2)$ , and reaction temperature) could be studied. Since oxygen excess in the reactant stream enhances the reaction rate, the variation of the feed (HCl/O<sub>2</sub>) composition allows us to correlate the reaction rate and the degree of chlorination. Results indicate that chemisorbed Cl is a poison of the catalytic reaction.

Chlorination/dechlorination experiments of a CeO<sub>2</sub> catalyst indicate that the rate of chlorination is not a function of the pre-chlorination degree, but lower oxygen over-stoichiometry increases the chlorination rate. Dechlorination is effective in high oxygen containing feeds and its rate is higher with stronger pre-chlorinated ceria. Parallel XRD experiments using CeCl<sub>3</sub> in HCl oxidation indicated the formation of CeO<sub>2</sub> as the active phase of the reaction. Electron Paramagnetic Resonance (EPR) experiments strongly suggests that oxygen activation is critically dependent on the surface chlorination degree. Surface intermediates of OH and Cl are the most abundant surface species and we followed the evolution of their coverage by *in situ* FTIR and PGAA as a function of the temperature and the partial pressure of O<sub>2</sub>, HCl and Cl<sub>2</sub>. Higher temperature and  $p(\text{O}_2)$  lead to the same effect in as much as the OH coverage increases and parallel the Cl coverage decreases, which concomitantly correlates with higher reactivity. The HCl partial pressure gives rise to opposite correlations and  $p(\text{Cl}_2)$  does not induce any measurable increase in the Cl coverage despite the strong inhibition by Cl<sub>2</sub> (Fig. 2). The results suggest that only a small fraction of ceria



◀ **Figure 2.** Influence of added Cl<sub>2</sub> on the rate of Cl<sub>2</sub> production in the Deacon reaction over CeO<sub>2</sub>-A. Conditions: 10 vol.% HCl and 90 vol.% O<sub>2</sub>, 703 K, space time = 5.6 g h mol<sup>-1</sup>, total volumetric flow = 166 cm<sup>3</sup> STP min<sup>-1</sup>, 1 bar, and dwelling time under each condition = 1.5 h.

surface sites are critically involved in the reaction and most of the surface probed in the *in situ* observation is not directly involved in the reaction.

### Quantitative Analysis and Distribution of Chloride in Archaeological Iron -

Archaeological iron objects corrode rapidly after excavation, and this is a function of their chloride ion content and the relative humidity. Quantitative measurement of this process and its effect on the physical integrity and longevity of the objects is vital to allow museums and other heritage organization to develop management and treatment strategies for their collections. *Cardiff University* is currently running a 3-year AHRC/EPSRC research project managed by *Prof. David Watkinson* and *Dr. Melanie Rimmer*, to investigate the relationships between relative humidity, chloride content, corrosion rate (measured by oxygen consumption) and physical damage to iron objects.

Currently available techniques for measuring the chloride content of the objects are destructive and provide only bulk data. The use of non-destructive neutron techniques provides the first opportunity to detect the effect of spatial distribution of chloride ions on the physical damage of objects, which is visible on the surface as cracking, lamination and loss of corrosion layers. It may be that corrosion rates and patterns of physical damage differ according to whether chloride is localized or more evenly distributed across the object.

Roman nails from two sites were analyzed both as whole objects, to provide bulk chloride content through PGAA, and using the NIPS facility, in incremental sections down the length of the objects, with a slice width of 3 mm. Corrosion rate of the objects had been previously measured at controlled relative humidity. The physical damage to objects was recorded by photographic images and x-radiography. Chloride concentration was high where there was significant mineralization of the iron core and increased damage to the overlying corrosion layers (Figure 1). PGAA bulk chloride data correlated well with the measured corrosion rate of objects (Figure 2), clearly distinguishing the objects from the two sites. 3D neutron tomography was also successfully trialed as a method of detailing the internal structure of corrosion layers and the metal core.

The neutron facilities at the BNC have provided much greater insight into the effect of localized chloride ions on the corrosion of archaeological iron, which contributes significantly to the interpretation of the wider project and is an excellent example of the power of non-destructive techniques in the analysis of heritage materials. PGAA, NIPS and neutron tomography have significant potential for further development in the investigation of archaeological iron corrosion.

Further information on the wider context of this project can be found at <http://www.cardiff.ac.uk/share/research/projectreports/conservationiron/index.html>

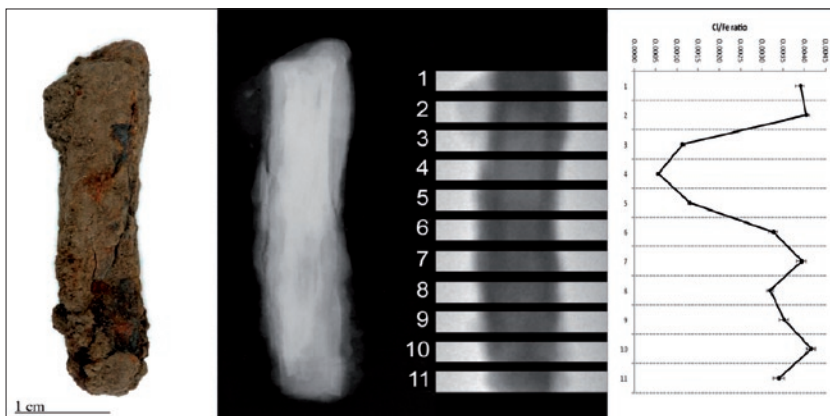


**Figure 3.** Results from NIPS analysis of iron nail CPF08\_062. Eleven 3 mm slices were analyzed, the position of each shown by the neutron radiograph (centre). The X-radiograph shows that areas of greater corrosion/pitting of the metal core correlate with high chloride content (graph on right) and visible surface damage (photograph).

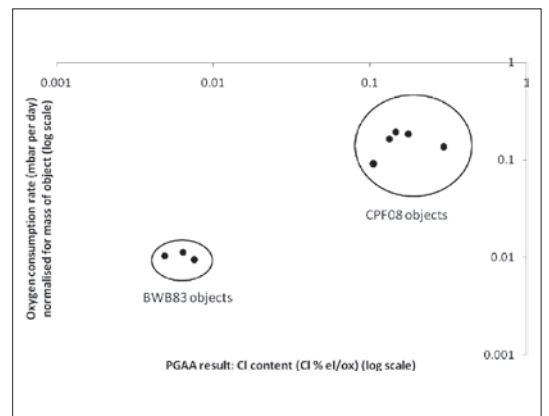


**Figure 4.** Relationship between chloride content of objects, as measured by PGAA, and their corrosion rate measured by oxygen consumption. The objects from the two sites are clearly distinguished on a logarithmic scale. Slow corrosion correlates with low chloride content (BWB83 objects) while higher chloride contents correlate with faster corrosion (CPF08).



### 4.3.1. STUDY OF THE DEACON REACTION WITH IN-SITU PGAA

Detre Teschner<sup>1,2</sup>, Ramzi Farra<sup>1</sup>, László Szentmiklósi<sup>2</sup>, Robert Schlögl<sup>1</sup>, Lide Yao<sup>1</sup>, Axel Knop-Gericke<sup>1</sup>, Miguel González Hevia<sup>3</sup>, Hary Soerijanto<sup>4</sup>, Reinhard Schomäcker<sup>4</sup>, Cecilia Mondelli<sup>5</sup>, Javier Pérez-Ramírez<sup>5</sup>, Núria López<sup>3</sup>, Timm Schmidt<sup>6</sup>

<sup>1</sup> Fritz-Haber Institute of the Max Planck Society, Berlin, D-14195, Germany

<sup>2</sup> Centre for Energy Research, Hungarian Academy of Science, Budapest, H-1525, Hungary

<sup>3</sup> Institute of Chemical Research of Catalonia (ICIQ), Av. Paisos Catalans 16, 43007 Tarragona, Spain

<sup>4</sup> Department of Chemistry, Technical University of Berlin, Berlin, D-10623, Germany

<sup>5</sup> Institute for Chemical and Bioengineering, Department of Chemistry and Applied Biosciences, ETH Zurich, Wolfgang-Pauli-Strasse 10, CH-8093 Zurich, Switzerland

<sup>6</sup> Bayer MaterialScience AG, PUR-PTI-PRI New Processes Isocyanates, Dormagen, D-41538, Germany

Chlorine is used as reactive intermediate in many processes to create thousands of often indispensable products of the chemical industry. On the large scale, it is produced using the electrolysis of NaCl (or HCl) water solution, however, these are very strongly energy demanding processes. The catalytic oxidation of (waste) HCl to Cl<sub>2</sub>, the Deacon process ( $2\text{HCl} + 1/2\text{O}_2 \rightarrow \text{Cl}_2 + \text{H}_2\text{O}$ ), is an energetically efficient yet environmentally friendly solution to recycle chlorine. The current state-of-the-art system is based on RuO<sub>2</sub> catalyst, which is highly competitive to the electrochemical process: However, ruthenium is a very expensive noble metal; therefore a cheaper alternative catalyst would be highly desirable.

Recently we demonstrated the high relevance of applying prompt gamma activation analysis PGAA in studying the mechanism of heterogeneous catalytic processes [1, 2]. Efforts to understand the reaction mechanism and design a proper catalyst for selective hydrogenation resulted in a low-cost alternative for palladium in heterogeneous hydrogenation reactions [3].

We adopted the same methodology to study the

chlorination of differently dispersed RuO<sub>2</sub> samples under the Deacon reaction in our in situ PGAA setup [4]. The quartz reactor (internal diameter=8 mm) was placed into the neutron beam and surrounded by a specially designed oven having openings for the incoming and outgoing neutrons and for the emitted gamma rays. These openings were covered by thin aluminum foils to minimize heat losses. The reaction feed, at constant total flow, was supplied by mass flow controllers, and used gases of HCl (4.5), O<sub>2</sub> (5.0) N<sub>2</sub> (5.0) and Cl<sub>2</sub> (4.0). The Cl<sub>2</sub> production was monitored by iodometric titration.

Based on the results from several techniques we revisited the mechanism of the reaction. We find [5] that the practically-relevant RuO<sub>2</sub>/SnO<sub>2</sub> Bayer catalyst consists of two major RuO<sub>2</sub> morphologies, namely 2-4 nm sized particles and 1-3 ML thick epitaxial RuO<sub>2</sub> films attached to the SnO<sub>2</sub> support particles. Steady-state Deacon kinetics indicates a weak-to-medium positive effect of the partial pressures of reactants and deep inhibition by both water and chlorine products. Temporal Analysis of Products and in situ Prompt Gamma Activation

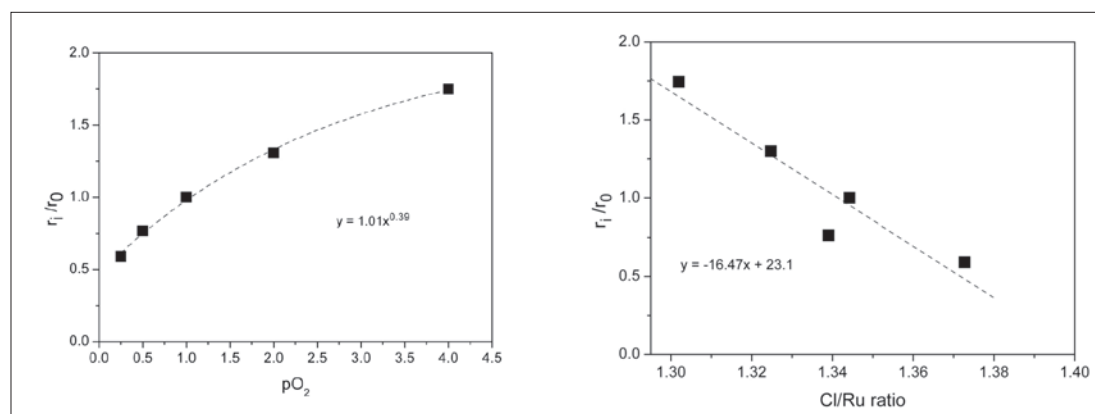


**Figure 1.** Influence of p(O<sub>2</sub>) (a) and the chlorine uptake (Cl/Ru ratio) (b) on the normalized reaction rate (r<sub>1</sub>/r<sub>0</sub>) over the RuO<sub>2</sub>/SnO<sub>2</sub>-Al<sub>2</sub>O<sub>3</sub> catalyst during in situ PGAA experiment carried out at atmospheric pressure. pO<sub>2</sub> is expressed in pHCl units. HCl flow was constant at 33.3 cm<sup>3</sup> min<sup>-1</sup> and the total flow was kept constant at 166.6 cm<sup>3</sup> min<sup>-1</sup> with the addition of inert N<sub>2</sub>. Rate is normalized to activity at O<sub>2</sub>:HCl: N<sub>2</sub> = 1:1:3.

Analysis strongly suggest a Langmuir-Hinshelwood mechanism and that adsorbed Cl poisons the surface. Under relevant operation conditions the reactivity is proportional to the coverage of a specific atomic oxygen species. On the extensively chlorinated surface, oxygen activation is the rate-determining step and not the energetically demanding recombination of Cl atoms.

Additionally, based on the *in situ* PGAA experiments, we find [6] that the chlorine production over RuO<sub>2</sub> can be expressed in a very simple form by the product of a rate coefficient and the coverage of non-Cl (O) species:

$$r = k \Theta(T, p)$$

The rate coefficient is independent of temperature and this is related to the so-called compensation effect [7]. Our results based on experiments and DFT calculations show that compensation effects are essentially linked to the balance between free sites and pressures and temperatures [6], thus giving a molecular level understanding to the compensation phenomenon.

After evaluating the mechanism of Deacon reaction over ruthenium-oxide based catalysts with success, a new generation of alternative catalysts, based on cerium-oxide and CuAlO<sub>2</sub> were designed and prepared. These catalysts are still capable of withstanding the corrosive Deacon condition, thus

showing long-term stability, as well as reasonable activity at a much lower material cost level.

In the next step these materials were studied using PGAA under Deacon condition. In the latest experiments, much more experimental conditions (such as feed compositions,  $p(\text{O}_2)$ ,  $p(\text{HCl})$  and  $p(\text{Cl}_2)$ , and reaction temperature) could be studied. Since oxygen excess in the reactant stream enhances the reaction rate, the variation of the feed ( $\text{HCl}/\text{O}_2$ ) composition allows us to correlate the reaction rate and the degree of chlorination. Results indicate that chemisorbed Cl is a poison of the catalytic reaction. Chlorination/dechlorination experiments of a CeO<sub>2</sub> catalyst indicate that the rate of chlorination is not a function of the pre-chlorination degree, but lower oxygen over-stoichiometry increases the chlorination rate. Dechlorination is effective in high oxygen containing feeds and its rate is higher with stronger pre-chlorinated ceria. Parallel XRD experiments using CeCl<sub>3</sub> in HCl oxidation indicated the formation of CeO<sub>2</sub> as the active phase of the reaction. Electron Paramagnetic Resonance (EPR) experiments strongly suggests that oxygen activation is critically dependent on the surface chlorination degree. Surface intermediates of OH and Cl are the most abundant surface species and we followed the evolution of their coverage by *in situ* FTIR and PGAA as a function of the temperature and the partial pressure of O<sub>2</sub>, HCl and Cl<sub>2</sub>. Higher temperature and  $p(\text{O}_2)$  lead to the same effect in as much as the OH coverage increases and parallel the Cl coverage decreases, which concomitantly correlates with higher reactivity. The HCl partial pressure gives rise to opposite correlations and  $p(\text{Cl}_2)$  does not induce any measurable increase in the Cl coverage despite the strong inhibition by Cl<sub>2</sub> (Fig. 2). The results suggest that only a small fraction of ceria surface sites are critically involved in the reaction and most of the surface probed in the *in situ* observation is not directly involved in the reaction.

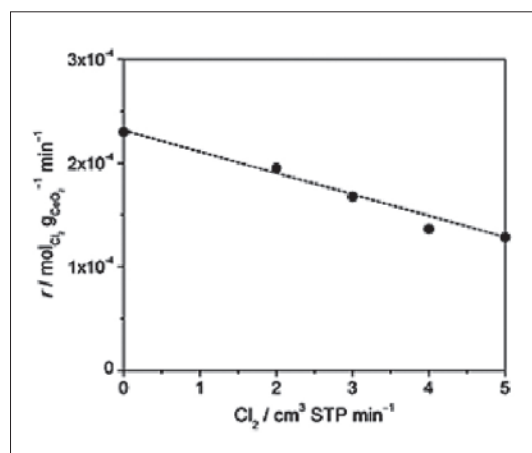


**Figure 2.** ▶

Influence of added Cl<sub>2</sub> on the rate of Cl<sub>2</sub> production in the Deacon reaction over CeO<sub>2</sub>-A. Conditions: 10 vol.% HCl and 90 vol.% O<sub>2</sub>, 703 K, space time = 5.6 g h mol<sup>-1</sup>, total volumetric flow = 166 cm<sup>3</sup> STP min<sup>-1</sup>, 1 bar, and dwelling time under each condition = 1.5 h.

## 4.4. CHARISMA FIXLAB HIGHLIGHT

### QUANTITATIVE ANALYSIS AND DISTRIBUTION OF CHLORIDE IN ARCHAEOLOGICAL IRON

*Prof. David Watkinson, Dr Melanie Rimmer*

Department of Archaeology and Conservation, Cardiff University, United Kingdom

Archaeological iron objects corrode rapidly after excavation, and this is a function of their chloride ion content and the relative humidity. Quantitative measurement of this process and its effect on the physical integrity and longevity of the objects is vital to allow museums and other heritage organisations to develop management and treatment strategies for their collections. Cardiff University is currently running a 3 year AHRC/EPSRC research project that is investigating the relationships between relative humidity, chloride content, corrosion rate (measured by oxygen consumption) and physical damage to iron objects.

Currently available techniques for measuring the chloride content of the objects are destructive and provide only bulk data. The use of non-destructive neutron techniques provides the first opportunity to detect the effect of spatial distribution of chloride ions on the physical damage of objects, which is visible on the surface as cracking, lamination and loss of corrosion layers. It may be that corrosion rates and patterns of physical damage differ according to whether chloride is localised or more evenly distributed across the object.

Roman nails from two sites were analysed both as whole objects, to provide bulk chloride content through PGAA, and using the NIPS facility, in incremental sections down the length of the objects, with a slice width of 3 mm. Corrosion rate of the objects had been previously measured at controlled relative humidity. The physical damage to objects was recorded by photographic images and x-radiography. Chloride concentration was high where there was significant mineralisation of the iron core and increased damage to the overlying corrosion layers (Figure 1). PGAA bulk chloride data correlated well with the measured corrosion rate of objects (Figure 2), clearly distinguishing the objects from the two sites. 3D neutron tomography was also successfully trialled as a method of detailing the internal structure of corrosion layers and the metal core.

The neutron facilities at the BNC have provided much greater insight into the effect of localised chloride ions on the corrosion of archaeological iron, which contributes significantly to the interpretation of the wider project and is an excellent example of the power of non-destructive techniques in

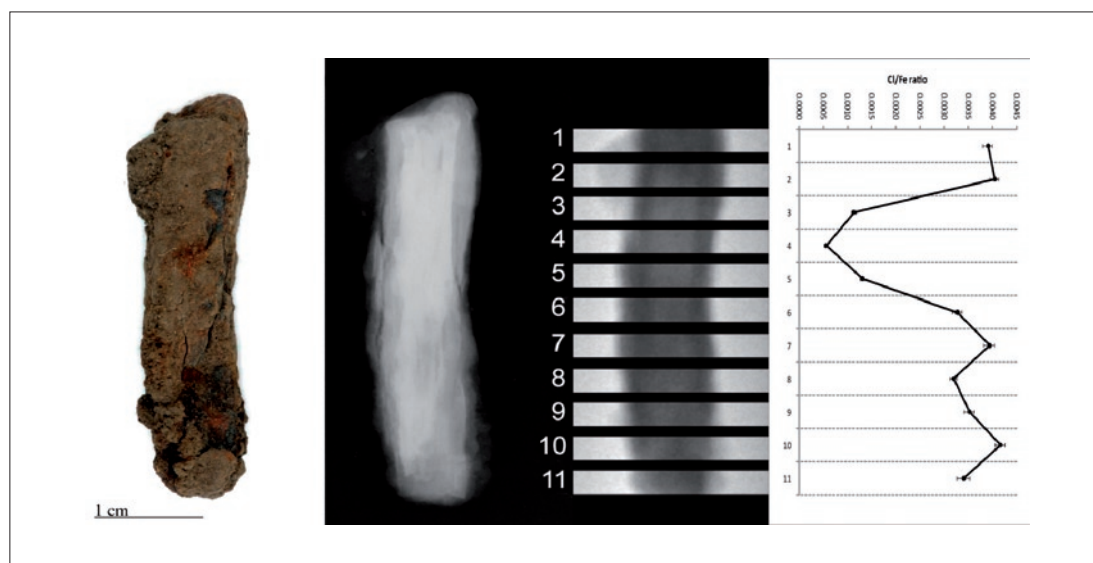
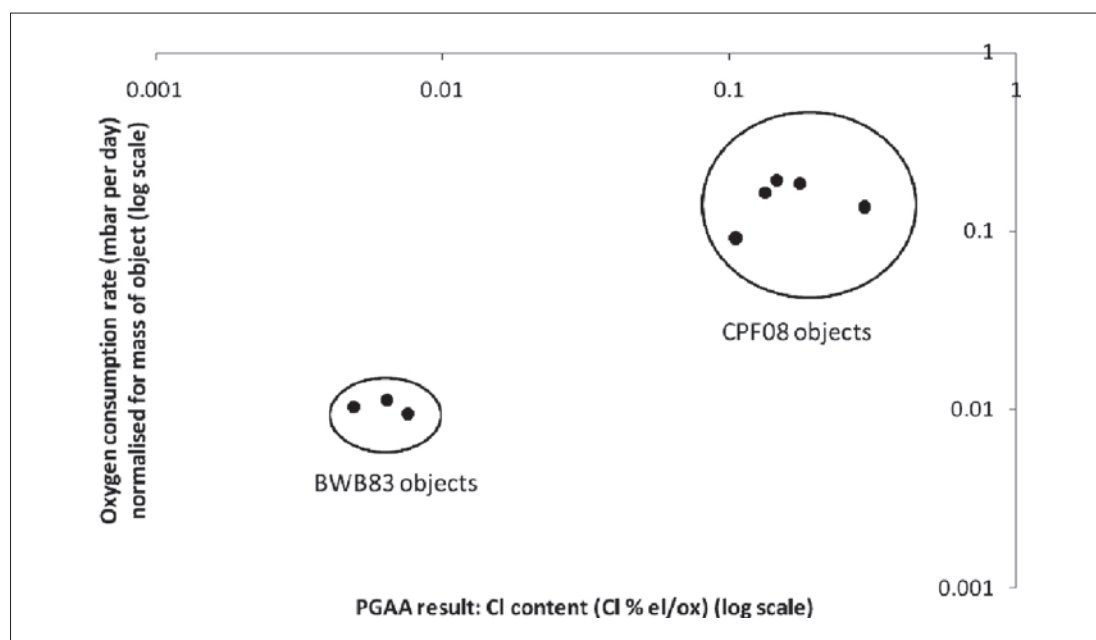


**Figure 1.** Results from NIPS analysis of iron nail CPF08\_062. Eleven 3 mm slices were analysed, the position of each shown by the neutron radiograph (centre). The X-radiograph shows that areas of greater corrosion/pitting of the metal core correlate with high chloride content (graph on right) and visible surface damage (photograph).

the analysis of heritage materials. PGAA, NIPS and neutron tomography have significant potential for further development in the investigation of archaeological iron corrosion.

Further information on the wider context of this project can be found at <http://www.cardiff.ac.uk/share/research/projectreports/conservationiron/index.html>

**Figure 2.** Relationship between chloride content of objects, as measured by PGAA, and their corrosion rate measured by oxygen consumption. The objects from the two sites are clearly distinguished on a logarithmic scale. Slow corrosion correlates with low chloride content (BWB83 objects) while higher chloride contents correlate with faster corrosion (CPF08).



### References:

1. Teschner, D., Borsodi, J., Wootsch, A., Révay, Z., Havecker, M., Knop-Gericke, A., Jackson, S. D., Schlogl, R. The roles of subsurface carbon and hydrogen in palladium-catalyzed alkyne hydrogenation, *Science* 320 (2008) 86. (doi: 10.1126/science.1155200)
2. Teschner, D., Révay, Zs., Borsodi, J., Hävecker, M., Knop-Gericke, A., Schlögl, R., Milroy, D., Jackson, D.S., Torres, D., Sautet, P., Understanding Palladium Hydrogenation Catalysts: When the Nature of the Reactive Molecule Controls the Nature of the Catalyst Active Phase, *Angewandte Chemie* 47 9274–9278 (2008) (doi: 10.1002/anie.200802134)
3. M. Armbrüster, K. Kovnir, M. Friedrich, D. Teschner, G. Wowsnick, M. Hahne, P. Gille, L. Szentmiklósi, M. Feuerbacher, M. Heggen, F. Girgsdies, D. Rosenthal, R. Schlögl, Yu. Grin, The Intermetallic Compound  $\text{Al}_{13}\text{Fe}_4$  Outperforms Expensive Noble-Metal Catalysts in Selective Hydrogenation, *Nature Materials* 11 (2012) 690. (doi: 10.1038/nmat3347)
4. Révay, Z., Belgya, T., Szentmiklósi, L., Kis, Z., Wootsch, A., Teschner, D., Swoboda, M., Schlogl, R., Borsodi, J., Zepernick, R. In Situ Determination of Hydrogen Inside a Catalytic Reactor Using Prompt  $\gamma$  Activation Analysis, *Anal. Chem.* 80 (2008) 6066 (doi: 10.1021/ac800882k)
5. D. Teschner, R. Farra, L. Yao, R. Schlögl, H. Soerijanto, R. Schomäcker, T. Schmidt, L. Szentmiklósi, A. P. Amrute, C. Mondelli, J. Pérez-Ramírez, G. Novell-Leruth, N. López, An integrated approach to Deacon chemistry on  $\text{RuO}_2$ -based catalysts, *J. Catalysis*, 285 (2012) 273 (doi: 10.1016/j.jcat.2011.09.039)
6. D. Teschner, G. Novell-Leruth, R. Farra, A. Knop-Gericke, R. Schlögl, L. Szentmiklósi, M. González Hevia, H. Soerijanto, R. Schomäcker, J. Pérez-Ramírez, and Núria López: In situ surface coverage analysis of the  $\text{RuO}_2$ -catalyzed HCl oxidation reveals the entropic origin of compensation in heterogeneous catalysis, *Nature Chemistry* 4 (2012) 739. (doi: 10.1038/nchem.1411)
7. G.C. Bond, M.A. Keane, H. Kral, J.A. Lercher, Compensation Phenomena in Heterogeneous Catalysis: General Principles and a Possible Explanation, *Catal. Rev. Sci. Eng.* 42 (2000) 323. (doi: 10.1081/CR-100100264)
8. R. Farra, M. Eichelbaum, R. Schlögl, L. Szentmiklósi, A.P. Amrute, C. Mondelli, J. Pérez-Ramírez, Detre Teschner, Do observations on surface coverage-reactivity correlations always describe the true catalytic process? A case study on ceria., submitted to *Journal of Catalysis*

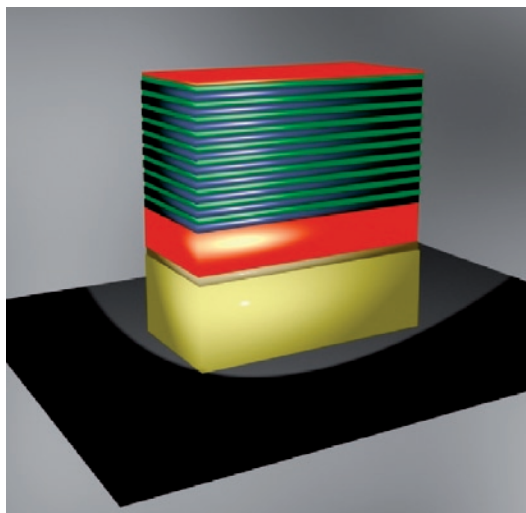
## 4.5. FE SELF-DIFFUSION IN FE/PD REVEALED BY REFLECTOMETRY

D.G. Merkel<sup>1</sup>, Sz. Sajti<sup>1</sup>, A. Rühm<sup>2</sup>, J. Major<sup>2</sup>, R. Ruffer<sup>3</sup> and L. Bottyán<sup>1</sup>

- <sup>1</sup> Wigner Research Centre, 1121 Budapest Konkoly Thege Miklós út 29-33
- <sup>2</sup> Max Planck Institute for Metals Research (now Institute for Intelligent Systems) Heisenbergstr. 3, 70569 Stuttgart, Germany
- <sup>3</sup> European Synchrotron Radiation Facility, BP 220, 38043 Grenoble CEDEX 9, France

The ever increasing demand for higher capacity magnetic storage media requires materials with strong perpendicular magnetic anisotropy. FePd, CoPd and their Pt-counterparts are attractive candidates for such purposes [1,2,3] The magnetic properties of the films depend on the local distribution of the L1<sub>0</sub> FePd phase fraction, which is controlled by short-range diffusion of a few angstroms. The anisotropic diffusion phenomena in L1<sub>0</sub> phase is of high interest from scientific and practical points of view alike.

Isotope-periodic multilayers of [<sup>nat</sup>Fe<sub>47</sub>Pd<sub>53</sub>]/[<sup>57</sup>Fe<sub>47</sub>Pd<sub>53</sub>]<sub>10</sub> were grown on MgO(100) at 350°C using MBE technique (Figure 1.). The samples were characterized by conversion electron Mössbauer spectroscopy (CEMS) and secondary neutral mass spectrometry (SNMS). Unpolarized neutron reflectivity (NR) at FRM II, Garching, polarized NR at BNC Budapest and Synchrotron Mössbauer reflectivity (SMR) at ESRF in Grenoble were performed at ambient conditions: as deposited and annealed at 310 °C to 530 °C for retention times 90 to 1800 min. In order to reveal the smoothening of the layer profiles the intensity variation of the isotopic Bragg peaks have been measured up to the second order. The logarithmic intensity decay of the Bragg peak of order *n* is proportional to *n*<sup>2</sup>. NR spectra were analyzed by the FitSuite code [4] in order to determine the diffusion lengths and further the activation energy and preexponential factor of self diffusion in the various local environments of FePd (determined by Mössbauer spectroscopy on the same samples). Figure 2 displays NR curves of the 500 °C annealed samples for various retention times and the calculated diffusion profile in a single period of the periodic multilayer. The first Bragg peak nearly vanishes after the longest annealing time of 1800 min, due to interdiffusion of the layers

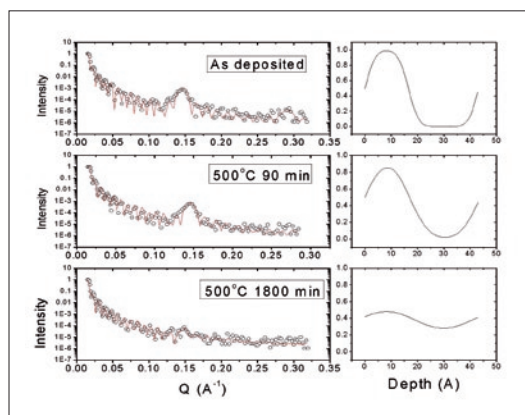


◀ **Figure 1.** Schematic image of the MgO/[<sup>nat</sup>Fe<sub>47</sub>Pd<sub>53</sub>]/[<sup>57</sup>Fe<sub>47</sub>Pd<sub>53</sub>]<sub>10</sub> isotope-periodic multilayer used in self diffusion studies

with natural Fe and <sup>57</sup>Fe isotope and a consequent flattening of the concentration profile. From these profiles the average diffusion coefficient and activation energy can be calculated according to the well known formula:

$$D(T) = D_0 e^{-\frac{Q}{kT}}$$

Experimental diffusion coefficients obtained from NR and SMR reflectivity measurements are shown in Figure 3. The red line indicates the fitting of the experimental data using the above formula and provides  $D_0 = 1.38 \cdot 10^{-13} \text{ m}^2 \cdot \text{s}^{-1}$  and  $Q = 1.51 \text{ eV}$ . The



◀ **Figure 2.** Neutron reflectivity curves and the corresponding diffusion profiles in <sup>57</sup>FePd/<sup>n</sup>FePd multilayer annealed at 500 °C for different retention times.

**Figure 3.** ▶  
Diffusion coefficients obtained from SMR and NR measurements as a function of the inverse temperature.

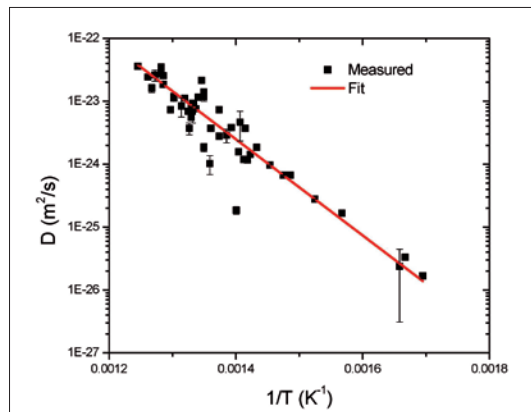
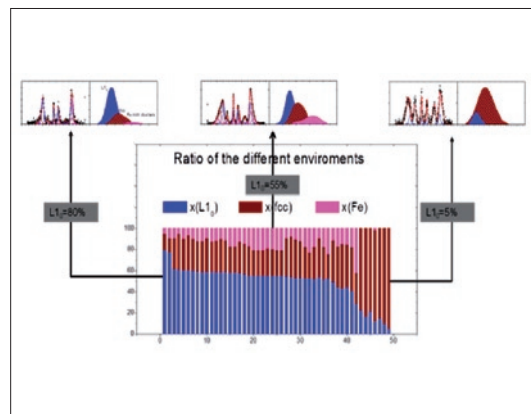


**Figure 4.** ▶  
The ratio of the three different <sup>57</sup>Fe environments in FePd determined from CEMS for each sample. Each column represents a sample and the colors correspond to the structural composition (spectral fraction in the CEM spectrum).

The results justify that the fractions of the different Fe environments namely: the L1<sub>0</sub>, the fcc and the iron-rich structure [5] are different in the samples and vary with the annealing. The detailed discussion of this theory and the determination of the partial diffusion coefficients for all the Fe environments have been determined and will be published elsewhere [6].

scattering of the data points in Figure 3 is rather large, far beyond the experimental error indicated by the error bars. This scattered behavior indicates that, in spite of the identical composition, the samples have different local atomic structures with different diffusion properties. In order to confirm or deny this assumption, CEMS measurements were taken on all samples (Figure 4)



#### References:

- 1 T. Devolder, H. Bernas, D.Ravelosona, C. Chappert, S. Pizzini, J. Vogel, J. Ferré, J. P. Jamet, J. Chen and V. Mathet, Nucl. Instr. and Meth. B 175-177, 375 (2001)
- 2 Piao, D. Lee, D. Wei, J. Magn. Magn, Mater 303, e39 (2006)
- 3 Suzuki, K. Harada, N. Honda and K. Ouchi, J. Magn. Magn, Mater 193, 85 (1999)
- 4 Sz. Sajti and H. Spiering, FitSuite, www.fs.kfki.hu
- 5 D. G. Merkel, M. Major, A. Németh, Sz. Sajti, F. Tanczikó, L. Bottyán, Z.E. Horváth, J. Waizinger, S. Stankov, A. Kovács; J Appl Phys 104 (2008) 013901
- 6 D.G. Merkel, Sz. Sajti, F.Tanczikó, M. Major, Cs. Fetzer, A. Kovács, A. Rühm, J. Major, R. Ruffer and L. Bottyán, <http://arxiv.org/ftp/arxiv/papers/1109/1109.4751.pdf>

## 4.6. CONDENSED MATTER RESEARCH BY NEUTRON SPECTROSCOPY

**L. Rosta, L. Almásy, L. Cser, G. Eszenyi, I. Füzesy, J. Füzi, A. Len, M. Markó, A. Meiszterics, F. Mezei, G. Nagy, J. Orbán, L. Riecsánszky, Zs. Sánta, N. Székely, Gy. Török, R. Ünnepp, T. Veres**

BNC – Research Institute for Solid State Physics and Optics, Neutron Spectroscopy Departmen

#### Neutron research activity

Our Department is one of the laboratories of the associate institutes forming the Budapest Neutron Centre, open for domestic and international users. Out of the 15 experimental stations of BRR, we operate on the cold neutron beams a small angle

scattering (SANS) spectrometer, a reflectometer (REFL) and a three axis spectrometer (TAS), a new focusing SANS instrument is under commissioning; on thermal beams – another TAS and a diffractometer (TOF-D).

Our thematic activity is mainly focused on topics of priority research areas according to the EU and domestic strategies. In particular, accent is made to utilize unique features of neutron scattering, namely the wide possibilities of isotope substitution and magnetic scattering. Materials aspects of nano- and life-sciences are in the scope of our activity; investigations include fields such as heterogeneous surface structures for spintronics; solid, liquid and soft nanocomposites based on specifically functionalized and stimuli-responsive nanoparticles; biocompatible and biofunctional nanoparticles including magnetic nanoparticles. Applied research for engineering sciences, structural characterization of materials for nuclear installations, non-destructive diagnostics of industrial components as well as archaeological objects are performed.

Methodical-instrumental development has been always in the focus of our activity. Hungarian and EU FP7 projects provide support for neutron optics, detector, control electronic etc. developments. Our experimental equipment consists of at large extent home-made optical and electronics components; choppers, detectors monitors have been recently installed on various spectrometers. These methodical developments are also aiming for commercialisation of neutron equipment via technology transfer to high-tech, spin-off companies. Several SMEs at our research centre site form the industrial cluster to provide a sizable production volume in neutron instrumentation.

Education and professional training is an important mission for us: we are involved in graduate and professional training, (teaching at several universities, performing PhD works, organising international training courses). Organization and co-ordination of international relations at BNC level is also in the

scope of our activity. The Hungarian membership to ILL in the context of the Central European Neutron Initiative (CENI, co-operation with AU, CZ, HU, SK) is managed also by our Department. Collaboration projects have been running with various domestic and international institutions in the frame of either bilateral agreements or various funded projects.

Experiments in condensed matter research SANS study of solvent effect on the structure of epoxy gels - A series of hydrophilic epoxy networks was prepared by end-linking reaction of  $\alpha,\omega$ -diamino terminated poly(oxypropylene)-block-poly(oxyethylene)-block-poly(oxypropylene) (POP-POE-POP) of molar mass  $600 \text{ g}\cdot\text{mol}^{-1}$ , and diglycidyl ether of Bisphenol A propoxylate (PDGEBA) at various initial ratio of reactive groups  $r=2[\text{NH}_2]_0/[\text{E}]_0$ . The networks prepared were swollen to equilibrium in deuterated methanol ( $\text{CD}_3\text{OD}$ ) and heavy water ( $\text{D}_2\text{O}$ ), respectively. Whereas methanol is good solvent for all the blocks built into the network (POE, POP and PDGEBA), water is good solvent for POE only. Consequently, SANS patterns of the gels obtained by swelling of networks in  $\text{CD}_3\text{OD}$  and  $\text{D}_2\text{O}$  differ significantly as illustrated in Fig. 1. In networks swollen in methanol (Fig. 1a), the scattering is governed by frozen and dynamic inhomogeneities, respectively, due to network connectivity and thermal movement of polymer segments. Unlike this, in networks swollen in water (Fig. 1b), above contributions to SANS are superimposed by inhomogeneities due to nanophase separation of the system into water-rich and water-poor domains. The domains exhibit a locally lamellar order as proved by successful fitting of SANS patterns to the Teubner-Strey model [Krakovsky\* I, Székely NK; *Small-angle neutron scattering study of nanophase separated epoxy hydrogels; Journal of Non-Crystalline Solids*; 356, 368-373, 2010].

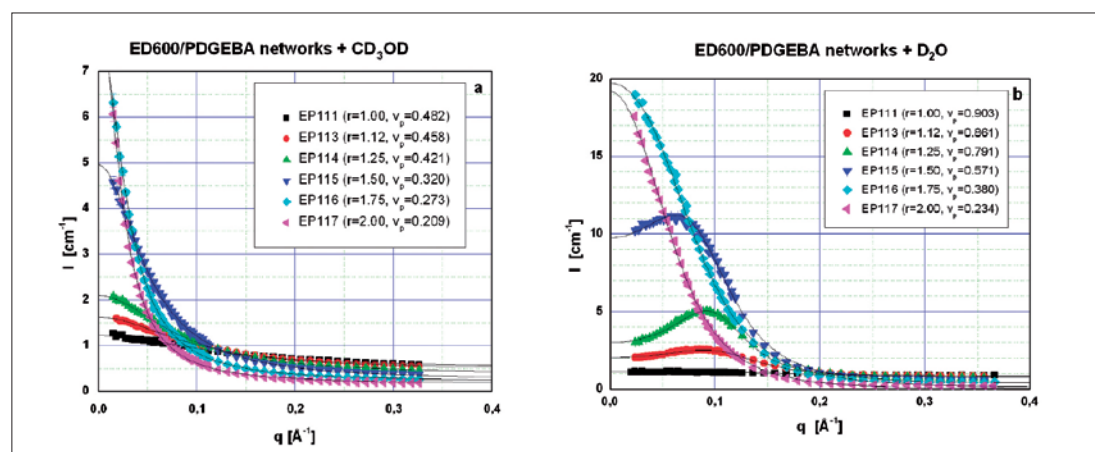


**Figure 1.** SANS scattering profiles obtained from the epoxy networks swollen to equilibrium in  $\text{CD}_3\text{OD}$  (a) and  $\text{D}_2\text{O}$  (b) at  $25^\circ\text{C}$ . Solid lines represent fits according to model developed for polymer networks swollen in good solvent (a) and Teubner-Strey model (b).  $v_p$  denotes the polymer volume fraction in gels.

Wool fibre structure. The nanoscale structure of various filaments attracts particular interest in their technical applications. Small angle neutron scattering (SANS) is an ideal tool for the investigation of such anisotropic systems. Recently we have performed pioneering experiments on wool and mohair fibres. They have a variety of properties that influence the texture and feel of the final woven textile products. Chemical treatment, washing and drying, moreover repeated stress procedures can considerably influence the fiber properties. In wool, individual polypeptide chains are joined together to form proteins by a variety of covalent chemical bonds, called cross-links, and non-covalent physical interactions. To improve the physical properties, for instance shrink resistance of textiles, they are often treated with environmentally unfriendly chemicals, so here we present set of SANS measurements to compare the effect of various chemical treatments (solution of chlorine, carot – potassium monopersulphate, enzyme and chlorine, and enzyme and carot). The SANS facility at the BNC was used with neutron wavelengths between 3.9 and 16 Å. The wool samples were packed into Al containers with the fibers aligned vertically. The results of SANS measurements are shown in Figure 1 in the form of 2D spectra.

The alignment of fibers, which is reflected in the scattering patterns due to the anisotropic nanoscale structure, tells about the treatment effect. The enzyme and chlorine treatment appeared to have the least disruptive effect on the fiber since the spectra were isotropic, whereas just the chlorine treatment had the greatest influence. We can also say that in the dry wool structure, we determined a density fluctuation with spherical

gyration radius  $\sim 7\text{-}9$  nm, which corresponds to the physical diameter of long cylindrical samples and this can be identified as the micro-fibril size of the studied wool filaments. Wetting experiments on samples of mohair with mean diameter  $25.3\ \mu\text{m}$  and  $37.3\ \mu\text{m}$  were also performed. 2D SANS spectra were measured for dry and saturated with D<sub>2</sub>O samples were studied. These results gave an indication of where and how the water molecules are attached to and detached from the wool fiber. This new knowledge will go far towards developing an understanding, at the molecular level, of the influence of the wetting and drying process of wool and mohair fibers. This project was performed as a science and technology collaboration between Hungary and South-Africa [Franklyn\* C; Török Gy; *The use of small-angle scattering to study wool and mohair fibres; Indonesian Polymer Journal; 14, 1-2, 2012*].

Nanoscale morphology of tungsten wires. Another filament structure study was related to the morphology of doped W used in lighting industry. Tungsten research has a long tradition in Hungary due to the GE TUNGSRAM Company, a leading manufacturer of lighting products worldwide. Our study was focused on the nanoscale structure of wires, in particular on the structure stabilizing feature of potassium doping using SANS. We investigated the potassium bubbles present in the tungsten matrix of the drawn wires to understand several qualitative and quantitative characteristics of the potassium-tungsten complex system. During the mechanical and thermal processing the potassium bubbles form a specific texture that delays the break of the wire and prolongs its life. During the wire drawing the sphere-like

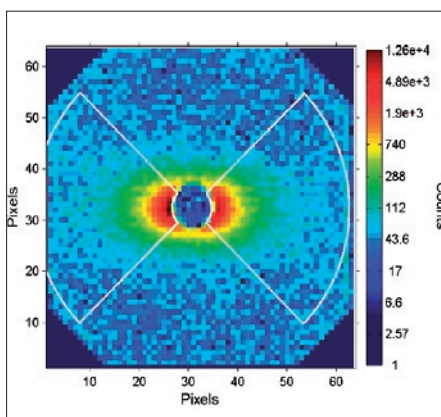


Figure 2a.  
chlorine

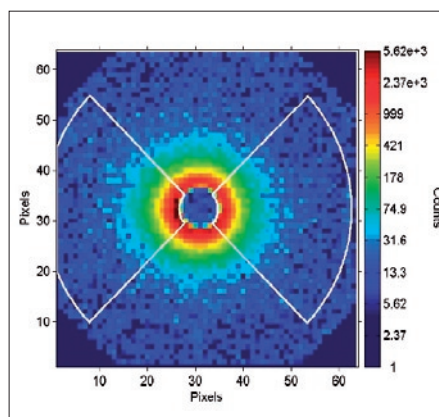


Figure 2b.  
carot

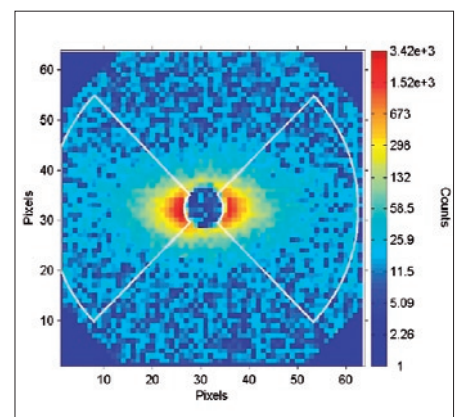


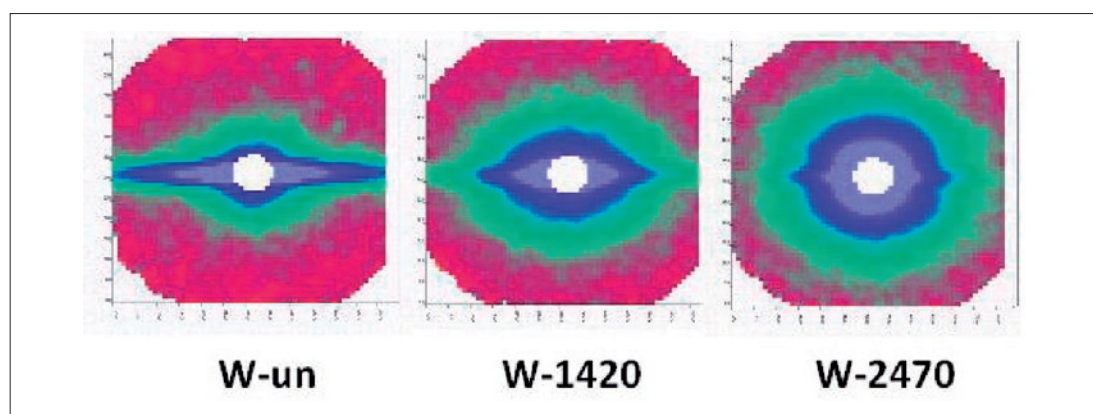
Figure 2c.  
enzyme



bubbles get elongated along the axis of the wire, forming ellipsoid or/and cylinder-like bubbles. Further the aspect ratio of a bubble reaches a critical value and becomes unstable: the ellipsoid splits into a row of elongated bubbles with a smaller aspect ratio. In the further steps of annealing the degree of the elongation decreases until all the bubbles adopt the spherical shape. These rows of bubbles guide the grain boundary migration allowing the growth of elongated grains along the axis of the wire. This structure gives a good tensile strength of the wires.

Analyzing the 2D SANS maps (Fig. 3) of series of samples annealed at different temperatures we can

determine the elongation ratio and give an accurate description of the maturation of the bubble system inside the wire during the production. Using a sophisticated 2D data treatment method we obtained the anisotropy of the scattering in a large Q range ( $10^{-5} \text{ \AA}^{-1}$  -  $10^{-1} \text{ \AA}^{-1}$ ) and enabled us to determine the size and shape of potassium bubbles. This lead us to understand that micro-crack formation during manufacturing of thin tungsten wires has always been presumed, and here it was finally demonstrated experimentally [Rosta L, Len A, Pépy G, Harmat\* P, *Nano-scale morphology of inclusions in tungsten wires - a complex SANS study, Neutron News, 23, 13-16, 2012*].



◀ **Figure 3.** 2D SANS scattering intensities of the 0.5 mm diameter tungsten samples taken from the different steps of the wire production. Temperatures of annealing: not annealed, 1420K and 2470K.

### Structure of photosynthetic membranes

The light reactions of oxygenic photosynthesis take place in thylakoid membranes; these reactions are responsible for the enzymatic splitting of water – leading to oxygen evolution, and the production of NADPH – responsible for the reduction of  $\text{CO}_2$  into carbohydrates. The high energy content ATP molecules are synthesized using the energized state of membranes, i.e. the light-induced trans-membrane electrical field and pH gradient that is formed between the inner and outer aqueous phases of the membrane vesicles. These vesicles form highly organized multilamellar systems, the exact structure of which depends on the organism and also on environmental factors. In plants, the thylakoid, flat (<20 nm thick) vesicles, are arranged into tightly stacked grana, which are interconnected in a regular fashion by stroma lamellar membrane sheets wound around the cylindrical grana, which are typically of about 500 nm in diameter and are several hundred nm high. The granum-stroma thylakoid membrane assembly is the most abundant membrane assembly on Earth and also one of the

most complicated one. The closely related green algal cells contain similar membrane systems but the grana are not fully developed compared to vascular plants. In diatoms, a family of algae responsible for almost one third of the atmospheric  $\text{CO}_2$  fixed in the Biosphere, the membranes are arranged into loosely stacked bundles of three thylakoid membranes but with no lateral differentiation into granal and stromal regions. The thylakoid membranes in cyanobacteria were found in concentric or radial arrays with relatively low packing densities due to the presence of large external light harvesting proteins, the phycobilisomes, attached to the membranes.

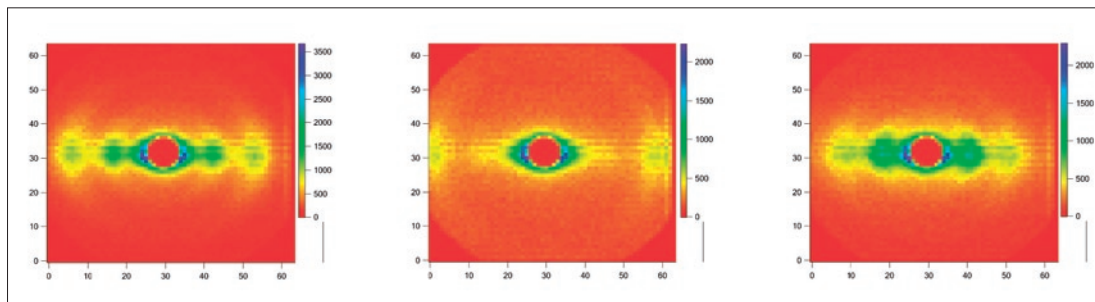
We used small angle neutron scattering (SANS) was to provide information on the average repeat distances and on some other ultra-structural parameters of this type of multilamellar membrane systems even in living cyanobacterial and algal cells as well as on intact leaves and isolated plant thylakoid membranes. Due to its non-invasive nature, SANS – in contrast to most

structural methods – can also be used to study the kinetics of structural changes in vivo. The origin of the most characteristic features of the scattering curves was identified via using mutants, different thylakoid preparation techniques, and various treatments. SANS in parallel with electron microscopy revealed the occurrence of changes in the repeat distances of membrane layers and also in the form-factors of paired membranes of

adjacent thylakoids. Small but well discernible changes were shown to occur in the repeat distances of the membranes in all systems studied, showing an unexpectedly high structural flexibility of the membranes upon illumination. Similar changes could also be induced and mimicked by varying the repeat distances by changes in the osmolarity and/or the ionic strength of the solvent medium (Fig. 4).

**Figure 4.** ▶

Reversible changes of living algal cells of the diatom *Phaeodactylum tricornutum* oriented in an external magnetic field of 1.5 T upon variation in the osmolarity of the suspending medium: left, untreated control algal cells; center, cells in 600 mM sorbitol-containing medium; and right, cells resuspended in sorbitol-free medium.

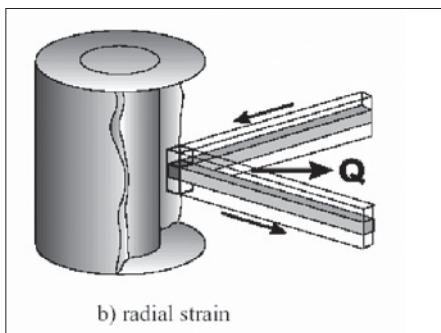


### Residual stress measurements in metal standards

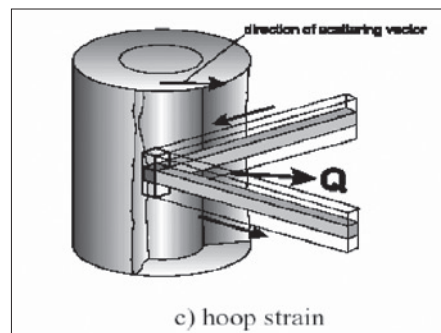
The deep penetration of thermal neutrons into the bulk of material makes neutron diffraction a powerful tool for the residual strains measurement by the high precision determination of lattice parameters and such non-destructive validation plays an important role in engineering sciences. For a series of “standard metal” samples a worldwide Round Robin test was performed; here we used the cold neutron triple axis spectrometer ATHOS in order to validate the followed procedure with our instrumental setup. ATHOS is an instrument with high flexibility and a relatively big sample table for investigation industrial samples. A vertically focusing PG monochromator provides continuously

changeable wavelength, the detector is 200x200 mm position sensitive delay line type detector. The Round Robin sample was VAMAS Aluminium Ring & Plug Aluminium Ring & Plug Set.

Figure 5/a shows the experimental setup, and the scheme for measuring radial and hoop stresses are shown in the Fig. 5/b. For stress measurement we used the 111 reflection using a gauge volume determined by the incident beam 20x3mm (HxW) and by the outgoing beam 20x3mm (HxW) at the detector direction. At the 111 reflection we used the wavelength of 0.33 nm giving us the 90 deg scattering angle.



▶ **Figure 5b.**



▶ **Figure 5b.**

◀ **Figure 5a.**

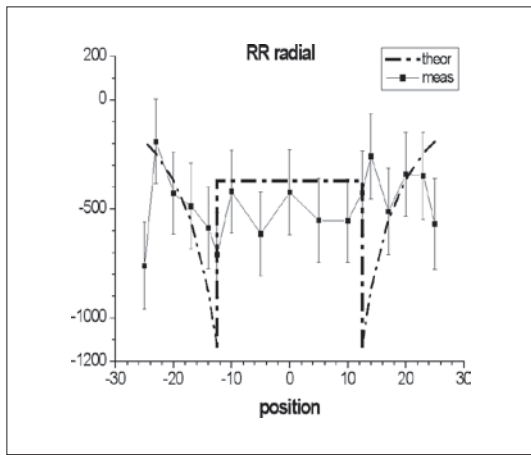


**Figure 6a.**  
The measured and calculated radial strain.

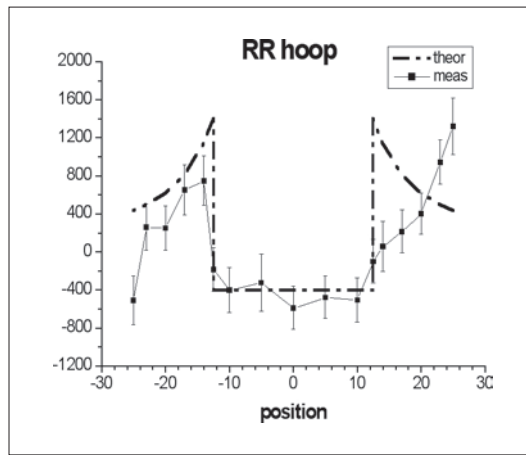


**Figure 6b.**  
The measured and calculated hoop strain.

The measured strain data fit well to the results measured elsewhere of the Round Robin series. It is seen that the strain fits well on the negative side of sample position, while on the positive side the fit is rather poor due to longer beam path in the sample well corresponding to the peak intensity weakening. In our case the used wavelength

0.33 nm results higher absorption than the usually applied thermal beam (0.1-0.2 nm), the used geometry, however is more comfortable. We have made another improvement, too: Using the 004 reflection of the PG monochromator gives much less error bar with no substantial intensity loss.

### Cultural heritage

Since 2009 we take part of a large EU FP7 project named CHARISMA, to provide analytical scientific approach and instrumentation for the investigation of ancient objects. In this regard a preliminary study of medieval swords by time of flight neutron powder diffraction (TOF-NPD) was performed at BRR. The aim of the experiment was to present the applicability of the method and the instrument itself for non invasive characterization of archeological artifacts made of carbon steel. The following characteristics were planned to determine: phase composition (for steel phases as ferrite, cementite, as far as possible martensite and non-steel phases), degree of alloying of the main phase, total carbon content, texture and the average internal stress and dislocation density. Four medieval – or believed to be that – swords have been studied. **Sword1** strongly

corroded but together with **Sword2** were visibly Damascus blades, certificated archeological objects. **Sword3** and **Sword4** were in good state but not certificated. Based in our experiments we assumed the following, concerning the texture: although the anisotropy in hot worked metal is much weaker than in a cold worked one, we have found that it is extremely low in the investigated objects thanks to the good manufacturing. On the other hand, the nature of the data seems to be typical for different style blades. In phase analysis: all the blades show high, but different cementite concentration, but no other phase has been found in the applied scattering vector range. Concerning the alloying degree of the main ferrite phase the peak shifts carries information rather on the final heat treatments, while the amount of the carbon in the ferrite depends mainly on the cooling rate.

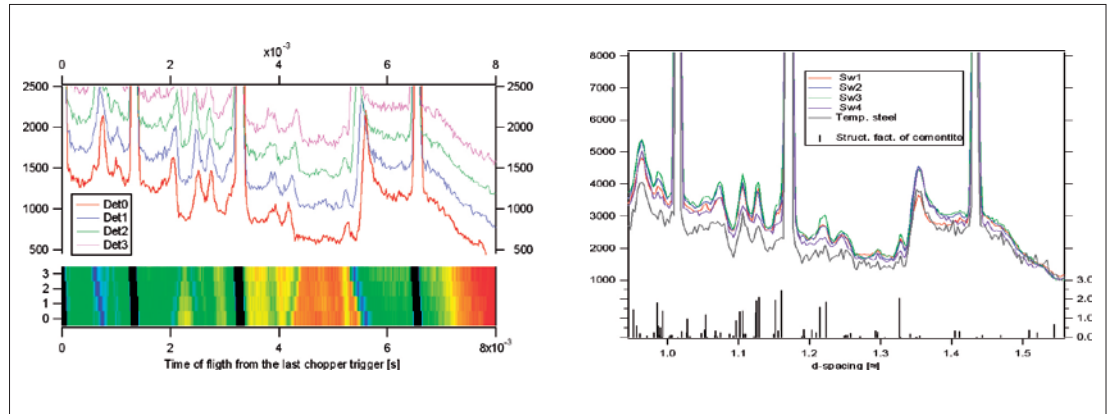


	Broadening [ $\text{\AA}$ ] ( $\pm 0.00006 \text{\AA}$ )	Relative peak shift ( $\pm 0.00005$ )	Cementite content [wt%] ( $\pm 3$ )	Carbon content in ferrite [at.%] ( $\pm 0.00003$ )
Sword1	0.00075	0.00059	13.1	0.0028
Sword2	0.00015	0.00011	16.0	0.0005
Sword3	0.00064	0.00031	17.8	0.0014
Sword4	0.00000	0.00041	8.76	0.0019

**Table 1.**  
The main parameters gained from the diffraction patterns.

**Figure 7.** ▶

The angular behavior of the inelastic part of the spectra. While weak elastic peaks are parallel to the other stronger peaks (black region) the inelastic ones are inclined depending on it whether due to annihilation or emission. b: A short part of the low resolution spectra of the four sword with a low carbon content commercial steel (C30) after some correction, together with the calculated cementite structure factor. Sword 1 shows somewhat weaker inelastic scattering, what can be attributed to the high carbon content in the ferrite phase and the high dislocation density.



To obtain information on stress and strains the peak shape analysis of the high resolution spectra were used. It was clearly visible, that the peak profiles show Lorentzian broadening compared to pure iron. These values – i.e. the broadening compared to pure iron

– are presented in Table 1. It is interesting to note that **one** of the swords shows no line broadening. More accurate results can be gained using a correct model for the inelastic scattering part, which is a completely new approach in this kind of studies.

### Neutron instrumentation development

**Neutron supermirrors** were discovered by F. Mezei in 1976 in Budapest; then since the application of magnetron sputtering techniques for the large scale productions of supermirrors (SM) in the middle of nineties, the construction of SM guides in neutrons centres has become a \$ multimillion venture. Due to multiple reflections in neutron guides, the reflectivity decrease of neutron supermirrors deserves careful examination. One possible cause of reflectivity loss is the contamination by hydrogen-containing compounds (large incoherent scattering cross section), from vacuum pumps and the atmosphere. In our experiments vacuum pump oil was deposited on the surfaces of supermirror samples and the average film thickness was measured by weighing before and after deposition, also locally by optical interference. Inhomogeneities and drop formation were observed by optical microscope. The reflectivities of clean and oil-covered supermirrors were measured at the

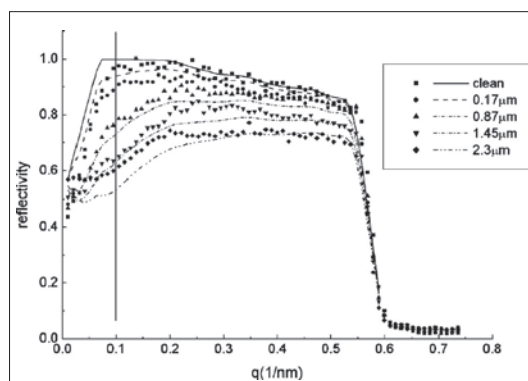
constant wavelength ( $\lambda=4.2 \text{ \AA}$ ) reflectometer of the Budapest Research Reactor.

We calculated the reflectivity applying the Parratt method. On figure 8. we see the comparison of the measured and calculated reflectivities (the finite sample and slit sizes are taken into account). The drop formation can not be taken exactly into account; there is some deviation between calculated and measured values for the thickest oil films. Monte Carlo simulations predict exponential decreasing of neutron yield as a function of the oil thickness. The shape of the beam is also distorted in the model calculation; this effect could be used to diagnose the presence of contamination using the pin-hole method.

**Time-of-Flight (TOF) method** for neutron diffraction is a very efficient alternative to the crystal monochromator techniques. High performance in diffraction is a most basic goal and requirement for all neutron sources now or in the future and a technique to achieve this is of central importance for the new generation of continuous or long pulse sources. In collaboration with HZ-Berlin at the Budapest Neutron Center (BNC) we undertook to develop a powerful TOF diffraction technique for both its own use and with the perspective of the establishing at a continuous source the foundations of TOF diffraction techniques for future long pulse sources. This project is described here in details in a separate paper by F. Mezei et al.

**Figure 8.** ▶

Measured (line) and calculated (dots) reflectivity of the supermirrors covered by oil of various thickness. (Left of the perpendicular line the reflectivity is distorted by geometrical effects.)



## 4.7. TIME-OF-FLIGHT NEUTRON DIFFRACTION FOR LONG PULSE NEUTRON SOURCES – BUDAPEST EXPERIMENTS

F. Mezei<sup>1,2</sup>, M. Russina<sup>3</sup>, Gy. Káli<sup>1</sup>

<sup>1</sup> BNC – Research Institute for Solid State Physics and Optics, Neutron Spectroscopy Department

<sup>2</sup> European Spallation Source ESS AB, Sweden

<sup>3</sup> Helmholtz Zentrum Berlin für Materialien und Energie, Germany

The Time-of-Flight (TOF) method for neutron diffraction was proposed half a century ago by Buras and Leciejewicz as a very efficient alternative to the crystal monochromator technique most often used at that time. It was the advent of the first pulsed spallation sources that has shown how farsighted this proposal was: the diffractometers naturally based on the TOF method have become most productive powerhouses at these sources. High performance in diffraction is of central importance for the new generation of long pulse sources pioneered by ESS. The central challenge is to produce short pulsed white neutron beams from the long pulses in order to meet all resolution requirements in diffraction. No efficient method for such pulse shaping could be successfully developed at the short pulse sources. In collaboration with HZB (then HMI), the Budapest Neutron Center (BNC) undertook in the second half of the 1990s the development powerful TOF diffraction for both its own use and with the perspective of establishing at a continuous source the foundations of TOF diffraction techniques for future long pulse sources.

On this basis a BNC-HZB team succeeded last year at BNC to experimentally implement and test the special chopper system capable of turning a long pulse spallation source into an ideal short pulse source with flexibly tunable pulse length for neutron diffraction work by Wavelength Frame Multiplication (WFM), a method proposed in 2002 in connection with the early ESS project. The experiments, using the TOF Diffractometer at BNC in an unconventional mode of operation for emulating long pulse sources, provided the full proof of principle of the WFM method with full success[3]. The results have shown that the combination of the neutron spectra coming from different chopper pulses into a single, broad-band diffraction pattern can be accomplished with such perfection that it is indistinguishable from a diffraction pattern that

would originate from a single pulse. This achievement is fundamental for instrument design on long pulse spallation sources. The WFM method is actually a variant of the by now fully developed Repetition Rate Multiplication (RRM) multiplexing technique for neutron spectroscopy at pulsed sources.

The TOF method using neutron beam choppers, e.g. disc type ones, is well established on both continuous and pulsed neutron sources. A multiplexing copper system, in contrast to the established configurations, produces a series of neutron pulses with different characteristics, e.g. different wavelengths. This is illustrated in the TOF diagram in Figure 1 which shows the archetypal WFM chopper system as it was first implemented at BNC [M. Russina, Gy. Káli, Zs. Santa and F. Mezei, *J. Nucl. Instr. and Meth. A654* (2011) 383]. The neutrons originating from pulses of a pulsed neutron source are cut by the pulse shaping fast chopper #1 into a sequence of pulses with a repetition rate that is the multiple of the source pulse repetition rate. The neutrons from one pulse shaping chopper pulse can propagate within one colored area and are represented by straight lines whose slope is the neutron velocity. For this purpose, the pulse repetition time  $T_i = 1/f_i$  of chopper #*i* must be proportional to the distance  $L_i$  of the chopper from the source (where  $f_i$  is the pulse frequency of chopper #*i*). In order to make sure that the pattern repeats itself for each source pulse, each chopper must have a pulse frequency which is a multiple of the source frequency  $f$ .

$$f_i L_i = \text{const}, \quad f_i / f = \text{integer}$$

It is important to observe that the chopper system defines its own virtual source pulses, i.e. well delimited time windows with repetition frequency  $f$  where the chopper system “looks” for neutrons. From outside these windows neutrons cannot make their way through the system. This virtual

source feature offers a very important capability to WFM chopper systems: to take the neutrons from the most intense flat top section of a long pulse. The colored sectors in Figure 1. also illustrate that detected neutron can only come from a single, well defined pulse shaping chopper pulse.

A final key ingredient of this work was the use of event recoding data collection [M. Russina, F. Mezei, T. Kozłowski, P. Lewis, S. Pentilla, J. Fuzi, E. David and G. Messing, in: *Proceedings of ICANS-XVI*, G. Mank, H. Conrad (Eds.), (FZ Jülich, 2003) p. 667], which is the standard data acquisition method on the BNC TOF diffractometer. All chopper pick up signals for each revolution and all neutron counts are time stamped and recorded. The data evaluation consists of analyzing all these records for each neutron count in view of all actually recorded chopper opening times and finding for each detected neutron the only possible pulse shaping chopper pulse it can come from. (Background neutrons that arrive in the

time gaps between colored sectors at the detector are discarded).

The first diffraction pattern ever observed with a multiplexing chopper system is shown in Figure 2. The dips in the background line show the crossover between two wavelength frames (colored sectors) in Figure 1 and amplified by the use of large safety margins in the event recording data evaluation. In a more recent experiment [M. Russina, F. Mezei and G. Kali, *Journal of Physics, conference series*, 340 (2012) 012018] we have tested two methods of fully eliminating the type of irregularities shown in Figure 2 at the limits of adjacent RRM frames. One of these consists of slewing the chopper phases in order to move the switching regions from one RRM frame to another around in a uniform fashion over the whole wavelength band observed. The result of such a phase slewing scan is shown in Figure 3 at higher intensity at lower resolution compared to Figure 2.

**Figure 1.** ▶  
The principle of Wavelength Frame Multiplication pulse shaping chopper system. Without multiplexing only the blue frame would be available for data collection within the time period between subsequent (virtual) source pulses. Figure from Ref. [M.Russina 2003].

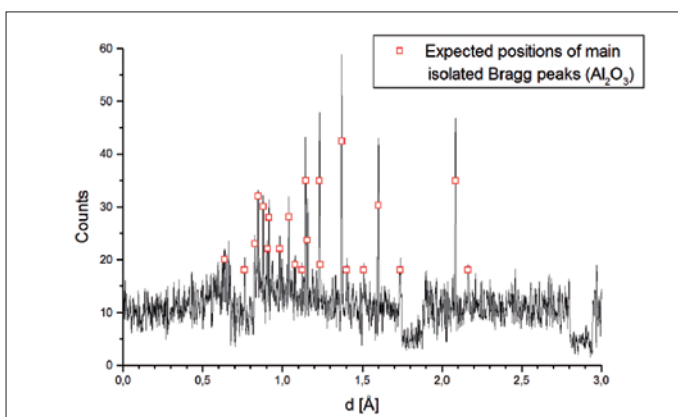
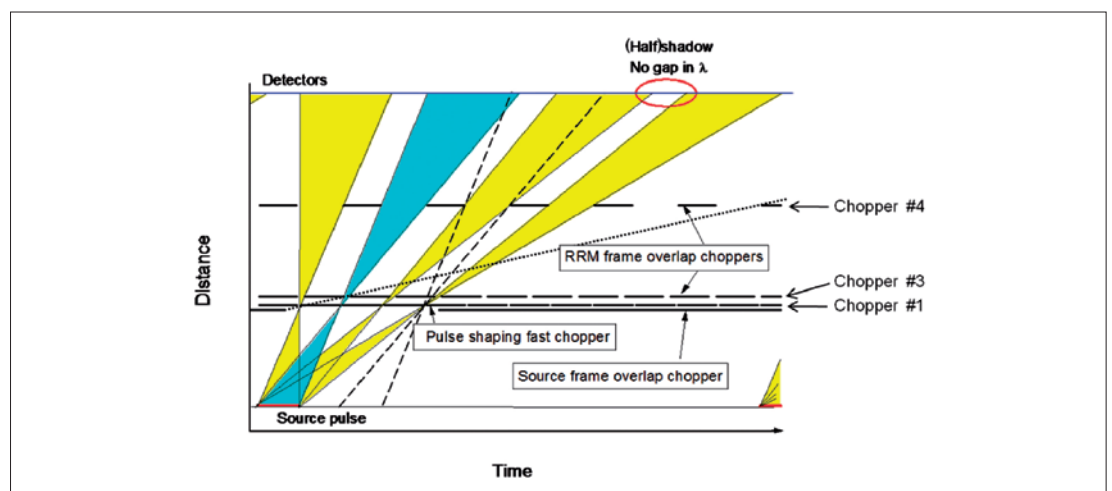


**Figure 2.**  
The first powder diffraction pattern obtained by Wavelength Frame Multiplication, showing marked transitions between adjacent RRM frames [M.Russina 2003].

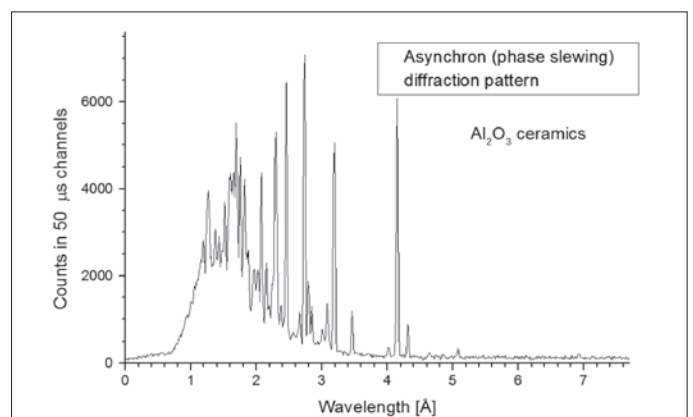


**Figure 3.**  
Diffraction pattern obtained by asynchron (phase slewing) WFM data collection mode for seamlessly joining together of multiple RRM frames. Figure from Ref. [M.Russina 2012]

*Detailed  
results  
(Experimental  
reports)* | **5.**

<b>B N C</b> <b>Experimental Report</b>	<i>Experiment title</i> <b>Active neutron multiplicity counting with guided cold neutrons</b>	<i>Instrument</i> NIPS
		<i>Local contact</i> L. Szentmiklósi
<i>Principal proposer</i> Bagi János – EC JRC ISPC, Ispra Italy <i>Experimental team</i> Bagi János, Hlavathy Zoltán, Szentmiklósi László-Institute of Isotopes		<i>Experiment Number</i> BRR-236 <i>Date</i> 06.02.2010-06.04.2010

## Objectives

To establish the active neutron multiplicity counting technique with guided neutrons, and investigate its performance in quantification of U-235 in various samples.

## Results

Successful experiments have been performed at the NIPS facility to establish the cold-neutron based neutron multiplicity counting technique. It is aimed at determining low amounts of nuclear material in different matrices, based on the detection of fission neutrons. The device consists of 19  $^3\text{He}$  neutron detector tubes embedded in a cylindrical polyethylene moderator (Figure 1.). The inside cavity – where the neutron beam passed through – was lined with Cd to shield against scattered slow neutrons. The sample, in form of a powder or liquid, was placed to the end of the NIPS flight tube. As the neutrons from neutron-induced fission are emitted in coincidence, contrary to the guided neutrons, a highly-selective discrimination is possible. The events were recorded with a digital pulse-train reader. For normalization, the incoming neutron flux was also monitored.

With the optimization of the shielding and geometry, the background was already low enough for useful experiments. A calibration curve was measured with a series of solid and liquid samples, containing U-235 from 1-250 g, which was found to be a linear over most of the investigated range. It was proven that the rate of coincidences (also called as doubles) is independent of the matrix and the volume of the sample. The achieved detection limit was as low as 1 g of U-235.

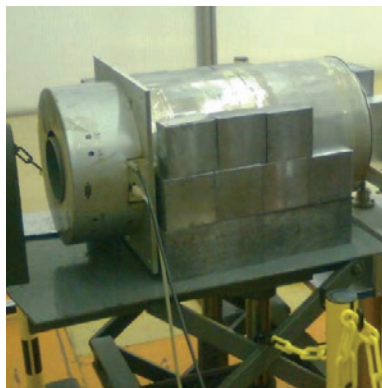


Figure 1. The photo of the neutron coincidence counter as it was placed at the NIPS experimental station

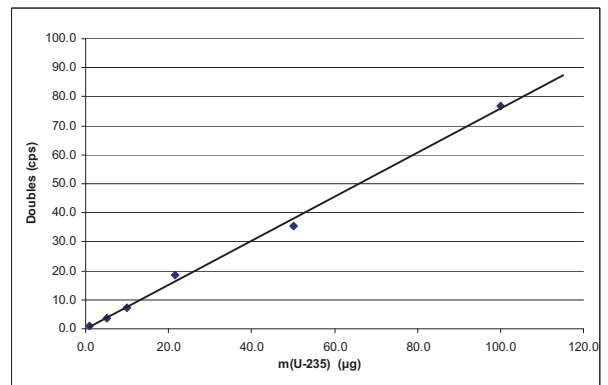


Figure 2. The count rate of coincident events (doubles) as a function of U-235 amount.

## Future prospects

The achieved DL could be further improved by employing a detector with better counting efficiency. The more precise sample positioning could also reduce the scattering of the measured points, as the beam was measured to be spatially inhomogeneous.

## References

1. J. Bagi; L. Szentmiklosi; Z. Hlavathy; Detection of fissile material using cold neutron interrogation combined with neutron coincidence counting, accepted for publication in *Nucl. Instr. Meth B*.



<b>B N C</b> <b>Experimental Report</b>	<i>Experiment title</i> <b>Fission fragment spectrometry by means of the time-of-flight method and fission gamma ray studies</b>	<i>Instrument.</i> NIPS <i>Local contact</i> Tamás Belgya
	<i>Principal proposer:</i> A. Oberstedt (U. Örebro, Sweden) <i>Experimental team:</i> Tamás Belgya, L. Szentmiklósi, Z. Kis, K. Takács (II-HAS), Andreas Oberstedt (U. Örebro, Sweden), Stephan Oberstedt, Franz-Josef Hamsch, Ruxandra Borcea, Imrich Fabry (EC JIR IRMM, Belgium), Trino Martinez (Nuclear Innovation Group Department of Energy CIEMAT), Alf Göök (Institut für Kernphysik Technische Universität Darmstadt)	<i>Experiment Number</i> NIPS_11_02_IC <i>Date</i> 2010.02.23- 2010.03.05

## Objectives

Fission fragment spectrometry by means of the time-of-flight method and fission gamma ray studies. Test measurement of the double-E and double-v fission fragment spectrometer VERDI.

## Results

The experimental set-up was installed at the cold neutron beam of the IKI Research Reactor in Budapest (Fig. 1). The neutron flux at the entrance window of the VERDI spectrometer was  $5 \times 10^7$  /s/cm<sup>2</sup>. During the experiment VERDI was operated in a single (v, E) configuration. Ten 450 mm<sup>2</sup> large PIPS detectors are placed at a distance of 50 cm from the fission source. As fissile target a 113 µg/cm<sup>2</sup> <sup>235</sup>U mounted on a 34 µg/cm<sup>2</sup> thick polyimide backing was used and placed directly on the diamond detector. Both the fission fragment distributions and prompt fission gamma-rays from the <sup>235</sup>U(n<sub>th</sub>,f) reaction were measured. Detail of the experimental results can be found in Ref. [1-2].

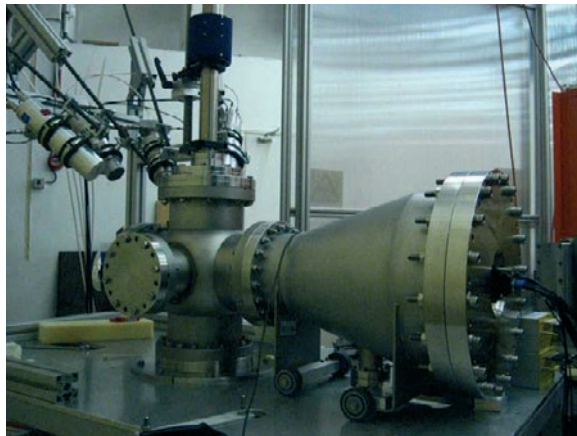


Figure 1: Photograph of the experimental set-up with the single (v, E) version of the fission fragment spectrometer VERDI and four lanthanum halide detectors (upper left corner).

This experiment was supported by the EFNUDAT (agreement number 31027) and NAP VENEUS OMF00186/2006 projects.

## References

1. A. Oberstedt, R. Billnert, A. Göök, J. Karlsson, S. Oberstedt, F.-J. Hamsch, R. Borcea, T. Martinez Perez, D. Cano-Ott, T. Belgya, Z. Kis, L. Szentmiklosi, and K. Takács. "Measurement of prompt fission  $\gamma$ -rays with lanthanum halide scintillation detectors." Proceedings of the Final Scientific EFNUDAT Workshop, Ed. Enrico Chiaveri, European Laboratory for Particle Physics (CERN), ISBN 978-92-9083-365-9 (2011) pp. 85-89. (<http://indico.cern.ch/conferenceDisplay.py?oww=True&confId=83067>).
2. S. Oberstedt, T. Belgya, R. Borcea, A. Göök, F.-J. Hamsch, Z. Kis, T. Martinez-Perez, A. Oberstedt, L. Szentmiklosi, T. Takács, Sh. Zeynalov. "VERDI – a double fission-fragment time-of flight spectrometer." Proceedings of the Final Scientific EFNUDAT Workshop, Ed. Enrico Chiaveri, European Laboratory for Particle Physics (CERN), ISBN 978-92-9083-365-9 (2011) pp. 91-97. (<http://indico.cern.ch/conferenceDisplay.py?oww=True&confId=83067>).

<b>B N C</b> <b>Experimental Report</b>	<i>Experiment title</i> <b>Composition of Reactor Graphite, Carbon Fiber and Cement samples</b>	<i>Instrument</i> PGAA and NIPS  <i>Local contact</i> Zs. Révay
	<i>Principal proposer</i> Eric Mauerhofer-Forschungszentrum Jülich GmbH IEF-6 <i>Experimental team</i> Révay Zsolt	<i>Experiment Number</i> NIPS_11_04_CW <i>Date</i> 2010.10.11- 2010.10.14

## Objectives

to determine the composition of 3 cement and 3 carbon fiber and 7 reactor graphite samples

## Results

About 2–5 g of each cement and carbon fibre samples was heat-sealed in fluorinated ethylene propylene (FEP) foils with the sizes of about 15×15 mm<sup>2</sup>. The masses of the graphite pieces were 0.6–0.7 g, except one that was 1.4g. The latter samples were measured without any packing, using just Teflon strings as sample holders. The cross-section of the neutron beam is 2×2 cm<sup>2</sup>. The background from carbon and fluorine (Teflon) and other structural materials (Al, Fe, Pb) were subtracted from the compositions.

The carbon fiber samples contained H, B, C, N, Cl above the detection limit:

Element	conc m%	unc %	conc m%	unc %	conc m%	unc %
H	3.00	2.8	2.93	2.9	2.9	6.2
B	1.51 ppm	3.4	1.40 ppm	3.7	1.20 ppm	3.4
C	92	0.3	92	0.3	92	0.3
N	4.8	4.5	4.9	4.8	4.9	3.7
Cl	0.25	20	0.23	16	0.059	6.5

The compositions of the three cement samples can be seen in the following table:

Element	Oxide conc m%	Unc %	Oxide conc m%	Unc %	c% ox/ox	unc %
H	13.1	1.4	12.5	1.4	11.9	1.2
B	297 ppm	1.4	307 ppm	1.3	311 ppm	1.2
Na	0.84	5	0.54	6.8	0.72	3.8
Al	9.4	2.1	9.1	1.9	9.3	2.2
Si	37	1.8	37	1.7	37	1.6
S	1.56	2.7	1.63	2.7	1.82	2.6
Cl	200 ppm	28	200 ppm	3.3	200 ppm	29
K	1.72	2.1	1.59	2.3	1.69	1.9
Ca	32	2.2	32	2.1	33	1.8
Ti	0.41	3.6	0.43	2.6	0.45	2.7
V					0.079	5.9
Mn	0.094	3.8	0.102	3.7	0.097	3.5
Fe	3.8	3.1	4.2	2.5	4.0	2.9
Co	130 ppm	5	400 ppm	17	210 ppm	9
Cd			0.4 ppm	13	0.7 ppm	14
Sm	0.086ppm	3.5	3.7 ppm	2	4.0 ppm	2.1
Gd	4.6 ppm	5.7	4.6 ppm	9.2	5.0 ppm	9.2

For reactor graphite samples, the concentration of carbon is more than 99.9 mass%. H, Li-6, B, N, Mg, Na, Al, Si, S, Cl, K, Ca, Sc, Ti, V, Cr, Mn, Fe, Co, Ni, Cu, Cd, Sm, Gd were identified in the samples in ppm amounts, whereas Eu and U were below detection limits (0.4 ppm, and 0.01%, respectively).

<h1 style="margin: 0;">B N C</h1> <p style="margin: 0;"><b>Experimental Report</b></p>	<i>Experiment title</i> <b>B in Silicon raw materials for solar cell industry</b>	<i>Instrument</i> NIPS
	<i>Principal proposer:</i> Undisclosed industrial partner <i>Experimental team:</i> László Szentmiklósi, Tamás Belgya	<i>Local contact</i> L. Szentmiklósi

## Objectives

to determine the boron content in solar cell raw materials

## Results

As a part of an exploratory study, the capabilities of the prompt gamma activation analysis technique was benchmarked for use in the on-line analysis of the material feed during the manufacturing process.

We have measured several samples representing key points of the process. About 2–3 g of samples, in a form of 10×10×10 mm<sup>3</sup> cubes or powders were analyzed. The latter type was first heat-sealed in fluorinated ethylene propylene (FEP) foils with the sizes of about 20×20 mm<sup>2</sup>. The background from carbon and fluorine (Teflon) and other structural materials (Al, Fe, Pb) were subtracted from the compositions.

As the major prompt-gamma peaks of silicon reached the area of a million, even the Si peaks with low relative intensities became significant. One of these lines appears on the top of the boron peak, at the energy of 477.13 keV. The net peak area of the boron was determined with an advanced peak fitting method.

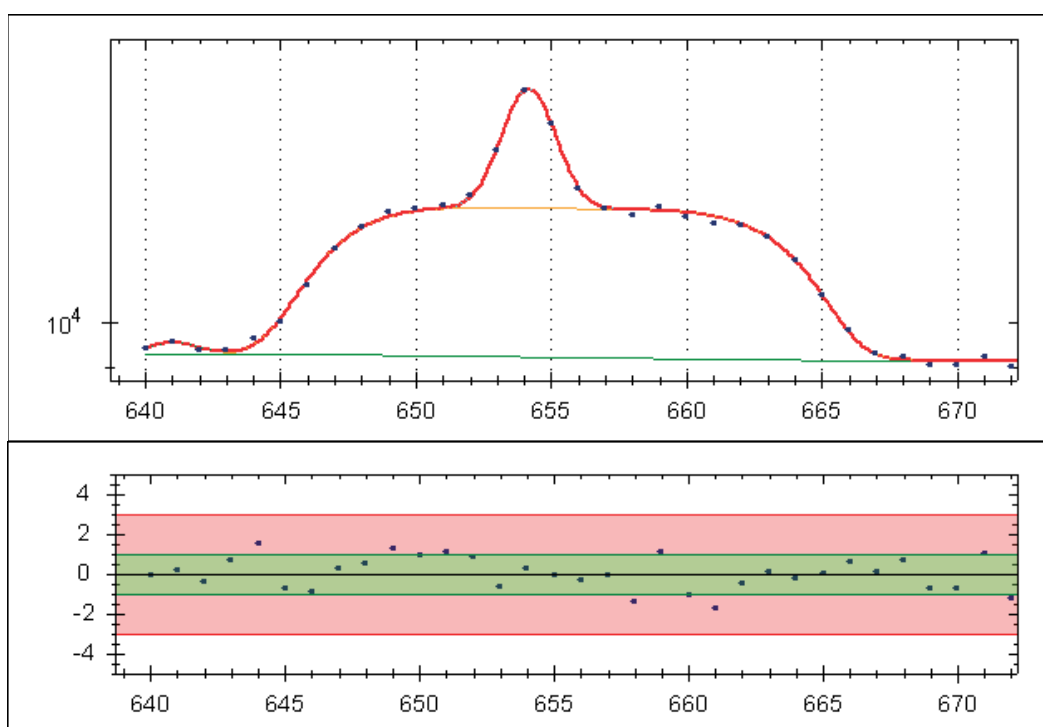


Figure 1. The fit of the Boron peak together with an interference line from the main component Silicon. The horizontal axis is the channel number. The Chi-square of the fit was  $1.11 \pm 0.29$ . The lower panel shows the residuals.

As a result, 0.28 ppm of B could already be quantified with an uncertainty of 6% at our facility, but this is not yet feasible at an industrial production site.

<b>B N C</b> <b>Experimental Report</b>	<i>Experiment title</i> <b>Compositions of Ni-Mo catalysts</b>	<i>Instrument.</i> NIPS <i>Local contact</i> Tamás Belgya
	<i>Principal proposer:</i> Tamás Ollár, Pál Tétényi II-HAS <i>Experimental team:</i> Tamás Belgya	<i>Experiment Number</i> NIPS_11_06_IH <i>Date</i> 2011.05.05

## Objectives

To measure number of atom ratios in five Ni-Mo catalyst samples.

## Results

The measurements were performed at the NIPS station with less than 10% accuracy for the Ni-Mo samples utilizing the comparator formula for PGAA [1]:

$$\frac{n_X}{n_C} = \frac{A_{X,\gamma} \sigma_{C,\gamma} \epsilon(E_{C,\gamma}) f(E_{C,\gamma})}{A_{C,\gamma} \sigma_{X,\gamma} \epsilon(E_{X,\gamma}) f(E_{X,\gamma})}$$

where  $n$  is the number of atoms,  $A$  is the measured peak area,  $\sigma$  is the partial gamma-ray production cross section for the characteristic gamma-ray with an energy of  $E$  of the element,  $\epsilon$  is the gamma-ray efficiency of the detector and the factor  $f(E)$  takes into the account the neutron and the gamma attenuation in the target. The index  $X$  is for the unknown and  $C$  is for the comparator.

The table below summarizes the results obtained for the samples.

	# of atom ratio			rel.unc%	rel.unc%	rel.unc%
	Ni/Al	Mo/Al	Ni/Mo	Ni/Al	Mo/Al	Ni/Mo
Ni	6.04%	<0.02%	>28981%	4.2	10.5	10.6
NiMo15	0.91%	5.48%	16.57%	5.3	4.2	5.9
NiMo35	0.84%	5.56%	15.04%	6.1	4.4	6.6
NiMo60	3.82%	6.70%	57.01%	7.2	6.0	7.5
Mo	<0.06%	6.33%	<0.91%	12.7	5.1	12.9

It can be seen from the table that except from the NiMo35 sample, the nominal Ni-Mo ratios (the number after NiMo shows the intended NiMo ratio in percentage) are in agreement with the expected values.

This experiment was supported by the NAP VENEUS OMFB 00186/2006 projects.

## Reference

1. Révay, Zs., Anal. Chem. **81**, (2009), 6851–6859.

<h1 style="margin: 0;">B N C</h1> <p style="margin: 0;"><b>Experimental Report</b></p>	<i>Experiment title</i> <b>Measurement of neutron distribution of the PGAA cold-neutron beam</b>	<i>Instrument.</i> PGAA <i>Local contact</i> Tamás Belgya
	<i>Principal proposer:</i> Tamás Belgya <i>Experimental team:</i> Tamás Belgya, László Szentmiklósi, Zoltán Kis	<i>Experiment Number</i> NIPS_11_07_IH <i>Date</i> 2011.04.05- 2011.04.08

## Objectives

Due to the changes in the neutron guide it was timely to repeat the neutron beam characterization using detailed time-of-flight (TOF) experiments.

## Results

The experiments have been performed using a 2D Position Sensitive Neutron Detector (PSND). The PSND detector and the acquisition system [1] were provided by the Neutron Optics Department of Research Institute for Solid State Physics and Optic, HAS. For the TOF experiments a flight path of 190 cm was used from the chopper blade rotated at 1250 rpm. The dwell time of the acquisition system was set to 5  $\mu$ s and the 2D positions were collected in 2048 channels. This made up a 256x256x2048 matrix with a position resolution of about 0.7 mm. The time of flight spectrum was calibrated with BeO and graphite Bragg filters for wavelength. The obtained 3D matrix is shown in Figure below. Details of the experimental results can be found in Ref. [2].

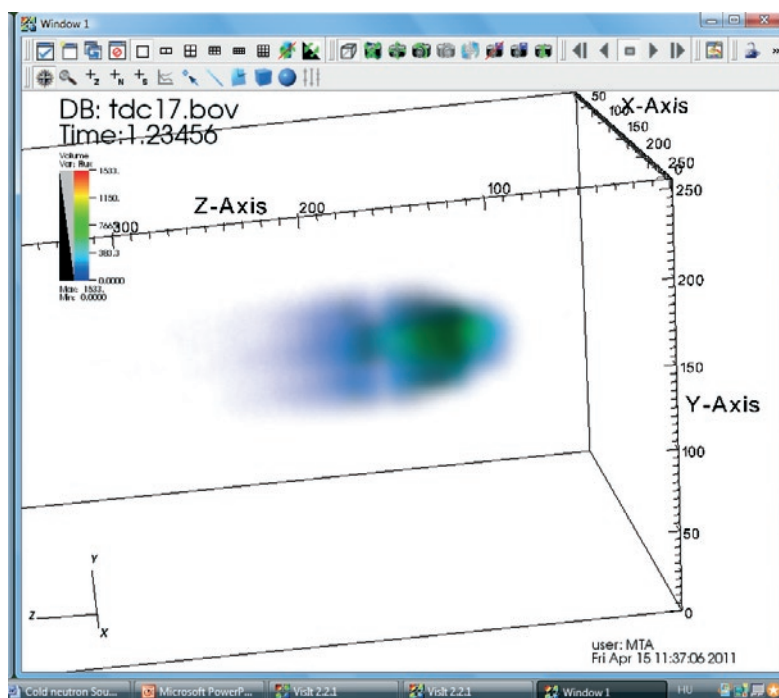


**Figure:** The 4D representation of the X-Y-T(Z axis on the figure) TOF matrix. The coloring codes the number of neutron counts analyzed by the 2D PSND at a given flight time T. The figure was made by the help of the VisIt 2.2.1 program.

This experiment was supported by the NAP VENEUS OMF0186/2006 projects.

## Reference

1. Füzi, J., Nucl Instrum. and Methods **A** 586 (2008) 41-45.
2. T. Belgya, L. Szentmiklósi, Z. Kis, Report on Consultant's meeting on Neutron sources spectra for EXFOR, INDC(NDS) 05-90, IAEA, 2011

<h1 style="margin: 0;">B N C</h1> <p style="margin: 0;"><b>Experimental Report</b></p>	<i>Experiment title</i> <b>Measurement of delayed neutrons from <math>^{235}\text{U}</math> produced by cold neutron interrogation</b>	<i>Instrument</i> NIPS
	<i>Local contact</i> L. Szentmiklósi	<i>Experiment Number</i>  <i>Date</i> 04.26.2011-04.30.2011
<i>Principal proposer:</i> Lakosi László – Institute of Isotopes <i>Experimental team:</i> Hlavathy Zoltán, Szentmiklósi László, Mesterházi Dávid – Institute of Isotopes		

## Objectives

to investigate the applicability of a cold neutron beam as an interrogating tool for quantifying small amounts of fissile material

## Results

The measurement of delayed neutrons for revealing fissile material is a well-established method. However, the use of cold neutrons opens up perspectives due to the high flux and the larger cross section. The beam at NIPS was modulated either by a revolving disk chopper or a linear beam shutter. Considering the half-lives of the nuclei emitting delayed neutrons (0.18 to 55 s) we chose a chopper speed of 275 rpm for the time scale up to 40 ms, whereas the beam shutter was programmed for being open for 15 seconds and being closed for 10 seconds. The neutrons emitted during the closed-beam phase were detected by a neutron collar equipped with 18  $^3\text{He}$  filled tubes. It was mounted at the flight tube in a horizontal arrangement. It had a though hole allowing the neutrons to pass through, before they reached the beam dump placed downstream. The inside of the collar was lined with Cd to absorb the scattered slow neutrons. The sample was fixed to the end of the beam guide, at the middle of the setup. The pulses were processed by a multichannel scaler. The signal characterizing the fissile-material content of the sample is obtained by integrating the delayed-neutron signal during the closed-beam periods. In this study uranyl-acetate powder with natural isotopic composition was measured with mass up to 200 mg, i.e. with  $^{235}\text{U}$  content up to 791  $\mu\text{g}$ . The presence of 28 mg uranyl-cetate (equivalent to 111  $\mu\text{g}$   $^{235}\text{U}$ ) could be proven.

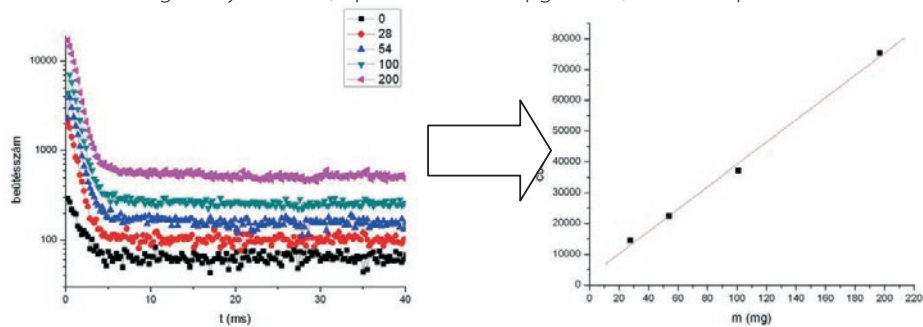
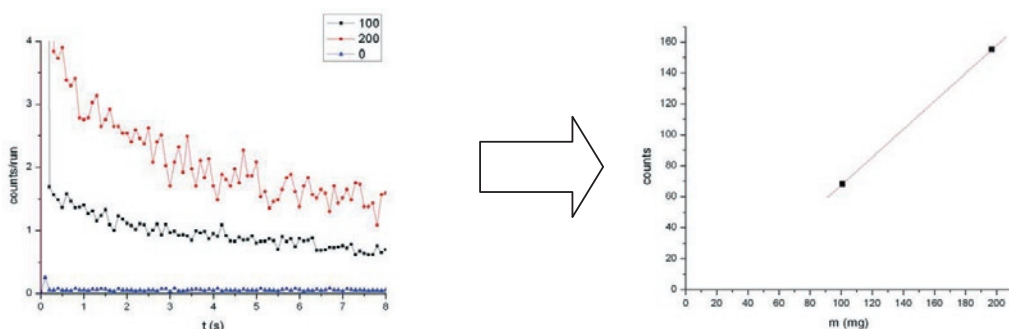


Figure 1-2: 50 000 runs at chopper speed of 275 rpm were recorded in 3000 sec. The curves were integrated from 6 to 40 ms, the blank background was removed and the results were plotted on the right hand side.



Figures 3-4: The beam shutter was open for 15 sec and closed for 10 seconds. 37 and 220 runs were recorded for 100 mg and blank samples and for 200 mg sample resp. The records were normalized for one run, integrated from 0.3 to 7.7 sec and the result was plotted on the right hand side.

## References

- [1] Hlavathy Zoltán, Szentmiklósi László, Bagi János, Nguyen Cong Tam, Serf Egyed, Lakosi László: OAH-ÁNI-ABA-12/10 report
- [2] Hlavathy Zoltán, Szentmiklósi László, Bagi János, Serf Egyed, Lakosi László, Mesterházy Dávid: OAH-ÁNI-ABA-04/11 report

<h1 style="margin: 0;">B N C</h1> <p style="margin: 0;"><b>Experimental Report</b></p>	<i>Experiment title</i> <b>Active neutron multiplicity counting with guided cold neutrons</b>	<i>Instrument</i> NIPS
	<i>Local contact</i> L. Szentmiklósi	<i>Experiment Number</i> BRR-262 <i>Date</i> 04.26.2011-04.30.2011
<i>Principal proposer:</i> Bagi János – EC JRC ISPC, Ispra Italy <i>Experimental team:</i> Bagi János, Hlavathy Zoltán, Szentmiklósi László – Institute of Isotopes		

## Objectives

This is a continuation of the previous proposal (BRR-236) to establish a new safeguards method, in-beam neutron coincidence counting.

## Results

During the last year, there has been an ongoing development of the methodology and data evaluation in order to optimize a new method, in-beam neutron coincidence counting. This time a neutron collar (Canberra JCC-13) with higher counting efficiency (about 35%, instead of the former detector with 10%) was used and an optimized Cd-lining was applied to achieve lower neutron background. As the square root of the efficiency determines the sensitivity, a much better signal-to-noise ratio could be achieved.

By optimizing the experiments, lower and lower amounts of U-235 could be quantified in the subsequent measurement series. It was studied if the powder and liquid samples indeed give the same response for the same amounts of fissile material, proving the matrix-independence of the method this way.

Sample	Uranium mass (mg)	U-235 content(µg)	S (cps)	D (cps)
Uc30	0.03	0.2133	135±1	0.12±0.01
Uc50	0.05	0.3555	492±1	0.16±0.04
Uc70	0.07	0.4977	116±1	0.22±0.02
Uc100	0.1	0.711	463±1	0.30±0.03
Uc150	0.15	1.0665	118±1	0.51±0.02
Uc500	0.5	3.55	384±1	1.29±0.15
Uc1000	1	7.11	583±1	2.6±0.2
Uc5000	5	35.55	711±1	12.1±0.1
Uc10000	10	71.1	973±1	25.1±0.5

Table 1. Singles and Doubles count rates for liquid samples

Sample	Total mass (mg)	Uranium mass (mg)	U-235 content (µg)	S (cps)	D (cps)	T (cps)
Up0011	1.1	0.62	4.42	25.4±0.2	1.2±0.03	0.05±0.03
Up0020	2	1.13	8.04	43.0±0.3	3.99±0.06	0.30±0.06
Up0051	5.1	2.88	20.5	152.3±0.4	9.44±0.14	0.24±0.13
Up0129	12.9	7.29	51.8	526.1±0.9	31.8±0.4	1.1±0.4
Up0277	27.7	15.66	111.3	1061.4±1.2	61.2±0.6	1.8±0.7
Up0540	54	30.52	217.0	1986.1±1.6	111.5±1.0	3.0±1.3
Up1009	100.9	57.0	405.5	3831.2±2.1	218.2±1.7	8.0±2.7
Up1969	196.9	111.3	791.3	7947.6±3.0	446.6±3.4	13.7±7.7

Table 2. Singles, Doubles and Triples count rates for powder samples

The results in Table 1 prove that with the new setup a detection limit as low as 0.2 g could be achieved.

## References

J. Bagi; L. Szentmiklosi; Z. Hlavathy, Detection of fissile material using cold neutron interrogation combined with neutron coincidence counting, accepted for publication in Nucl. Instr. Meth B.

<b>B N C</b> <b>Experimental Report</b>	<i>Experiment title</i> <b>Neutron capture of enriched Er, Eu, W isotopes with LeGe detector</b>	<i>Instrument</i> NIPS
	<i>Principal proposer:</i> Shamsu Basunia, Richard B. Firestone – Lawrence Berkeley National Laboratory, CA, USA <i>Experimental team:</i> László Szentmiklósi, Shamsu Basunia	<i>Local contact</i> L. Szentmiklósi

## Objectives

To determine low-energy transitions of enriched rare earth and tungsten isotopes.

## Results

Traditionally, HPGe (high-purity germanium) detectors with few hundred cm<sup>3</sup> volumes are applied in prompt gamma activation analysis in order to have sufficient efficiency even at 12 MeV. These detectors, however, have only about 1.6-1.7 keV resolution at low energies and the lower threshold level is usually set at about 40-60 keV. This makes difficult or even impossible to resolve the complicated multiplets in the <200 keV region of heavy elements. One way to reduce the complexity of the spectrum is the use of enriched isotopes. In collaboration with Lawrence Berkeley National Laboratory (LBNL), we managed to obtain highly enriched of isotopes of Eu-151, Eu-153, and Er-167 and W-186. The other way is to achieve better energy resolution. This is made possible with the use of a LeGe (low-energy germanium) detector.

The usual PGAA measurements on natural oxides of Eu, Er were and the above mentioned isotopes were completed in an earlier run. This time the aim was to collect more detailed information about the first few-hundred keV range of the spectra. Delayed gamma spectra were also collected to identify the lines originating from radioactive decay.

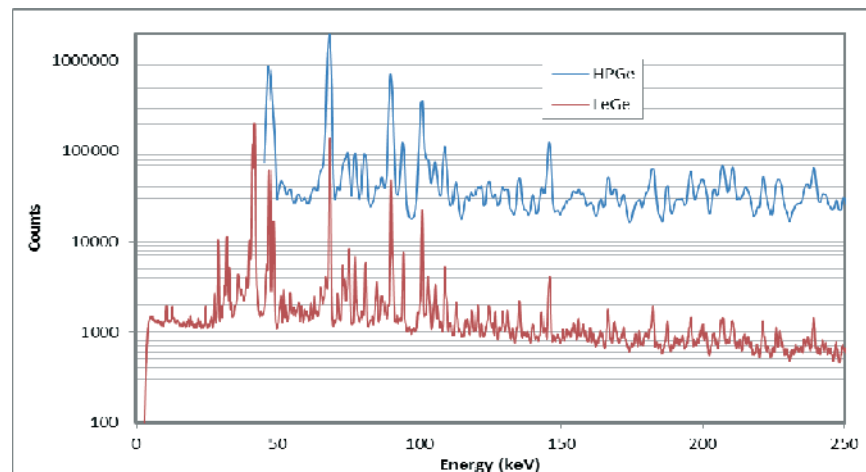


Figure 1. The comparison of the Eu-153 spectra taken with conventional HPGe and LeGe detectors. Note the sharper peaks in the LeGe spectrum due to the superior energy resolution.

The data analysis is still ongoing at LBNL. The determined energies and intensities serve as input to level scheme and cross-section calculations with the program DICEBOX [1-2]. Preliminary results show that the low energy transitions play an important role in achieving correct intensity balances.

## References

1. F. Becvár, Nucl. Instrum. Methods A **417**, 434 (1998).
2. F. Becvár, Statistical gamma Cascades Following Thermal and keV Neutron Capture in Heavy Nuclei. in S. Wender, ed., Gamma-Ray Spectroscopy and Related Topics. American Institute of Physics, New York (2000), 504.



<h1 style="text-align: center;">B N C</h1> <p style="text-align: center;"><b>Experimental Report</b></p>	<i>Experiment title</i> <b>Installation, tuning and testing of the NORMA imaging instrument</b>	<i>Instrument</i> NIPS
	<i>Principal proposer:</i> Révay Zsolt – Institute of Isotopes <i>Experimental team:</i> Kis Zoltán, Szentmiklósi László, Belgya Tamás – Institute of Isotopes	<i>Local contact</i> Z. Kis

## Objectives

to install and carry out the first tests of a new and complex facility called NORMA for neutron imaging coupled to prompt-gamma activation analysis

## Results

There are several separate PGAA and neutron radiography (or tomography) facilities at neutron research centers worldwide, however, there are no integrated setups offering both features at the same time and same instrument. Having set up NORMA makes possible the visualization of the structure and the elemental analysis of the inner part of the object without using two separate facilities. A neutron beam is well applicable to produce the radiographic (2D) and tomographic (3D) image of an object, and the interesting parts could be positioned into a collimated neutron beam to determine their elemental composition with PGAA.

During the installation the components were aligned to each other and the main parameters of the system were measured. As a fine tuning the verticality and horizontality, and the precision of the movements of the system were checked and adjusted. Then the spatial resolution and the L/D ratio (a measure of the beam divergence), the two most important parameters of an imaging facility were measured. A freshly cut Gd-stripe of 0.25 mm in thickness was positioned at different distances to the scintillator screen, and the edge spread function of the projection was evaluated to obtain the spatial resolution at that distance (see Fig. 1a). The inverse of the fitted straight line's slope yields the L/D ratio, of which value is 211. This value is higher than it is expected for a guided beam with a  $2\Theta$  supermirror guide ( $L/D \approx 24$ ), which should be later explained by Monte Carlo simulation of the beam with the given energy distribution. The best available spatial resolution is given if the Gd-stripe is positioned directly on the screen. The measured value of 0.37 mm was worse than previously anticipated. It needs further fine tuning of the optical system to reach the planned value of  $0.2 \pm 0.05$  mm, which work is still in progress.

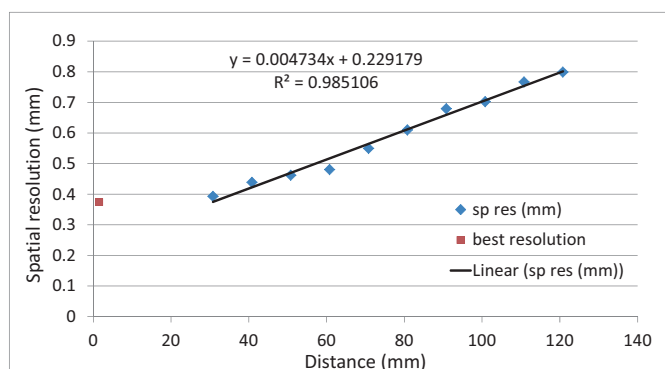


Figure 1: Spatial resolution as a function of the distance to the scintillator screen.

<h1 style="margin: 0;">B N C</h1> <p style="margin: 0;"><b>Experimental Report</b></p>	<i>Experiment title</i> <b>Optimization of the NIPS Compton suppressor</b>	<i>Instrument</i> NIPS
	<i>Principal proposer:</i> Tamás Belgya – Institute of Isotopes <i>Experimental team:</i> László Szentmiklósi, Tamás Belgya, Zoltán Kis, – Institute of Isotopes	<i>Local contact</i> L. Szentmiklósi

## Objectives

to install a Compton-suppressed gamma spectrometer at the NIPS facility

## Results

An important aspect of the ongoing upgrade at the Budapest PGAA-NIPS facility has been the design and installation of a second Compton suppressed gamma spectrometer. This was aimed at providing better spectroscopic conditions for future position sensitive and large sample prompt gamma activation analysis applications. The optimum geometry of the setup was determined by Monte Carlo calculations with the MCNP CP code, as a trade-off between performance and cost.

Based on the above mentioned parameters the final design and the production of the detector were made by the Scionix, B.V. Netherlands. The installed detector works according to the specifications and can deliver the expected suppression factors.

Figure 1 shows the present status of the NIPS station, whereas Figure 2 compares the measured and calculated spectra of a Urea-D calibration sample.

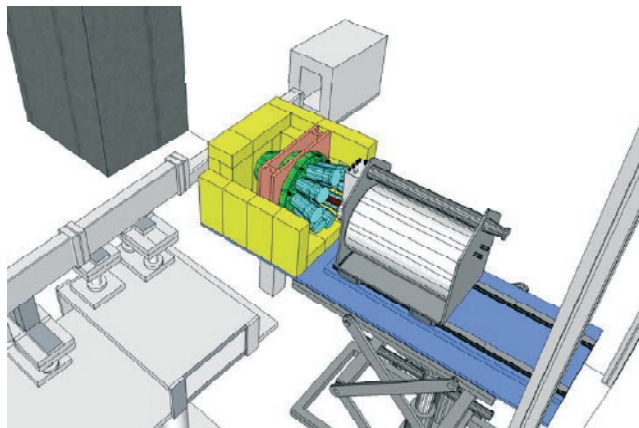


Figure 1. The sketch of the Compton-suppressed NIPS detector.

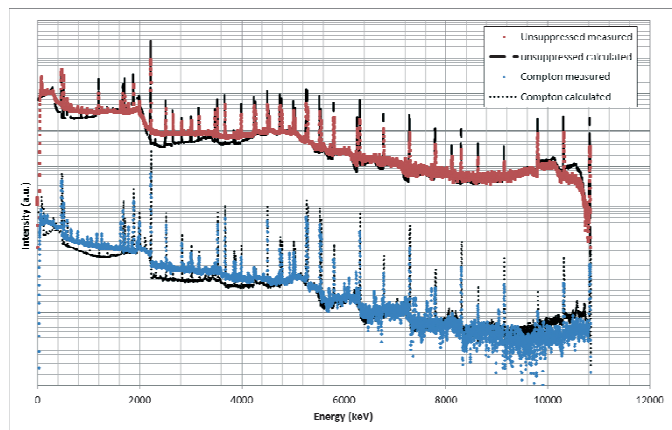


Figure 2. Measured and calculated spectra of a Urea-D calibration sample.

## Reference

L. Szentmiklósi, Z. Kis, T. Belgya, A.N. Berlizov: On the Design and Installation of a Compton-Suppressed HPGe Spectrometer at the Budapest Neutron-Induced Prompt gamma Spectroscopy (NIPS) facility, J Radioanal Nucl Chem. online first, DOI: 10.1007/s10967-013-2555-2

<h1 style="margin: 0;">B N C</h1> <p style="margin: 0;">Experimental Report</p>	<p><i>Experiment title</i></p> <p><b>Implementation of neutron tomography at NORMA imaging instrument</b></p>	<p><i>Instrument</i></p> <p>NIPS-NORMA</p> <p><i>Local contact</i></p> <p>Kis Zoltán</p>
	<p><i>Principal proposer:</i></p> <p>Kis Zoltan – Centre for Energy Research</p> <p><i>Experimental team:</i></p> <p>Kis Zoltán, Szentmiklósi László, Belgya Tamás – Centre for Energy Research</p>	<p><i>Experiment Number</i></p> <p>NIPS_12_13_IH</p> <p><i>Date</i></p> <p>2012.01.10- 2012.01.17</p>

## Objectives

to improve the spatial resolution and to carry out the first tomographic tests of NORMA

## Results

After having set up the NORMA imaging facility it makes possible the visualization of the structure of the inner part of objects using a neutron beam, which is well applicable to produce the radiographic (2D) and tomographic (3D) image.

Spatial resolution results from the very first installation showed that its improvement is necessary. After the fine tuning of the optical system the spatial resolution and the L/D ratio, the two most important parameters of an imaging facility were remeasured. A freshly cut Gd-stripe of 0.25 mm in thickness was positioned at different distances to the scintillator screen. The modulation transfer function (MTF) and the edge spread function (ESF) of the projections were evaluated to obtain the spatial resolution at various distances (see Fig. 1a-b). The inverse of the fitted straight line's slope yields the L/D ratio, of which value is 233. The best available spatial resolution is given if the Gd-stripe is positioned directly on the screen. The measured values (about 0.23 mm on the screen and about 0.45 mm at 84 mm distance to the screen) are close to what was previously anticipated.

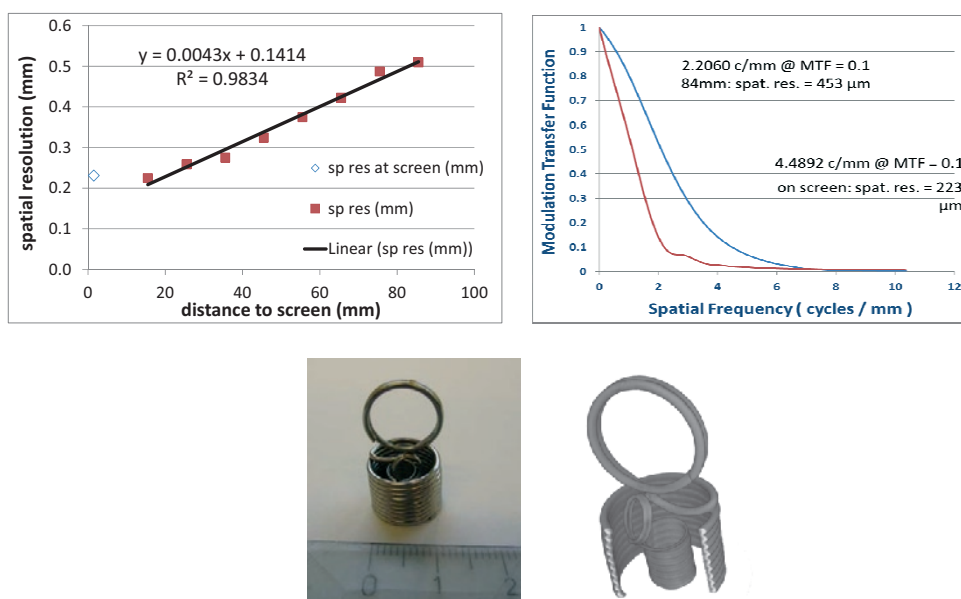


Figure 1a-b: Spatial resolution as a function of the distance to the scintillator screen based on ESF and MTF;

Figure 1c-d: photo and tomographic image of two springs (diameters: 12.7 mm, and 5.3 mm)

An important step of the setup is to be able to reconstruct tomographic images of objects. An example is shown in Fig. 1b-c, where the photo and 3D reconstruction of two tiny springs put into each other are shown.

<p style="text-align: center;"><b>B N C</b></p> <p style="text-align: center;"><b>Experimental Report</b></p>	<p><i>Experiment title</i>  <b>Mapping the fracture surface of ODS steels by neutron tomography and 3D visualization</b></p>	<p><i>Instrument</i>  NIPS  <i>Local contact</i>  László Szentmiklósi</p>
<p><i>Principal proposer:</i>  Ákos Horváth – Centre for Energy Research  <i>Experimental team:</i>  László Szentmiklósi, Zoltán Kis – Centre for Energy Research</p>		<p><i>Experiment Number</i>  NIPS_12_14_IH  <i>Date</i>  2012.01.18-  2012.01.19</p>

**Objectives**

to map the fracture surface of ODS steels by neutron tomography and 3D visualization

**Results**

The samples were casted in rectangular bars with 10x10 mm cross-section. After the tensile tests, the two halves of the steel bars were separately imaged in 3D at the NORMA experimental station. Three experimental alloys were investigated.

601 or 1201 projections were recorded per 180 degree rotation, and they were corrected with the beam- and dark images. The tomography reconstruction software Octopus was used to obtain the slices of the objects that were visualized with VG Studio 2.1 volume rendering program.

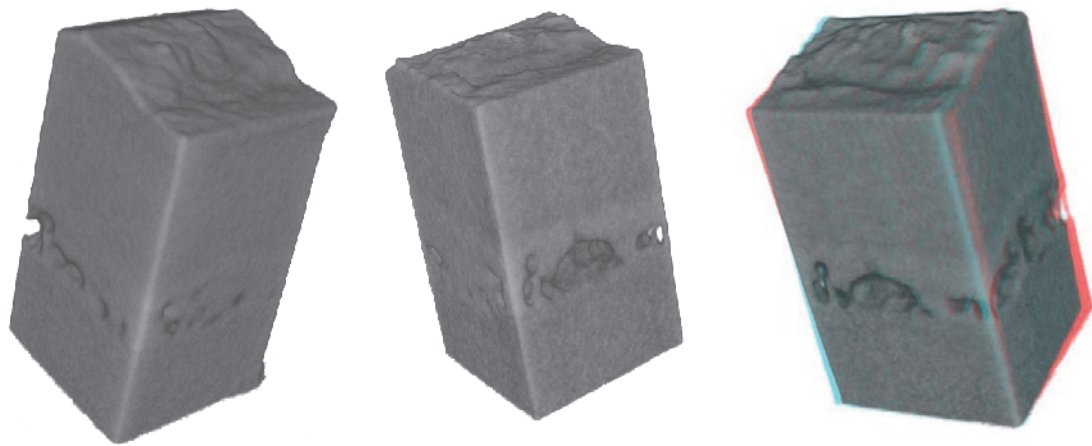


Figure 1. 3D visualization of selected tomographies. The picture to the right can be seen in 3D with appropriate glass

The raw data are available as a stack of TIFF images, and also in the form of a 3D matrix (RAW format). The numerical grayscale values have to be converted to a 3D mesh of nodes before mathematical analysis. This conversion is still in progress. A comparison to laser scan is also foreseen.

The developed methodology and the measured dataset can form the basis of modeling the behavior ODS steels under tensile stress.

<b>B N C</b> <b>Experimental Report</b>	<i>Experiment title</i> <b>Non-destructive characterization of <math>^{10}\text{B}</math> targets</b>	<i>Instrument</i> NIPS <i>Local contact</i> Kis Zoltán
	<i>Principal proposer:</i> Jan Heyse – EC-JRC-IRMM <i>Experimental team:</i> Kis Zoltán, Szentmiklósi László, Belgya Tamás – Centre for Energy Research	<i>Experiment Number</i> NIPS_12_15_IC <i>Date</i> 2012.02.14- 2012.02.23

## Objectives

to characterize the total amount of  $^{10}\text{B}$  and the areal density profile of boron coated reference disks

## Results

The neutron induced  $^{10}\text{B}(n,\alpha)$  reaction is widely used as a reference standard for neutron induced reaction cross section measurements. The flux monitors developed at EU JRC IRMM (Geel, Belgium) institute were investigated by PGAI techniques. The sample was a stainless steel backing ( $\varnothing 50$  mm) with a boron layer ( $\varnothing 38$  mm), having a nominal thickness of  $30 \mu\text{g}/\text{cm}^2$ . The projection of the  $2.50 \times 5 \text{ mm}^2$  collimated neutron beam was  $5 \times 5 \text{ mm}^2$  on the surface of the sample, as its plane was set in  $30^\circ$  relative to the beam. The aim of the project was to characterize  $^{10}\text{B}$  layers by the detection of gamma-rays emitted after the  $^{10}\text{B}(n,\alpha)\gamma$  reaction at one of the BNC's cold neutron guides. There were two sets of layers, one with an aluminum backing and one with a stainless steel backing. Both sets were characterized for total amount of  $^{10}\text{B}$  and a sample of each set was characterized for the areal density profile.

Having known the production process it was presumed that the layer thickness changes along the radius. Therefore, a scanning along the diameter of the disk was carried out in 7 spots (see Fig. 1.). To reach the statistical uncertainty of 0.25%, the acquisition time at each irradiated spot was 18000 sec. According to the results, the original assumption was proven. The thickness of the boron layer is decreasing radially from the middle point to the perimeter. The change was 1.5%. The total amount of the boron could be determined based on this result taking into consideration both the detection efficiency measurements performed with Co and Eu samples, and the background determined experimentally with open beam, empty target frame and empty backing. The importance of this measurement is that due to the lack of availability of  $^3\text{He}$ , the future neutron detectors will apply surfaces covered with boron layers.

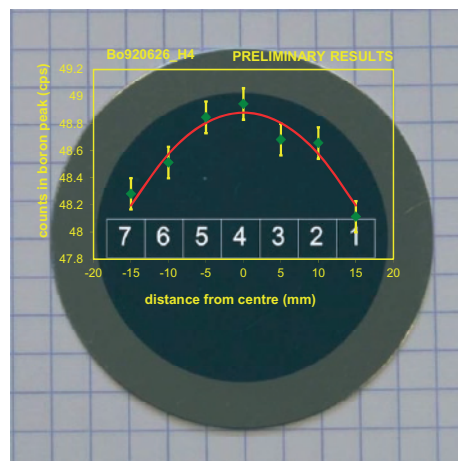


Figure 1: Scanning the  $^{10}\text{B}$  areal density profile for IRMM flux monitor

<b>B N C</b> <b>Experimental Report</b>	<i>Experiment title</i> <b>Characterization of supermirror guides by neutron radiography technique</b>	<i>Instrument</i> NIPS-NORMA <i>Local contact</i> Kis Zoltán
	<i>Principal proposer:</i> Miskolczi Tibor – Mirrotron Kft. <i>Experimental team:</i> Kis Zoltán, Szentmiklósi László, Belgya Tamás – Centre for Energy Research	<i>Experiment Number</i> NIPS_12_16_IH <i>Date</i> 2012.02.14- 2012.02.23

### Objectives

to prove the ability that the total reflection of the neutron guide surface using neutron radiography technique could be characterized

### Results

Pilot studies were carried out on supermirrors ( $m=2.5$ ) produced by the Mirrotron Ltd. to characterize the total reflection angle of their surface. Series of neutron radiography images were taken at several positions during the rotation of the object. The object was firstly positioned parallel to the beam, and then is rotated between  $-5.25^\circ - 5.25^\circ$  in  $0.075^\circ$  steps. Altogether 140 images were acquired for each mirror, separately. A neutron collimator of  $2 \times 20 \text{ mm}^2$  (WxH) was used to irradiate only the reflection surface of the mirrors.

We were able to prove that the position of the reflected neutron beam could be recorded in the function of the rotation angle. In certain conditions the change of the intensity of the reflected beam according to the rotational angle could be measured as an average gray value of a region of interest, which is covered by the reflected beam.

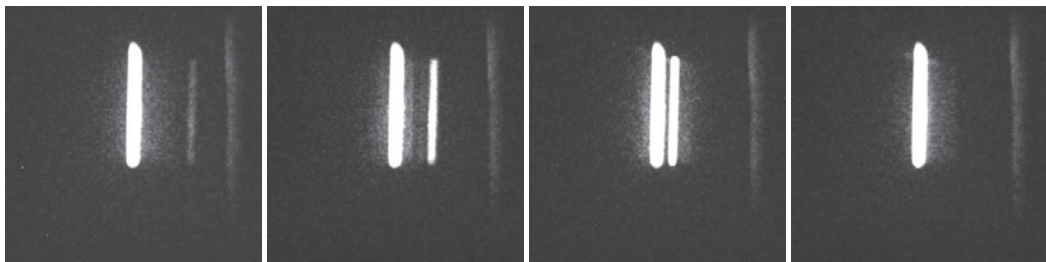


Figure 1: Some example image from a series taken for the mirror No. 040520\_A5 (1:  $-5,25^\circ$ , 2:  $-3,375^\circ$ , 3:  $-1,5^\circ$ , 4:  $0^\circ$ ).

<h1 style="margin: 0;">B N C</h1> <p style="margin: 0;"><b>Experimental Report</b></p>	<i>Experiment title</i> <b>Quality assessment for neutron imaging and computed tomography (CT)</b>	<i>Instrument</i> NIPS-NORMA <i>Local contact</i> Kis Zoltán
	<i>Principal proposer:</i> Anders Kaestner and Eberhard Lehmann – PSI, Switzerland <i>Experimental team:</i> Kis Zoltán, Szentmiklósi László – Centre for Energy Research	<i>Experiment Number</i> NIPS_12_17_IC <i>Date</i> 2012.04.17- 2012.04.27

## Objectives

to take part in the initiative of IAEA and PSI, Switzerland to measure the neutron computed tomography performance of neutron imaging beamlines

## Results

For X-ray tomography, driven by medical imaging, there are quality assessment methods developed and available to certify the quality of the delivered images. This is not the case for neutron tomography therefore IAEA and PSI initiated a set of test bodies to evaluate the performance of neutron computed tomography. We took part in this round robin test as one of the ten laboratories worldwide. The method included measurements on three different QA phantoms and aimed at measuring the ability of detecting different contrasts and the resolution of reconstructed CT slices from a neutron imaging instrument. One sample was intended for contrast samples evaluation while the other two are for resolution measurements. The resolution samples handled the cases of resolution with negative and positive contrast. This approach was a first step into the direction of creating a quality assessment (QA) routine for neutron tomography.

The purpose of the contrast sample was to show the variation in reconstructed neutron attenuation coefficients for different materials. The original sample design contained the following materials: Sample body, Al, and insets rods of Pb, PE, Fe, Ni, Al, and Cu. The most important finding was that the PE is attenuating the beam so much that the remaining intensity is insufficient for a correct reconstruction of the projection data as it can be seen in Fig 1a. These so-called starvation artefacts occurred mainly in combinations of PE and Fe, Cu, and Ni.

The purpose of the resolution sample was to determine the thinnest feature that can be detected with the resolution provided by the current imaging configuration. The resolution samples consisted of two blocks that were assembled with two screws. The gap between the two blocks was used to insert a thin contrast feature (a number of Al or Cu foils to provide the positive or negative contrast). The sample profile in all cases but one are clearly cupped. This is an expected result since it is caused by the scattered neutrons. In the case of Hungary, the profile is very flat which could be explained by the fact that the beam comes from a guide with cold neutrons. The width of the slit was estimated as 0.62 mm. This deviates from the true value only with 3.33%.

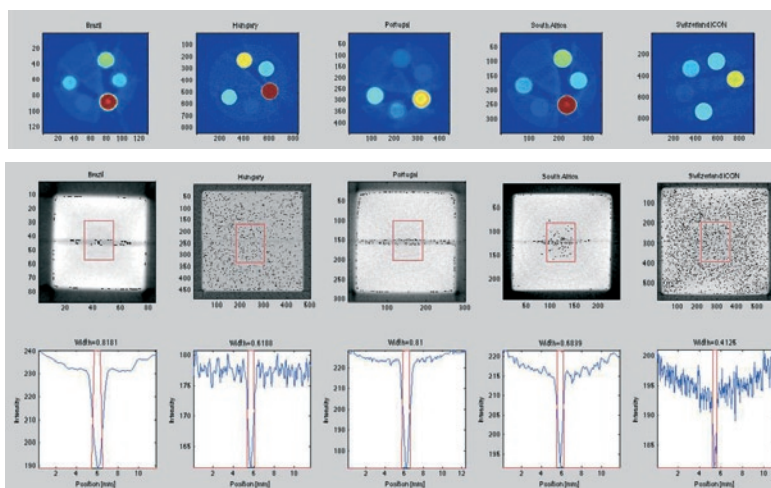


Figure 1a: Contrast images returned from five different facilities. The slice from ICON, Switzerland was measured using a revised sample with Ti replacing PE; 1b: Slice images of the resolution sample returned from five different facilities. The profile plots are averaged in the red box marked in each slice.

<b>B N C</b> <b>Experimental Report</b>	<i>Experiment title</i> <b>Design and installation of the gamma shielding at the NIPS experimental station</b>	<i>Instrument</i> NIPS <i>Local contact</i> László Szentmiklósi
	<i>Principal proposer:</i> László Szentmiklósi, Zoltán Kis <i>Experimental team:</i> László Szentmiklósi, Zoltán Kis – Centre for Energy Research	<i>Experiment Number</i> PGAA_12_18_IH <i>Date</i> 2012

## Objectives

to upgrade the shielding of the NIPS Compton-suppressed HPGe detector

## Results

An important aspect of the ongoing upgrade at the Budapest PGAA-NIPS facility has been the design and installation of a second Compton-suppressed gamma spectrometer. The aim was to provide excellent spectroscopic conditions for future position-sensitive and large-sample prompt gamma activation analysis applications.

The optimum geometry of the suppressor and the shielding was determined by Monte Carlo calculations with the MCNP-CP code. Both the suppressed and unsuppressed spectra were generated from the same run into 1-keV wide energy bins; and the suppression ratios, i.e. the ratio of counts in the suppressed vs. unsuppressed spectra were calculated. The comparison was done at energies of 500 keV, 2223 keV, 4000 keV, 6000 keV, 8000 keV and 10000 keV.

Based on the above mentioned results the final design and the production of the BGO detector were made by the Scionix, B.V. Netherlands. The delivered BGO suppressor was mounted onto a solid Al frame, whose dimensions were determined to exactly fit into the lead shielding made of lead bricks. The thickness of the lead is 10 cm all around, except for the rear side, where it is only 5 cm due to geometrical limitations (Figure 4 b). The gross weight of the lead is 996 kg. The HPGe detector can be pushed back from the measurement position for maintenance on a trolley.

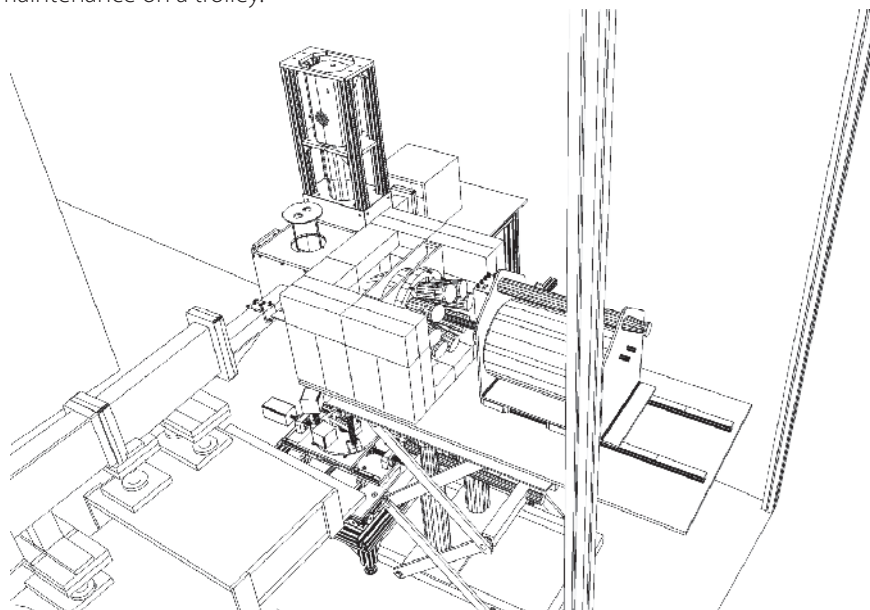


Figure 1. The layout of the NIPS-NORMA experimental station after completion of gamma shielding and installation of the BGO Compton suppressor (the top and rear lead layers were made transparent to reveal the internal details)

## Reference

1. L. Szentmiklósi, Z. Kis, T. Belgya, A.N. Berlizov: On the Design and Installation of a Compton Suppressed HPGe Spectrometer at the Budapest Neutron-Induced Prompt gamma Spectroscopy (NIPS) facility, J Radioanal Nucl Chem. online first, DOI: 10.1007/s10967-013-2555-2



<h1 style="margin: 0;">B N C</h1> <p style="margin: 0;"><b>Experimental Report</b></p>	<i>Experiment title</i> <b>Tomography with the Compton-camera concept</b>	<i>Instrument</i> NIPS <i>Local contact</i> László Szentmiklósi
	<i>Principal proposer:</i> Dávid Légrády, Tímea Hülber – Budapest University of Technology and Economics <i>Experimental team:</i> László Szentmiklósi, Zoltán Kis – Centre for Energy Research	<i>Experiment Number</i> NIPS_12_20_IH <i>Date</i> 2012.

**Objectives**

To investigate the idea of combining prompt-gamma neutron activation analysis and gamma detection with Compton-camera concept

**Results**

The electric collimation is based on two position- and energy-sensitive detectors as a detector system. A photon is Compton scattered in the first detector and afterwards absorbed in the second one. From the released energies and the interaction positions the emitting place of the photon can be determined with an uncertainty of a conical surface.

We used two miniPET detectors produced by the Institute of Nuclear Research, Debrecen. It contains a matrix of LYSO (lutetium-yttrium-orthosilicate) crystal pins coupled to a position-sensitive photomultiplier tube (PSPMT). Dedicated data acquisition software was written and combined with stepping motor moving. This made the whole system to be capable of executing gamma tomography.

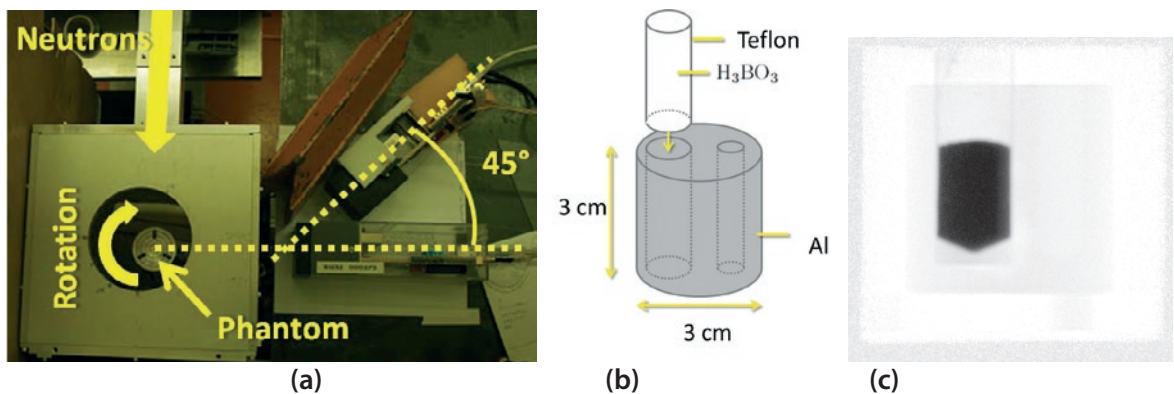


Figure 1. Measurement set-up, the Aluminum phantom with boric acid in a Teflon vial and the neutron transmission image taken with the NORMA CCD camera

A custom software was made using C# in order to handle all of the steps from data acquisition to coincidence sorting.

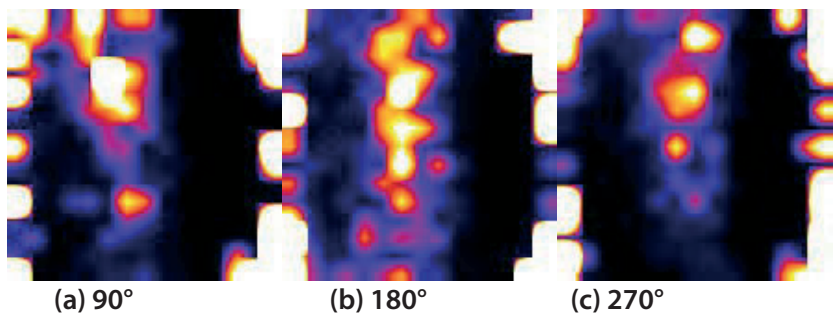


Figure 2: Boron data reconstructions of three projections with different angles relative to the neutron beam direction

**Reference**

Tímea Hülber: Transmission, emission and excitation gamma tomography, Master's Thesis, Budapest University of Technology and Economics, Institute of Nuclear Techniques, 2012

<b>B N C</b> <b>Experimental Report</b>	<i>Experiment title</i> <b>The use of neutron analysis techniques for detecting the concentration and distribution of chloride ions in archaeological iron</b>	<i>Instrument</i> NIPS-NORMA <i>Local contact</i> Kis Zoltán
	<i>Principal proposer:</i> David Watkinson, Melanie Rimmer – Cardiff University, UK <i>Experimental team:</i> Kis Zoltán, Szentmiklósi László – Centre for Energy Research	<i>Experiment Number</i> BRR_281 CH <i>Date</i> 2012.05.14- 2012.05.16

## Objectives

to analyse the distribution of Cl in archaeological iron objects

## Results

Chloride (Cl) ions diffuse into iron objects during burial and drive corrosion after excavation. Although the basic principles of this process are well-understood, information regarding the three-dimensional distribution of chloride ions within the object and its relationship to patterns of cracking and the development of corrosion behaviour is not currently available. This is due to the difficulty in analysing for chloride ions, which are located deep within the object under the corrosion layers, and are not accessible to surface analytical techniques such as X-ray fluorescence, X-ray diffraction and Raman spectroscopy without cross-sectioning of objects or removal of overlying corrosion. Neutron analysis offers non-destructive avenues for determining Cl content and distribution in objects.

A pilot study used Prompt Gamma Activation Imaging (PGAI) to analyse the longitudinal distribution of Cl in archaeological iron objects. High Cl areas were linked with visible damage to the corrosion layers and attack of the iron core. Neutron techniques have significant advantages in the analysis of archaeological metals including penetration depth and low detection limits. For the element analysis, the neutron beam was shaped to the desired size ( $3 \times 20 \text{ mm}^2$  area) with a collimator, to reach the optimal count rate of  $\gamma$ -photons. At present, elemental ratios can be determined with this technique, based on precise evaluation of a pair of peaks with similar energies. In this study, five objects were mounted vertically in a sample holder using Teflon strings, and the Cl/Fe ratios in the nails were analysed along the long axis, in steps of 3 mm (Fig. 1).

From these pilot results it could be assumed that areas of high Cl correspond with areas of remaining metal core, which are already attacked, and usually have visual corrosion phenomena, and areas in objects that are fully mineralised tend to have negligible Cl.

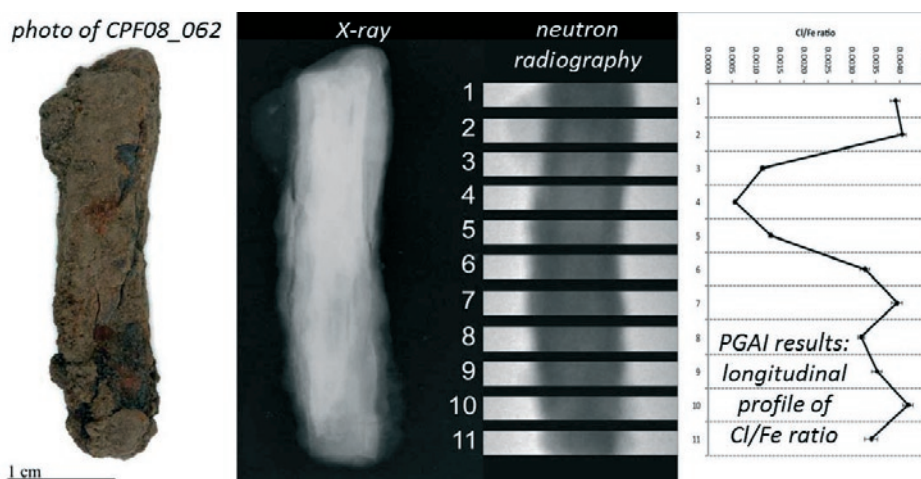


Figure 1: The photo, the X-ray image, the neutron radiography image and the Cl/Fe ratio from PGAI measurement of the object No. CPF08\_062.

<h1 style="margin: 0;">B N C</h1> <p style="margin: 0;">Experimental Report</p>	<i>Experiment title</i> <b>Brass and other copper alloys of the Meuse valley in the middle Ages: links between market and techniques</b>	<i>Instrument</i> : PGAA/NIPS <i>Local contact</i> Zsolt Kasztovszky
	<i>Principal proposer</i> : Nicolas Thomas - INRAP – Laboratoire de médiévisitque occidentale de Paris <i>Experimental team</i> : Nicolas Thomas, David Bourgarit – INRAP Laboratoire de médiévisitque occidentale de Paris	<i>Experiment Number</i> BRR 297 CH <i>Date</i> 2012.06.26-06.29.

## Objectives

The aim was to study the nature and the scale of the metal productions, by characterizing the ancient metallurgical processes and documenting the organization of workshops within their economic and social contexts using position sensitive PGAA and Neutron Radiography.

## Results

Four archaeological cauldrons were analysed. In addition, an experimental reconstruction of a cauldron was studied for comparison's sake. The comparison of metal composition between feet and body for a given cauldron will definitely answer the question whether the different parts have been cast separately or not. The experimental results are under evaluation yet.

Positioning and irradiation of the objects were carrying out using Gd markers, which can be very well seen in radiographic images (Fig.1).



Figure 1: a, Photo of a cauldron with Gd marker; b, Neutron radiography of one of the cauldron's legs with the Gd marker

		Cl	Cu	Zn	As	Ag	Cd	Sn	Sb	Nd	Au	Pb
		0.003	0.24	0.16	0.2	0.03	0.0004	0.5	0.9	0.002	0.07	1
C2RMF 68705	One of the legs	0.022	66.2			0.037		9.2	2.4			22
C2RMF 66689	Leg1	0.179	70.8		0.24	0.067	0.00050	6.8		0.0085		22
C2RMF 66689	Leg2, shorter measurement	0.018	63.1			0.050	0.00042	4.9				29
C2RMF 66689	Leg2, longer measurement	0.021	66.4			0.063	0.00055	5.1		0.0062		28
C2RMF 66689	body	0.032	62.2			0.256	0.00050	5.7	3.5	0.0100		28
C2RMF 66688	body	0.061	67.6	12.2		0.099	0.00369	3.2		0.0055		17
C2RMF 66688	Leg1, shorter measurement	0.023	64.8	14.4		0.127	0.00516	3.4				17
C2RMF 66688	Leg1, longer measurement	0.023	64.3	14.7		0.118	0.00515	3.3				17
C2RMF 66688	Leg2	0.015	65.2	14.1			0.00496	4.9		0.0087		16
C2RMF 66688	Bec	0.029	65.1	12.6		0.167	0.00513	6.4		0.0074		16
C2RMF 66688	Handle	0.029	67.7	15.5		0.032	0.0053	4.5				12
C2RMF CTIF6	Bronze standard, CTIF6		67.2	6.6	4.0	1.1	0.014	4.7	7.1		0.75	9

Table 1: Composition of the different parts of the cauldrons, measured by PGAA

## References

THOMAS N., BOURGARIT D., VERBEEK M., PLUMIER J., ASMUS B., « Commerce et techniques métallurgiques : les laitons mosans dans le marché européen au Moyen Âge (XIII<sup>e</sup>-XVI<sup>e</sup> siècles) », Actes du colloque international *L'archéologie au laboratoire*, organisé par l'Inrap, la Fondation EDF et Universcience, Cité des Sciences et de l'Industrie, Paris, 27-28 janvier 2012, Paris, La découverte, 2013, p. 169-182.

BOURGARIT D., THOMAS N., « Late Medieval copper alloying practices: a view from a Parisian workshop of the 14th century AD », *Journal of Archaeological Science*, 39, 10, 2012, p. 3052-3070.

<b>B N C</b> <b>Experimental Report</b>	<i>Experiment title</i> <b>Inspection of possible ceramic core residues in inner gas path of a turbine blade by neutron radiography techniques</b>	<i>Instrument</i> NIPS-NORMA <i>Local contact</i> Kis Zoltán
	<i>Principal proposer:</i> Málits József – Alcoa-Howmet Hungary Ltd. <i>Experimental team:</i> Balaskó Márton, Kis Zoltán, Horváth László, Szentmiklósi László – Centre for Energy Research	<i>Experiment Number</i> NIPS_12_23_IH <i>Date</i> 2012.09.05- 2012.09.14

## Objectives

to inspect possible ceramic core residues in inner gas path of a turbine blade by thermal and cold neutron radiography

## Results

Alcoa-Howmet Hungary is performing post cast operations of investment castings. The investment castings are cobalt and nickel-based superalloys for aerospace and industrial gas turbine blades and vanes. Depending on the design castings are solid or having an inner gas path. The investment casting technology uses embedded ceramic core in a wax phase to give gas path in a metal form. All parts are subject to a non-destructive testing such as penetrant- and X-ray inspection.

Due to a core residue, which at the time was not detectable with traditional X-ray technology, Alcoa Howmet contacted BNC, if there was a method to reveal core residue with other method. The trial was conducted on parts, which had evidence of core material on our X-ray films. BNC developed a technique to be able to visualize the residues. According to this method objects were immersed in a bath of cadmium sulphate solution so that possible residues could uptake some cadmium. Due to the initial cost of the gadolinium this method uses cadmium sulphate instead of gadolinium nitrate.

Pilot studies were carried out for four blades at the DNR and the NIPS-NORMA facilities using thermal and cold neutrons, respectively. We were able to prove that the position of the core residues can be detected by both kinds of the neutrons (Fig. 1).

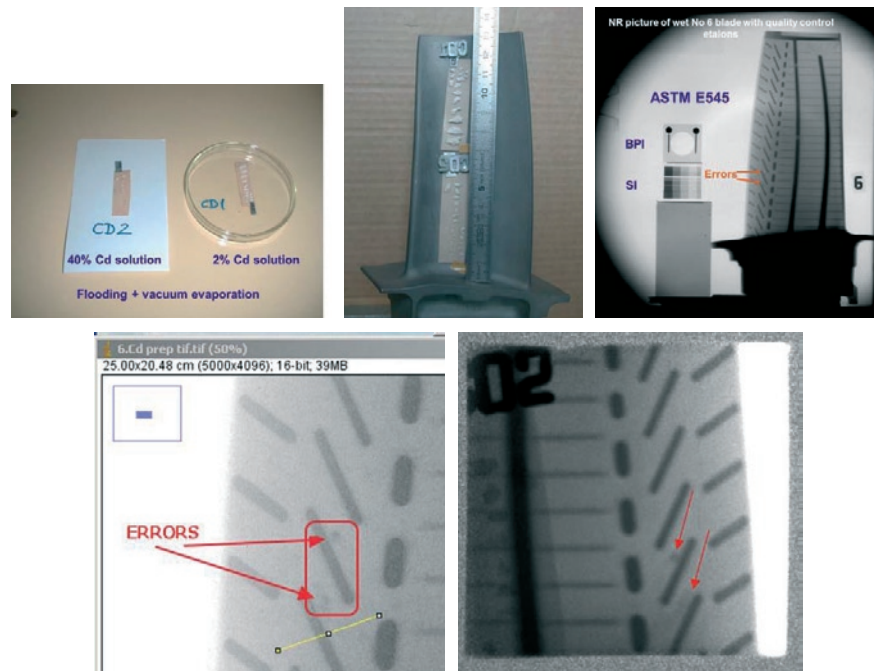


Figure 1: a, Examples of ceramic core material after a Cd solution bath; b, Photo of the blade; c, Full image of the blade at DNR (thermal neutrons); d, Detailed images of the positions of core residues by thermal and cold neutrons

<h1 style="text-align: center;">B N C</h1> <p style="text-align: center;"><b>Experimental Report</b></p>	<i>Experiment title</i> <b>Tomography of small items at NORMA experimental station</b>	<i>Instrument</i> NIPS <i>Local contact</i> László Szentmiklósi
	<i>Principal proposer:</i> Stefan Söllradl – Univeristy of Bern <i>Experimental team:</i> László Szentmiklósi, Zoltán Kis – Centre for Energy Research	<i>Experiment Number</i> NIPS_12_24_IC <i>Date</i> 2012.11.13- 2012.11.15

**Objectives**

to explore the 3D imaging capabilities of NORMA and compare it to the corresponding facility of FRM II

**Results**

Small technical and geological samples were tomographed at the NORMA station. 601 projections were recorded per 180 degree rotation, and they were corrected with the beam- and dark images. The tomography reconstruction software Octopus was used to obtain the slices of the objects that were visualized with VG Studio 2.1 volume rendering program.

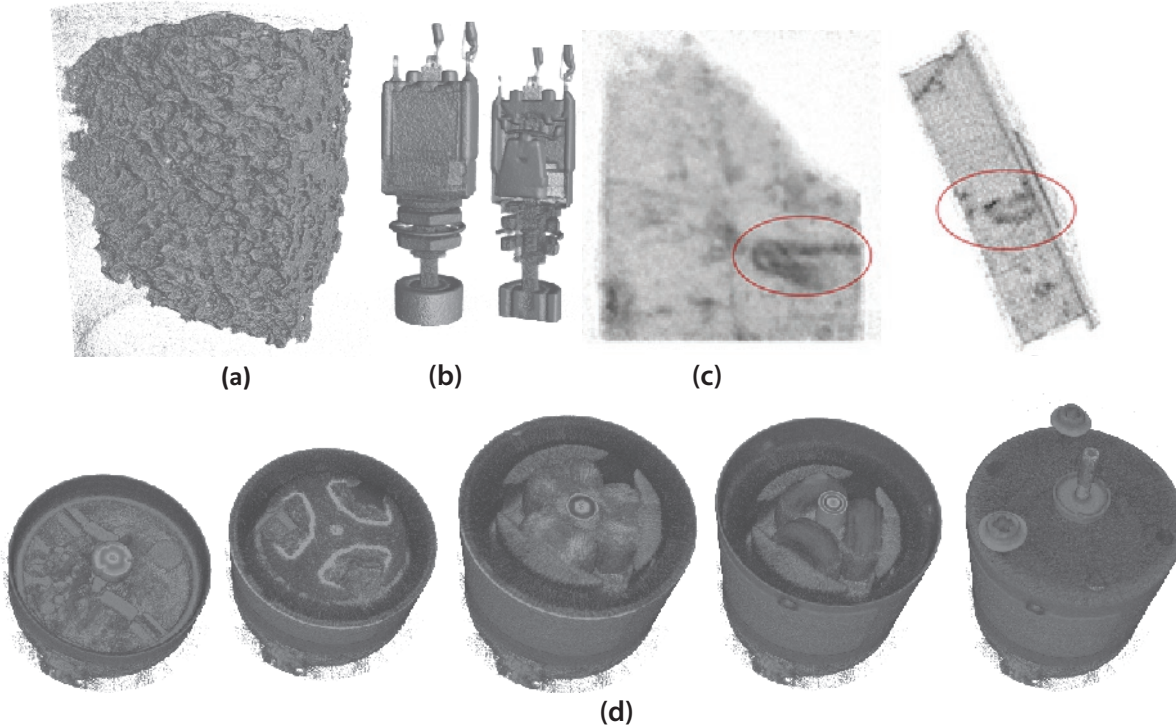


Figure 1: 3D visualization of a Hawaiian basalt (a), a limit switch (b), a lapis lazuli (c) and a stepper motor (d)

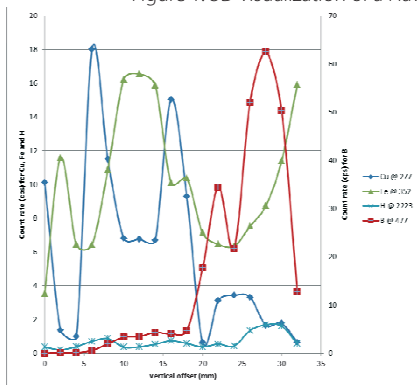


Figure 2. the axial distribution of selected elements in the stepper motor 0 mm=top, 32mm=bottom

A PGAI scan was also performed along the long axis of the stepper motor with a step size of 2 mm in order to reveal the composition of the main components.

It is easy to recognize the parts in the Fig. 2 based on the characteristic elements, such as the iron cover, the ankle, the iron core of the magnets and components of the electronic board.

The experiment demonstrated the capability of NORMA imaging station to scrutinize small technical items and to find inhomogeneities in geological samples.

<h1 style="margin: 0;">B N C</h1> <p style="margin: 0;"><b>Experimental Report</b></p>	<i>Experiment title</i> <b>PGAI with neutron radiography for mapping of materials' heterogeneity</b>	<i>Instrument</i> NIPS-NORMA <i>Local contact</i> Kis Zoltán
	<i>Principal proposer:</i> Kis Zoltán – Centre for Energy Research <i>Experimental team:</i> Kis Zoltán – Centre for Energy Research	<i>Experiment Number</i> NIPS_12_25_IC <i>Date</i> 2012.11.15- 2012.11.16

## Objectives

to combine PGAI (I for imaging) technique with neutron radiography and tomography (NR/NT) for mapping of materials' heterogeneity

## Results

The combination of PGAI (I for imaging) elemental analysis technique with neutron radiography and tomography (NR/NT) for mapping of materials' heterogeneity will be developed as complementary tool in EU FP7 NMI3-II Imaging JRA (WP18 Task 18.3: energy-selective neutron imaging). NR or NT provides a 2D or 3D visual representation of the sample, and the spatial data of internal regions could be linked to the positions of a motorized sample stage. This way one can localize and move selected parts of the sample into the neutron beam, where the subsequent acquisition of gamma-spectra results in characterization of these selected spots in a selective way.

In a pilot experiment with a stainless steel plate (Type 304) we measured the uniformity of the thickness of the plate based on radiography, and the Fe, Ni and Cr content of the irradiated areas, which were next to each other along a line. As a hypothesis test we could find inhomogeneities at 1-sigma level, but no inhomogeneity was found at 2-sigma level (the 2-sigma error bars in Fig. 1. show this). Longer acquisition times in the future could decrease the statistical uncertainty of the peak areas.

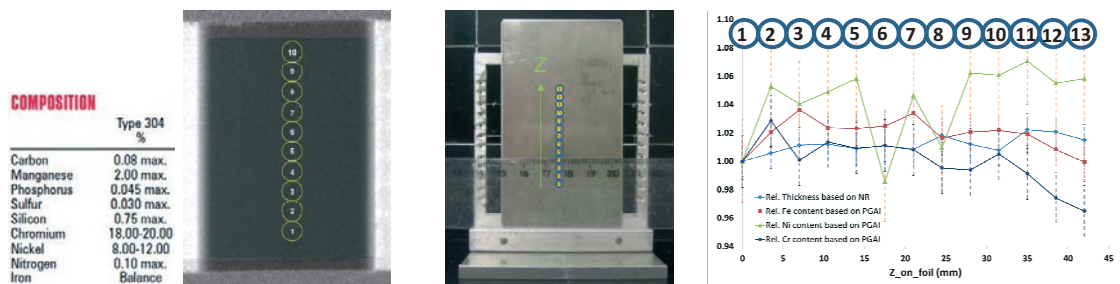


Figure 1: The nominal composition of the SS plate of type 304; part of the irradiated spots in its NR image in the field of view; the irradiated spots in the photo of the plate; relative Fe, Ni and Cr content along Z-axis.

<h1 style="margin: 0;">B N C</h1> <p style="margin: 0;">Experimental Report</p>	<i>Experiment title</i> <b>Gamma-ray transmission of the applied lead collimator as a function of energy for PGAI measurements</b>	<i>Instrument</i> NIPS <i>Local contact</i> Kis Zoltán
	<i>Principal proposer:</i> Kis Zoltán – Centre for Energy Research <i>Experimental team:</i> Kis Zoltán – Centre for Energy Research	<i>Experiment Number</i> NIPS_12_26_IC <i>Date</i> 2012.09.14- 2012.12.12

## Objectives

to measure the spatial resolution of the gamma-ray transmission of the applied lead collimator as a function of energy for PGAI

## Results

The knowledge of the spatial resolution of PGAI for this position sensitive elemental analysis technique is inevitable for the different gamma collimators applied. In the framework of EU FP7 NMI3-II Imaging JRA (WP18 Task 18.3: energy-selective neutron imaging) a method is developed to be able to measure this quantity. The extension of the irradiated volume, which is sensed by the HPGe detector is the source of the analytical information, of which spatial data could be linked to the gamma-spectra results.

We developed a method to measure the FWHM (full width at half maximum) of the gamma-ray transmission of the actually applied lead collimator as a function of energy. Point-like radioactive source is positioned in the so-called isocentre, and then it is moved around it. During the movement several gamma-ray spectra are collected, and the intensities at the different energies are linked to the actual position. This transmission curves determine basically the spatial resolution of the PGAI. The spatial resolution of the method reached to date the range of few mm in the case of using a 2x20 mm<sup>2</sup> lead collimator for lower energy gamma-rays (for some hundreds of keV).

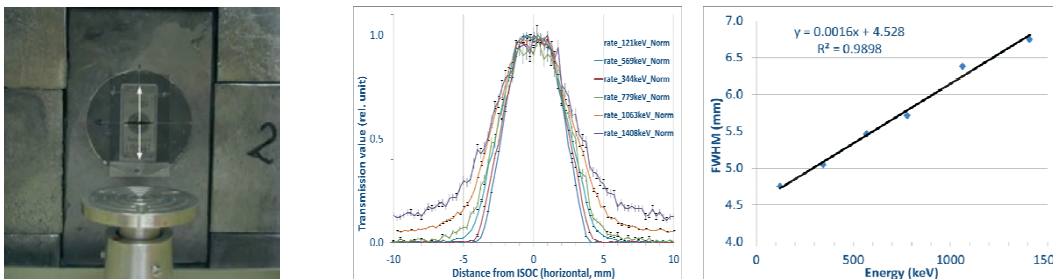


Figure 1: Point-like radioactive source is positioned in front of the lead collimator, and by moving it up and down the transmission curves of the gamma-ray spectrometer at different energies were measured.

<b>B N C</b> <b>Experimental Report</b>	<i>Experiment title</i> <b>Radiography of medieval arms and armours from Q'alat al Marqab (Margat Castle) Syria</b>	<i>Instrument</i> NIPS-NORMA <i>Local contact</i> Kis Zoltán
	<i>Principal proposer:</i> Vágner Zsolt – Syro-Hungarian Archaeological Foundation <i>Experimental team:</i> Kis Zoltán, Szentmiklósi László – Centre for Energy Research	<i>Experiment Number</i> NIPS_12_27_IH <i>Date</i> 2012.06.14- 2012.06.14

## Objectives

to have more information about the elements of the metal and copper based objects comparing to other archaeological material

## Results

The Syro-Hungarian Archaeological mission of Pázmány Péter Catholic University made several excavation sessions from 2007 to 2011. The studied castle is the largest crusader castle situated on the middle of the coastal region of Syria 3 km from the sea. The castle is firstly known from the middle of the 11th Century as a local tribe fortification. Permanent crusaders settled down later and built a proper fortified residence as the first known castle on the site. It then became an administrative centre until 1285 when the mamluk Sultan Baybars sieged it successfully.

At the summer session of 2011 Zsolt Vágner found a unique collection of late 13th century of arms and armours. That contained different types of chain mails, two types of helmets, a decorative dagger and almost 300 pieces of arrowheads belong to bows and crossbows over several other small metal finds. The first archaeological analysis suggest the finds belonged to a mamluk (muslim) warrior who could be died at the 1285 siege of the castle when the crusaders lost it.

The major aim of the proposed analysis (PGAA) was to have more information about the elements of the metal and copper based objects comparing to other archaeological material and creating a reference collection. The other aim was to get information about the physical structure and conditions of the studied objects (NR) to understand their making techniques and help to do best conservation process. The studied objects have only few known parallel finds from the age of crusades. The results will be able to give some new fix points for further comparative archaeometrical researches as well.

Helmet fragments Nr. 20. and 10., arrow heads Nr. 3., 6. and 7, piece of chain-mail (Nr. K2/6) and the blade of the dagger (Nr. 11/1) are made of iron, with 56.0 to 68.6 wt% Fe content, which correspond to 80.04 to 97.97 Fe<sub>2</sub>O<sub>3</sub>, supposing that the iron is totally corroded. Minor and trace elements of H, B, Si, S, Cl, K, Ca and Ti are attributed to contamination from the soil and/or to corrosion. The Nr. K2/2 piece of chain-mail turned out to be tin-bronze with 66.2 wt% Cu, 2.8 wt% Sn and 0.29 wt% As. Nr. K2/E piece of chain turned out to be made of brass with 58.0 wt% Cu, 13.7 wt% Zn and 1.0 wt% Sn. The knob of the dagger shows a composition of typical brass with 51.3 wt% Cu, 8.5 wt% Zn and 1.26 wt% Sn. In this measurement, the amount of Fe is probably due to the central nail in the knob.

The objects were not cleaned so extraneous parts could affect the attenuation of the neutron beam, and as a result, artefacts could appear in the final images. As a consequence these studies should be considered as preliminary ones. A thorough cleaning before later investigations is essential. Some structural details of the objects could, however, be recognized (Fig. 1.).

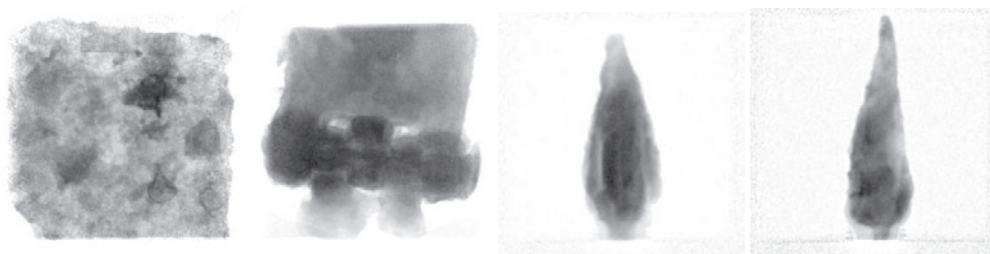


Figure 1: Neutron radiographies: Helmet fragment; Door hinge; Arrowheads with segmented and compact structure



<h1 style="margin: 0;">B N C</h1> <p style="margin: 0;"><b>Experimental Report</b></p>	<i>Experiment title</i> <b>Non-destructive Prompt Gamma Activation Analysis of Swords and Helmets</b>	<i>Instrument</i> . PGAA/NIPS <i>Local contact</i> <i>Kasztovszky Zsolt</i>
	<i>Principal proposer:</i> Alan Williams - The Wallace Collection, London <i>Experimental team:</i> Alan Williams, David Edge - The Wallace Collection, London	<i>Experiment Number</i> BRR 282 CH <i>Date</i> 2012.04.24-04.26.

## Objectives

The aim was to determine the carbon contents (and of equal importance, the phase contents) of swords and helmets with non-invasive methods

## Results

This knowledge would be particularly desirable for the high-carbon steels of Oriental arms. It is not simply of interest to describe their metallurgy, fascinating though that is, but to reconstruct their original appearance. Many will originally have had the surface finish resembling “watered-silk” (misleadingly described as “Damascus steel”) but have been polished by over-zealous 19th century collectors, destroying their intended appearance, which illustrated their metallurgy. Determination of this will be needed to precede, and inform, any ethical decisions to be made about their conservation and display.

Eight objects have been analysed - these included 3 swords and 2 daggers both European and Indian, a katar, a kukri, an Indian steel bow, and a collar from a "Maximilian" harness. Positioning and irradiation of the objects were carrying out using Gd markers, which can be very well seen in radiographic images (Fig.1).

Besides Fe, we were able to detect B, P, S, Cl, Ca, Mn, Co, Ni, Cu, Ag and Au in many instances. Despite the expected high levels of carbon in Oriental Steels, it was still below the detection limit of PGAA. The presence of manganese and sulphur would suggest manganese sulphide inclusions which would in turn suggest modern steel. This could be a very useful test for museums wishing to authenticate arms and armour offered to them for purchase.

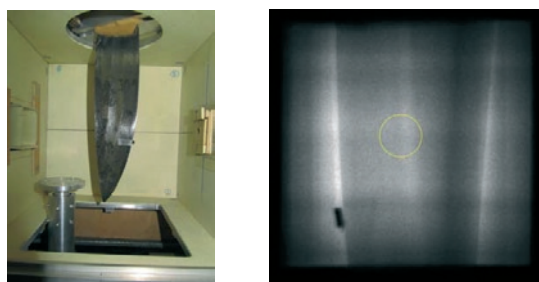


Figure 1: a, Photo of a dagger with Gd marker in the sample chamber; b, The irradiated spot is indicated by yellow circle in the neutron radiography of the dagger

	H	B	P	S	Cl	Ca	Mn	Fe	Co	Ni	Cu	Ag	Au	C
	0.005	0.0001	1	0.05	0.001	0.05	0.005	0.2	0.005	0.01	0.02	0.003	0.003	3
<i>Indian Steel Bow 1A, blued surface</i>	0.0112	0.00021	n.d.	n.d.	n.d.	n.d.	0.377	99.6	n.d.	n.d.	0.021	0.025	0.004	n.d.
<i>Indian Steel Bow 1A, not blued surface</i>	0.0082	0.00024	n.d.	n.d.	0.0052	n.d.	0.270	99.7	0.006	n.d.	0.050	n.d.	0.005	n.d.
<i>Indian Steel Bow 1B, blued surface</i>	0.0071	0.00023	n.d.	n.d.	0.0033	n.d.	0.283	99.6	0.007	n.d.	0.051	n.d.	0.003	n.d.
<i>Indian Blade, crucible steel</i>	n.d.	n.d.	1.0	n.d.	n.d.	n.d.	0.025	98.9	n.d.	n.d.	n.d.	n.d.	n.d.	n.d.
<i>Rear-plate of collar</i>	0.0903	0.00024	n.d.	n.d.	0.0240	n.d.	0.024	99.5	n.d.	n.d.	0.120	0.109	0.084	n.d.
<i>Sword</i>	0.0187	n.d.	n.d.	n.d.	n.d.	n.d.	0.186	97.8	0.039	n.d.	2.0	n.d.	n.d.	n.d.
<i>Sword</i>	n.d.	0.00026	n.d.	n.d.	0.0047	n.d.	0.124	99.5	0.018	0.045	0.29	n.d.	n.d.	n.d.
<i>Knife</i>	0.0068	n.d.	n.d.	n.d.	n.d.	n.d.	0.014	99.95	n.d.	n.d.	n.d.	0.025	n.d.	n.d.
<i>iron sword</i>	n.d.	0.00023	n.d.	n.d.	0.0109	n.d.	0.008	99.8	0.022	n.d.	0.15	n.d.	n.d.	n.d.
<i>iron sword</i>	n.d.	0.00021	n.d.	n.d.	0.0098	0.06	0.019	99.7	0.018	0.027	0.18	n.d.	n.d.	n.d.
<i>pendray sample</i>	n.d.	n.d.	n.d.	n.d.	0.0046	n.d.	0.156	99.8	0.005	n.d.	n.d.	n.d.	n.d.	n.d.
<i>iron dagger</i>	n.d.	n.d.	n.d.	n.d.	n.d.	n.d.	0.014	99.99	n.d.	n.d.	n.d.	n.d.	n.d.	n.d.
<i>guard</i>	n.d.	n.d.	n.d.	n.d.	0.0042	n.d.	0.085	99.9	n.d.	n.d.	0.042	n.d.	0.009	n.d.
<i>steel dagger</i>	n.d.	0.00065	n.d.	n.d.	0.0018	n.d.	0.005	99.99	n.d.	n.d.	n.d.	n.d.	n.d.	n.d.
<i>pendray sample</i>	0.021	n.d.	n.d.	0.06	0.0048	n.d.	0.118	99.8	0.0057	n.d.	n.d.	n.d.	0.022	n.d.

Table 1. The detected elements' concentrations in iron objects, measured by PGAA.

## References

<b>B N C</b> <b>Experimental Report</b>	<i>Experiment title</i> <b>Geochemical study of riolites from the Tokaj Mts.  Cooperation with ELTE TTK, PhD study.</b>	<i>Instrument.</i> PGAA <i>Local contact</i> Katalin Gméling
	<i>Principal proposer:</i> Péter Kiss <i>Experimental team:</i> Péter Kiss, Katalin Gméling, Ferenc Molnár, Zoltán Pécskay	<i>Experiment Number</i> PGAA_10_01_IH <i>Date</i> 2010.01.17

### Objectives

In the Tokaj Mts, which is a part of the Inner Carpathian Volcanic Arc, large amounts of intermediate-acidic calc-alkaline volcanic rocks accumulated in a N–S oriented graben-like structure, in relation with the closure of the Alpine Tethys (Penninic) ocean. Although previous research on volcanism and related hydrothermal processes produced a huge number of K/Ar age data no systematic petrochemical database has been available from the Tokaj Mts. In this study we publish new results of geochemical analyses completed on systematically collected basaltic, andesitic, dacitic and rhyolitic rocks, and of the spatial-temporal evaluation of petrochemical signatures, with special reference to origin of magmatism and relationships of rhyolite to hydrothermal mineralization.

### Results

In the southern Tokaj Mts rhyolite contains K-feldspar phenocrysts, while this phenomenon is absent in the rhyolite from the northern areas of the mountains. In accordance with this, significant potassium enrichment occurs in the south (whole rock K<sub>2</sub>O content varies between 4.35 and 5.61 wt%), whereas rhyolite from the northern Tokaj Mts is less enriched in potassium (K<sub>2</sub>O content is from 3.28 to 5.1 wt%). The most significant difference between the northern and southern dacite is the age of their formation. They were formed at the same time as rhyolite and andesite (between 13.4 and 11 Ma) in the northern Tokaj Mts, while they are much younger (10.57–10.1 Ma) in the southern Tokaj Mts, where they post-date hydrothermal activity. The boron content (10.1–52.12 µg/g) and the patterns of other trace elements of the volcanic rocks show typical subduction-related features; however, direct influx of subduction-related fluids during magma generation can be excluded. A more plausible explanation for the magma genesis is decompression melting of a previously metasomatized mantle, enriched with subduction-related components. Additionally, the unmineralized northern rhyolite samples contain much less Cl (usually below 0.2 wt%) than the high-K rhyolite in the southern part of the Tokaj Mts (usually more than 0.2 wt%), which correlates with the presence/absence of spatially and temporally related epithermal mineralization in these areas.

### References

- Kiss, P., Gméling, K., Molnár, F., Pécskay, Z. (2010): Geochemistry of Sarmatian volcanic rocks in the Tokaj Mts (NE Hungary) and their relationship to hydrothermal mineralization. *Central European Geology*, 53, 4, 377–403.
- Kiss, P., Molnár, F., Gméling, K., Pécskay, Z., (2010): Geochemical characteristics of Sarmatian volcanic rocks in the Tokaj Mts., Hungary. *Acta Mineralogica-Petrographica Abstr. Ser. (XX IMA2010)* 6, GM74, 484.
- Kiss P., Molnár F., Gméling K., Pécskay Z. (2010): Petrochemical signatures of Sarmatian volcanic rocks in the mineralized and unmineralized areas of the Tokaj Mountains, NE-Hungary. *Geologica Balcanica, Abstr. Vol. (XIX CBGA)* 39. 1-2, 191.

<p style="text-align: center;"><b>B N C</b></p> <p style="text-align: center;"><b>Experimental Report</b></p>	<p><i>Experiment title</i>  <b>Geochemical studies of intrusive volcanic rocks from the Apuseni Mts., Romania.</b></p>	<p><i>Instrument.</i>  PGAA  <i>Local contact</i>  Katalin Gméling</p>
<p><i>Principal proposer:</i>  Ioan Seghedi  <i>Experimental team:</i>  Katalin Gméling, Ioan Seghedi, Zoltán Pécskay</p>		<p><i>Experiment Number</i>  PGAA_10_03_IH  <i>Date</i>  2010.01.20                      and  2010.02.14</p>

### Objectives

Bontău is a major eroded composite volcano filling the Miocene Zărand extensional basin, near the junction between the Codru-Moma and Highiş-Drocea Mountains, at the tectonic boundary between the South and North Apuseni Mountains. It is a quasi-symmetric structure (16-18 km in diameter) centered on an eroded vent area (9x4 km), buttressed to the south against Mesozoic ophiolites and sedimentary deposits of the South Apuseni Mountains. The volcano was built up in two sub-aerial phases (14-12.5 Ma and 11-10 Ma) from successive eruptions of andesite lava and pyroclastic rocks with a time-increasing volatile budget. The initial phase was dominated by emplacement of pyroxene andesite and resulted in scattered individual volcanic lava domes associated marginally with lava flows and/or pyroclastic block-and-ash flows. The second phase is characterized by amphibole-pyroxene andesite as a succession of pyroclastic eruptions (varying from strombolian to subplinian type) and extrusion of volcanic domes that resulted in the formation of a central vent area. Numerous debris flow deposits accumulated at the periphery of primary pyroclastic deposits. Several intrusive andesitic-dioritic bodies and associated hydrothermal and mineralization processes are known in the volcano vent complex area.

### Results

Chemical analyses show that lavas are calc-alkaline andesites with SiO<sub>2</sub> ranging from 56–61 wt%. The major oxide distribution along petrographical data support minor fractional crystallization processes during evolution of the magmas in crustal-level chambers, compatible with the extensional setting that not favoured long stage magma chamber processes. All the samples have H<sub>2</sub>O content below 3 wt%. Boron content of the measured samples varies between 1.8 and 7.7 µg/g. The Cl content of the samples are changeable (18-350 µg/g). The petrographical differences between the two stages are an increase in amphibole content at the expense of two pyroxenes (augite and hypersthene) in the second stage of eruption; CaO and MgO contents decrease with increasing SiO<sub>2</sub>. In spite of a ~4 Ma evolution, the compositions of calc-alkaline lavas suggest similar fractionation processes. The extensional setting favoured two pulses of short-lived magma chamber processes.

### References

Seghedi, I., Szakács, A., Rosu, E., Pécskay, Z., Gmeling, K. (2010): Note on the evolution of a Miocene composite volcano in an extensional setting, Zărand Basin (Apuseni Mts., Romania). *Central European Journal of Geosciences*, 2(3), 321-328.

<b>B N C</b> <b>Experimental Report</b>	<i>Experiment title</i> <b>PGAA analysis of Basalts from Ireland and Greenland. Main interest on their B and Cl content.</b>	<i>Instrument.</i> PGAA <i>Local contact</i> Katalin Gméling
	<i>Principal proposer:</i> Christoph Schnabel and Joyce Wilcox <i>Experimental team:</i> Katalin Gméling, Christoph Schnabel and Joyce Wilcox	<i>Experiment Number</i> PGAA_10_05_IC <i>Date</i> 2010.10.06            and 2011.07.13

## Objectives

We were asked from Scotland (NERC Cosmogenic Isotope Analysis Facility, SUERC, East Kilbride) to measure basalt rock samples (fourteen from Ireland and seven from Greenland) with PGAA. Analysis needed for the following elements: Si, Ti, Al, Fe, Mn, Mg, Ca, Na, K, C, H, B, Cl, Cr, Sm, Gd. The proposer needed the analytical results for the interpretation of Cl-36 concentrations in these samples.

## Results

Concentrations of major components and their oxides (except P and P<sub>2</sub>O<sub>5</sub>) and some trace elements (B, Cl, Sc, V, Cr, Co, Ni, Nd, Sm, Gd) have been determined in all samples using the prompt gamma neutron activation analysis (PGAA) facility at the Budapest Research Reactor (Hungary).

The claimed Cl content could be determined in all the seven samples from Greenland, and showed wide range between 20 and 183 µg/g. The UBE20(1) sample has the lowest Cl content, which is close to the detection limit, thus the result has higher uncertainty than for the others. Next to Cl, B, Sc, V, Sm and Gd could be measured in all the samples. Other trace elements, like Cr, Co, Ni and Nd could be measured only in some of the samples. The measured samples have also variable B content (0.6-19.5 µg/g). The UBE01 sample looks more altered by its chemical composition (with its high H<sub>2</sub>O, Cl and B content), compared to basalts and the other samples measured in this run.

The Cl content could not be determined in every Ireland basalt. In those samples where we gave the Cl data are also low and those results have high uncertainty. B, V, Cr, Co, Ni, Sm and Gd could be measured in all the samples. Trace elements, like Sc, and Nd could be measured only in some of the samples. The measured samples have very low Cl content, around and below 30 µg/g. The B content is also low, below 1.5 µg/g.

PGAA is highly sensitive of B, Cl, Gd and H, and provides more satisfactory and reliable results, than other analytical methods.

## References

<b>B N C</b> <b>Experimental Report</b>	<i>Experiment title</i> <b>Geochemical and environmental studies of rocks and sediments from St Ana Lake (Balea rock)</b>	<i>Instrument</i> PGAA  <i>Local contact</i> K. Gmélíng
	<i>Principal proposer:</i> Carmen Olteanu (Cristache) <i>Experimental team:</i> Carmen Olteanu, Katalin Gmélíng	<i>Experiment Number</i>  <i>Date</i> 02.15.2010-02.16.2010

### Objectives

Romanian geologist and physicist proposed a project with the main objective of determining the pollutants in water and sediments of the lakes (St Ana and Balea), in order to find the polluting area along river basins pouring into the lakes. Mud, sediments and basin rocks were collected from St Ana Lake and from Balea to examine the sedimentology, geophysics, mineralogy, and geochemistry. We were asked to measure the samples chemical composition with PGAA.

Saint Ane Lake is the only alpine lake (on an altitude of 946 m) of volcanic origin throughout Romania and also in Europe. It is situated in the Great Ciumatul Mt., with the Olt river on its left, near Tuşnad. The lake is situated on the bottom of a volcanic crater. This volcano erupted most recently, few tens of thousands years ago (probably less than 42,000 years ago) in the Carpathian Volcanic Region in Eastern Europe.

### Results

Using the PGAA techniques, it was possible to determine all major elements (Si, Ti, Al, Fe, Mn, Mg, Ca, Na, K, H) and some trace elements (like: B, Cl, Sc, Cd, V, Cr, Co, Nd, Sm, Gd) in order to obtain information about the formation of rocks and sediments. Mud from St Ana Lake had high CO<sub>2</sub> content (>57 wt%) and also high H<sub>2</sub>O content (above 20 wt%) and average B content (6-9 µg/g). While volcanic rock samples from St. Ana Lake have H<sub>2</sub>O content around 1 wt% and relatively high B content (20-48 µg/g). Soil samples from Balea Lake have lower H<sub>2</sub>O content than the mud samples from St. Ana Lake, but higher B content (H<sub>2</sub>O: 6-12 wt%; B: 17-32 µg/g). Only one rock sample from Balea Lake was measured, which is a limestone. The limestone has low H<sub>2</sub>O (0.22 wt%) and B (0.74 µg/g) content.

### References:

<b>B N C</b> <b>Experimental Report</b>	<i>Experiment title</i> <b>PGAA Analysis of Balkanic Flint for Comparison with Neolithic Artefacts from South Eastern Romania</b>	<i>Instrument</i> PGAA/NIPS  <i>Local contact</i> Zs. Kasztovszky
	<i>Principal proposer:</i> Madalina Dimache - Valahia University in Targoviste, Romania <i>Experimental team:</i> Madalina Dimache, Zsolt Kasztovszky	<i>Experiment Number</i> BRR_226 <i>Date</i> 2010.04.21-04.24

### Objectives

PGA Analyses of 10 chipped stone artefacts and 10 geological reference samples of Balkanic flint was the aim of the project. 5 geological flint samples are from the Dobrogea area of Romania and 5 are from Prut Valley. The artefacts are from late Neolithic sites in south western Romania. The results from the analyses of the artefacts would be compared to the results of the analyses of the geological samples. The purpose of this analysis is to understand if the artefacts are from local material or imported material.

### Results

Elemental compositions of 20 flint rock samples (both artefacts and geological references) were determined with PGAA. Major components (H, Na, Al, Si, K, Ca, Ti, Mn and Fe) as well as traces (B, S, Cl, Nd, Sm and Gd) were quantified. Based on the analytical data, we tried to determine whether the artefacts closely match the chemical signature of the flint from Northern Dobruja (where it's suspected they came from). During the evaluation of the analytical results we have faced the problem of the large variation in the composition of the geological materials. This is a frequent problem with microcrystalline quartz, which can cause overlap between the sources. The other problem is that it can't be excluded that the material didn't come from another nearby source - e.g. the limestone formations from across the Danube in Bulgaria. It is also difficult to determine to what degree bleaching/leaching from the soils around the artefacts (at the archaeological site) have affected the composition of the artefacts. It may cause the artefacts to be a bit different from their original raw materials, so it will be hard to tell whether the artefacts are at the periphery of what characterises the raw materials or if they are from a different material altogether.

According to preliminary investigations, the following elemental composition data are the most useful for characterisation: H, B, Si, Cl, K, Ca, Fe and Gd. Furthermore, Cl, Ti, and Sm will also be useful because there were not measurable in only a few samples.

<h1 style="margin: 0;">B N C</h1> <p style="margin: 0;"><b>Experimental Report</b></p>	<i>Experiment title</i> <b>PGAA analysis of 15 geological silicate samples from Central Transylvania for comparison with analysis of 5 prehistoric artefacts</b>	<i>Instrument</i> PGAA
	<i>Principal proposer:</i> Otis Crandell, University Babeş-Bolyai, Cluj-Napoca, Romania <i>Experimental team:</i> Otis Crandell, Zsolt Kasztovszky	<i>Local contact</i> Zs. Kasztovszky

The objective of this project was to analyse jasper samples (prehistoric artefacts and geological samples) by PGAA. The samples came from archaeological sites and geological outcrops in Transylvania (central Romania). The purpose of these analyses was determine whether it was possible to distinguish between jasper artefacts of different geographic origin made of similar raw materials. The artefacts were compared to the geological samples. In this project, jasper artefacts and geological samples were used as they contain a higher amount of impurities than most other cherts and would therefore have a higher probability of exhibiting regional variations.

## Results

It was possible to correctly predict group membership (based on geographic origin) of the geological samples, although the same results obtained for artefacts must be viewed with caution because four out of 18 geological samples had an extremely low prediction level, and another six were low enough to be unacceptable for predictions. All of the artefacts analysed received a prediction of their source but all had extremely low or non-existent levels of accurately of the predictions. The predictions may be correct but they must be considered with suspicion.

Difficulties: The statistical significance of results is too low to give conclusive results, particularly relating to the archaeological samples. It is possible that a larger sample set would increase the reliability of the predictions.

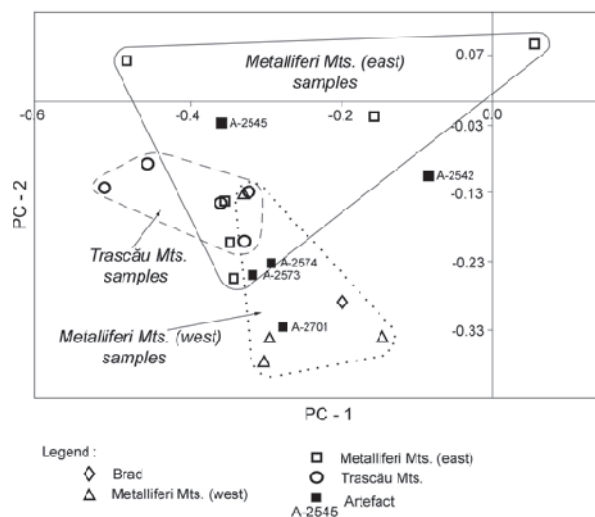


Figure 1. Principal component analysis plot of the PGAA data

## References

1. Otis Crandell: Evaluation of PGAA data for provenance of lithic artifacts, *Studia UBB Geologia*, 2012, **57** (1), 3 – 11

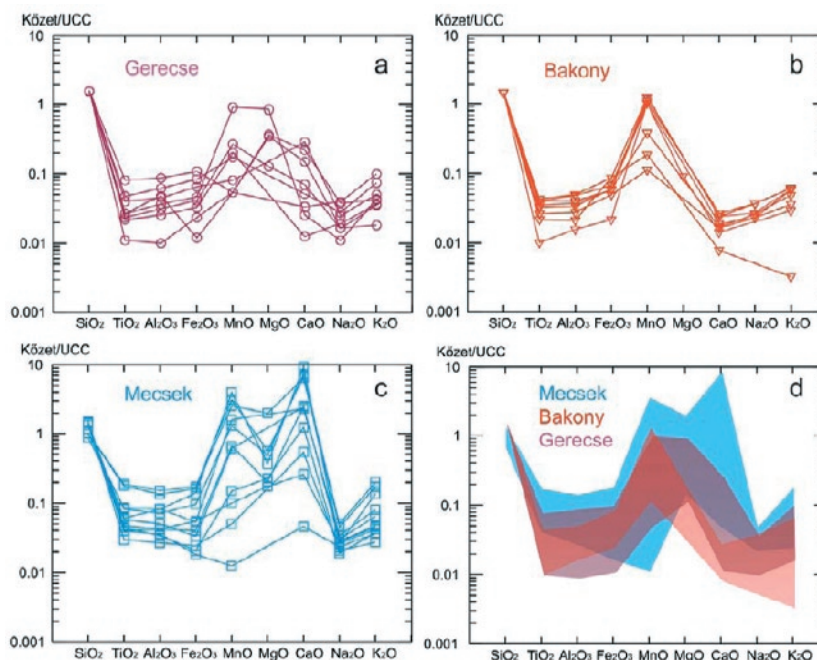
<h1 style="margin: 0;">B N C</h1> <p style="margin: 0;">Experimental Report</p>	Experiment title	Instrument
	<b>Provenance study of radiolarite stone tools (Hárskút, Nagytevel, Városlőd and Sümeg - Hungary)</b>	PGAA/NIPS
Principal proposer: Katalin T. Biró – Hungarian National Museum Experimental team: Zsolt Kasztovszky, Veronika Szilágyi		Local contact Zs. Kasztovszky
		Experiment Number PGAA_10_16_NC Date 2010.10.06-2010.10.10

## Objectives

Radiolarites represent one of the most numerous and most important raw material for chipped stone tools in the Carpathian Basin. They have a basic role in the regional supply, especially in Transdanubia and some other parts outside Hungary (Moravia, W Slovakia and probably Austria and Croatia as well). Long distance trade of attractive and high quality radiolarites has also been proved. The objective of the present study was the geochemical characterisation of individual source regions.

## Results

Different, macroscopically separable types were studied by PGAA. Siliceous rocks in general represent a difficult subject because the main chemical compound, SiO<sub>2</sub> makes up over 95% of the total composition. PGAA results indicate that radiolarites will be separable on the level of smaller regions (mountains). Gerecse Mts. seem to have a very wide range; Mecsek and Bakony mts. are centred more tightly. For statistical relevance, more (geological and archaeological) samples are needed.



Major element composition of the Hungarian radiolarite source collected samples, normalised for UCC

## References

1. TÉT homepage <http://www.ace.hu/tet/am2009-10-29/TBK-09-10-29.pdf>
2. T. Biró Katalin, Szilágyi Veronika, Kasztovszky Zsolt Archeometriai Műhely 6/3 25-44



<h1 style="margin: 0;">B N C</h1> <p style="margin: 0;"><b>Experimental Report</b></p>	<i>Experiment title</i> <b>Lapis lazuli and "false" lapis lazuli in the royal tomb of Qatna (Syria)</b>	<i>Instrument</i> : PGAA/NIPS  <i>Local contact</i> Zs. Kasztovszky
	<i>Principal proposer</i> : Judit Zöldföldi - University of Tübingen, Institute of Geoscience <i>Experimental team</i> : Judit Zöldföldi, Zolt Kasztovszky, Veronika Szilágyi, György Káli, Imre Kovács	<i>Experiment Number</i> BRR 250 CH <i>Date</i> 2010.11.13-11.18; 2012.09.04-09.06

## Objectives

Lapis lazuli, "false" lapis lazuli, variscite from the royal tomb of Qatna (Syria) and other comprehensive lapis lazuli, such as archaeological pieces from Kulke's excavation in Afghanistan, have been investigated. In this project PGAA,  $\mu$ -PIXE and external-beam PIXE have been applied to characterise the lapis lazuli raw material in details, because of its inhomogeneity. Additionally, TOF-ND method has been applied to identify the minerals in lapis lazuli non-destructively. The ultimate goal of the study is to determine the provenance of archaeological objects, made of lapis lazuli

## Results

For this purposes, we have investigated geological reference samples from Afghanistan, Lake Baikal, Pakistan, Ural Mountains, Canada and Chile in this study. With PGAA we were able to measure all the major and accessory components of lapis lazuli. We have already prepared a preliminary database of chemical composition, based on which we succeeded to distinguish between the most relevant quarries. Furthermore, identification of forgeries is also possible in a non-destructive way. This bulk technique has been used, because of the inhomogeneity of the lapis lazuli raw material. PGAA is one of the few non-destructive methods, which is applicable in bulk elemental analysis of valuable archaeological objects, like beads and cylinder seals, as well. Furthermore, the external-beam PIXE technique makes possible the elemental analysis of macroscopically different surface regions, such as darker blue areas and white patches on lapis lazuli.

Additionally, TOF-ND method has been applied to identify the minerals in lapis lazuli non-destructively.

In some fortunate instances, the different sources can be distinguished, based on their elemental composition, for example, based on their S and Cl content. However, the elemental compositions of lapis lazuli from Baikal and from Afghanistan are very similar, however, according to its Cl-, S- and Fe-content it is possible to differentiate between them.

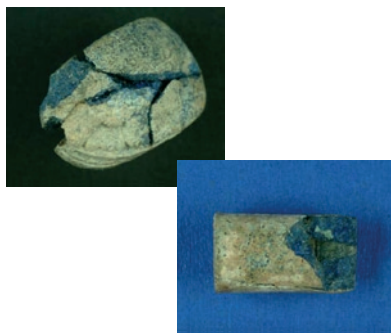


Fig. 1: Photos of lapis lazuli beads from Syria

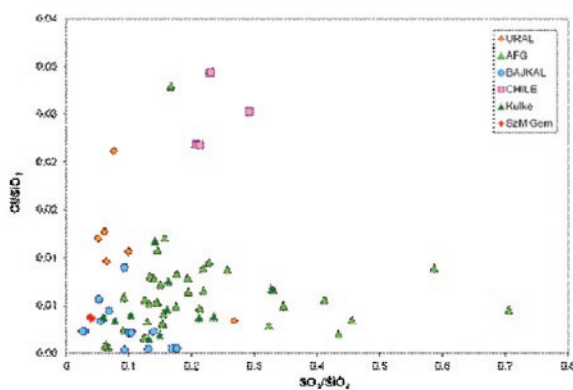


Fig. 2: Differentiation between lapis lazulis of various origin

<b>B N C</b> <b>Experimental Report</b>	<i>Experiment title</i> <b>Non-destructive chemical and mineralogical analysis of lithic implements from Vojvodina</b>	<i>Instrument</i> PGAA  <i>Local contact</i> Zs. Kasztovszky
	<i>Principal proposer:</i> Peter Ritz – City Museum Subotica, Serbia <i>Experimental team:</i> Andor Hajnal, Zsolt Kasztovszky, Veronika Szilágyi	<i>Experiment Number</i> BRR 254  <i>Date</i> 12.01.2010-12.04.2010

## Objectives

The stone implements found at the coast of the Ludas lake constitute the substance of the examination. The lake is situated nearby Subotica (Szabadka) in northern Serbia, about 20 km from the border with Hungary. The characteristic of the area is the exploitable raw stone material which cannot be found in the neighbouring areas (cca. 100 km radius). The mentioned area, primarily in the prehistoric age, layed in meeting-points or borders of different cultures. The stone implements found here certainly do not come from the neighbourhood. The most important aim of the additional researches is to find out the commercial contacts of the area, in which way were people living here in the prehistoric age, where was the raw material of their tools obtained from?

## Results

The following archeological objects have been investigated with non-destructive PGAA:

-21 chipped objects (igneous and sedimentary rocks such as obsidian, silex, radiolarite).

-14 polished objects (metamorphic and igneous rocks such as diorite, andesite, serpentinite, gabbro, dolerite, hornfels, aplite and greenshist).

Major components ( $H_2O$ ,  $Na_2O$ ,  $CaO$ ,  $K_2O$ ,  $MgO$ ,  $Al_2O_3$ ,  $SiO_2$ ,  $TiO_2$ ,  $MnO$  and  $Fe_2O_3$ ) as well as accessory and trace elements (B, Sc, V, Nd, Sm and Gd) have been quantitatively determined.

The obtained composition data are compared with those of similar materials compiled in our database. Based on the comparison with similar sort of materials, we were able to distinguish two types of Serbian obsidians according to the origin of their raw materials. The evaluation of the results is in progress.

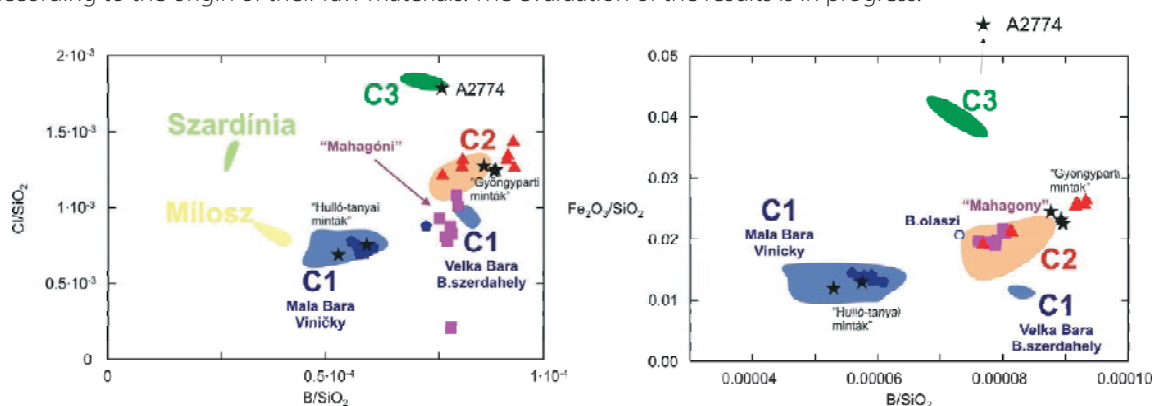


Figure 1-2: Separation of Serbian obsidians (black stars label)

## References

1. Zs. Kasztovszky et al.: Recent provenance study of obsidian artefacts found in Central Europe, 39th Int. Symposium on Archaeometry, 2012, Leuven, Belgium

<b>B N C</b> <b>Experimental Report</b>	<i>Experiment title</i> <b>Determination of Raw material of prehistoric stone Artifacts and their possible sources by mean of Prompt Gamma Activation Analyses</b>	<i>Instrument. PGAA/NIPS</i>  <i>Local contact</i> Zs. Kasztovszky
	<i>Principal proposer:</i> Elisabetta Starnini - Ministry of Cultural Heritage, Archaeological Superintendency <i>Experimental team:</i> Elisabetta Starnini, Zsolt Kasztovszky, Veronika Szilágyi	<i>Experiment Number</i> BRR 250  <i>Date</i> 11.13.2011-11.18.2011

## Objectives

The research concentrates on lithic raw material sourcing, a well based topic in archaeometry.

Previous research in this matter was conducted throughout more traditional petrographical approaches, such as TS-OM, XRD, XRF, Magnetic Susceptibility (MS) measurements. Most of these analytical methods can be successfully used for the analysis of raw material (rocks) samples, however they are considered invasive. Therefore, they cannot be always employed for archaeological artefacts, or, as in case of MS, they are useful only as a first step for a broad discrimination of rock groups. Previous experience in PGAA was achieved thanks to a bilateral research project, during which some measurements were performed on Hungarian late Neolithic polished stone tools found in Gorzsa (SE-Hungary). The present project has the aim to create a more complete database of the main lithic raw materials of the Hungariana Neolithic axe blades and to test the presence of long-distance imports from western European sources.

## Results

The main result is that we have successfully demonstrated the effectiveness of the PGAA as one of the powerful, absolutely non-destructive methods in discrimination of stone artefacts made of metamorphic rocks. Contrary to other non-invasive chemical methods this technique has the advantage that it measures bulk composition. As regards in particular polished stone tools, PGAA measures all major elements (H, Na, Mg, Al, Si, K, Ca, Mn, Fe and Ti) and few trace elements (B, Cl, Co, Cr, Nd, Sm, Eu and Gd), which are extremely useful for raw material sourcing. According to our knowledge, this was the first application of PGAA to characterise HP-metaophiolite sources of N-W Italy, in order to create the first reference database for the comparison with archaeological artefacts. We have investigated 42 samples altogether, including geological and archaeological artefacts. After the complete evaluation of the results, the presence of W-Alpine origin prehistoric artefacts in various Hungarian museums collections can be proved. Further achievement is to detect the presence of possible utilizable rocks in form of river pebbles in the alluvial deposits of the Maros (HU-RO) and Staffora and Curone Rivers (I), which might have constituted an alternative source of raw materials to primary outcrops. As a conclusion, we can assess that macroscopic description combined with PGAA successfully help to determine raw materials of polished stone tools for several rock types. From archaeological point of view, the results revealed the presence of unexpected lithotypes and rocks which are exotic in the Carpathian Basin. They unquestionably show long-distance connections and interactions with areas, such as the Moravian region, the Bohemian Massif and, possibly, the W-Alps, for the procurement of specific raw materials.

**Figure:** Photo of a greenschist axe, analysed with PGAA



## References

1. Gy. Szakmány, et al: Discrimination of prehistoric polished stone tools from Hungary with non-destructive chemical Prompt Gamma Activation Analyses (PGAA), Eur. J. Mineral. 2011, 23, 883–893

<b>B N C</b> <b>Experimental Report</b>	<i>Experiment title</i> <b>Geochemical characterisation of Japanese obsidians</b>	<i>Instrument</i> PGAA/NIPS  <i>Local contact</i> Zsolt Kasztovszky
	<i>Principal proposer:</i> Katalin T. Biró, Viola Dobosi – Hungarian National Museum <i>Experimental team:</i> Zsolt Kasztovszky, Veronika Szilágyi / Boglárka Maróti	<i>Experiment Number</i> PGAA_11_26_NC <i>Date</i> 2011.01.14-01.19

## Objectives

The Lithotheca Collection of the Hungarian National Museum received a representative set of obsidian samples from Japan. Although the Japanese obsidian is not relevant from archaeological point of the Carpathian Basin, with extension of our geochemical reference database, we wish to find correlation between the chemical composition and geological formation of various obsidians. This information, in turn, may help in provenance studies of Carpathian obsidians.

## Results

Altogether 29 obsidian samples have been analysed with PGAA, the largest ones being more kgs. Similarly to earlier obsidian analysis, we were able to quantify the major components (Si, Ti, Al, Fe, Mn, Ca, Na, K, H) and traces of B, Cl, Sc, Nd, Sm and Gd. Among the trace elements, B and Cl were found to be discriminative. Preliminary results on separation of Japanese obsidians from different origin are shown on Figure. For comparison, Carpathian and Lipari obsidians are displayed, too.

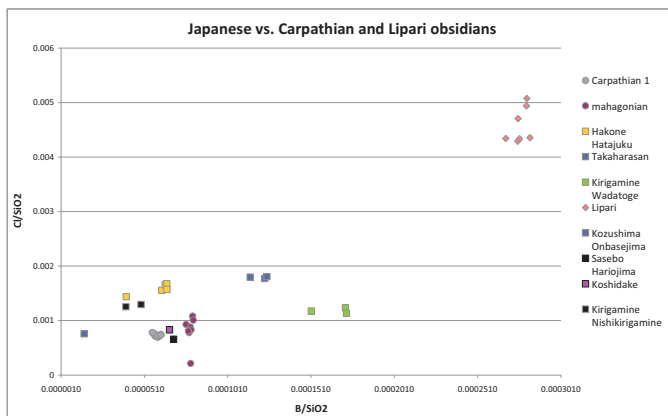


Fig. 1: Distribution of Japanese obsidians from different origin, compared with Carpathian and Lipari ones



Fig. 2: Origin of the Japanese obsidians

<h1 style="margin: 0;">B N C</h1> <p style="margin: 0;"><b>Experimental Report</b></p>	<p><i>Experiment title</i></p> <p><b>Provenance study of Szeletian felsitic porphyry archeological objects</b></p>	<p><i>Instrument</i></p> <p>PGAA/NIPS</p>
	<p><i>Principal proposer:</i> Katalin T. Biró, András Markó – Hungarian National Museum</p> <p><i>Experimental team:</i> Zsolt Kasztovszky, Veronika Szilágyi / Boglárka Maróti</p>	<p><i>Local contact</i></p> <p>Zs. Kasztovszky</p>

## Objectives

In this work we outline the distribution data of a single raw material called felsitic porphyry, used almost continuously in the Palaeolithic period in the Carpathian basin and in exceptional cases outside too. The largest part of this relatively closed basin, the Great Hungarian Plain is formed by the alluvial deposits of the Danube and the Tisza rivers, with a Quaternary layer sequence up to 450 m in thickness. In the southern part of this region the 20-16 kys old *Ságvárian* and *Epigravettian* culture bearing layers are the earliest traces of the human presence, excavated in the depth of 4-5 meters. The aim of the study was to identify the most characteristic chemical components, with which it was possible to differentiate between objects of similar appearance.

## Results

Based on PGAA data, we were able to distinguish between two main groups of the objects. Objects of the first group typically contain relatively lower amount (75.3-82.4) wt% SiO<sub>2</sub>, while for the second group, SiO<sub>2</sub> content was found between 95.5 and 98.5 wt%. (Fig.) The first group contain the Szeletian porphyry objects, whereas the second type objects proved to be hornstone, radiolarite and limnique quartzite. Besides the silica content, concentrations of alkalis (Na<sub>2</sub>O and K<sub>2</sub>O), and TiO<sub>2</sub> turned out to be discriminative factors. Partly on the basis of the analytical results, the most interesting feature is observed in the case of the Vanyarc-type industry and the Bábonyian in the Cserhát, where the intense use of the felsitic porphyry and occasionally the obsidian is well documented, with on-site exploitation and tool rejuvenation even at the distance of 100-125 km from the source area.

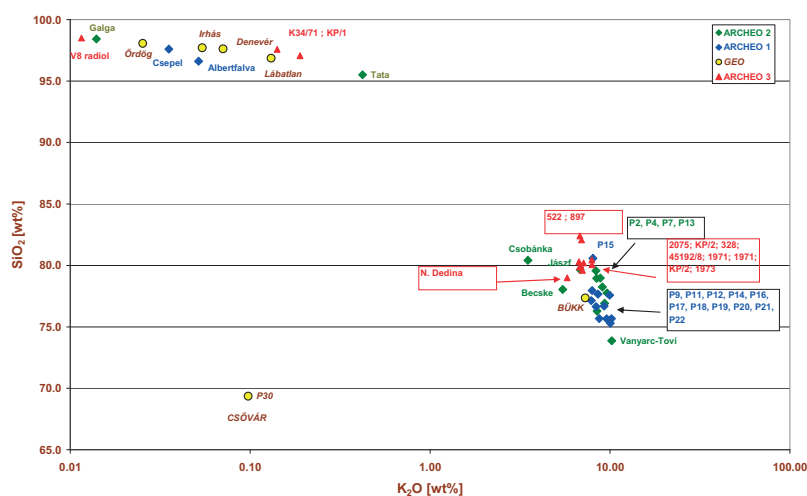


Figure: Differentiation between various stone objects, based on their Si and K content

## References

1. Markó A., T. Biró K., Kasztovszky Zs.: 'Szeletian felsitic porphyry': use and the determination of the raw material, SKAM 2012 Brno, Czech Republic

<b>B N C</b> <b>Experimental Report</b>	<i>Experiment title</i> <b>Bronze-Age Usage and Development of Defensive Armour in Hungary</b>	<i>Instrument</i> PGAA/NIPS  <i>Local contact</i> Zs.Kasztovszky
	<i>Principal proposer:</i> Marianne Mödlinger - Landesmuseum Kärnten, Klagenfurt, Austria <i>Experimental team:</i> Marianne Mödlinger, Zsolt Kasztovszky, Veronika Szilágyi, György Káli, Imre Kovács	<i>Experiment Number</i> BRR 253CH  <i>Date</i> 02.16.2011-02.19.2011

## Objectives

Weapons design applies the most advanced technologies a society has to offer. Until now, only one study on the composition and manufacture techniques of Central and Eastern European defensive armour have been published. Fundamental aspects of manufacture, use and functionality of cuirasses, greaves and helmets have not been comprehensively analysed yet and we are still left with a very incomplete picture of this aspect of Bronze Age life. By analysing material properties, shape and manufacture we gain insights not only into their manufacture, but also into the capability of these weapons to withstand impact during a fight. In cooperation with the Magyar Nemzeti Múzeum and museums in Szekszárd, Kaposvár, Paks and Keszthely, one cuirass, two complete greaves and further fragments of greaves as well as seven helmets have been studied and analysed. Especially for such rare and unique archaeological objects, carrying out non-invasive analyses is of high importance. Therefore, the carried out analyses as PGAA, PIXE and ToF-ND were chosen.

## Results

The results will allow us to identify and explain technological changes through time. Furthermore, we achieve more information on the production technique (the texture, structure and phases of the bronzes, analysed with the ToF-ND) and we gain information if the Bronze Age workshops were using different alloys for the same type of objects (PIXE, PGAA). Additional, while having a look at the structure, we can identify the intensity of post casting treatment. As well, the alloy-composition might indicate the dating of helmets and fragments of helmets.

With the PGAA, the alloying components of the bulk material, e.g. Cu and Sn were quantified. As far as we can say now, the Sn-content of the armour is around 10-15% or even lower. The trace elements – depending on their concentration in the different objects – were detected as well. The most important trace elements concerning archaeological bronzes were: S, Fe, Pb, As, Sb, Ag and Ni. With the PIXE, smaller areas of the objects were studied, which could not be analysed with the PGAA or the ToF-ND, as e.g. rivets and the thin wires of the greaves. Additionally, we were gaining more information about the composition of the corrosion.

On several elements such as Ni, Au, Pb and Bi XRS methods have a higher sensitivity than PGAA. Sb was more difficult, for both methods. Nevertheless, referring to already carried out analyses on Bronze Age objects, the exact amount of small quantities of Sb usually is of higher importance just for studies on Early Bronze Age or Copper Age objects for gaining more information about the ore source. For the Late Bronze Age, this is not necessary due to the high rate of recycling.



Figure: PGAA of a Bronze Age helmet (property of the Hungarian National Museum)

<h1 style="margin: 0;">B N C</h1> <p style="margin: 0;"><b>Experimental Report</b></p>	<i>Experiment title</i> <b>Characterization of Bükk Neolithic Culture pottery by non-destructive micro-PIXE, micro-PIGE and PGAA methods</b>	<i>Instrument</i> PGAA/NIPS
	<i>Local contact</i> Zs. Kasztovszky	<i>Experiment Number</i> BRR 252CH
<i>Principal proposer:</i> Viktoria Leno - University of Tübingen, Institute of Geoscience <i>Experimental team:</i> Daniel Schökle, Christian Luthardt, Veronika Szilágyi, Imre Kovács, András Kocsonya		<i>Date</i> 03.02.2011-03.05.2011

## Objectives

The objective of this part of the project was to achieve a bulk chemical description of Slovakian and Hungarian Bükk pottery samples by PGAA at BNC. PGAA was chosen because of its applicability for non-destructive chemical analysis of ancient ceramics samples. Especially, the Slovakian samples constitute a new contribution to earlier investigations, since up until now mostly Hungarian samples were investigated.

Together with micro-PIXE and -PIGE measurements conducted in Debrecen, the gained data can then be used for further investigations on provenance, possible long distance trade, manufacturing processes and fingerprinting of the Neolithic Bükk potteries.

## Results

We achieved a description of the bulk chemical composition of 29 Bükk pottery samples from Slovakia and Hungary. Together with further studies by micro-PIXE and -PIGE in Debrecen concerning the investigation of the incrustation of those ceramics, those results will contribute to current studies concerning the Bükk culture. PGAA made it possible to extend our knowledge of the composition of the ceramics on several Slovakian sites (Silica cave, Domica cave, Blatné and Stúrovo) while meeting the condition of preserving the samples by non-destructive measurements. With these data the Slovakian Bükk pottery can be included in the investigations concerning the provenance of the ceramics; it can extend the studies of the chemical composition of Bükk fineware as well as a possible chemical "fingerprint" of those ceramics.

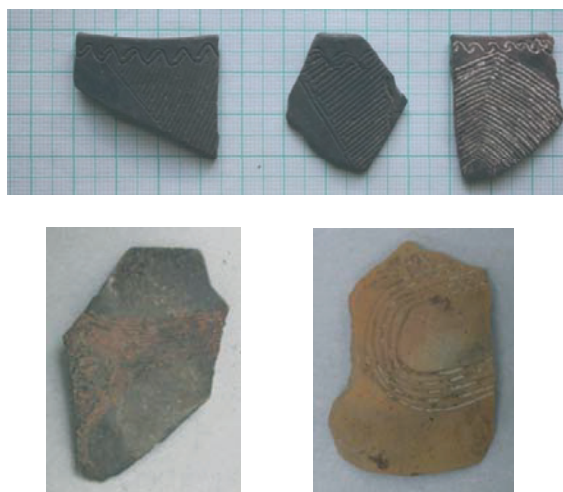
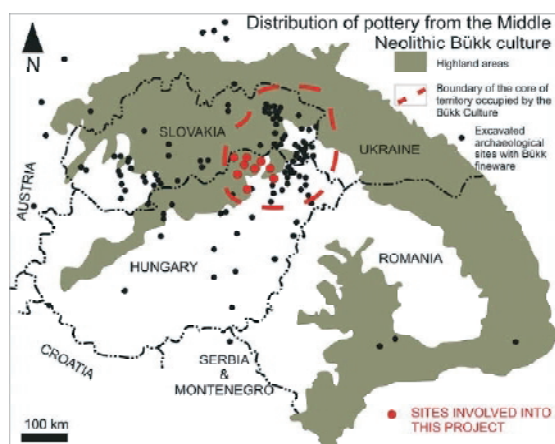


Figure: Photo of some investigated potteries

Further evaluation of the results still has to be done.

<h1 style="margin: 0;">B N C</h1> <p style="margin: 0;"><b>Experimental Report</b></p>	<p><i>Experiment title</i></p> <p><b>Defining border zones of people and goods in south Pannonian Basin during the Neolithic and Copper Age</b></p>	<p><i>Instrument</i></p> <p>PGAA/NIPS</p> <p><i>Local contact</i></p> <p>Zs. Kasztovszky</p>
	<p><i>Principal proposer:</i> Tihomila Težak-Gregl - Department of Archaeology, Faculty of Humanities and Social Sciences University of Zagreb</p> <p><i>Experimental team:</i> Marcel Buric, Rajna Šošić Klindžić, Zsolt Kasztovszky, Veronika Szilágyi</p>	<p><i>Experiment Number</i></p> <p>BRR 267 CH</p> <p><i>Date</i></p> <p>2011.03.07-03.11</p>

## Objectives

Participation in CHARISMA helps us to perform more analysis on obsidians and radiolarites using PGAA, both from present day Croatia and Hungary, in order to establish reliable criteria for distinction of different raw material sources using the PGAA method. Results will be combined with other analysis, such as micropaleontological and geochemical analysis. Special attention will be brought to efforts to determine Mecsek and Bakony radiolarites spread to the south in space and time span, as well as the obsidians originating from Tokaj area, both in terms of Neolithic period.

## Results

In the frame of CHARISMA we processed 26 stone tools samples from various archaeological sites in Croatia. Four of them were obsidians and 22 were radiolarites. We were able to quantify the major and some trace elements in the samples with non-destructive way. This Hungarian-Croatian CHARISMA collaboration is an extension of previous collaborations during which the very first interdisciplinary analyses of the Neolithic stone industry from Croatia were obtained. Based on PGAA results, we have found evidences to reconstruct the networks of trade routes developed between present-day Hungary and Croatia during prehistoric times. The analysis of origin-specific raw materials, such as obsidians and radiolarites, are especially suitable for studying the networks of that kind.

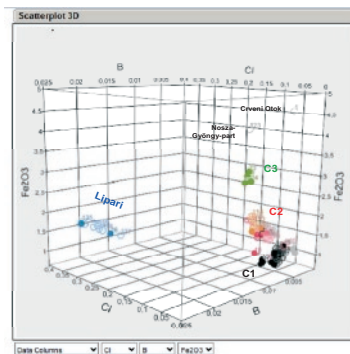


Fig.1 : 3D Scatter Plot of the investigated obsidians

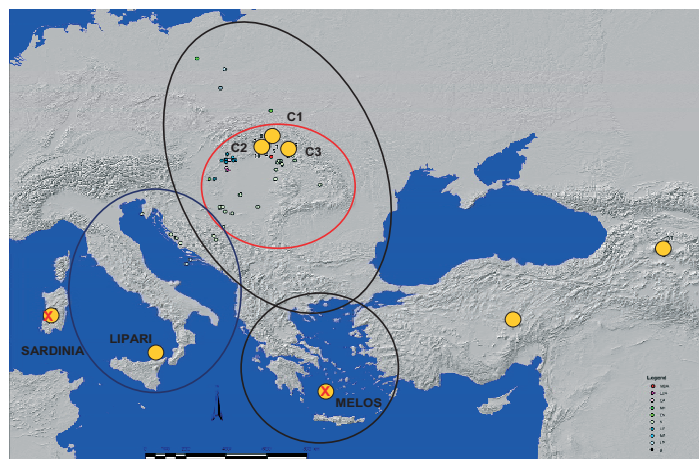


Fig. 2: Distribution of the investigated objects, supported by PGAA measurements

## References

1. Zs. Kasztovszky et al.: Recent provenance study of obsidian artefacts found in Central Europe, *39th Int. Symposium on Archaeometry, 2012, Leuven, Belgium*



<b>B N C</b> <b>Experimental Report</b>	<i>Experiment title</i> <b>Study of Copper Age shaft-hole axes found in Caput Adriae by non-destructive Prompt Gamma Activation Analysis</b>	<i>Instrument</i> PGAA/NIPS
	<i>Principal proposer:</i> E. Montagnari Kokelj - University of Trieste, Dipartimento di Storia e Culture dall'Antichita' al Mondo Contemporaneo <i>Experimental team:</i> Federico Bernardini, Zsolt Kasztovszky, Veronika Szilágyi	<i>Local contact</i> Zs. Kasztovszky

## Objectives

1. to control the PGAA efficacy for the rock types most used in the Caput Adriae; to perform PGAA on artefacts which have been already analysed by different analytical techniques and compare the geochemical results.
2. to create an initial database of PGAA results of the most important raw materials of polished stone tools of Caput Adriae. These data will be compared with the data available for neighbouring areas.
3. to better characterize the shaft-hole axes made from metaultramafite, which is one of the most used raw material during the Copper Age and whose origin is still debated.

## Results

We have measured more than 30 Copper Age polished stone axes from Caput Adriae by non-destructive PGAA. The archaeological objects were mainly made of meta-ultramafic rocks; additional reference rock samples have been analysed for major and few trace elements.

The obtained results were compared with the large amount of mineralogical and geochemical data available and in part already published. In fact, thin sections and a few geochemical analyses by Inductively Coupled Plasma-Mass Spectrometry (ICP-MS) are available from broken meta-ultramafite artefacts. Moreover, some thin sections have also been analysed by Electron Microprobe Analysis (EMPA). The results allow us to discover the provenance of the meta-ultramafite shaft-hole axes and in this manner to shed light on prehistoric exchange systems between north Adriatic and southeast Europe during Copper age (IV millennium-III millennium BC).

PGAA has proven its efficacy for the chemical analysis of the most used rock types for the production of prehistoric polished stone axes found in the Caput Adriae. The collected data have allowed creating an initial database of PGAA results of the most important raw materials. These data were compared with the PGAA data available for neighbouring areas and in particular for Pannonian basin.

## References

1. F. Bernardini, et al.: Mineralogical and chemical constraints about the provenance of copper age polished stone axes of "Ljubljana type" from Caput Adriae, *submitted to Archaeometry*.

<h1 style="margin: 0;">B N C</h1> <p style="margin: 0;"><b>Experimental Report</b></p>	<i>Experiment title</i> <b>Provenance study of various high silica content archaeological stone objects from Central Europe – A case study: Kup</b>	<i>Instrument</i> PGAA/NIPS  <i>Local contact</i> Zs. Kasztovszky
	<i>Principal proposer:</i> Katalin T. Biró – Hungarian National Museum <i>Experimental team:</i> Zsolt Kasztovszky, Veronika Szilágyi, Boglárka Maróti	<i>Experiment Number</i> PGAA_12_35_NC <i>Date</i> 2011.08.31-2012.09.18

## Objectives

Kup-Egyes is a Neolithic settlement in West Central Hungary, close to Pápa. Production of stone tools is one of the most important activity on the site. Local and regional raw materials, flint and radiolarite can be found in large quantities and instances of polished stone tools can also be found here. Their geochemical investigation is essential in providing reference material for provenance studies. Moreover, polished stone tools were also found and chemically investigated from the site (basalt, greenschist, metabasite) that will contribute to the assesment of polished stone tool trade database apart from the significance of the Kup site.



Photo: Photo of some stone objects from Kup

## Results

Based on PGAA our lithics database, containing major and trace concentrations is being extended (See Table). Evaluation of the analytical results is in progress.

	SiO <sub>2</sub>	TiO <sub>2</sub>	Al <sub>2</sub> O <sub>3</sub>	Fe <sub>2</sub> O <sub>3</sub>	MnO	MgO	CaO	Na <sub>2</sub> O	K <sub>2</sub> O	H <sub>2</sub> O	CO <sub>2</sub>
<i>Kup, zöldpala nyéllukas balta</i>	48.2	1.865	10.2	15.8	0.190	13.4	4.8	0.62	1.37	3.35	
<i>Kup, zöldpala vésőbalta</i>	49.3	1.247	16.9		8.360	7.4	8.8	3.91	0.07	3.54	
<i>Kup, zöldpala csiszolt balta</i>	53.3	1.209	15.8	7.8	0.119	6.3	7.6	4.98	0.06	2.83	
<i>Kup, ékvéső, zöldpala</i>	51.0	3.402	13.0	14.6	0.255	6.1	8.3	1.34	0.16	1.10	
<i>foltos tűzkő, Szerbia</i>	99.0		0.1		0.003		0.0	0.03	0.04	0.74	
<i>Kup, sárgásfehér, meszes</i>	1.8	0.022	0.4	0.6	0.041	0.7	52.0		0.10	0.46	43.9
<i>Kup, sárgásfehér, meszes</i>	42.2	0.523	9.9	16.0	0.981	16.1			2.29	10.92	
<i>Kup, kőeszköz töredék</i>	55.1	0.794	18.6	4.3	0.095	5.8	10.1	0.74	2.55	1.78	

	B	S	Cl	Sc	V	Cr	Co	Ni	Nd	Sm	Gd
<i>Kup, zöldpala nyéllukas balta</i>	1.50E-03		0.0138	0.0025	0.020	0.044				2.91E-04	3.41E-04
<i>Kup, zöldpala vésőbalta</i>	5.57E-05	0.067	0.0024	0.0049	0.030	0.085				2.08E-04	3.58E-04
<i>Kup, zöldpala csiszolt balta</i>	8.67E-05		0.0019	0.0040	0.022				1.54E-03	1.91E-04	3.13E-04
<i>Kup, ékvéső, zöldpala</i>	1.96E-04	0.206	0.0040	0.0029	0.034	0.032			4.20E-03	5.36E-04	7.40E-04
<i>foltos tűzkő, Szerbia</i>	1.80E-02		0.0023						7.39E-04		1.18E-05
<i>Kup, sárgásfehér, meszes</i>	5.36E-04		0.0012		0.022	0.146			7.25E-04	5.49E-05	8.53E-05
<i>Kup, sárgásfehér, meszes</i>	1.28E-02		0.0279		0.518	0.006			1.73E-02	1.32E-03	2.03E-03
<i>Kup, kőeszköz töredék</i>	6.05E-03		0.0137	0.0020	0.014				3.73E-03	5.14E-04	5.78E-04

Table: Chemical composition of some stone objects from Kup

## References

1. Preliminary results were presented on the 5<sup>th</sup> Petroarchaeology Symposium, Brno 25.11.2012.

<b>B N C</b> <b>Experimental Report</b>	<i>Experiment title</i> <b>Technological and Provenance Studies of Peloponnese Archaeological Glass: Blue Mycenaean Objects and Roman Coloured Mosaic Tesserae</b>	<i>Instrument</i> PGAA/NIPS  <i>Local contact</i> Zs. Kasztovszky
	<i>Principal proposer:</i> Nikolaos Zacharias - Lab of Archaeometry, University of the Peloponnese, Greece <i>Experimental team:</i> Nikolaos Zacharias, Maria Kaparou, Zsolt Kasztovszky, Veronika Szilágyi, György Káli, Imre Kovács	<i>Experiment Number</i> BRR 278 CH <i>Date</i> 09.11.2011-09.16.2011

## Objectives

A key question in archaeological research remains the assignment of provenance for glass objects and this has been the core issue for glass material recovered from sound Peloponnese Mycenaean Palatial centers namely Mycenae, Pylos, Tiryns but also from archaeological sites excavated in the Argolid, Messinia and Lakonia. The study is focused on the analytical examination of blue/dark blue glass artifacts (namely, beads and plaques) from the above mentioned Peloponnese archaeological sites within a twofold aim of: exploring the intra-Peloponnese correlations on a technological and analytical level for the studied objects and also investigating the inter Peloponnese / Egypt and Mesopotamia associations. A second research direction of the proposed study aims at investigating Late Roman mosaic tesserae artefacts excavated at the archaeological site of Ancient Messene (SW- Peloponnese). They are securely dated to the third century AD but it is not clear whether they were part of a wall or floor decoration due to the fact that they were found scattered. The blue, white, red and purple tesserae were opacified by calcium antimonate crystals, whereas lead and antimony compounds acted both as colouring and opacifying agents for yellow and green specimens. As the main goal, the determination of the origin of calcium antimonate minerals (stibnite or roasted stibnite) is an essential parameter for provenance and technological issues to be explored.

## Results

The application of PGAA on all glass samples (totally 19) provided useful data to be evaluated within the very next months. Based on the results, elemental concentrations of light elements and actinides proved to be unique indicators of base glass used for the production of the material. Concentration values for major and minor elements were compared with those acquired from earlier applications of SEM/EDAX and EDS/XRF and found to be in good agreement. Additionally, the application of PIXE on selected corroded samples was initiated to provide a better spotted (restricted areas of the samples) information on clean and possibly intact from corrosion effects, areas of the samples.

The rest of laboratory measurements performed for the study of the mosaic tesserae (totally 15 samples), TOF-ND indicated for low counting statistics thus the additional use of Neutron Diffraction (PSD) measurements was undertaken.

## References

1. Nikolaos Zacharias, et al.: A Technological and Provenance Study of Two Mycenaean Glass Collections Using X-Rays and Ion-Beam Analyses, *39<sup>th</sup> International Symposium on Archaeometry, Leuven, Belgium*

<b>B N C</b> <b>Experimental Report</b>	<i>Experiment title</i> <b>Application of PGAA for the study of the late- and post-medieval glass from Hungary and Poland. A comparative study</b>	<i>Instrument</i> PGAA/NIPS  <i>Local contact</i> Zs. Kasztovszky
	<i>Principal proposer:</i> Jerzy Kunicki-Goldfinger - Institute of Nuclear Chemistry and Technology <i>Experimental team:</i> Jerzy Kunicki-Goldfinger, Zsolt Kasztovszky, Veronika Szilágyi	<i>Experiment Number</i> BRR 265 CH <i>Date</i> 2011.09.18-09.22

### Objectives

The proposed experiment aimed to recognise the possible differences in chemical composition between glasses made and utilized in Hungary and Poland from late-medieval times to the 18th century. The results will contribute to the knowledge about Central European glass.

In addition to major and minor glass constituents, we also analysed some trace elements, such as gadolinium, samarium, and boron. The PGAA allowed us to analyse them with an extremely low detection limit.

### Results

Thirty five historical glass fragments, such as vessel fragments, window panes as well as slags and moils from chosen glasshouses and other archaeological sites have been analysed. They were examples excavated from the 14-15th century Hungarian glasshouse in Diósjenő and 18-19th century Hungarian glasshouse in Gyertyánvölgy; a selection of archaeological glass material from Buda castle (14-15th and 18-19th centuries) and Visegrád castle (14-15th and 18-19th century) as well as post-medieval window glass panes excavated in the Old Town in Elbląg (Poland). Additionally, a set of glass reference materials was analysed.

All fragments were analysed non-destructively without any sampling of material, which might be considered as a one of the main advantages of the PGAA in glass archaeometry.

The possibility to compare the chemical composition of glasses made and/or utilized in Hungary and Poland might be considered as a main achievement of the project. There are no such comparative studies published.

The most important difficulty encountered concerns the possibility to analyse severely corroded items (with deposits and thick leached layers), as PGAA is a bulk analysis and the results received concern the entire investigated object or its fragment.

<b>B N C</b> <b>Experimental Report</b>	<i>Experiment title</i> <b>The Charecterisation of Middle Bronze Age smelting slags from the Southern Urals</b>	<i>Instrument</i> PGAA/NIPS  <i>Local contact</i> Zs. Kasztovszky
	<i>Principal proposer:</i> Roger Doonan - The University of Sheffield <i>Experimental team:</i> Derek Pitman, Zsolt Kasztovszky, Veronika Szilágyi	<i>Experiment Number</i> BRR 275 CH <i>Date</i> 10.05.2011-10.08.2011

### Objectives

This analytical program is part of a broader program archaeological investigation that centres on material from the southern Ural steppe that dates to the Middle Bronze Age (2100-1500BC). The region which is known archaeologically as 'the country of towns' is associated with the so called Sintashta Culture and is a significant case study into the emergence of complexity and the early developments of metallurgy. The primary aim of this analytical project was to characterise the slag material excavated from these sites in order to establish the technological choices employed by ancient smelters. Specifically, we sought to answer the following questions:

- 1) To what extent does the evidence for metal production from the Stepnoye and Ust'ye settlements support the concept of a uniform Sintashta metallurgical tradition?
- 2) What technological parameters were chosen by Bronze Age metallurgists and how is this captured in slag chemistry.

### Results

A total of 30 samples were able to be analysed in the allotted time which represents a significant sample of slag from both settlements.

In terms of the project aims it is possible, based on an initial examination of the dataset, to suggest that the metallurgical process was not uniform at the two sites; in fact there seems to be noticeable chemical variation between the sites and even within each settlement. This could have potentially significant implications regarding our understanding of metallurgy in the southern Urals. In the future the results will be accompanied by complimentary techniques such as XRF, SEM-EDS, this will allow a full characterisation of the slag assemblage which will hopefully reveal even more about the smelting practices that took place during the Middle Bronze Age.

Due to areas of tourmaline rich geology in the Southern Urals a secondary aim of the work was to establish the presence of Boron in the slags, which has proved difficult with other analytical techniques. The results do show very small amounts of boron in the samples, which will important when attempting to explore resource procurement strategies.

<b>B N C</b> <b>Experimental Report</b>	<i>Experiment title</i> <b>Provenancing Iron: Sourcing Iron Produced from Bog Ore</b>	<i>Instrument</i> PGAA/NIPS  <i>Local contact</i> Zs. Kasztovszky
	<i>Principal proposer:</i> Thomas Birch - University of Aberdeen, UK <i>Experimental team:</i> Thomas Birch, Tim Michall, Zsolt Kasztovszky, Boglárka Maróti, György Káli, László Almásy	<i>Experiment Number</i> BRR 276 CH <i>Date</i> 10.10.2011-10.13.2011

### Objectives

The research project had very specific aims and objectives outlined below:

- to analyse and study the element composition of all iron production residues (ore, fuel, clay, slag, iron);
- to analyse and study the behaviour of trace elements in multiple smelting systems (four);
- to assess the variability of chemical composition within a bog-ore deposit;
- to assess the differences between tree species used for charcoal;
- to assess the variability of chemical composition within the slag produced from a single smelt, and
- to construct a 'bog-ore' provenance model.

### Results

PGAA and other neutron beam techniques are invaluable non-destructive means of learning material composition and properties;

- The accuracy and precision of the PGAA instrument was very impressive, particular for majors and particular traces
- The analytical results proved to be very informative and provided useful detail on aspects of the smelting system
- Other techniques provided at the BNC (TOF-ND, SANS) will provide complimentary data to the compositional data being obtained
- The prospect of establishing future collaboration in developing the project appeared promising.

The following feedback is submitted here:

- The range of elements analysed at trace level was less than hoped for
- Time needed for analysis can be long and influenced the number of samples analysed (this point was resolved)

### References

1. Thomas Birch, et al.: Using PGAA to determine the composition of experimental iron smelting residues: strengths and limitations of a non-destructive analytical technique, *39<sup>th</sup> International Symposium in Archaeometry, Leuven, Belgium*
2. Thomas Birch, et al.: Ore, slag and inclusion: measuring variability in the direct process and assessing its implications for provenancing iron using the SI method, *39<sup>th</sup> International Symposium in Archaeometry, Leuven, Belgium*

<h1 style="margin: 0;">B N C</h1> <p style="margin: 0;">Experimental Report</p>	<i>Experiment title</i> <b>Searching for the provenance of the lithic geoarchaeological material from Micula, Carei (Satu Mare County) and Târgu Mureş (Mureş County), Romania</b>	<i>Instrument</i> PGAA/NIPS
	<i>Principal proposer:</i> Corina Ionescu - Babes-Bolyai University of Cluj Napoca, Romania <i>Experimental team:</i> Corina Ionescu, Zsolt Kasztovszky, Boglárka Maróti	<i>Local contact</i> Zs. Kasztovszky

## Objectives

To study the geochemical composition of the obsidian and limnoquartzite lithic tools from Micula - 10 pc. and obtain the provenance based on the comparison to the PGAA database.

To study the geochemical composition of the obsidian and silex lithic tools from Carei - 9 pc. and obtain the provenance based on the comparison to the PGAA database.

To study the geochemical composition of the obsidian and silex lithic tools from Mureş County Museum - 10 pc. and obtain the provenance based on the comparison to the PGAA database.

## Results

1. We used the first measuring chamber for the smaller (approx. less than 8 cm in diameter) samples.
2. We were able to measure the geochemical composition of the obsidian and limnoquartzite tools from Micula and obtained their provenance based on the comparison to the PGAA database.
3. We were able to measure the geochemical composition of the obsidian and silex tools from Carei and obtained their provenance based on the comparison to the PGAA database.
4. We were able to measure the geochemical composition of the obsidian and silex tools from Mures County Museum and obtained their provenance based on the comparison to the PGAA database.
5. By combining the mineralogical-petrographical and geochemical data with the archaeological background, new social, technological and economical information resulted (the obsidian might originate from the Tokaj Mts. while the silex and limnoquartzite material might have local sources, it could be supposed that the Eastern Carpathians and Apuseni Mts. provided the raw material for these ancient societies).
6. By using the small and large chambers (PGAA and NIPS) for the same tool, it was possible to compare and double check the results achieved by the two different measuring locations.



Figure: Measurement of large obsidian core at the NIPS/NORMA station

## References

1. Zs. Kasztovszky et al.: Recent provenance study of obsidian artefacts found in Central Europe, 39th Int. Symposium on Archaeometry, 2012, Leuven, Belgium

<b>B N C</b> <b>Experimental Report</b>	<i>Experiment title</i> <b>Mankind's earliest iron – investigating the meteoritic beads from Gerzeh, 3,500 BC</b>	<i>Instrument</i> PGAA/NIPS  <i>Local contact</i> Zs. Kasztovszky
	<i>Principal proposer:</i> Thilo Rehren - University College London <i>Experimental team:</i> Thilo Rehren, Zsolt Kasztovszky, Boglárka Maróti, Zoltán Kis, László Szentmiklósi	<i>Experiment Number</i> BRR 277 CH <i>Date</i> 12.12.2011-12.15.2011

### Objectives

The aim was to determine the nature of the iron from which these earliest iron beads are made - can we demonstrate that they are meteoritic in origin, as has been speculated based on their early date? Specifically, can we determine the crystal structure of the beads (presence of schreibersite  $Fe_3P$  crystals, grain size of remaining metallic iron), their chemical composition (particularly full body composition of nickel, cobalt, germanium), and any other related information.

### Results

The main achievements were that the neutron imaging showed in much detail how the beads were formed from wrapping a sheet of metal around to make a tube, with some overlap at the join. It also indicated that there is no metallic iron left. The ToF-ND confirmed this assumption, with no clear crystal phases being identifiable (but data processing is still ongoing). Chemical characterisation of the beads with PIXE and PGAA revealed a very strong signal for nickel, in the order of 5 to 8 percent by weight, and a significant cobalt peak, around 0.2 wt%, as well as a small peak for germanium in one of the three beads (data processing ongoing). Thus, the main objectives were achieved; however, there were a number of difficulties, for instance the small size and severely corroded state of the material, preventing successful ToF-ND application. Similarly, germanium determination by PGAA was hampered by the presence of Ge in the detector. However, the analytical approach has been adjusted, including accommodation the analysis of comparative material to determine the reasons for the analytical difficulties (hydrogen content of the corroded material) and finding ways to address them (spectra overlay of Ge-free comparative samples to compensate for detector germanium levels).

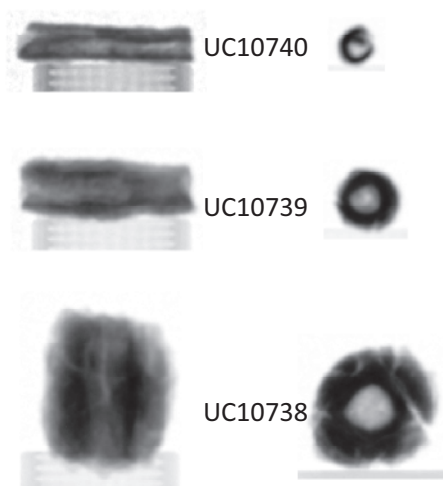


Fig. 1: Neutron radiography image of Egyptian iron beads



Fig. 2: Positioning of iron beads at NORMA station



<b>B N C</b> <b>Experimental Report</b>	<i>Experiment title</i> <b>PGAA of neolithic Ceramic vessels from Nagytétény</b>	<i>Instrument</i> PGAA/NIPS
	<i>Principal proposer:</i> Katalin T. Biró – Hungarian National Museum <i>Experimental team:</i> Zsolt Kasztovszky, Veronika Szilágyi	<i>Local contact</i> Zs. Kasztovszky

## Objectives

In 1936, a grave with four ceramic vessels, allegedly belonging to 4 different prehistoric cultures was found at Nagytétény. This grave is one of the most famous instances of Neolithic pottery trade, established only on archaeological typological argumentation so far. The aim of the PGA analysis was to check pottery chemical composition to support / modify this view. Comparative samples from coeval sites from Budapest area were also measured.

## Results

Two of the Nagytétény vessels are chemically different from the others. Vessel 4/1936.1. („Bükk”) and 4/1936.3. („Zseliz”) are chemically very close; 4/1936.2. („Vinča”) and 4/1936.4 („TLBC/undecorated Zseliz”) are chemically different from each other and the other two.

Results were compared to Bükk pottery vessels investigated in the MÖB-DAAD 3 project. The „cloud” of Bükk pottery vessels could include all four Nagytétény vessels. The most distinctive elements are seemingly Ti and Sm (especially in respect of the („Vinča”) pot. The chemical composition of the Nagytétény vessels were also compared to shards from coeval sites from Budapest. The Budapest shards also fit in the established Bükk cloud. It seems that the Növény utca pieces are in fact closer to the most local element of the Nagytétény grave 4/1936.4 („TLBC/undecorated Zseliz”) and they form no group with the shards from the Northern parts of Budapest. The vessels of the Nagytétény grave can be typologically assigned into –at least – three different cultural units (1,2, 3-4). We can separate them on the basis of chemical composition into three units, too, but in a different way. (2, 4, 1-3). The Bükk pottery „cloud” embraces all of them (perhaps 2 as outlier). The number of comparative material from Budapest sites is very small as yet; it seems that local (Növény utca) shards are closest to the „local” (4) pot.

We need a lot more data from regional studies to have a final solution of the problem.



## References

1. Katalin T. Biró, Veronika Szilágyi, Zsolt Kasztovszky, Zsuzsanna M. Virág: Nagytétény: the grave of a prehistoric cosmopolitan EMAC '11 Conference, Vienna

<b>B N C</b> <b>Experimental Report</b>	<i>Experiment title</i> <b>Carpathian Regional Exchange Materials of the Eneolithic and Neolithic Eras</b>	<i>Instrument</i> PGAA/NIPS  <i>Local contact</i> Zsolt Kasztovszky
	<i>Principal proposer:</i> Otis Crandell - Babes-Bolyai University, Cluj-Napoca, Romania <i>Experimental team:</i> Otis Crandell, Zsolt Kasztovszky, Boglárka Maróti	<i>Experiment Number</i> BRR 301 CH <i>Date</i> 2012.01.24-01.28.

### Objectives

There were two main objectives to this study. The first was to determine how well several macroscopically similar materials could be distinguished by PGAA analysis. The investigated categories were flint, opal, jasper and chert – all very similar macroscopic appearance showing very high SiO<sub>2</sub> content with slightly changing amount of minor and trace elements. The second objective was to compare archaeological artefacts with rock samples to help determine the source of the material from which the artefacts were made.

### Results

Thirty samples - 25 rock samples and 5 artefacts – have been analyzed by PGAA. Preliminary comparison of spectra for rock samples suggests that the three rock categories analysed in this study (i.e. opal, jasper, and chert) can be distinguished from each other based on PGAA data. After careful statistical analysis of the results, it turned out that Fe distinguishes well between the two kinds of flints from Dobrogea and from Moldavia. This confirms the idea that the artefacts are from the Dobrogea area. On the contrary, Fe is not good element for distinguishing between general cherts and flints. The iron content seems to be connected to outcrops. When comparing Ca and Na content of flints and cherts, Ca in cherts seems to be much higher. It may be the calcium carbonate in the rock that was not changed to silica. Na might also be useful for distinguishing the two materials.

When comparing jasper and opal, the hydrogen content seems to be highest in the opals (probably connected to water content). The jaspers also seem to have higher hydrogen content than the cherts but not as much as the opals. The iron content in the jaspers appears to be higher than in the cherts.

The artefact spectra which were observed show a higher presence of iron. This is consistent with the high iron oxide content observed in petrographic thin sections. These preliminary observations, along with petrographic analyses and previous PGAA analyses of rock samples suggest that the source of the artefacts can be identified (which in turn supports the theory that they were long distance imported objects).

### References

<h1 style="margin: 0;">B N C</h1> <p style="margin: 0;"><b>Experimental Report</b></p>	<i>Experiment title</i> <b>Origin and distribution of obsidian in Poland</b>	<i>Instrument</i> PGAA/NIPS  <i>Local contact</i> Zsolt Kasztovszky
	<i>Principal proposer:</i> Iwona Sobkowiak-Tabaka - Insitute of Archaeology and Ethnology Polish Academy of Sciences, Poznan, Poland <i>Experimental team:</i> Iwona Sobkowiak-Tabaka, Zsolt Kasztovszky, Boglárka Maróti	<i>Experiment Number</i> BRR 298 CH <i>Date</i> 2012.02.14-02.18

## Objectives

It was aimed to investigate 49 obsidian archaeological objects originated from 4 sites of different archaeological periods, located in different parts of Poland, using Prompt Gamma Activation Analysis. The biggest collection originates from Cichmiana (Polish Lowland) and is connected with Late Palaeolithic, the second one is from Rudna Wielka (Pogorze Karpackie, SE part of Poland) and it is dated to the Neolithic (Linear Band Pottery Culture) and two last objects are from Kowalewko (Polish Lowland, Linear Band Potery Culture) and Mokrsko Szlacheckie (Krakow-Czestochowa Upland, Late Palaeolithic). Based on chemical composition compared with existing data base, we aimed to determine the provenance of the objects.

## Results

During the available beamtime, it was possible to analyse 25 pieces. Unfortunately, the rest of the collection consist of too small to achieve statistically significant data, We were able to quantify the major elements H, Na, Al, Si, S, Cl, K, Ca, Ti, Mn, Fe, and traces of B, Nd, Sm and Gd. Based on the PGAA results, and using statistical methods, all of the investigated objects turned to show a typical composition, which is characteristic for the so-called "Carpathian 1" obsidian type, a well localized geological source region on North of the Tokaj mountains (Vinicky or Cejkov locations). Most of the pieces measured with PGAA, were measured with portable XRF Spectroscopic device. Since the XRF machine is only in testing mode yet, the data will be useful to check the reliability of it, and to define further calibration routine for the XRF.

A possibility to investigate the small pieces at FRM II PGAA facility has been considered.

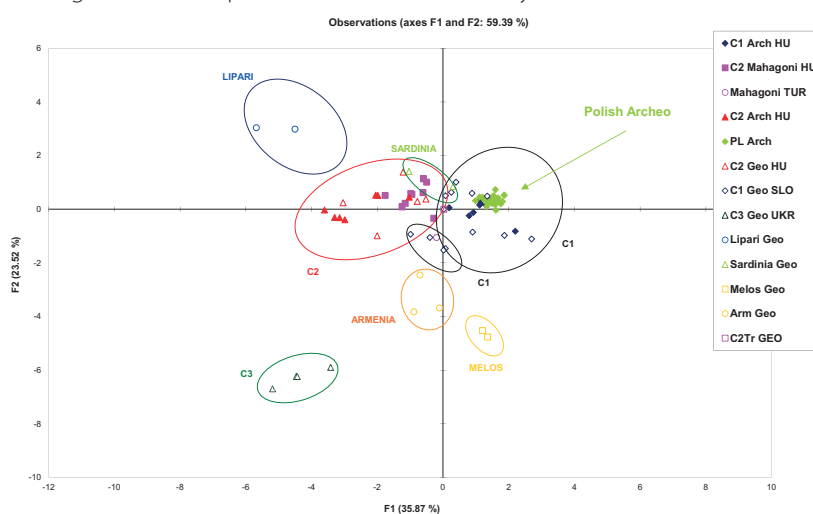


**Fig. 1:** PCA of measured obsidian compositional data. Geological references, Polish and Hungarian archaeological pieces are compared

## References

<b>B N C</b> <b>Experimental Report</b>	<i>Experiment title</i> <b>Bronze measurements</b>	<i>Instrument</i> PGAA <i>Local contact</i> Boglárka Maróti
	<i>Principal proposer:</i> Boglárka Maróti <i>Experimental team:</i> Boglárka Maróti, Tamás Belgya, Zsolt Kasztovszky – Centre for Energy Research	<i>Experiment Number</i> PGAA_12_51_IH <i>Date</i> 2012.02.23- 2012.02.24

### Objectives

Several bronze alloys were measured by PGAA our routine method, to compare the results of the newly acquired handheld XRF equipment.

### Results:

For the reason, that PGAA is a bulk analytical method, and XRF is for surface composition measurement, first measurements were done several bronze samples with corrosion-free surface. One of these, well demonstrative example is presented. There were no significant differences between the 3 PGAA results, taken in 3 different points with a 24 mm<sup>2</sup> neutron collimator. In case of XRF a 7 mm<sup>2</sup> X-ray beam was used. Because of the lack of the corrosion layer, differences can be derived from the inhomogeneity of the bronze.

Bronze VII.	Cu	±	Zn	±	Sn	±	Pb	±
XRF 1	<b>62.01</b>	0.19	<b>0.81</b>	0.03	<b>27.78</b>	0.19	<b>7.92</b>	0.09
XRF 2	<b>62.26</b>	0.18	<b>0.52</b>	0.03	<b>27.6</b>	0.19	<b>8.24</b>	0.1
XRF 3	<b>63.74</b>	0.19	<b>0.43</b>	0.03	<b>27.68</b>	0.19	<b>6.88</b>	0.09
XRF 4	<b>63.06</b>	0.19	<b>0.43</b>	0.03	<b>27.63</b>	0.19	<b>7.26</b>	0.09
XRF 5	<b>63.17</b>	0.19	<b>0.51</b>	0.03	<b>27.52</b>	0.19	<b>7.31</b>	0.09
PGAA (3)	<b>67.24</b>	0.82	<b>N.D.</b>		<b>26.56</b>	0.63	<b>6.20</b>	0.71

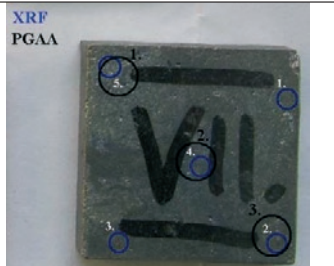


Figure 1/A and B: Comparison of the PGAA and XRF results (A). Measured points by XRF and PGAA (B).

<h1 style="margin: 0;">B N C</h1> <p style="margin: 0;"><b>Experimental Report</b></p>	<i>Experiment title</i> <b>Provenance study of Central European obsidian archaeological objects – A case study: Red obsidians</b>	<i>Instrument</i> PGAA/NIPS  <i>Local contact</i> Zsolt Kasztovszky
	<i>Principal proposer</i> : Katalin T. Biró, András Markó – Hungarian National Museum <i>Experimental team</i> : Zsolt Kasztovszky, Veronika Szilágyi, Boglárka Maróti – Centre for Energy Research	<i>Experiment Number</i> PGAA_12_53_NC <i>Date</i> 2011.08.31- 2012.09.18

### Objectives

For provenance study of archaeological obsidians, large database of references from the main geological sources is necessary. Besides the Mediterranean sources, three types of the Carpathian (Tokaj) obsidians are known. One sub-type of the C2 is called red or mahagonian obsidian (T2r) with characteristic red-brown colour. We aimed to extend our database with measurements of T2r geological and archaeological pieces from Tolcsva, Kálló and Arka, respectively.

### Results

At the moment, our PGAA obsidian database consists of 160 archaeological pieces from Central Europe, and about 100 geological references from all the major European- (so-called, Mediterranean) sources, incl. Tokaj-Prešov mts. (Slovakia, Hungary), Lipari, Sardinia, Palmarola, Melos, Yali, Antiparos, Armenia and Anatolia. Reddish coloured ('Mahogany') obsidian has been previously poorly represented in our collection, but with the help of the Hungarian National Museum we were able to increase the number of the investigated objects. The pieces came from the geological occurrence in "Tolcsva-Ciróka árok" and excavation material from "Arka-Herzsa rét", both in the Tokaj Mountains, NE Hungary. Red obsidian from more distant sites e.g. Kálló and Legénd were also included. B-Cl diagram proved to be very efficient in separating individual source regions. C2Tr pieces fit well into former models; they show consistent B content but Cl content seemingly varies quite a bit that must be geochemically explained.



**Fig. 1:** Mahogany obsidian from Kálló

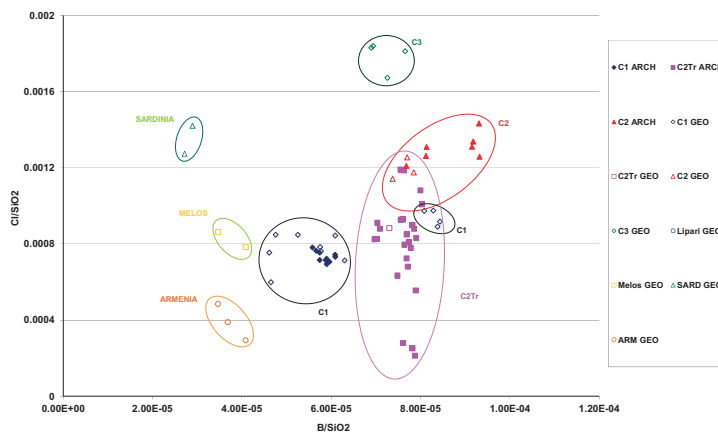


**Fig. 2:** Classification of the main obsidian sources according to their B- and Cl content

### References

Biró, Katalin T., Markó, A., Kasztovszky, Zs., 'Red' obsidian in the Hungarian Palaeolithic. Characterisation studies by PGAA *Præhistoria* (2005) **6** 91–101.

<h1 style="margin: 0;">B N C</h1> <p style="margin: 0;"><b>Experimental Report</b></p>	<i>Experiment title</i> <b>Archaeological obsidian characterization using PGAA, External milli-PIXE and XRF</b>	<i>Instrument</i> PGAA/NIPS  <i>Local contact</i> Zsolt Kasztovszky
	<i>Principal proposer:</i> Bogdan Constantinescu - National Institute of Nuclear Physics and Engineering, Bucharest, Romania <i>Experimental team:</i> Bogdan Constantinescu, Daniela Cristea-Stan - - National Institute of Nuclear Physics and Engineering, Bucharest, Romania	<i>Experiment Number</i> BRR 317 CH <i>Date</i> 2012.08.29-09.04.

## Objectives

Thirty archaeological samples from different regions of Romania and from different prehistorical periods were analysed by PGAA and by external milli-beam PIXE: Iclod, Tzaga, Silagiu sites in Transylvania, Neolithic period; Cuina Turcului site at Iron Gates (on Danube border, between Romania and Serbia), Early Neolithic (Neolithisation) and Neolithic period; Magura site in Teleorman County (South of Bucharest, near Danube), Early Neolithic (Neolithisation period).

The aim of the study was to identify obsidian geological sources used in each region and period. Two main geological regions are presumed to be the obsidian sources for Romanian territory: Tokaj Mountains (Carpathian I – now in Southern Slovakia and Carpathian II – now in Northern Hungary) and Greek Islands – especially Melos (Aegean Sea).

## Results

PGAA proved to be the most convenient method to quantify the major components and some characteristic trace elements in the bulk material, most of all B and Cl, in a non-invasive way. Compositions of archaeological objects were compared with our own reference database including the major European and Mediterranean sources. B/SiO<sub>2</sub> vs. Cl/SiO<sub>2</sub> ratios and Principal Components Analysis (PCA) proved to be the most indicative in determination of different groups.

Our results indicate all the Transylvanian Neolithic samples fit the “Carpathian I” pattern. The same pattern can be attributed to Neolithic Cuina Turcului samples. A special situation is for the Neolithisation period, both for Cuina Turcului and Teleorman. These samples fit Carpathian II pattern, however, based on K<sub>2</sub>O content, these samples are very similar to those from Yali Island (Aegean Sea). Since the latter are known to show weak mechanical quality, it has been less probably used for tools production.



Fig. 1: Map of occurrences of the studied obsidians

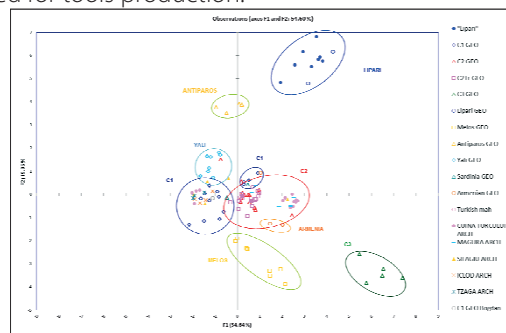


Fig. 2: PCA of the measured PGAA data.

## References

- [1] Constantinescu, B. et al., PGAA analysis of some Neolithic obsidian samples from Romanian regions, NINMACH 2013, Garching, Germany
- [2] Constantinescu, B. et al., External beam milli-PIXE as analytical tool for Neolithic obsidian provenance studies, 13<sup>th</sup> Int. Conference on Particle Induced X-ray Emission, 2013, Gramado, Brazil
- [3] B. Constantinescu, D. Cristea-Stan, I. Kovács, Z. Szőkefalvi-Nagy, Provenance studies of Central European Neolithic obsidians using external beam milli-PIXE spectroscopy (2013), NIM-B *in press*

<h1 style="margin: 0;">B N C</h1> <p style="margin: 0;">Experimental Report</p>	<p><i>Experiment title</i>  <b>Provenance Oriented Interdisciplinary Glass Studies: the Hagia Sofia at Constantinopolis Glass Tesserae and a Mycenaean Glass Collection from Patras, Archaia</b></p>	<p><i>Instrument</i>  PGAA  <i>Local contact</i>  Zsolt Kasztovszky</p>
	<p><i>Principal proposer:</i>  Nikolaos Zacharias - Department of History, Archaeology and Cultural Resources Management, University of Peloponnese  <i>Experimental team:</i>  Nikolaos Zacharias, Tonia Moropoulou, Maria Kylafi, Zsolt Kasztovszky, Boglárka Maróti</p>	<p><i>Experiment Number</i>  BRR 320_CH  <i>Date</i>  2012.10.16-  2012.10.19</p>

## Objectives

Hagia Sophia (532-537 A.D.) dome stands as one of the most well-known and dazzling monuments of world cultural heritage. The glass tesserae of the Hagia Sophia dome mosaics consists of opaque, colored glasses and metallic gold glasses (16 samples in total). The proposal suggests the examination of blue/dark blue glass artifacts (namely, beads and plaques, in total 14 samples) from a Mycenaean cemetery (12<sup>th</sup> c BC) excavated at Achaia in order to explore the intra-Peloponnese correlations on a technological and analytical level for the studied objects and also investigating the inter Peloponnese / Egypt and Mesopotamia associations.

## Results

All samples –with the exception of the metallic tesserae– were studied by combining PGAA and PIXE measurements; the metallic tesserae were studied only by PIXE on both their metal and glass substrate part. The analytical data from the Mycenaean samples indicate for a provenance center(s) outside the Peloponnese/Greece while for the Hagia Sofia samples a local (Byzantine) origin should be assigned.

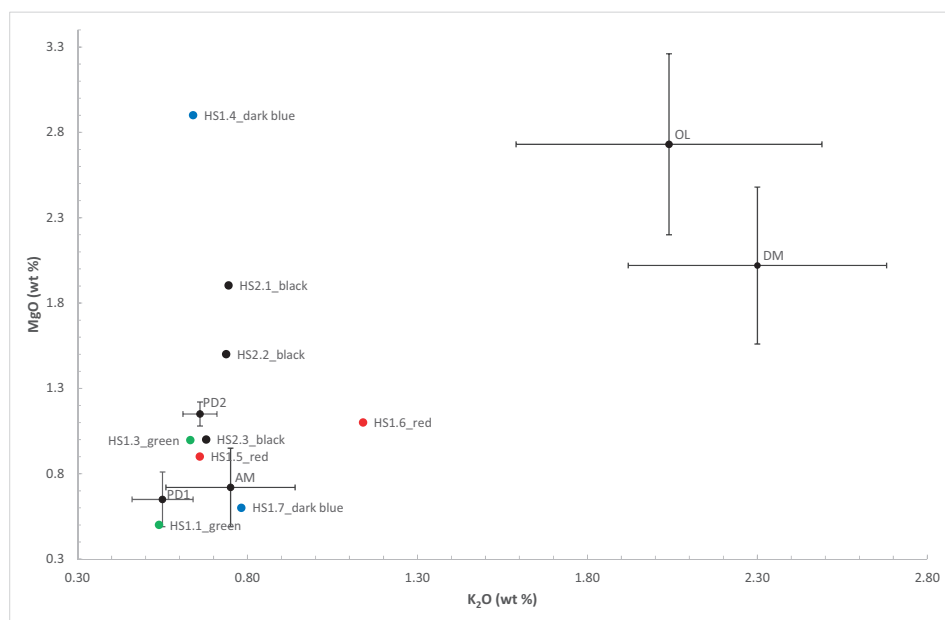


**Figure 1.** Hagia Sofia samples (labelled as HS) plotted against other published Byzantine glass tesserae collections from Greece and Italy.

## References

Moropoulou, A., et al. *A diagnostic study of glass tesserae from the dome of Hagia Sofia*, 125-133, in N. Zacharias, M. Georgakopoulou, K. Polikreti, Y. Facorellis, T. Vakoulis (eds.) 5<sup>th</sup> HSA Symposium Proceedings, Publications of the University of Peloponnese, Athens 2012

<h1 style="margin: 0;">B N C</h1> <p style="margin: 0;">Experimental Report</p>	<i>Experiment title</i> <b>Prompt Gamma Activation Analysis of Byzantine Glass fragments</b>	<i>Instrument. PGAA/NIPS</i> <i>Local contact</i> Zsolt Kasztovszky
	<i>Principal proposer:</i> Bogdan Constantinescu - National Institute of Nuclear Physics and Engineering, Bucharest, Romania <i>Experimental team:</i> Bogdan Constantinescu, Daniela Cristea-Stan - National Institute of Nuclear Physics and Engineering, Bucharest, Romania	<i>Experiment Number</i> BRR 319 CH <i>Date</i> 2012.11.14-11.15.

## Objectives

PGAA of coloured glass fragments from some Byzantine bracelets of Romanian museums was performed. The bracelets have been discovered during the archaeological excavations from Isaccea - Noviodunum, a commercial town situated before Danube Delta. The aim was to determine the chemical components responsible for the colour of the glass

## Results

Bulk elemental composition of 13 Byzantine glass samples have been determined by non-destructive PGAA. PGAA was able to quantify all the major components, as H<sub>2</sub>O, Na<sub>2</sub>O, K<sub>2</sub>O, MgO, CaO, SiO<sub>2</sub>, TiO<sub>2</sub>, MnO, Fe<sub>2</sub>O<sub>3</sub>, minor elements of S, Cl, colorants of Co and Cu, traces of B, Nd, Sm and Gd. In one instance, significantly high amount of As and trace level of Ag was measured in "Byz 4" sample. All the investigated glass proved to be sodium-glass, except one, which turned to be potassium glass ("Byz 4"). Higher concentrations of H in samples "Byz 18, 22, 23 and 36" are attributed to the elevated corrosion states of the objects. As colourants, Iron and Manganese for black, Chromium for yellow, Lead also for yellow in other samples, Fe and Cu was identified in red, Fe in blue, Ti "silver" glass. The variety of pigments and the artistic quality are arguments for the provenance of the bracelets from a specialized workshop somewhere in an important Byzantine city, possibly even Constantinople. Further measurements on recent archaeological discoveries in near Danube Dobroudja sites are necessary to distinguish between Byzantine-imported and local produced glass.

	H2O	Na2O	MgO	Al2O3	SiO2	SO3	K2O	CaO	TiO2	MnO	Fe2O3
Byz 2	0.11	14.1	2.3	2.8	65.9		1.87	7.56	0.15	0.84	1.12
Byz 4	0.11	0.1	1.4	1.1	65.9	0.47	18.16	10.69	0.02	0.52	0.34
Byz 5	0.14	15.1	2.8	2.2	64.8		1.76	7.65	0.14	0.75	3.99
Byz 9	0.13	14.0	3.1	2.2	67.2	0.35	1.90	7.74	0.11	0.90	1.21
Byz 18	0.45	15.0	3.1	2.0	67.3	0.28	1.51	6.69	0.10	0.60	1.53
Byz 19	0.14	13.8	2.5	2.5	67.5	0.31	1.82	7.59	0.12	1.00	1.57
Byz 20	0.12	15.2	3.0	2.6	66.3		1.42	7.37	0.11	0.49	2.06
Byz 31	0.11	14.0	2.6	2.4	67.7		1.77	7.49	0.11	0.86	1.53
Byz 22	0.63	15.5	3.3	2.1	66.1		1.40	7.50	0.11	0.71	1.32
Byz 23	0.96	14.7		2.5	68.4		1.78	7.68	0.12	0.88	1.75
Byz 36	0.35	15.3	2.8	2.5	65.5	0.19	1.54	7.06	0.13	0.67	2.51
Byz 24	0.18	14.7	3.8	2.5	66.0		1.41	7.48	0.10	0.54	2.07
Byz 34	0.16	16.3	2.4	2.1	65.7	0.35	1.73	6.55	0.12	2.66	0.92
	CoO	CuO	As2O3	B	Cl	Ag	Cd	Nd	Sm	Gd	
Byz 2		2.46		0.0567	0.671			3.0E-03	7.8E-05	1.1E-04	
Byz 4			1.13	0.00914	0.018	0.0131	7.63E-05	2.2E-03	3.0E-05	3.4E-05	
Byz 5	0.033			0.0452	0.599			1.8E-03	7.7E-05	1.1E-04	
Byz 9	0.052	0.16		0.0432	0.773			2.1E-03	8.0E-05	1.0E-04	
Byz 18	0.070	0.23		0.0518	0.865			2.4E-03	7.0E-05	9.9E-05	
Byz 19	0.040	0.21		0.0309	0.849		6.65E-05	3.5E-03	8.4E-05	1.1E-04	
Byz 20	0.060	0.15		0.0517	0.892				7.3E-05	1.2E-04	
Byz 31	0.117	0.38		0.0408	0.788			2.3E-03	8.4E-05	1.6E-04	
Byz 22	0.049	0.16		0.0627	0.853			1.6E-03	7.2E-05	1.1E-04	
Byz 23	0.051	0.22		0.0490	0.789			4.1E-03	7.0E-05	1.2E-04	
Byz 36	0.038	0.38		0.0863	0.737			2.4E-03	8.3E-05	1.1E-04	
Byz 24	0.061	0.19		0.0465	0.849			2.6E-03	7.8E-05	9.5E-05	
Byz 34	0.011			0.0362	0.950			2.7E-03	1.0E-04	1.4E-04	

Table 1: Composition of coloured glass fragments, measured by PGAA



<h1 style="margin: 0;">B N C</h1> <p style="margin: 0;"><b>Experimental Report</b></p>	<i>Experiment title</i> <b>PGAA of archaeological megaliths excavated in Kevermes, Hungary</b>	<i>Instrument</i> PGAA/NIPS <i>Local contact</i> Zsolt Kasztovszky
	<i>Principal proposer:</i> István Oláh, Attila Gyucha – Hungarian National Museum, National Heritage Protection Center <i>Experimental team:</i> Boglárka Maróti, Zsolt Kasztovszky	<i>Experiment Number</i> PGAA_12_67_CW <i>Date</i> 2012.09.14.

## Objectives

The aim was to determine the elemental composition of rock samples from a megalith, in order to determine the provenance of the valuable archaeological finds.

The prehistoric object was found during plowing in the vicinity of Kevermes, located in the southeastern part of Békés County, near the Rumanian border. The megalith is decorated with a complex pattern of carvings unparalleled in the Carpathian Basin.

## Results

Three samples taken from Kevermes megalith have been analyzed by PGAA. "Kevermes 2" represents the average composition of the megalith, while "Kevermes 1/a" and "Kevermes 1/b" were taken from albite-rich and epidot-rich parts of the same object, respectively. The obtained compositions are shown in Table 1.

The results are in agreement with the macroscopic description of the rock, i.e. it is greenschist. With the help of comparison with the literature data – especially with use of the average "Kevermes 2" data – the provenance study of the object can be performed. Based on preliminary results, we expelled most of the well-known source regions of the Carpathian Basin and the Czech Massif-Moldanubian zone. The most perspective provenance regions are the Maros zone in Transylvania or the Vardar zone, but more fieldwork and collecting samples will be necessary to verify this assumption.

El	Det.Limit wt%	979 Kevermes 2			980 Kevermes 1/a			981 Kevermes 1/b		
		wt%	rel. unc %	abs. unc %	wt%	rel. unc %	abs. unc %	wt%	rel. unc %	abs. unc %
H2O	0,09	2,443	1,5	0,037	2,037	1,6	0,032	2,448	1,5	0,038
Na2O	0,01	3,87	2,1	0,08	4,99	2,2	0,11	0,74	2,6	0,020
MgO	0,1	4,76	6,	0,27	3,65	6,	0,22	N.D.		
Al2O3	0,5	21,61	1,8	0,38	20,62	1,8	0,37	22,03	1,7	0,38
SiO2	0,1	48,61	1,2	0,60	50,87	1,2	0,61	39,51	1,6	0,63
K2O	0,01	4,89	2,0	0,09	3,66	2,1	0,076	0,33	3,5	0,012
CaO	0,02	4,02	2,7	0,11	4,90	2,8	0,14	20,90	2,3	0,49
TiO2	0,003	0,705	2,5	0,017	0,694	2,5	0,017	0,664	2,4	0,016
MnO	0,02	0,0884	3,7	0,0033	0,0732	2,0	0,0015	0,159	3,2	0,0051
Fe2O3t	0,02	8,96	2,4	0,21	8,48	2,2	0,18	13,13	2,2	0,29
B	3,0E-05	4,93E-03	1,1	5,33E-05	2,34E-03	0,8	1,86E-05	1,95E-02	0,8	1,62E-04
Cl	1,0E-03	9,04E-03	6,	5,15E-04	6,81E-03	6,	3,85E-04	4,13E-03	22,	9,29E-04
Sc	1,0E-03	1,56E-03	9,	1,37E-04	1,65E-03	10,	1,58E-04	2,22E-03	10,	2,17E-04
Nd	4,0E-04	5,70E-03	8,	4,51E-04	5,26E-03	9,	4,63E-04	6,71E-03	7,	4,55E-04
Sm	5,0E-05	5,32E-04	1,8	9,41E-06	5,23E-04	1,6	8,58E-06	6,86E-04	1,7	1,16E-05
Gd	5,0E-05	5,54E-04	11,	6,09E-05	5,37E-04	12,	6,44E-05	8,02E-04	9,	7,15E-05

Table 1: Composition of different sample taken from the megalith

<b>B N C</b> <b>Experimental Report</b>	<i>Experiment title</i> <b>Background characterisation</b>	<i>Instrument</i> PGAA <i>Local contact</i> Boglárka Maróti
	<i>Principal proposer:</i> Boglárka Maróti <i>Experimental team:</i> Boglárka Maróti, László Szentmiklósi – Centre for Energy Research	<i>Experiment Number</i> PGAA_12_63_IH <i>Date</i> 2012.10.20- 2012.10.24

### Objectives

To measure the PGAA background depending on the neutron collimator size, and the effect of the on/off state of the NIPS station.

### Results

Four days were needed to take nine background spectra. An aluminium frame with Teflon strings and teflon bag were used in all cases. The quantity of carbon and fluorine (components of teflon) in the background spectra depend on the collimator size. After our measurements it was found that iron and lead components in the background are less dependent from the collimator size, but strongly dependent on the on/off state of the NIPS station. Measured nitrogen is dependent solely on the collimator size. In case of boron, hydrogen, aluminium and germanium as background components both the collimator size and the on/off state of the NIPS station have effect on the quantity. It is highly recommended to take a background spectrum with the same conditions, if one of the above listed elements are present as a minor or trace components in the examined sample.

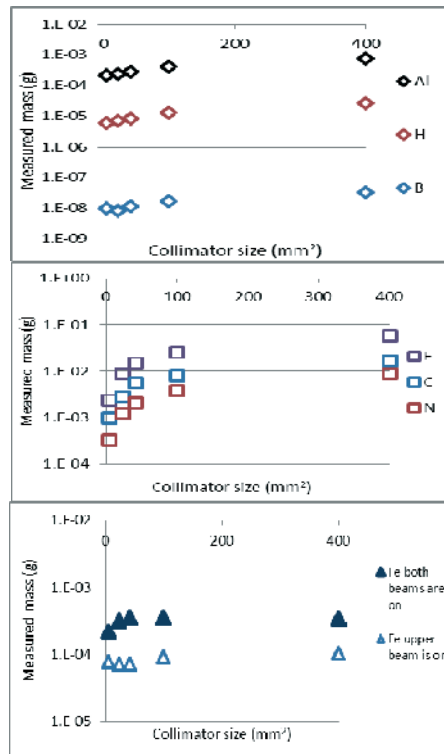


Figure 1/a, b and c: Changes in the quantity of some background components by the collimator size in logarithmic scale.

<h1 style="text-align: center;">B N C</h1> <p style="text-align: center;"><b>Experimental Report</b></p>	<i>Experiment title</i> <b>Neutron flux and collimator characterisation</b>	<i>Instrument</i> PGAA <i>Local contact</i> Boglárka Maróti
	<i>Principal proposer:</i> Boglárka Maróti <i>Experimental team:</i> Boglárka Maróti, László Szentmiklósi – Centre for Energy Research	<i>Experiment Number</i> PGAA_12_64_IH <i>Date</i> 2012.11.10- 2012.11.12

## Objectives

To estimate the spreading of the neutron beam spot size using Al plate.

## Results

Based on the background measurements completed in October, 2012, which reflected on the irregular changing of iron and lead quantity in the background, significant measurement options have been considered. It was suspected that the count rate is not in direct proportion with the collimator size because of the beam inhomogeneity and the spreading of the beam, however, our aim was to examine the extent of it. An aluminium plate (larger than the 30° projection of the 20x20 mm collimator) was measured using different neutron collimators, from an attenuator layer to a maximum collimator size of 20x20 mm. The count rate of two selected aluminium prompt-gamma lines (983 keV and 7723 keV) were observed and compared with each different spectrum.

The changing of the count rate is not with linear correlation with the collimator size. Using these measurements, our background corrections become more accurate.

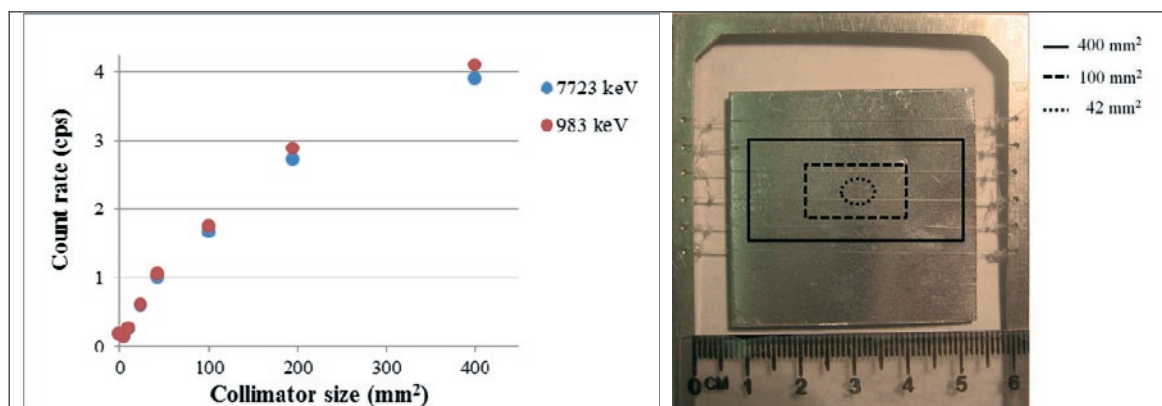


Figure 1/A and B: Changing of the count rate of the 983 and 7723 keV prompt-gamma Al peak by the neutron collimator size (A). Aluminium plate placed between the teflon strings (B).

<h1 style="margin: 0;">B N C</h1> <p style="margin: 0;">Experimental Report</p>	<i>Experiment title</i> <b>Measurement of B segregation at grain boundaries in experimental Co-Re polycrystalline alloys being developed for high temperature gas turbine applications</b>	<i>Instrument</i> PGAA
	<i>Principal proposer:</i> Debashis Mukherji – Technische Universität Braunschweig <i>Experimental team:</i> László Szentmiklósi, Zsuzsanna Mácsik – Institute of Isotopes	<i>Local contact</i> L. Szentmiklósi
<i>Experiment Number</i> BRR_261		<i>Date</i> 2011.03.24, 2011.06.20- 2011.06.23

## Objectives

To determine the boron content and its surface distribution in Co-Re experimental alloys

## Results

Co-Re based alloys are being developed at the TU Braunschweig to supplement Ni-base Superalloys at ultra-high temperature (>1200°C) applications. Grain boundaries in these polycrystalline alloys are strengthened by boron. B is known to segregate to grain boundaries in Ni-alloys and improve low temperature ductility. The mechanisms to strengthen the grain boundaries are being explored for the Co-Re alloys. To have a better understanding of the effect of Boron addition, a set of experimental alloy was manufactured with known added Boron amounts up to 1000 ppm. However, as Boron is volatile, the quantity remained in the alloy is presumably lower than added.

The aims of the present experiments were to quantify the B content of Co-Re-Cr alloys, coded as CoRe L7 (200 ppm nominal B), L8 (500 ppm), L9 (1000 ppm) L0 (no added boron); L1BST (200 ppm B and with carbides)/L1ST (no added boron), L2BST (200 ppm B+ 1.2% Ta)/L2ST (no added boron) by PGAA, and to investigate the possibilities to map the distribution of the boron in the alloys. Thanks to the high cross-section of the  $^{10}\text{B}(n, \gamma)^{11}\text{Li}$  reaction, we could quantify boron already in a few ppm quantity, based on its 477.6 keV gamma-ray. However, PGAA, or even PGAI, did not have the sufficient spatial resolution (in the order of 10 m) to map the segregation. Therefore a new method had to be worked out and tested, based on the solid state nuclear track detector (SSNTD) technique. In this matrix, the only source of alpha particles is the above mentioned reaction, thus if we make a close contact between a polished surface of the sample and the track detector during the irradiation, the spots will represent the near-surface boron distribution. The track detectors were etched in hot NaOH, and imaged by an optical microscope.

Test irradiations have been carried out at the PGAA beamline. The guided beam of slow neutrons provided favourable irradiation conditions, in contrast to the conventional way, when it is done in the reactor core. The irradiation, etching and imaging conditions were optimized. Blanks, boron-free alloys, and a homogeneous NIST  $^{10}\text{B}$  standard were irradiated to prove that the signal is indeed related to the boron content of the sample. There are preliminary indications that in some samples the segregation was detectable, but the results were not yet fully conclusive. A follow-up study is planned to draw further conclusions. The gained information can help the material scientists to develop better materials for the aviation and energy sector.

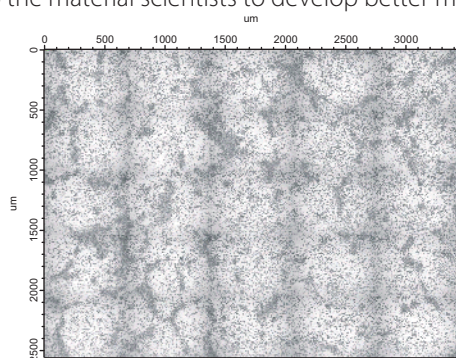


Figure 1. SSNTD image of a boron-containing L1BST sample.

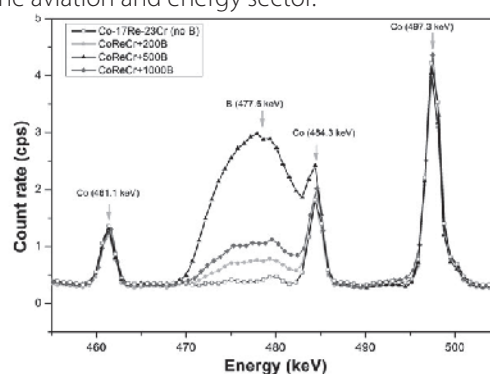


Figure 2. Compositions of the Co-17Re-23Cr samples

## References

1. D. Mukherji, et al, Scripta Materialia **66** (2012) 60–63

<b>B N C</b> <b>Experimental Report</b>	<i>Experiment title</i> <b>Non-destructive determination of hydrogen contents in zircaloy samples by <math>k_0</math>-based PGAA</b>	<i>Instrument.</i> PGAA  <i>Local contact</i> Zs. Révay
	<i>Principal proposer:</i> Kathi Sudarshan – Radiochemistry Division, Bhabha Atomic Research Centre, Mumbai, India <i>Experimental team:</i> Révay Zsolt, László Szentmiklósi	<i>Experiment Number</i>  <i>Date</i> 03.27.2010-04.02.2010

## Objectives

To determine the hydrogen content of zircalloy samples.

## Results

Presence of excess hydrogen in zircaloy, used as cladding material of reactor fuel, makes them brittle and changes the material properties including reduction of mechanical strength. To study the properties of zircaloys in presence of varying hydrogen concentrations, accurate determination of H is essential. In this respect Prompt Gamma ray Neutron Activation Analysis (PGAA) is superior compared to many conventional methods including Mass Spectrometry (MS), Differential Scanning Calorimetry (DSC) and Inert Gas Fusion (IGF). The PGAA facility was used for determination hydrogen contents in four samples each of Zircaloy 2 and Zr-2.5%Nb alloys. Samples in the mass range of 0.5-1.0 g were irradiated in vacuum and the prompt  $\gamma$ -rays were measured for 2-4 h with a Compton suppressed detection system (HPGe-BGO detectors). The absolute counting efficiency of the detector was determined using  $^{133}\text{Ba}$  and  $^{152}\text{Eu}$  and prompt gamma rays from  $^{14}\text{N}(n,\gamma)^{15}\text{N}$  and  $^{35}\text{Cl}(n,\gamma)^{36}\text{Cl}$ . Hydrogen concentrations were determined by  $k_0$ -PGAA utilizing 2223 keV prompt gamma rays obtained from  $^1\text{H}(n_{\text{th}}, \gamma)$  reaction. The concentration results obtained in the range of 26-287  $\text{mg kg}^{-1}$  are given in Table 1. The uncertainties quoted in Table 1 combined uncertainties at  $\pm 1$ . Since all major elements in three zircaloys were amenable to PGAA, H contents were determined by a standard-less approach. The determined hydrogen contents were found to be in good agreement with the expected values based hydrogen charging. For validation purposes, the samples were analyzed IGF as well as DSC methods.

Sample	This work	Expected Value
Zr-Nb-2	$42 \pm 5$	40
Zr-Nb-3	$58 \pm 3$	60
Zr-Nb-4	$82 \pm 6$	80
Zr-Nb-5	$99 \pm 6$	100
Zry-2-1	$287 \pm 14$	290
Zry-2-2	$155 \pm 8$	158
Zry-2-3	$135 \pm 8$	130
Zry-2-4	$26 \pm 2$	32

Table 1. H contents ( $\text{mg kg}^{-1}$ ) in different Zircaloy 2 and Zr-2.5%Nb alloy samples

## Reference

- 1 K. Sudarshan, R. Acharya, Zs. Révay, L. Szentmiklósi, T. Belgya, R.V. Kulkarni, V. D. Alur, G.K. Mallik, P.K. Pujari: *Non-destructive determination of hydrogen contents in zircaloy samples by  $k_0$ -based Prompt Gamma-ray NAA*, Proc. Fourth International Symposium on Nuclear Analytical Chemistry (NAC-IV) Bhabha Atomic Research Centre, Trombay, Mumbai, India, November 15-19, 2010

<b>B N C</b> <b>Experimental Report</b>	<i>Experiment title</i> <b>Short lives nuclides with chopped beam PGAA</b>	<i>Instrument</i> PGAA <i>Local contact</i> Zs. Révay, L. Szentmiklósi
	<i>Principal proposer:</i> Dong Hui Huang – China Institute of Atomic Energy, Beijing, China <i>Experimental team:</i> László Szentmiklósi	<i>Experiment Number</i> PGAA_10_15_IC <i>Date</i> 2010.05.26- 2010.05.27

### Objectives

to assess the feasibility of a PGAA and short-lived NAA facility at CARR

### Results

The China Advanced Research Reactor (CARR) is a multi-purpose, tank-in-pool, inverse neutron trap type research reactor. The Government approved the CARR project formally in July 1997. The engineering construction began on September 27, 2001.

In order to explore full use of CARR after completing, it's important and necessary to program the utilization and develop the facilities with associated equipments and instruments. The major task of this project includes programming neutron utilization all-round for CARR, installing various irradiation utilization facilities with associated instruments and equipments, constructing cold neutron source and related neutron guide tube. One of the planned instrument is the PGAA.

The purpose of the scientific visit was to make experiment with the continuous-beam and chopped-beam PGAA facility of the Budapest Neutron Centre, in order to assess the feasibility of constructing such an experimental station at CARR.

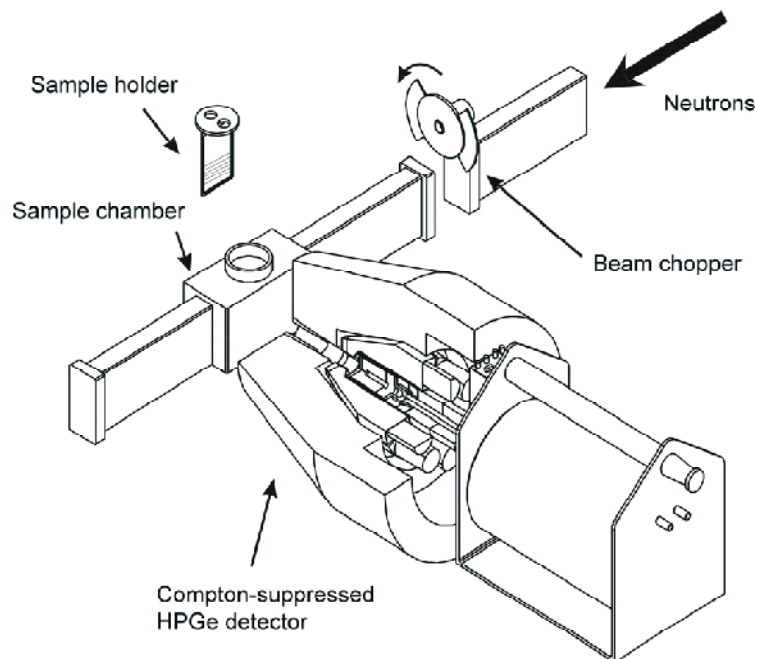


Figure 1. the Budapest PGAA setup with the chopped-beam option

Short-lived decay lines from the elements Na, V, Hf, Sc, Se were measured and the possible suppression of the background was also studied in details.

<h1 style="margin: 0;">B N C</h1> <p style="margin: 0;">Experimental Report</p>	<i>Experiment title</i> <b>Studying the Deacon process using in-situ Prompt Gamma Activation Analysis</b>	<i>Instrument</i> PGAA
	<i>Local contact</i> L.Szentmiklósi	<i>Experiment Number</i> PGAA_10_18_IC <i>Date</i> 2010.10.25- 2010.11.05
<i>Principal proposer:</i> Detre Teschner – Fritz-Haber-Institute, Berlin, Germany <i>Experimental team:</i> Detre Teschner, Ramzi Farra, László Szentmiklósi		

## Objectives

To clarify the mechanistic details of the Deacon reaction.

## Results

An alternative process to the conventional electrolysis for producing chlorine is the Deacon process, based on the heterogeneous gas phase oxidation of HCl. In 1999, Sumitomo Company patented a novel RuO<sub>2</sub>-based catalyst, which is highly competitive to the electrochemical process. As, however, ruthenium is a very expensive noble metal, a cheaper alternative catalyst would be highly desirable.

The Deacon process over ruthenium-oxide based, Cu-based and CeO<sub>2</sub>-based catalysts was this time studied using in situ Prompt Gamma Activation Analysis [1]. Since oxygen excess in the reactant stream enhances the reaction rate, the variation of the feed (HCl/O<sub>2</sub>) composition allows us to correlate the reaction rate and the degree of chlorination. Results indicate that chemisorbed Cl is a poison of the catalytic reaction. The chlorine coverage is near saturation and only a small part of it can be removed from the surface by the increasing oxygen content of the feed gas. However, the activity was linearly proportional to the amount of Cl removed indicating that a catalytic material stable under this corrosive condition but binding chlorine somewhat weaker could be a very effective catalyst.

On the other hand, the rate coefficient of a chemical reaction typically follows the classical Arrhenius equation, and thus the reaction rate varies as a function of temperature. Here an alternative formulation was demonstrated consisting of a temperature-independent rate coefficient and a coverage term that depends on temperature and pressures. This formulation, derived from the experimental determination of the oxygen and chlorine coverages during HCl oxidation to Cl<sub>2</sub> on a RuO<sub>2</sub> catalyst is substantiated by theory and DFT calculations.

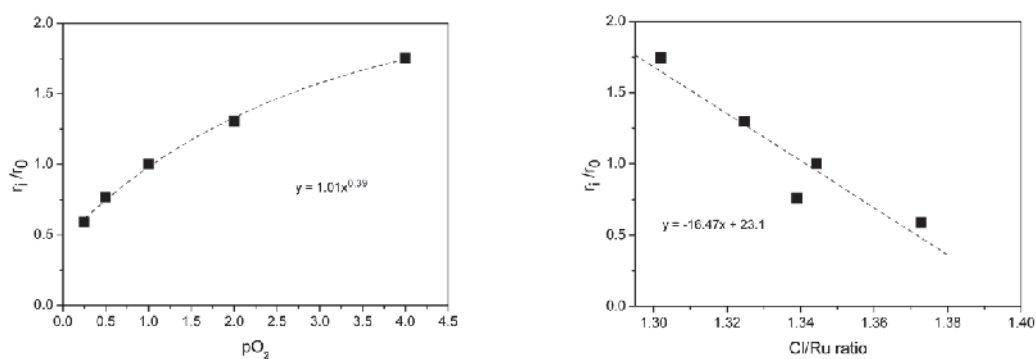


Figure 1. Influence of  $p(O_2)$  (a) and the chlorine uptake (Cl/Ru ratio) (b) on the normalized reaction rate ( $r_1/r_0$ ) over the RuO<sub>2</sub>/SnO<sub>2</sub>-Al<sub>2</sub>O<sub>3</sub> catalyst during in situ PGAA experiment carried out at atmospheric pressure.  $pO_2$  is expressed in pHCl units. HCl flow was constant at 33.3 cm<sup>3</sup> min<sup>-1</sup> and the total flow was kept constant at 166.6 cm<sup>3</sup> min<sup>-1</sup> with the addition of inert N<sub>2</sub>. Rate is normalized to activity at O<sub>2</sub>:HCl:N<sub>2</sub> = 1:1:3.

## References

- Zs. Révay et al. Anal. Chem. 80 (2008) 6066.
- D. Teschner, R. Farra, L. Yao, R. Schlögl, H. Soerijanto, R. Schomäcker, T. Schmidt, L. Szentmiklósi, A. P. Amrute, C. Mondelli, J. Pérez-Ramírez, G. Novell-Leruth, N. López, J. Catalysis, 285 (2012) 273–284
- D. Teschner, G. Novell-Leruth, R. Farra, A. Knop-Gericke, R. Schlögl, L. Szentmiklósi, M. González Hevia, H. Soerijanto, R. Schomäcker, J. Pérez-Ramírez, and N. López: In situ surface coverage analysis of the RuO<sub>2</sub>-catalyzed HCl oxidation reveals the entropic origin of compensation in heterogeneous catalysis, accepted for publication in Nature Chemistry

<b>B N C</b> <b>Experimental Report</b>	<i>Experiment title</i> <b>Non-destructive determination of hydrogen contents in zircaloy samples by <math>k_0</math>-based PGAA</b>	<i>Instrument.</i> PGAA <i>Local contact</i> Zsolt Révay
	<i>Principal proposer:</i> Kathi Sudarshan – Radiochemistry Division, Bhabha Atomic Research Centre, Mumbai, India <i>Experimental team:</i> Révay Zsolt, László Szentmiklósi	<i>Experiment Number</i> PGAA_10_09_IC <i>Date</i> 2010.03.27 - 2010.04.02.

## Objectives

to determine the hydrogen content of zircaloy samples

## Results

Presence of excess hydrogen in zircaloy, used as cladding material of reactor fuel, makes them brittle and changes the material properties including reduction of mechanical strength. To study the properties of zircaloys in presence of varying hydrogen concentrations, accurate determination of H is essential. In this respect Prompt Gamma ray Neutron Activation Analysis (PGAA) is superior compared to many conventional methods including Mass Spectrometry (MS), Differential Scanning Calorimetry (DSC) and Inert Gas Fusion (IGF). The PGAA facility was used for determination hydrogen contents in four samples each of Zircaloy 2 and Zr-2.5%Nb alloys. Samples in the mass range of 0.5-1.0 g were irradiated in vacuum and the prompt  $\gamma$ -rays were measured for 2-4 h with a Compton suppressed detection system (HPGe-BGO detectors). The absolute counting efficiency of the detector was determined using  $^{133}\text{Ba}$  and  $^{152}\text{Eu}$  and prompt gamma rays from  $^{14}\text{N}(n,\gamma)^{15}\text{N}$  and  $^{35}\text{Cl}(n,\gamma)^{36}\text{Cl}$ . Hydrogen concentrations were determined by  $k_0$ -PGAA utilizing 2223 keV prompt gamma rays obtained from  $^1\text{H}(n_{\text{th}}, \gamma)$  reaction. The concentration results obtained in the range of 26-287 mg  $\text{kg}^{-1}$  are given in Table 1. The uncertainties quoted in Table 1 combined uncertainties at  $\pm 1$ . Since all major elements in three zircaloys were amenable to PGAA, H contents were determined by a standard-less approach. The determined hydrogen contents were found to be in good agreement with the expected values based hydrogen charging. For validation purposes, the samples were analyzed IGF as well as DSC methods.

Sample	This work	Expected Value
Zr-Nb-2	$42 \pm 5$	40
Zr-Nb-3	$58 \pm 3$	60
Zr-Nb-4	$82 \pm 6$	80
Zr-Nb-5	$99 \pm 6$	100
Zry-2-1	$287 \pm 14$	290
Zry-2-2	$155 \pm 8$	158
Zry-2-3	$135 \pm 8$	130
Zry-2-4	$26 \pm 2$	32

Table 1. H contents (mg  $\text{kg}^{-1}$ ) in different Zircaloy 2 and Zr-2.5%Nb alloy samples

## Reference

K. Sudarshan, R. Acharya, Zs. Revay, L. Szentmiklósi, T. Belgya, R.V. Kulkarni, V. D. Alur, G.K. Mallik, P.K. Pujari: *Non-destructive determination of hydrogen contents in zircaloy samples by  $k_0$ -based Prompt Gamma-ray NAA*, Proc. Fourth International Symposium on Nuclear Analytical Chemistry (NAC-IV) Bhabha Atomic Research Centre, Trombay, Mumbai, India, November 15-19, 2010



<h1 style="margin: 0;">B N C</h1> <p style="margin: 0;"><b>Experimental Report</b></p>	<i>Experiment title</i> <b>Short lives nuclides with chopped beam PGAA</b>	<i>Instrument</i> PGAA <i>Local contact</i> Zs.Révay, L. Szentmiklósi
	<i>Principal proposer:</i> James J. Carroll – Department of Physics and Astronomy Youngstown State University, USA <i>Experimental team:</i> Révay Zsolt, László Szentmiklósi	<i>Experiment Number</i> PGAA_10_19_IC <i>Date</i> 2010.11.08- 2010.11.13

## Objectives

To determine the gamma spectrum and cross-section of  $^{185}\text{Re}$ .

## Results

Long-lived nuclear excited states, or isomers, have proven important in the development of the shell and collective models of nuclear structure. For example, the existence of rotational bands was first demonstrated from the sequence of gamma rays emitted following decay of the  $T_{1/2} = 5.47$  hour isomer of  $^{180}\text{Hf}$ .

About thirty truly metastable isomers exist with half-lives of years, decades or longer. The longest-lived isomer is  $^{180\text{m}}\text{Ta}$ , with  $T_{1/2} > 10^{16}$  years, while the highest energy metastable isomer is  $^{178\text{m}2}\text{Hf}$ , with  $E_m = 2.446$  MeV and  $T_{1/2} = 31$  years. The specific energy of the latter isomer corresponds to 1.2 GJ/g, compared with about 45 kJ/g for gasoline. Thus, it is no surprise that the possibility of utilizing nuclear energy stored in isomers has provided an added motivation for basic research.

The high energy density is, however, not by itself sufficient to realize any application: another necessary component is a means by which to efficiently release the stored energy on a useful time scale and upon demand. Nuclear structure holds the keys to both energy storage and release from isomers.

One of the above mentioned potential storage isomers is the  $^{186\text{Re}}\text{m}2$  with a half-life of  $2 \times 10^5$  years. It is produced from the  $^{185}\text{Re}(n, \gamma)$  reaction with a cross section of about 0.3 barns.

In the present experiments, the thermal neutron capture cross-section and the capture gamma spectrum of the  $^{185}\text{Re}$  were to be determined. For this purpose prompt and decay spectra were taken of an enriched sample, whereas the precision of the Re elemental cross section was improved using a  $\text{ReCl}_3$  sample. Some spectra were taken at higher gains to have a more detailed tabulation of the low energy spectrum part.

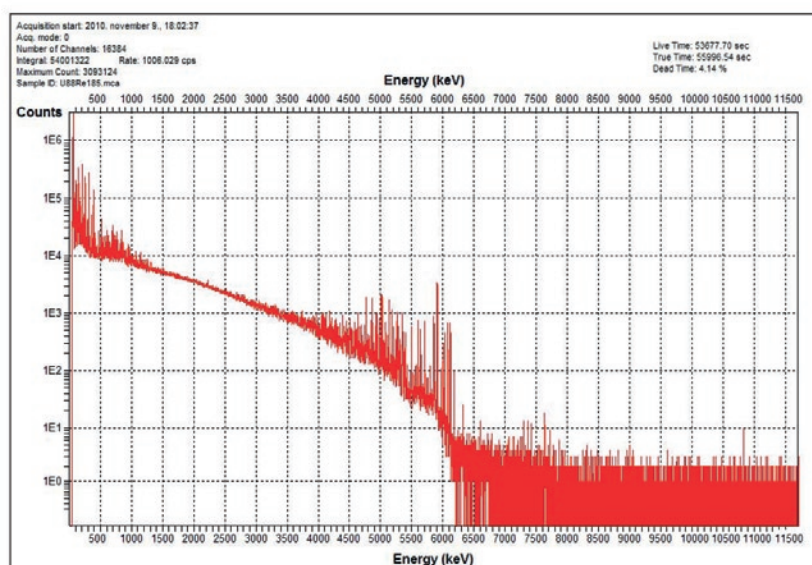


Figure 1. The PGAA spectrum of the  $^{185}\text{Re}$  sample

In a parallel study, the spectroscopy of the  $^{186\text{m}}\text{Re}$  is being studied with the complementary (d, p) reaction in an LBNL-LLNL-YSU collaboration.

<b>B N C</b> <b>Experimental Report</b>	<i>Experiment title</i> <b>A structural evaluation of the tungsten isotopes via thermal neutron capture</b>	<i>Instrument</i> PGAA  <i>Local contact</i> Zs. Révay
	<i>Principal proposer:</i> Aaron Hurst, Richard B. Firestone – Lawrence Berkeley National Laboratory, CA, USA <i>Experimental team:</i> Révay Zsolt, László Szentmiklósi, Kis Zoltán	<i>Experiment Number</i> PGAA_10_21_IC <i>Date</i> 2010.11.18 - 2010.11.19

## Objectives

To determine the neutron capture cross-sections of tungsten isotopes

## Results

Total radiative thermal neutron-capture  $\gamma$ -ray cross sections of the tungsten isotopes have been measured with PGAA in isotopically-separated tungsten samples. These quantities have been determined as the sum of the experimentally observed partial neutron-capture gamma-ray cross sections feeding the ground state directly, in addition to the modeled contribution from the (unobserved) quasi continuum that feeds the ground state. In each of the tungsten isotopes investigated, a new critical energy, exceeding the current RIPL-3-suggested value, is proposed based upon consistency between theoretical calculations and experimental data. The analysis of the capture-gamma spectra, together with the DICEBOX simulations, has led to new independent measurements of the total radiative thermal neutron-capture cross section ( $\sigma_0$ ) for each of the isotopes. The new measurements for the three  $^{183,185,187}\text{W}$  compounds bear excellent agreement with the current literature, although that of  $^{184}\text{W}$  displays strong disagreement by as much as 40 % with the current adopted value. Furthermore, an independent decay-scheme normalization has been extracted from the decay of radioactive  $^{187}\text{W}$  and is found to be in excellent agreement with previous gamma-ray emission probabilities, thus, providing further validation of our analysis technique. Additionally, the adopted analysis methods, provide both confirmation and new insights into the decay schemes and structure of the major tungsten isotopes under investigation in the present study.

$E_\gamma$ [keV]	$\sigma_\gamma$ [b]	$P_\gamma^a$	$P_\gamma^b$	$P_\gamma^c$
71.97(7)	2.115(77)	0.209(12)	-	0.203(11)
134.34(7)	1.100(31)	0.109(6)	0.102(5)	0.106(5)
479.47(5)	2.760(82)	0.273(15)	0.261(12)	0.266(14)
551.22(9)	0.629(16)	0.062(3)	0.061(3)	0.061(3)
617.96(6)	0.725(20)	0.072(4)	0.075(4)	0.070(3)
625.03(10)	0.120(6)	0.0118(8)	0.0131(7)	0.0115(7)
685.74(5)	3.352(86)	0.331(17)	0.331(16)	0.322(16)
772.99(10)	0.505(19)	0.050(3)	0.049(2)	0.049(3)

Table 1. Partial gamma-ray cross sections and  $P$  values corresponding to decay lines observed in the delayed  $^{187}\text{W}$  beta decay spectrum, in comparison to earlier literature data (a-c).

## Reference

1. A. M. Hurst, R. B. Firestone, M. S. Basunia, B. Sleaford, N. C. Summers, J. E. Escher, Zs. Révay, L. Szentmiklósi, T. Belgya, H. Choi, M. Krticka: *A structural evaluation of the tungsten isotopes via thermal neutron capture*. to be submitted to Phys. Rev. C.

<b>B N C</b> <b>Experimental Report</b>	<i>Experiment title</i> <b>Neutron capture of enriched Gd and Eu isotopes</b>	<i>Instrument.</i> PGAA  <i>Local contact</i> Zs. Révay
	<i>Principal proposer:</i> H.D. Choi, Richard B. Firestone – Lawrence Berkeley National Laboratory, CA, USA <i>Experimental team:</i> Révay Zsolt, Kis Zoltán, László Szentmiklósi	<i>Experiment Number</i> PGAA_10_23_IC <i>Date</i> 2010.12.03- 2010.12.04

## Objectives

To determine the neutron capture cross-sections of separated Gd and Eu isotopes

## Results

The rare earth elements have more than one stable isotopes and each of them have highly complicated neutron capture gamma spectrum. This makes difficult or even impossible to resolve the complicated multiplets and assign them to isotopes. Amongst the stable nuclides, gadolinium has the highest radiative capture cross section for thermal neutrons, e.g. those of  $^{157}\text{Gd}$  and  $^{155}\text{Gd}$  are 254000 b and 60900 b, respectively. These high cross sections of  $^{157}\text{Gd}$  and  $^{155}\text{Gd}$  for the capture of thermal neutrons are due to the fact that their lowest resonances, 0.0314 eV and 0.0267 eV, are close to the thermal neutron energy, 0.0253 eV, in comparison to their total widths, 106 meV and 108 meV, respectively.

One way to reduce the complexity of the spectrum is the use of enriched isotopes. In collaboration with Lawrence Berkeley National Laboratory (LBNL), we managed to obtain some milligrams of highly enriched of isotopes: Gd-157, Gd-155, Eu-151, Eu-153 in oxide form. In addition, the corresponding samples with natural isotopic abundances were also measured for normalization.

The standardization was based in case of Gd on the stoichiometric compound of  $\text{GdB}_6$ , normalizing to the of 478 keV  $\gamma$ -rays from the  $^{10}\text{B}(n, \gamma)^7\text{Li}$  reaction, whereas the Eu was standardized in a HCl-solution.

There were theoretical predictions implying that the deexcitation scheme of the compound nucleus may differ if thermal or cold neutrons are used for the irradiations. This may be due to the high density of the nuclear levels close to the capture state. In this context, the kinetic energy of the neutron would not be negligible. To prove or disprove this theory, all measurements were done twice, in a thermal and in a cold beam.

The analysis of the data is still in progress, in collaboration with the Berkeley Lab Isotopes Project team.

## Reference

1. H.D. Choi, R.B. Firestone, M.S. Basunia, A. Hurst, B. Sleaford, N. Summers, J. Escher, Zs. Révay, T. Belgya, and M. Krtička, Radiative capture cross sections of Gd isotopes for thermal neutrons, to be submitted

<b>B N C</b> <b>Experimental Report</b>	<i>Experiment title</i> <b>Measuring the Compton-suppressed response function of the PGAA detector</b>	<i>Instrument</i> PGAA  <i>Local contact</i> L. Szentmiklósi
	<i>Principal proposer:</i> Tamás Belgya – Institute of Isotopes <i>Experimental team:</i> László Szentmiklósi – Institute of Isotopes	<i>Experiment Number</i> PGAA_11_28_IH <i>Date</i> 2011.01.25- 2011.02.04

## Objectives

To measure and calculated the response function of the Budapest PGAA detector (continuation).

## Results

The detector system of the PGAA facility consists of an n-type HPGe detector (Canberra GR 2720) and a Bismuth Germanate (BGO) guard detector arranged in a coaxial geometry. The eight main segments of the suppressor are complemented by two additional “catchers” behind the HPGe crystal. The whole detector is surrounded by a 10 cm-thick lead shielding.

The interpretation of the highly complicated elemental PGAA spectra and the prediction of the spectroscopic conditions for multi-component analytes require the accurate knowledge of the detector response function. The first step towards the characterization of our spectrometer was the accurate measurements of well-known and simple gamma spectra. Unfortunately there are only a few commercially available radioactive sources for this purpose, while some additional nuclides with short half-lives could be prepared by activation in the neutron beam, and could be measured with the pulsed-beam technique using the recently installed computer-controlled beam shutter. A few, simple capture gamma spectra were also involved.

The earlier studies on the previous detector were repeated and extended. In contrast to the former calculations with MCNP-CP, the analysis of the present data was completed with an other Monte Carlo code, geant4. It was found that geant4 can better reproduce the gamma-spectra then MCNP-CP; therefore it will be used in our future calculations. Now the absolute counting efficiency, as well as the Compton-suppressed spectra could also be well reproduced.

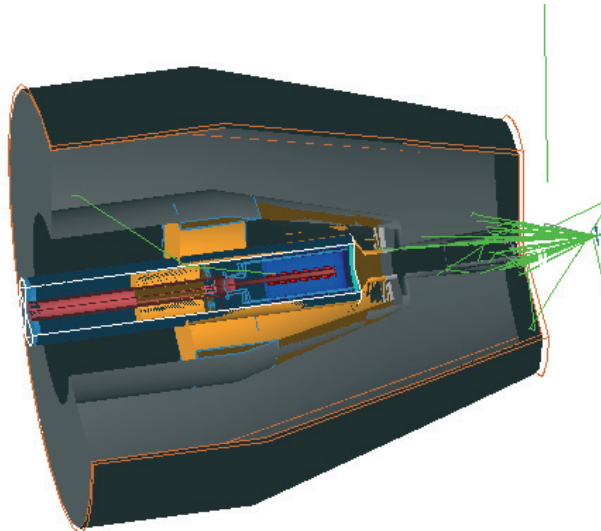


Figure 1. a screenshot from the Monte Carlo code geant4 during the simulation of the gamma-ray interactions in the PGAA detector. Quarter of the detector was made transparent to visualize the inner parts.

<b>B N C</b> <b>Experimental Report</b>	<i>Experiment title</i> <b>Hydrogen Trapping due to Severe Plastic Deformation (SPD)</b>	<i>Instrument</i> PGAA  <i>Local contact</i> L. Szentmiklósi
	<i>Principal proposer:</i> Matthias Boenisch, Gerhard Krexner – Faculty of Physics, University of Vienna <i>Experimental team:</i> László Szentmiklósi	<i>Experiment Number</i> BRR-263  <i>Date</i> 05.01.2011-05.05.2011

## Objectives

To determine the amounts of H in Pd and Ti-based hydrogen storage materials

## Results

Nanostructured metal-hydrogen systems produced by techniques of Severe Plastic Deformation exhibit unusually high concentrations of vacancies which possibly are stabilized by trapped hydrogen. Preliminary work on PdH has shown that the methods applied so far (X-ray, DSC, SEM, TEM, gravimetry) provide only indirect and highly inaccurate estimates on the amount of hydrogen which is stored not on regular interstitial sites but trapped at vacancies and, possibly, other lattice defects. The method of PGAA allows a direct determination of the total amount of hydrogen (H) present in the sample irrespective of any prior sample treatment.

Altogether 13 samples were measured, 12 of which were PdH and one was TiH. The dimensions of a typically disk-shaped sample were 6 mm in diameter and 0.5 to 1 mm in thickness. The period of time for a single measurement ranged from 1.5 to 19 h and the gamma count rates were 300 to 2160 cps. Each sample was packed in a Teflon bag for the measurement. Measurements were to be conducted at room temperature under air for both PdH and TiH samples. The hydrogen content in the order of several atomic per cents has been properly detectable by PGAA.

For samples of PdH the treatment prior to the measurement consisted of storing at room temperature (RT) immediately after the hydrogenation process, torsional deforming of the H-loaded samples under hydrostatic pressure to high plastic strains by High Pressure Torsion (HPT), or a combination of HPT on H-loaded samples followed by heat treatment in a DSC. In samples that had been loaded with H (atomic ratio H/Pd = 0.78 and 0.71) and subsequently stored at RT for 14 and 2.5 months a H content of 0.26 and 0.56 was detected, respectively. In contrast, samples loaded to the same initial H concentrations, but deformed by HPT prior to storing at RT, a significantly smaller amount of H was found. For storage times of 31, 14 and 2.5 months the H content dropped to few  $10^{-3}$  (31 and 14 months storage time) and below 0.26 (2.5 months storage time), respectively. Samples that were additionally subjected to heat treatment in the DSC up to 870K after HPT, yielded a H content of few  $10^{-3}$ . The single sample of TiH had been loaded with H up to a concentration of 1.91 and then heat treated in the DSC to a maximum temperature of 860 K. A H/Ti atomic ration of 0.28 was measured, showing that the temperature of the heat treatment was too low to allow for desorption of all interstitial H.

<i>Sample code</i>	<i>AVG RATIO</i>	<i>UNC.</i>	<i>COMMENT</i>
<b>Pd10</b>	0.255	0.004	good sample
<b>Pd25</b>	0.005	0.001	slightly above bkg
<b>Pd22</b>	0.004	0.003	~ bkg
<b>Pd29</b>	0.0018	0.0009	~ bkg
<b>Pd23</b>	0.0026	0.0010	~ bkg
<b>Pd54</b>	0.256	0.004	good sample
<b>Pd28</b>	0.0029	0.0010	~ bkg
<b>Pd63</b>	0.194	0.003	good sample
<b>Pd72</b>	0.0155	0.0017	slightly above bkg
<b>Pd75</b>	0.5577	0.0077	best sample
<b>PdS</b>	0.0053	0.0008	slightly above bkg
<b>PdT</b>	0.0042	0.0017	~ bkg
<b>Ti51</b>	0.278	0.008	good sample

Table 1. The measured H/Pd or H/Ti atomic ratios

The accuracy of measurement fulfilled the expectations and the results obtained provided valuable stimulus for experiments to come.

<b>B N C</b> <b>Experimental Report</b>	<i>Experiment title</i> <b>New generation of Deacon catalysts: in-situ Prompt Gamma Activation Analysis</b>	<i>Instrument</i> PGAA  <i>Local contact</i> L. Szentmiklósi
	<i>Principal proposer:</i> Detre Teschner – Fritz-Haber-Institute, Berlin, Germany <i>Experimental team:</i> Detre Teschner, Ramzi Farra, László Szentmiklósi	<i>Experiment Number</i> PGAA_11_43_IC <i>Date</i> 2011.11.15- 2011.11.25

## Objectives

To clarify the characteristics of the Deacon reaction on Ceria catalysts

## Results

An alternative process to the conventional electrolysis for producing chlorine is the Deacon process, based on the heterogeneous gas phase oxidation of HCl. As a continuation of our experiments in October 2010, two CeO<sub>2</sub>-based catalysts (CeO<sub>2</sub>-A, CeO<sub>2</sub>-R) and much more experimental conditions (such as feed compositions,  $p(\text{O}_2)$ ,  $p(\text{HCl})$  and  $p(\text{Cl}_2)$ , and reaction temperature) were studied using in situ Prompt Gamma Activation Analysis [1]. The quartz reactor (i.d. = 8 mm) was placed into the neutron beam and surrounded by a specially designed oven having openings for the incoming and outgoing neutrons and for the emitted gamma rays. These openings were covered by thin aluminum foils to minimize heat losses. About 0.8 g of CeO<sub>2</sub> (sieve fraction 0.1-0.32 mm) was loaded into the reactor. The reaction feed, at constant 166.6 cm<sup>3</sup> STP min<sup>-1</sup> total flow, was supplied by mass flow controllers, and used gases of HCl (4.5), O<sub>2</sub> (5.0) N<sub>2</sub> (5.0) and Cl<sub>2</sub> (4.0). The Cl<sub>2</sub> production was monitored by iodometric titration.

The experiments indicate that the rate of chlorination is not a function of the pre-chlorination degree, but lower oxygen over-stoichiometry increases the chlorination rate. Dechlorination is effective in high oxygen containing feeds and its rate is higher with stronger pre-chlorinated ceria. Parallel XRD experiments using CeCl<sub>3</sub> in HCl oxidation indicated the formation of CeO<sub>2</sub> as the active phase of the reaction. Electron Paramagnetic Resonance (EPR) experiments strongly suggests that oxygen activation is critically dependent on the surface chlorination degree. Surface intermediates of OH and Cl are the most abundant surface species and we followed the evolution of their coverage by *in situ* FTIR and PGAA as a function of the temperature and the partial pressure of O<sub>2</sub>, HCl and Cl<sub>2</sub>. Higher temperature and  $p(\text{O}_2)$  lead to the same effect in as much as the OH coverage increases and parallel the Cl coverage decreases, which concomitantly correlates with higher reactivity. The HCl partial pressure gives rise to opposite correlations and  $p(\text{Cl}_2)$  does not induce any measurable increase in the Cl coverage despite the strong inhibition by Cl<sub>2</sub>. The results suggest that only a small fraction of surface sites are critically involved in the reaction and most of the surface probed in the *in situ* observation is not directly involved in the reaction.

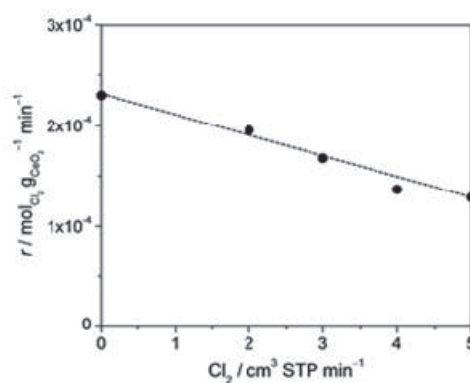


Figure 1: Influence of added Cl<sub>2</sub> on the rate of Cl<sub>2</sub> production in the Deacon reaction over CeO<sub>2</sub>-A. Conditions: 10 vol.% HCl and 90 vol.% O<sub>2</sub>, 703 K, space time = 5.6 g h mol<sup>-1</sup>, total volumetric flow = 166 cm<sup>3</sup> STP min<sup>-1</sup>, 1 bar, and dwelling time under each condition = 1.5 h.

## References

1. Zs. Révay et al. Anal. Chem. **80** (2008) 6066.
2. R. Farra, M. Eichelbaum, R. Schlögl, L. Szentmiklósi, A.P. Amrute, C. Mondelli, J. Pérez-Ramírez, D. Teschner, to be submitted to the J. Catalysis

<b>B N C</b> <b>Experimental Report</b>	<i>Experiment title</i> <b>New generation of Deacon catalysts: in-situ Prompt Gamma Activation Analysis</b>	<i>Instrument</i> PGAA <i>Local contact</i> László Szentmiklósi
	<i>Principal proposer:</i> Detre Teschner – Fritz Haber Institute, Berlin <i>Experimental team:</i> Ramzi Farra – Fritz Haber Institute, Berlin; László Szentmiklósi– Centre for Energy Research	<i>Experiment Number</i> BRR_287 <i>Date</i> 2012.10.02- 2012.10.12

## Objectives

The role of trivalent (La, Y) and tetravalent (Hf, Zr) dopants was investigated on the catalytic properties of ceria in Deacon reaction.

## Results

The catalytic oxidation of (waste) HCl to Cl<sub>2</sub>, the Deacon process (2HCl + 1/2O<sub>2</sub> → Cl<sub>2</sub> + H<sub>2</sub>O), is an energetically efficient yet environmentally friendly solution to recycle chlorine. Earlier in situ Prompt Gamma Activation Analysis experiments made a significant contribution in evaluating the state-of-the-art RuO<sub>2</sub> system, and provided us a clear view how bulk ceria works. In this experiment we evaluated various doped ceria catalysts by in situ PGAA.

A reference CeO<sub>2</sub> system was measured first, followed by a series with different amounts of hafnium (Ce<sub>99</sub>Hf<sub>1</sub>, Ce<sub>97.5</sub>Hf<sub>2.5</sub>, Ce<sub>95</sub>Hf<sub>5</sub>, Ce<sub>90</sub>Hf<sub>10</sub>). Finally at fixed 5 atomic percent doping concentration, the effect of Hf, Zr, Y and La was compared (Ce<sub>95</sub>Zr<sub>5</sub>, Ce<sub>95</sub>Y<sub>5</sub>, Ce<sub>95</sub>La<sub>5</sub>).

About 0.25 g of doped and undoped CeO<sub>2</sub> with the sieve fraction of 0.1-0.315 mm was loaded into the reactor. Various gas feeds, at constant 166.7 cm<sup>3</sup> min<sup>-1</sup> total flow, were supplied by mass flow controllers. HCl (4.5), oxygen (5.0) and nitrogen (5.0) were used. The standard reaction condition was set to O<sub>2</sub>:HCl:N<sub>2</sub> = 9:1:0 at 703 K, and the reaction was monitored by iodometric titration. Molar ratios, Cl/(Ce+M), (M: dopant) were determined from the characteristic peak areas corrected by the detector efficiency and the nuclear data of the observed elements.

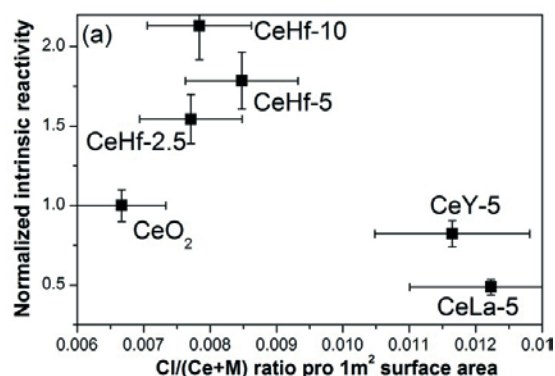


Figure 1. Intrinsic reactivity as a function of the Cl uptake pro surface area, at 703 K temperature, in a reaction mixture of O<sub>2</sub>:HCl = 9:1. For convenient comparison, the intrinsic reactivity of 1 corresponds to CeO<sub>2</sub>.

The experiments indicate the lowest Cl uptake for undoped CeO<sub>2</sub>, the largest uptake for catalysts with trivalent dopants and a weak volcano-shaped trend. The higher chlorination upon trivalent doping is in good agreement with the DFT prediction. It was found that the intrinsic reactivity of ceria in HCl oxidation can be improved by a factor of 2 when doping with Hf and Zr in appropriate quantities, whereas trivalent dopants are detrimental.

The analysis of the doping elements was a technical challenge for PGAA. New spectroscopic data were generated for this set of uncommon elements to allow accurate analysis. A lead gamma attenuator was applied for the first time with success to avoid the overload of the signal processing electronics by the elements with high capture cross section in percentage amounts.

## Reference

Ramzi Farra, Max García-Melchor, Maik Eichelbaum, Maik Hashagen, Wiebke Frandsen, Jasmin Allan, Frank Girgsdies, László Szentmiklósi, Núria López, and Detre Teschner: Promoted Ceria: A Structural, Catalytic, and Computational Study, ACS Catal. 2013, **3**, 2256–2268, doi:10.1021/cs4005002

<b>B N C</b> <b>Experimental Report</b>	<i>Experiment title</i> <b>Composition of Ti/Ru,Ir catalyst samples</b>	<i>Instrument</i> PGAA  <i>Local contact</i> L. Szentmiklósi
	<i>Principal proposer:</i> Antal Tungler – Institute of Isotopes, Department of Surface Chemistry and Catalysis <i>Experimental team:</i> László Szentmiklósi	<i>Experiment Number</i> PGAA_11_44_IH <i>Date</i> 2011.12.06- 2011.12.16

## Objectives

To determine the composition of Ti/Ru,Ir catalyst samples.

## Results

The compositions of eight Ti-based monolith catalysts were analysed by PGAA. The samples were small fragments of Ti mesh, covered with precious metal oxides, weighting about 50-250 mg. Some of them were new, obtained with different preparation methods or from a commercial supplier, while others were already used in wet oxidation of high organic content wastewaters.

PGAA offered a unique opportunity for analysis without destruction of the samples. The results of PGAA revealed both the performance of the preparation of the catalysts and their ageing during wet oxidation under harsh conditions. The latter could be determined by the decrease of precious metal content which occurred by leaching.

The samples were irradiated in Teflon bags for 40-70 000 seconds at the PGAA facility. The concentration of Ti was found to be more than 99.9% in every sample, while the amounts of the trace elements are summarized in the table below.

	<i>Sample 1</i>	<i>Sample 2</i>	<i>Sample 3</i>	<i>Sample 4</i>	<i>Sample 5</i>	<i>Sample 6</i>	<i>Sample 7</i>	<i>Sample 8</i>
<b>V</b>					340 ppm	210 ppm	200 ppm	230 ppm
<b>Cr</b>					430 ppm			
<b>Ru</b>	0.14	0.29		0.21	0.10	0.11		
<b>Pd</b>								0.12
<b>Cd</b>	2.6 ppm	1.2 ppm	0.5 ppm		0.13 ppm			
<b>Ta</b>							19 ppm	
<b>Ir</b>	0.35	0.23	360 ppm	0.40	0.052		330 ppm	

Table 1. the trace elements found in the samples, in addition to the main component Ti. The typical uncertainties are 10-20 %.

## References

1. Arezoo M. Hosseini, Antal Tungler, Zoltán Schay, Sándor Szabó, János Kristóf, Éva Széles, László Szentmiklósi, Comparison of precious metal oxide/titanium monolith catalysts in wet oxidation of wastewaters, submitted to Applied Catalysis B Environmental



<h1 style="margin: 0;">B N C</h1> <p style="margin: 0;"><b>Experimental Report</b></p>	<i>Experiment title</i> <b>Measurement of the content and segregation of B at grain boundaries in experimental Co-Re polycrystalline alloys</b>	<i>Instrument</i> PGAA <i>Local contact</i> László Szentmiklósi
	<i>Principal proposer:</i> Debashis Mukherji – Technische Universität Braunschweig <i>Experimental team:</i> László Szentmiklósi, Zsuzsanna Mácsik– Centre for Energy Research	<i>Experiment Number</i> BRR_303 <i>Date</i> 2012.01.30- 2012.02.03

## Objectives

To determine the boron content and its surface distribution in Co-Re experimental alloys

## Results

Co-Re based alloys are being developed at the TU Braunschweig to supplement Ni-base Superalloys at ultra-high temperature (>1200°C) applications. Grain boundaries in these polycrystalline alloys are strengthened by boron. B is known to segregate to grain boundaries in Ni-alloys and improve low temperature ductility. The mechanisms to strengthen the grain boundaries are being explored for the Co-Re alloys. To have a better understanding of the effect of Boron addition, a set of experimental alloy was manufactured with known added Boron amounts up to 1000 ppm. However, as Boron is volatile, the quantity remained in the alloy is presumably lower than added.

The aims of the present experiments were to quantify the B content by PGAA, and to map its distribution in the alloys, looking for signs of segregation. Thanks to the high cross-section of the  $^{10}\text{B}(n, \gamma)^7\text{Li}$  reaction, we could detect boron already in a few ppm quantity, based on its 477.6 keV gamma-ray. A complementary technique, solid state track detectors (SSTD) was used to map the near-surface B density. The alpha particles, emitted from the same nuclear reaction, create tracks in the SSTDs, if we make a close contact between a polished surface of the sample and the track detector during the irradiation. The track detectors were etched in hot NaOH and imaged with an optical microscope. In some samples the segregation was clearly detectable. This information allows the material scientists to develop a new generation of materials.

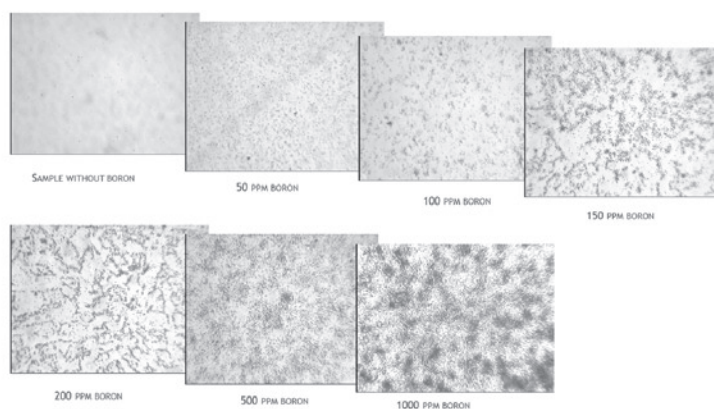


Figure 1. Surface boron distribution patterns as a function of boron content

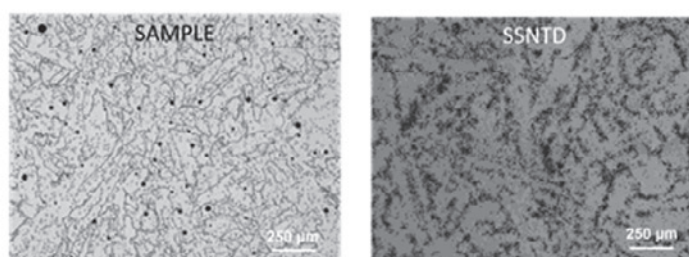


Figure 2. Correlation of the metal structure and the boron distribution

## Reference

D. Mukherji, J. Rösler, J. Wehrs, P. Strunz, P. Beran, R. Gilles, M. Hofmann, M. Hölzel, H. Eckerlebe, L. Szentmiklósi, Z. Mácsik, Metallurgical and Materials Transactions A, 44 (1) 22-30 2013, (doi: 10.1007/s11661-012-1363-6)

<b>B N C</b> <b>Experimental Report</b>	<i>Experiment title</i> <b>Composition of six graphite samples and three rock samples</b>	<i>Instrument</i> PGAA <i>Local contact</i> László Szentmiklósi
	<i>Principal proposer:</i> Eric Mauerhofer – Forschungszentrum Jülich GmbH IEF-6 <i>Experimental team:</i> László Szentmiklósi– Centre for Energy Research	<i>Experiment Number</i> PGAA_12_56_IC <i>Date</i> 2012.01.30- 2012.02.03

## Objectives

to determine the composition of 3 rock and 6 reactor graphite samples

## Results

About 2 g of rock samples were heat-sealed in fluorinated ethylene propylene (FEP) foils with the sizes of about 25×15 mm<sup>2</sup>. The masses of the graphite pieces were 0.6–0.7 g, except one that was 1.4g. The neutron flux at the sample position of the PGAA station was about 9×10<sup>7</sup> cm<sup>-2</sup>s<sup>-1</sup>. The cross-section of the neutron beam was 2×2 cm<sup>2</sup> for the graphites and 1×1 cm<sup>2</sup> for the soils.

The latter samples were measured without any packing, using just Teflon strings as sample holders. The cross-section of the neutron beam is 2×2 cm<sup>2</sup>. The background from carbon and fluorine (Teflon) and other structural materials (Al, Fe, Pb) were subtracted from the compositions.

The compositions of the three graphite samples can be seen in the following table:

Z	El	c% el/el	unc %	c% el/el	unc %	c% el/el	unc %	c% el/el	unc %	c% el/el	unc %	c% el/el	unc %
1	H	46.1ppm	3.1	48 ppm	3.5	46.7 ppm	3.2	59.8 pm	3.1	34 ppm	3.5	39 ppm	3.4
5	B	0.051ppm	5.	0.456 ppm	3.1	0.409ppm	3.1	0.875ppm	3.1	0.458ppm	3.1	0.563ppm	3.1
6	C	99.977	0.002	99.938	0.004	99.933	0.004	99.912	0.004	99.939	0.004	99.932	0.004
13	Al	0.179	3.8	390 ppm	8.	340 ppm	8.	440 ppm	7.	380 ppm	7.	450 ppm	7.
14	Si	150 ppm	11.			70 ppm	11.	110 ppm	7.	60 ppm	25.	90 ppm	18.
16	S			90 ppm	13.	54 ppm	9.	2 ppm	74.	50 ppm	17.	22 ppm	16.
20	Ca			38 ppm	10.	58 ppm	6.	200 ppm	6.	0 ppm	291.	8.1 ppm	4.
22	Ti			11 ppm	6.	10.7 ppm	5.	15 ppm	5.	5 ppm	37.	3.9 ppm	11.
23	V	2.4 ppm	4.	6 ppm	11.	6.0 ppm	5.	0.9 ppm	25.	7.8 ppm	6.	40 ppm	19.
26	Fe	220 ppm	6.	30 ppm	34.	50 ppm	13.	40 ppm	21.	40 ppm	18.	0.0093ppm	5.
62	Sm			0.015ppm	7.	0.0170ppm	4.	0.036ppm	5.	0.014ppm	5.	0.0064ppm	7.
64	Gd			0.023ppm	6.	0.032ppm	6.	0.033ppm	6.	0.9 ppm	9.		

In the soil samples, elements H, B, C, N, Na, Mg, Al, Si, S, Cl, K, Ca, Ti, V, Cr, Mn, Fe, Ni, Cu, Zn, Cd, Nd, Sm, Gd were quantified.

<b>B N C</b> <b>Experimental Report</b>	<i>Experiment title</i> <b>Fission fragment spectrometry by means of the time-of-flight method and fission gamma ray studies</b>	<i>Instrument</i> NIPS
	<i>Principal proposer:</i> A. Oberstedt (U. Örebro, Sweden) <i>Experimental team:</i> Tamás Belgya, L. Szentmiklósi, Z. Kis, K. Takács (IL-HAS), Andreas Oberstedt (U Örebro, Sweden), Stephan Oberstedt, Franz-Josef Hamsch, Ruxandra Borcea, Imrich Fabry (EC JIR IRMM, Belgium), Trino Martinez (Nuclear Innovation Group Department of Energy CIEMAT), Alf Göök (Institut für Kernphysik Technische Universität Darmstadt)	<i>Local contact</i> T. Belgya

## Objectives

Fission fragment spectrometry by means of the time-of-flight method and fission gamma ray studies. Test measurement of the double-E and double-v fission fragment spectrometer VERDI.

## Results

The experimental set-up was installed at the cold neutron beam of the IKI Research Reactor in Budapest (Fig. 1). The neutron flux at the entrance window of the VERDI spectrometer was  $5 \times 10^7$  /s/cm<sup>2</sup>. During the experiment VERDI was operated in a single (v, E) configuration. Ten 450 mm<sup>2</sup> large PIPS detectors are placed at a distance of 50 cm from the fission source. As fissile target a 113 µg/cm<sup>2</sup> <sup>235</sup>U mounted on a 34 µg/cm<sup>2</sup> thick polyimide backing was used and placed directly on the diamond detector. Both the fission fragment distributions and prompt fission gamma-rays from the <sup>235</sup>U(n<sub>th</sub>,f) reaction were measured. Detail of the experimental results can be found in Ref. [1-2].

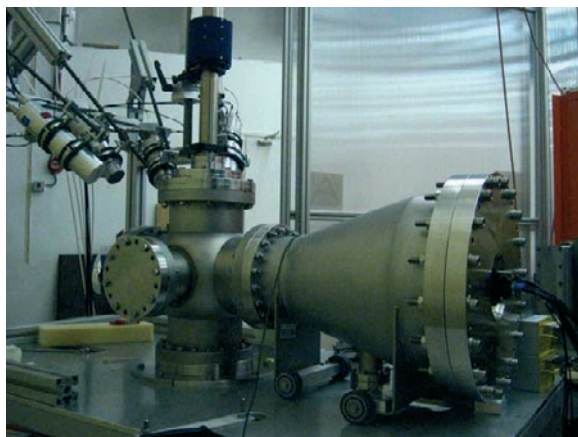


Figure 1: Photograph of the experimental set-up with the single (v, E) version of the fission fragment spectrometer VERDI and four lanthanum halide detectors (upper left corner).

This experiment was supported by the EFNUDAT (agreement number 31027) and NAP VENEUS OMFB 00186/2006 projects.

## References

1. A. Oberstedt, R. Billnert, A. Göök, J. Karlsson, S. Oberstedt, F.-J. Hamsch, R. Borcea, T. Martinez Perez, D. Cano-Ott, T. Belgya, Z. Kis, L. Szentmiklosi, and K. Takács. "Measurement of prompt fission  $\gamma$ -rays with lanthanum halide scintillation detectors." Proceedings of the Final Scientific EFNUDAT Workshop, Ed. Enrico Chiaveri, European Laboratory for Particle Physics (CERN), ISBN 978-92-9083-365-9 (2011) pp. 85-89. (<http://indico.cern.ch/conferenceDisplay.py?ovw=True&confId=83067>).
2. S. Oberstedt, T. Belgya, R. Borcea, A. Göök, F.-J. Hamsch, Z. Kis, T. Martinez-Perez, A. Oberstedt, L. Szentmiklosi, T. Takács, Sh. Zeynalov. "VERDI – a double fission-fragment time-of flight spectrometer." Proceedings of the Final Scientific EFNUDAT Workshop, Ed. Enrico Chiaveri, European Laboratory for Particle Physics (CERN), ISBN 978-92-9083-365-9 (2011) pp. 91-97. (<http://indico.cern.ch/conferenceDisplay.py?ovw=True&confId=83067>).

<b>B N C</b> <b>Experimental Report</b>	<i>Experiment title</i> <b>Compositions of Ni-Mo catalysts</b>	<i>Instrument</i> NIPS
	<i>Principal proposer:</i> Tamás Ollár, Pál Tétényi II-HAS <i>Experimental team:</i> Tamás Belgya	<i>Local contact</i> T. Belgya
		<i>Experiment Number</i>  <i>Date</i> 05.05.2011

## Objectives

To measure number of atom ratios in five Ni-Mo catalyst samples.

## Results

The measurements were performed at the NIPS station with less than 10% accuracy for the Ni-Mo samples utilizing the comparator formula for PGAA [1]:

$$\frac{n_X}{n_C} = \frac{A_{X,\gamma} \sigma_{C,\gamma} \varepsilon(E_{C,\gamma}) f(E_{C,\gamma})}{A_{C,\gamma} \sigma_{X,\gamma} \varepsilon(E_{X,\gamma}) f(E_{X,\gamma})}$$

where  $n$  is the number of atoms,  $A$  is the measured peak area,  $\sigma$  is the partial gamma-ray production cross section for the characteristic gamma-ray with an energy of  $E$  of the element,  $\varepsilon$  is the gamma-ray efficiency of the detector and the factor  $f(E)$  takes into account the neutron and the gamma attenuation in the target. The index  $X$  is for the unknown and  $C$  is for the comparator.

	# of atom ratio			rel.unc%	rel.unc%	rel.unc%
	Ni/Al	Mo/Al	Ni/Mo	Ni/Al	Mo/Al	Ni/Mo
Ni	6.04%	<0.02%	>28981%	4.2	10.5	10.6
NiMo15	0.91%	5.48%	16.57%	5.3	4.2	5.9
NiMo35	0.84%	5.56%	15.04%	6.1	4.4	6.6
NiMo60	3.82%	6.70%	57.01%	7.2	6.0	7.5
Mo	<0.06%	6.33%	<0.91%	12.7	5.1	12.9

*The table below summarizes the results obtained for the samples.*

It can be seen from the table that except from the NiMo35 sample, the nominal Ni-Mo ratios (the number after NiMo shows the intended NiMo ratio in percentage) are in agreement with the expected values.

This experiment was supported by the NAP VENEUS OMFB 00186/2006 projects.

## Reference

1. Révay, Zs., Anal. Chem. **81**, (2009), 6851–6859.

<b>B N C</b> <b>Experimental Report</b>	<i>Experiment title</i> <b>Neutron Prompt gamma ray activation measurements on enriched Hafnium isotopes</b>	<i>Instrument.</i> PGAA  <i>Local contact</i> T. Belgya
	<i>Principal proposer:</i> N. Vasilev (INRNE, Sofia) and Peter Schillebeeckx (DG JRC IRMM, Geel, Belgium) <i>Experimental team:</i> Tamás Belgya, Lászlo Szentmiklósi, Zoltán Kis	<i>Experiment Number</i>  <i>Date</i> 02.23.2010-03.05.2010

## Objectives

To measure the isotopic composition of enriched Hf samples which will be used to measure and improve the resonance capture cross section of Hf isotopes. Natural hafnium is used in regulatory rods of reactors.

## Results

Hf samples originating from Bulgaria to be used for energy differential neutron capture experiments at the JRC IRMM were measured in the EFNUDAT project at the PGAA experimental station operated by II-HAS at the Budapest Research Reactor. The HfO<sub>2</sub> enriched samples were packed in Al disks with a diameter of 3 cm and with thicknesses between 1-3 mm. Since the cross sections of Hf-isotopes are high, the neutron beam was collimated to about 1 mm<sup>2</sup> area, which yielded sufficient count rate for the experiments. The gamma ray spectra were measured with a 27% efficient and 2.2 keV resolution HPGe detector, surrounded with BGO Compton-shield. Auxiliary measurements of Al<sub>2</sub>O<sub>3</sub> powder, Nat-HfO<sub>2</sub> powder, empty Al container and Nat-HfOCl<sub>2</sub>·xH<sub>2</sub>O powder samples were also performed to determine the background components and to re-measure the natural Hf partial gamma-ray cross sections using chlorine as comparator. The natural HfO<sub>2</sub> measurement was used to determine the enrichment of the samples.

The isotopic identification was made by careful comparison of the spectra. If a gamma ray had higher intensity for a given enriched sample than in all of the others then we could assign this gamma ray to that isotope. Of course the literature data helped to perform this identification. Data for <sup>176</sup>Hf is very sparse in the literature, there were only 5 gamma rays identified for this nucleus. This little knowledge of Hf isotopes may induce further research (identification of gamma rays), when enrichment determination is required.

The results of the abundances are shown in the table below. They must be checked for other identified gamma-rays to exclude possibilities of mistakes from unresolved gamma-ray doublets [1].

Samples→ ↓Isotopes	E	<sup>176</sup> Hf	<sup>177</sup> Hf	<sup>178</sup> Hf	<sup>179</sup> Hf	Natural
176	395	46.9±1.9	11.5±1.1	0.4±0.2	0.3±0.2	5.3
177	1419	33.4±0.3	75.2±0.2	2.8±0.1	0.9±0.1	18.6
178	1003	11.7±0.3	12.2±0.8	89.6±0.1	4.9±0.2	27.3
179	1065	2.6±0.1	0.3±0.2	5.7±0.2	72.4±0.2	13.6
180	5694	5.4±0.3	0.8±0.2	1.5±0.2	21.5±0.4	35.1

This experiment was supported by the EU FP6 EFNUDAT and the NAP VENEUS OMF 00186/2006 projects.

## Reference

1. Belgya, T, and Z. Kis. "PGAA Analysis of Isotopically Enriched Samples." Proceedings of the Final Scientific EFNUDAT Workshop, Ed. Enrico Chiaveri, European Laboratory for Particle Physics (CERN), ISBN 978-92-9083-365-9 (2011) pp. 1-8. (<http://indico.cern.ch/conferenceDisplay.py?ovw=True&confId=83067>)

<b>B N C</b> <b>Experimental Report</b>	<i>Experiment title</i> <b>Determination of the photon strength function in <math>^{114}\text{Cd}</math> in joint experiments on photon scattering at FZD-ELBE and on thermal neutron capture into <math>^{113}\text{Cd}</math> at IKI Budapest</b>	<i>Instrument</i> PGAA
	<i>Principal proposer:</i> Arnd Junghans FZD Dresden, Germany <i>Experimental team:</i> Evert Birgersson FZD Dresden, Georg Schramm FZD Dresden, Tamás Belgya	<i>Local contact</i> T. Belgya

### Objectives

The reaction  $^{113}\text{Cd}(n, \gamma)^{114}\text{Cd}$  was measured in order to get insight of the photon strength functions and level density in  $^{114}\text{Cd}$ . Since the capture of the neutron leads to a  $1^+$  state in  $^{114}\text{Cd}$ , the transitions to the ground state and low lying states are M1 transitions and thus suppressed in favour of E1 transitions. This leads to a higher intensity of the quasi continuum transitions under the discrete lines. The shape of this quasi continuum region is crucial for deducing information about photon strength functions and level density.

### Results

The spectrum from the reaction  $^{113}\text{Cd}(n, \gamma)^{114}\text{Cd}$  was measured using a natural target as well as a enriched target. A large portion of the detected gamma rays are not seen as peaks in the spectrum but rather as a continuum. It is very important to have good knowledge of the detector response for a high quality measurement of this kind, since the Compton scattered events from high energy transitions has to be separated to obtain a spectrum containing only the full energy transitions. The HPGe detector at the Prompt Gamma Activation Analysis (PGAA) station at the Budapest research reactor was used for the experiment. Its response is understood and no problem should arise during analysis of the spectrum. The rather high capture cross section in combination with the high flux cold neutron source gave initially too high count rates with the standard  $5 \text{ mm}^2$  collimator. This caused a spectral shape change of the peaks. In order to avoid this, we constructed an even smaller collimator. The collimator consists of  $^6\text{LiF}$  loaded plastic. The beam spot size was approximately  $2 \text{ mm}^2$ . The detector at the PGAA station is routinely used and calibration measurements with sources as well as with calibration targets in the beam had already been performed before the measurement started. Because of this and the high capture cross section, a beam time of three days was sufficient. This experiment was followed by a  $^{114}\text{Cd}(\gamma, n)$  experiment in Dresden at the ELBE facility in April 2012 which is supported by the EU FP7 ERINDA project. The analysis of the data is still in progress, in collaboration with the FZD project team.

This experiment was supported by the EU FP6 EFNUDAT and the NAP VENEUS OMF00186/2006 projects.

<h1 style="margin: 0;">B N C</h1> <p style="margin: 0;"><b>Experimental Report</b></p>	<p><i>Experiment title</i> <b><sup>237</sup>Np standardization</b></p>	<p><i>Instrument</i> PGAA</p> <p><i>Local contact</i> T. Belgya</p>
	<p><i>Principal proposer:</i> Matthias Rossbach, Jülich, Germany <i>Experimental team:</i> Tamás Belgya, Zoltán Kis, Cristoph Genreith, Jülich, Germany</p>	<p><i>Experiment Number</i> PGAA_11_36_IC</p> <p><i>Date</i> 2010.02.23- 2010.03.05</p>

## Objectives

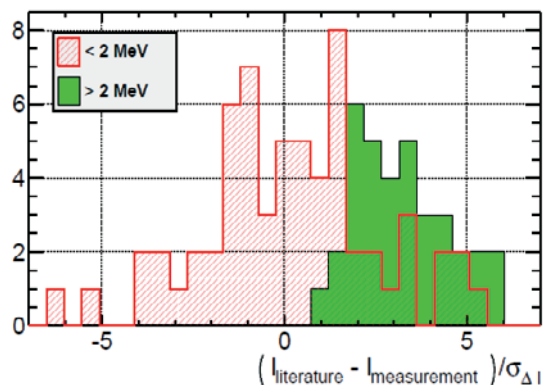
To measure PGAA neutron capture gamma-ray spectra of <sup>237</sup>Np for identification in nuclear waste and determine partial gamma ray cross sections.

## Results

Due to their importance in nuclear waste management transuranic actinides are of particular interest in research and technology. Radiotoxicity, longevity and decay radiation of these elements require the development of innovative non-destructive methods for the characterization of nuclear waste.

Prompt gamma activation analysis (PGAA) offers an alternative to standard gamma spectroscopic techniques for the identification and quantification of transuranic actinides in complex waste matrices. <sup>237</sup>NpO<sub>2</sub> powder was obtained from Oak Ridge National Laboratory via TU München. The preparation was performed in a glove box at Forschungszentrum Jülich. About 8.6 mg of the powder was pressed to form a pill of 3mm diameter using a pill press with a maximum pressure of 1 t. The pill was mounted between two circular foils of 99.99% pure aluminium with a thickness of  $d = 0.25\text{mm}$  held in a screw cap frame made from industrial aluminium. In addition a blank sample without <sup>237</sup>NpO<sub>2</sub> was prepared. The irradiation of the sample was performed at the PGAA facility at the Budapest Research Reactor using a guided cold neutron beam with a thermal equivalent flux of  $1.2 \times 10^8 \text{ cm}^{-2}\text{s}^{-1}$ . The sample has been placed within a neutron shielded sample chamber 23.5 cm in front of a collimated HPGe/BGO Compton-suppression spectrometer.

Among 800 detected peaks, 97 prompt gamma lines of <sup>237</sup>Np have been identified. The comparison of the obtained values with literature values showed a reasonable agreement with respect to the energies of the identified lines but significant differences with respect to the relative intensities (see Figure below) [1].



This experiment was supported by the NAP VENEUS OMF 00186/2006 project.

## Reference

1. C. Genreith, M. Rossbach, E. Mauerhofer, T. Belgya, G. Caspary, *First results of the prompt gamma characterization of <sup>237</sup>Np*, NUKLEONIKA, in print

<b>B N C</b> <b>Experimental Report</b>	<i>Experiment title</i> <b>Characterisation of prompt gamma signature of actinides</b>	<i>Instrument</i> PGAA <i>Local contact</i> Belgya Tamás
	<i>Principal proposer:</i> Matthias Rossbach Research Center of Juelich, IEK-6 <i>Experimental team:</i> Chritoph Genreith, Matthias Rossbach, IEK-6, Kis Zoltán, Belgya Tamás – MTA EK IKI	<i>Experiment Number</i> PGAA_12_52_IC <i>Date</i> 2012.03.03- 2012.03.12

### Objectives

- 1) To study the prompt gamma radiation emitted from selected actinide nuclides under cold neutron irradiation in the beam of the Budapest Research Reactor and compare results with theoretical values.
- 2) Determine intensities of  $(n, \gamma)_{\text{prompt}}$  lines and partial gamma ray production cross sections.
- 3) Determine thermal equivalent neutron capture cross sections from the activated decay.

### Results

The encapsulation of the radioactive  $^{237}\text{NpO}_2$  and  $^{242}\text{PuO}_2$  samples were done in quartz vials and sealed in FEP foil. Quantities per sample were approximately 5 mg per nuclide with and without gold monitor. Blank vial was also irradiated. After irradiation the samples were counted in the low level DÖME facility to determine the neutron flux with the gold monitor. It was then used to determine the prompt and delayed partial gamma-ray production probabilities for the  $^{238}\text{Np}$  and  $^{243}\text{Pu}$  nuclei.

The thermal neutron capture cross sections of  $^{237}\text{Np}$  and  $^{242}\text{Pu}$  were evaluated from the obtained prompt and delayed gamma ray data. The thermal neutron capture cross sections for  $^{237}\text{Np}(n, \gamma)^{238}\text{Np}$  was found to be  $\sigma(^{237}\text{Np}) = 170.4 \pm 7.4$  b and for  $^{242}\text{Pu}(n, \gamma)^{243}\text{Pu}$  to be  $\sigma(^{242}\text{Pu}) = 19.6 \pm 3.9$  b.

A typical spectrum is shown in Fig 1.

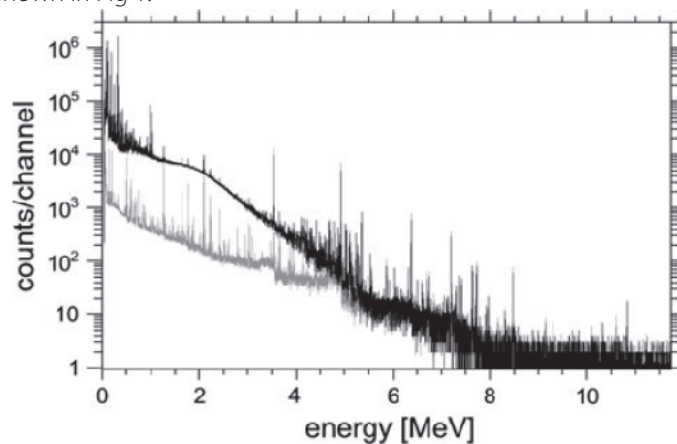


Fig 1. The prompt gamma ray spectrum obtained during a 24 h measurement of the  $^{237}\text{NpO}_2$  (black) along with prompt gamma ray spectrum of the blank sample irradiation (gray). The spectrum of the blank sample irradiation was renormalized to the live time of the  $^{237}\text{NpO}_2$  sample.

### References

- [1] Genreith C., Rossbach M., Mauerhofer E., Belgya T., Caspary G., First results of the prompt gamma characterization of Np-237, Nukleonika 57 (2012) 443-446.
- [2] Genreith, C., M. Rossbach, E. Mauerhofer, T. Belgya, and G. Caspary: Measurement of thermal neutron capture cross sections of  $^{237}\text{Np}$  and  $^{242}\text{Pu}$  using prompt gamma neutron activation, J. Radioanal. Nucl. Chem., 296 (2013) 699-706.



<b>B N C</b> <b>Experimental Report</b>	<i>Experiment title</i> <b>Characterisation of prompt gamma signature of actinides</b>	<i>Instrument</i> PGAA <i>Local contact</i> Belgya Tamás
	<i>Principal proposer:</i> Tamás Novotny , Erzsébet Feró MTA EK <i>Experimental team:</i> Tamás Belgya, László Szentmiklósi and Boglárka Maróti – MTA EK IKI	<i>Experiment Number</i> PGAA_12_58_IH_ <i>Date</i> 2012.06.28- 2012.07.05

### Objectives

To measure the hydrogen content of several zirconium fuel cladding treated with high pressure hot water.

### Results

PGAA is especially good for measurement of hydrogen content of various materials. In collaboration with the Fuel and Reactor Materials Department a number of Russian zirconium cladding were traded LOCA equivalent circumstances and the treated claddings were investigated with PGAA and other methods to determine the hydrogen content of the cladding. The hydrogen contents were then correlated with the mechanical properties of the treated cladding. The result of the PGAA experiment is presented in Figure 1.

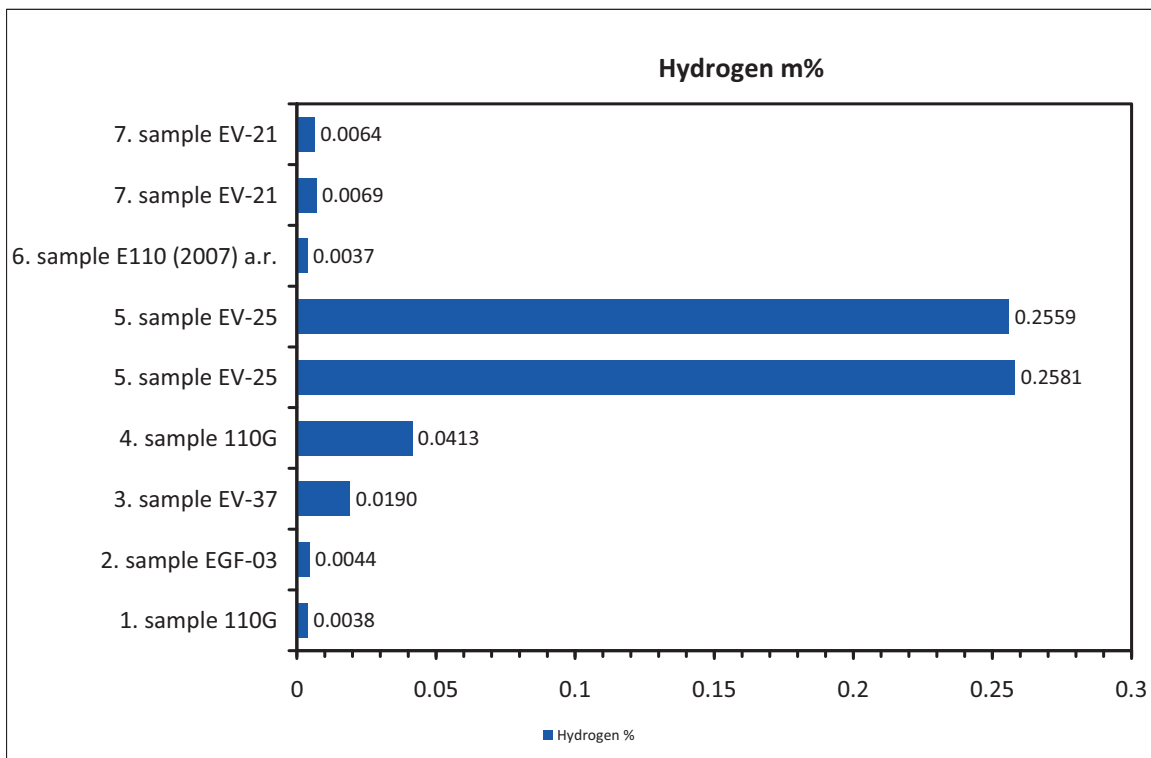


Fig 1. Hydrogen content of the investigated samples.

### Future

More collaboration on this topic should be done.

<b>B N C</b> <b>Experimental Report</b>	<i>Experiment title</i> <b>Correlation measurements of prompt fission gamma rays and fission fragments</b>	<i>Instrument</i> PGAA <i>Local contact</i> Belgya Tamás
	<i>Principal proposer:</i> Andreas Oberstedt U. Oerebro, Sweden <i>Experimental team:</i> S. Oberstrdt, R. Billnert, M. Vidali IRMM, Geel, Belgium Tamás Belgya, László Szentmiklósi and Kis Zoltán – MTA EK IKI	<i>Experiment Number</i> PGAA_12_66_IC <i>Date</i> 2012.05.23- 2012.07.01

### Objectives

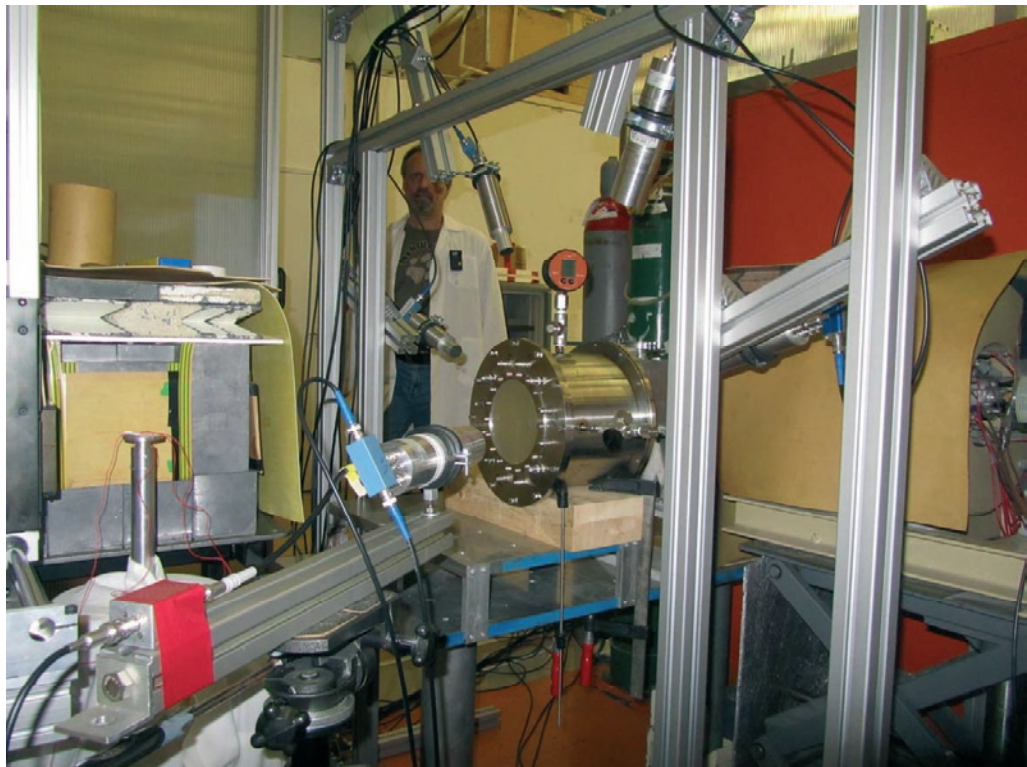
To measure the correlation of prompt fission gamma-rays and fission fragments.

### Results

Gamma energy and efficiency calibrations were performed using several La based scintillation detectors, followed by the fission gamma experiments on U-235 target in a Frisch-grid ionization chamber.

A good knowledge about particle emission in fission is essential for the peaceful use of nuclear power. Prompt gamma-rays contribute considerably to the fission heat in a reaction core, whereas prompt neutrons are responsible for maintaining a chain reaction. The precision, with which their characteristics are known, is of course important for both safety reasons and economy. Apart from the technological aspects, there are also indications that in particular prompt fission gamma-rays reveal detailed information on the dynamics of the fission process.

The experimental setup is shown in picture below. The analysis of the data is in progress.



### References

Andreas OBERSTEDT et al., Measurements of prompt fission gamma-rays and neutrons with lanthanide halide scintillation detectors, The ERINDA 2013 Workshop, CERN, Geneva (Switzerland) from 1st to 3rd October 2013, Talk

<h1 style="margin: 0;">B N C</h1> <p style="margin: 0;"><b>Experimental Report</b></p>	<i>Experiment title</i> <b>DEVELOPMENT OF CONTROL OF THE SUPER CRITICAL WATER LOOP</b>	<i>Instrument</i> DNR
	<i>Principal proposer:</i> Attila Kiss <sup>2</sup> and Attila Aszódi <sup>2</sup> <i>Experimental team:</i> Márton Balaskó <sup>1</sup> , László Horváth <sup>1</sup> , Ákos Horváth <sup>1</sup> , Kiss Attila <sup>2</sup> <sup>1</sup> MTA KFKI Atomic Energy Research Institute, Budapest, Hungary <sup>2</sup> BME Institute for Nuclear Technology, Budapest, Hungary	<i>Local contact</i> Horváth László  <i>Experiment Number</i> DNR_12_10_IH <i>Date</i> 2012. multiple occasions

### Objectives

Important task to measure the streaming properties of the supercritical water in a closed circle loop.

### Results

The supercritical water has an extraordinary feature. Its density is changing dramatically above 374°C, 22.1 MPa. This basic event is available to study by ANCARA (MTA KFKI **A**EKI-BME **N**TI Budapest super**C**ritical w**A**ter test **f**Acility) natural circulation loop in the dynamic neutron radiography (DNR) station. The loop is essentially a bended closed pipe with many different measurement equipments (absolute and differential pressure transducers, mass flow meter, thermocouples, and heaters with a total power of 6000W) mounted on an aluminium alloy frame.

The experiment is controlled by a datalogger software, which measures the state of the supercritical water on 26 places. It stores the measured values of the temperatures, pressures, mass flow, and heating powers on the computer disc and displays it on a graph. The software can hold the state of the water in a precise value. The software saves the picture of the neutron radiography camera too.

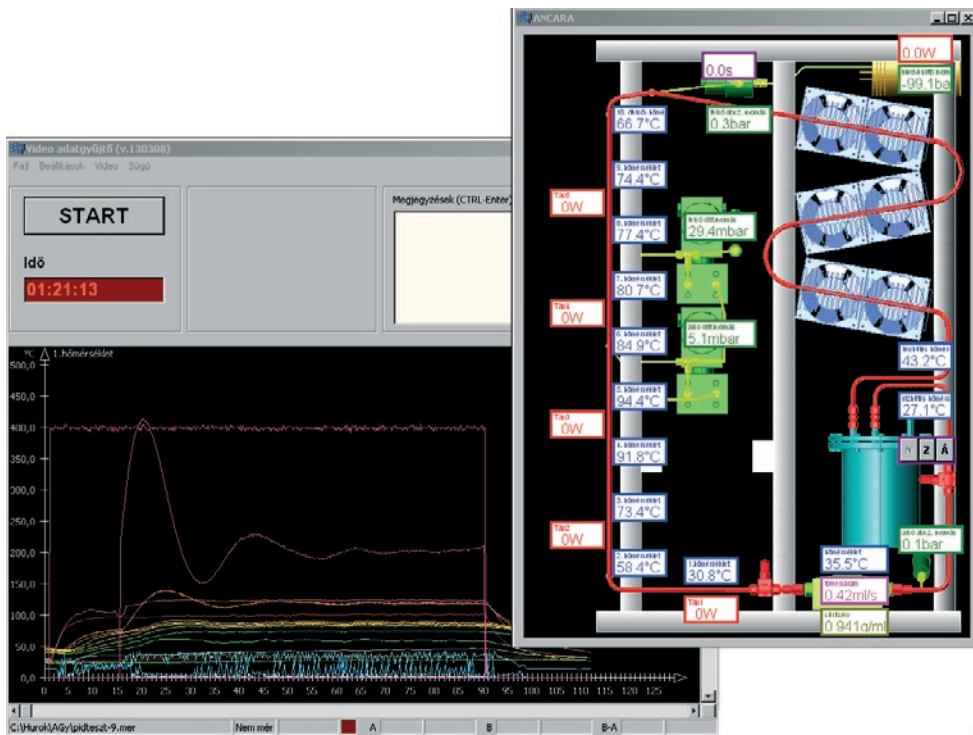


Figure 1.

### Future prospects

This project will be continued, as a co-operation work between EK and BM

<b>B N C</b> <b>Experimental Report</b>	<i>Experiment title</i> <b><sup>197</sup>Au Mössbauer spectroscopy of stabilised nanoparticles</b>	<i>Instrument.</i> IMBS  <i>Local contact</i> Károly Lázár
	<i>Principal proposer:</i> Imre Dékány, MTA-SZTE Research Team for Supramolecular and Nanostructured Materials, Szeged <i>Experimental team:</i> S. Stichleutner, K. K. Lázár	<i>Experiment Number</i>  <i>Date</i>

### Objectives

The probability of the Mössbauer effect strongly depends on the size of particles beyond a certain threshold value. This threshold depends on various factors (e.g. the energy of Mössbauer  $\gamma$ -transition, the stabilisation of the emitting particles, the temperature of measurement, etc.). In the case  $^{197}\text{Au}$  Mössbauer spectroscopy this limit is a few nm provided the measurements are performed at liquid He temperature (4.2 K). At an intermediate stage of the installation of the in-beam Mössbauer spectrometer (in particular the liquid He facility) the threshold size of gold particles was estimated from measurements performed at higher temperature, 80 K (with liquid nitrogen). 29, 20 and 4.5 nm gold particles were stabilised, and the relative intensities of their spectra compared.

### Results

Nanodisperse gold particles were prepared by two reduction methods. Depending on the speed of reduction the particle size may be modified. First the particles were reduced and stabilised by aminodextrane, particles with 29 and 20 nm were obtained this way.  $\text{NaBH}_4$  was used in the second case with octanethiol stabiliser, the average particle size of the product was 4.5 nm.  $^{197}\text{Au}$  spectra were collected, the relative intensities determined and compared in four cases, by using 50 micron thick gold foil as a reference material.

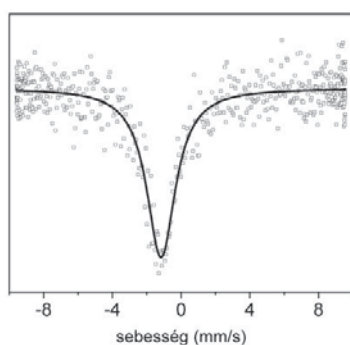


Figure: 80 K spectrum of the Au(Dext-1) sample

Sample	Diameter nm	Rel. Intensity %
Au 50 $\mu$ foil	$\infty$	1.0
Au(Dext-1)	29	0.73
Au(Dext-2)	20	0.68
Au-Thiol	4.5	$\sim 0$

Table  
Comparison of the probability of  $^{197}\text{Au}$  Mössbauer effect on particles of different size (80 K)

From these measurements only a rough estimation can be provided as for the detectable threshold size of particles at 80 K under the experimental conditions applied. Namely ca. particles of  $\sim 10$  nm diameter can probably still be investigated at 80 K. For studying particles of smaller size the installation of the liquid He facility is indispensable.

### Reference

Lázár K., Belgya T., Csapó E., Dékány I., Hornok V., Stichleutner S.: In-beam Mössbauer-spektroszkópia, *Nukleon*, 5 (2012) 120.

<b>B N C</b> <b>Experimental Report</b>	<i>Experiment title</i> <b>BAGIRA3 irradiation loop</b>	<i>Instrument</i> BAGIRA
	<i>Principal proposer:</i> Ferenc Gillemot <i>Experimental team:</i> Ákos Horváth, Gábor Uri, Marta Horváth,	<i>Local contact</i> F. Gillemot

## Objectives

To built an neutron irradiation device satisfying the up-to date requirements

At the Budapest Research Reactor two gas cooled irradiation rigs (BAGIRA 1 and 2) have been operated since 1998 and 24 different irradiation researches have been performed to testing irradiation ageing of reactor and fusion devices structural materials as low alloyed and stainless steels, Al, Ti and W alloys, ceramics etc. The devices served more than 12 years, they material aged by irradiation and corrosion, and their capacity can't satisfy the up-to date requirements of the newly developing materials.

Presently the main interest of the nuclear industry is the development of fusion reactors and Generation Four fission reactors. To increase the efficiency and decrease the impact on the environment high operation temperature will be used. Consequently high temperature irradiation combined with in pile creep and fatigue testing are the future tasks of the irradiation devices.

## Description of the new device

The new device is called BAGIRA3. The main features of it are:

The rig capacity is 36 Charpy size specimen ( $\approx 1200$  gr steel) or similar. The specimen sizes and shape can be varied according to the requirements, since only the target simple holder has to be changed.

Each of the new six zone electric heating can be separately controlled, ensuring to keep the required irradiation temperature within  $\pm 5^\circ\text{C}$ . Irradiation temperature can be controlled between  $150^\circ\text{C}$ - $650^\circ\text{C}$ .

The maximum fluence rate is  $1\text{-}5 \cdot 10^{13}$  n/cm<sup>2</sup> E>1MeV

The irradiation rig is shielded with boron carbide to filter the thermal neutrons, reducing the activity of the irradiated specimens and the nuclear heating. Reduced target activity reduces the cost of the testing or transportation of the irradiated specimens.

The target holder is separated from the thermocouples and electric heating system. This way the cost of the heating elements and thermocouples decreasing, and only minor quantity of aluminium or titanium heat removal material goes into the radioactive waste

The new target pick up and eject system allows the quick target change during the reactor stop, and active target also can be used (e.g irradiated and annealed material can be reirradiated)

The target can be rotated during irradiation to ensure the same irradiation of the specimens located on the same level

The rig design allows irradiation creep or irradiation-low cycle fatigue study too.

The device is designed for automatic operation, programmable, and it has several safety features, (including emergency passive cooling system, automatic reset in case of any malfunction of the control system, etc.)

## The present situation and the remaining work

The equipment is ready and the control software is tested several hundred hours. Twelve different safety tests performed successfully, and the Hungarian National Saftz Authority permitted the installation into the reactor and to make the test run, planned in 2012 august. According to the plan the rig will be continuously operated from January 2013.

## References

1. Gillemot, F.: „Study of Irradiation Effects at the Research Reactor” Strengths of materials, Vol 42. No 1. 2010, Springer Science pp.78-83

<b>B N C</b> <b>Experimental Report</b>	<i>Experiment title</i> <b>Water chemistry at the Budapest Research Reactor</b>	<i>Instrument.</i> <i>Gamma-spectrometry</i>
	<i>Principal proposer:</i> Ibolya Sziklai-László, Centre for Energy Research, HAS <i>Experimental team:</i> Dénes Elter, Centre for Energy Research, HAS	<i>Local contact</i> Ibolya Sziklai-László <i>Experiment Number</i> NAA-11-01-IH <i>Date</i> 31. 12. 2011.

## Objectives

The main objective of this study is to measure the activity concentrations of characteristic fission and corrosion products in the primary cooling water and the chemical concentrations of different impurity components in various water systems of the Budapest Research Reactor (BRR).

## Results

The increase of fission product activities in the primary coolant indicates the presence of fuel defects. In order to investigate the status of fuel cladding integrity and to detect any failure at the earliest stage during the fuel conversion from the highly enriched uranium (HEU) to low enriched uranium (LEU), samples from the primary cooling water were measured in every reactor cycle. Samples were taken three (1st) and nine days (2nd) after the reactor start and at the time of the shutdown (3rd). The water purification system was put into operation after the second sampling process in every cycle. In 2010, one of the main tasks of the project was to monitor the activities of two characteristic iodine nuclides during the normal operation of the BRR. Based on a comparison of  $^{131}\text{I}$  and  $^{133}\text{I}$  activities in Cycles 28, 29 (reactor core with mixed HEU and LEU) and Cycle 27 (before the fuel conversion procedure began) no damage to the fuel elements was indicated. Figure 1. and 2. show the variation of activity concentrations of  $^{131}\text{I}$  and  $^{133}\text{I}$  nuclides in water samples, taken from the primary circuit during normal operations and reactor shutdown. The highest concentrations were generally measured for  $^{131}\text{I}$  in the 2nd samples. Comparing the maximum values of activity concentrations of measured radionuclides to the total authority limit (40 MBq/l), it can be stated that the data are well below the specified limit. The total activity concentration levels (minimum and maximum) ranged only from 1.5 to about 4.9% of the referred limit.

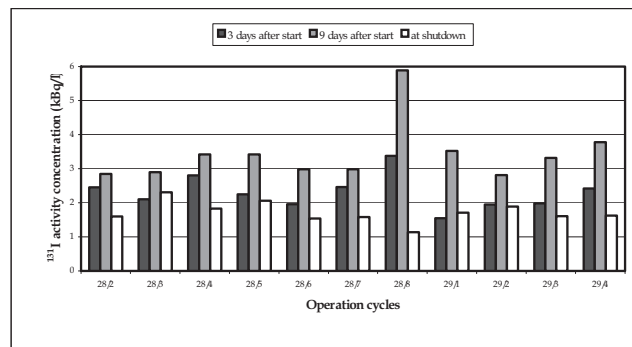


Figure 1: Variation of activity concentrations of  $^{131}\text{I}$  nuclide in the primary water of the BRR in 2010

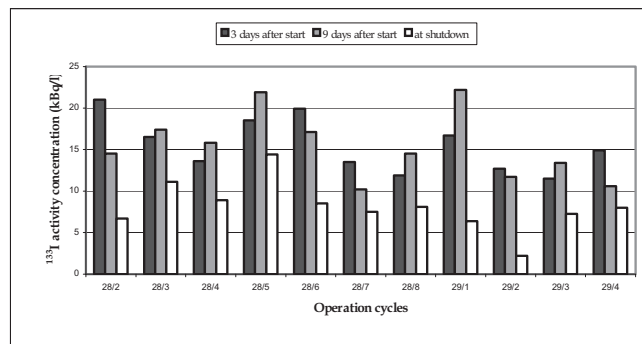


Figure 2: Variation of activity concentrations of  $^{133}\text{I}$  nuclide in the primary water of the BRR in 2010

<b>B N C</b> <b>Experimental Report</b>	<i>Experiment title</i> <b>New materials based on biogenic iron oxides - study of composition, features and behaviour: INAA study of synthetic and natural iron bacteria products</b>	<i>Instrument: INAA and Gamma-spectrometry</i>  <i>Local contact: Ibolya Sziklai-László</i>
	Principal proposer: Kiril Krezhov, Institute for Nuclear Research and Nuclear Energy, Bulgarian Academy of Sciences, Sofia, Bulgaria, Experimental team: Ibolya Sziklai-László, HAS Centre for Energy Research, Lubomir Slavov, Ivan Nedkov, Institute of Electronics, B.A.S.Veneta Groudeva, Ralitsa Angelova, Faculty of Biology, Sofia University "Saint Kliment Ohridski"	<i>Proposal No. BRR_339</i>  <i>Date of experiment: 2012.10.01.</i>

## Objectives

The remarkable feature of some of the Fe-oxidizing bacteria are the unique morphology structures they produce, such as powders, sheaths or stalks, acting as organic matrices upon which the deposition of hydrous ferric oxides can occur. The aim of the present study was the determination of the elemental constitution of the products of the bacteria group *Sphaerotilus – Leptothrix* which can be found in different natural habitats. As a result of their metabolism, they form biogenic iron oxides/(oxy)hydroxides, accumulating in their sheaths. Several investigations provide information about their important application as pigments, catalysts, absorbents etc, obtained in different environmental conditions. The Instrumental neutron activation analysis (INAA) based measurements should help in revealing an optimized scheme for isolation and enrichment of bacteria in laboratory conditions and possible implications for nanotechnology.

## Results

The samples studied were prepared in the laboratory Faculty of Biology, Sofia University, Romania. Seven different samples were studied. Three samples are products from poly bacterial action of *Sphaerotilus* and *Leptothrix* (Vitoshka, 1783 m) in solution with nutrient media of ferro ammonium sulphide and different days of cultivation. Two samples are from monobacterial *Leptothrix* with nutrient media of ferro ammonium sulphide. One sample is a product from *Leptothrix* with nutrient media of iron sulphide. Reference sample picked from a natural source, from the locality Aleko, Vitoshka mountain at the altitude of 1840 m.

Irradiations of the samples were carried out at the BRR. INAA based on short-lived radionuclides was applied for the determination of Al, Ba, Cu, Mn, V and S. The long-lived radionuclides were applied for the determination of Ag, As, Br, Ca, Co, Cr, Cs, Fe, K, La, Na, Rb, Sb, Sc, Th, U and Zn. The concentrations of the elements in bacteria samples cultivated in different nutrient media were compared to those found in reference sample. High enrichment level of iron was found in all samples in comparison with the reference sample. The enrichment rate varied between 3.8 and 7.4. Comparing the Mn concentration with that of the reference sample, the high enrichment level was found in only one sample. Somewhat higher concentration of As found in two samples (23.9 and 25.7 mg/kg versus 18.3 mg/kg) is probably due to the presence of a small quantity of arsenic processing bacteria. This will be the subject of further bio-experiments. The increased amounts of Cu and Cr found in all tested samples, compared to the concentration in the basic sample is of high interest. The traces of Th, U and Sb found in the basic sample raise possible ecological issues. The Zn concentrations found in the different samples were orders of magnitude higher than in the reference. The reasons for this high accumulation in sample 1, 4 and 5, will be subject of further studies.

The results obtained so far demonstrate that the experiments directed to obtain iron compounds by biotechnology routes were correctly organized and final products have iron content with an order of magnitude higher than the natural product (reference). Additional interest comes from the registered highly selective increase of several essential elements which supports the ability of the NAA technique to reveal and quantify the presence of specific trace elements in the biosphere.

## Future prospects

The study is in progress. New set of samples will be prepared in order to clarify possible contributions from the starting culture media, the iron containing additives and the basic sample. Additional XRD analyses are carried out to reveal actual phase constitutions.

<b>B N C</b> <b>Experimental Report</b>	<i>Experiment title</i> <b>Test of the pneumatic transfer system of the BRR</b>	<i>Instrument</i> <i>Gamma-spectrometry</i>
	<i>Local contact</i> <i>Ibolya Sziklai-László</i>	<i>Experiment Number</i> <i>NAA-11-02</i>
<i>Principal proposer:</i> Ibolya Sziklai-László, Centre for Energy Research, HAS		<i>Date</i> 31. 12. 2011.
<i>Experimental team:</i> József Janik, Attila Matisz, Centre for Energy Research, HAS		

## Objectives

The control and data acquisition electronics and software of the fast rabbit system of the BRR has been upgraded recently. In the new system Field Point modular based I/O was implemented (National Instruments, USA). In order to extend the irradiation period (up to 20 minutes) a new sample holder capsule made from a high purity polymer (DuPont™ Vespel® SP-1) was used for short irradiations in the fast rabbit system. The main objectives of the present work were to test of the cleanliness of this new material by INAA method and to measure the surface contamination of the capsule during irradiations and to check on the sample temperature inside the capsule. In addition, overall neutron flux characterizations and the investigation of the reproducibility/reliability of the irradiations were performed in the irradiation channel used for short irradiations.

## Results

Table 1. shows the results of the INAA measurement in comparison with the Vespel test results. The results are in fair agreement and the relatively high measured concentration of iron is acceptable in use of this capsule in short irradiation cycles thanks to its long half life. The concentrations of the Al, As, Cu, Mg, Mn, and Na producing short half life isotopes with impurities <0.7 ppm, have no limiting affect on the usage of these capsules in several irradiation cycles per day. The typical uncertainties of the results are about 1-3 %. The temperature was also tested using Temperature Sensing Labels (Spirig, Switzerland). The temperature increased up to 110°C inside the sample holder after 4.25 minutes of irradiation time. The decontamination efficiency of the Vespel sample holder after three irradiation cycles (3x2 minutes) was ~95% and only a very low activity of <sup>60</sup>Co nuclide originating from the tubing of the fast rabbit system, was detected on the surface of the sample holder. For the determination of thermal and fast fluxes high purity foils of Al-0.1% Au, Zr and Fe were used (Table 2.).

**Table 1.** Analytical results on Vespel SP-1 polyimide sample

Element	Concentration (ppm)	
	Vespel test by ICP method	INAA results
Al	0.12	0.21
As	-	0.12
Ca	0.31	0.45
Cr	<0.1	0.14
Co	-	0.32
Cu	0.21	0.63
Fe	0.14	0.37
K	<0.1	0.15
Mg	0.12	0.18
Mn	<0.1	0.09
Mo	<0.1	0.09
Na	0.23	0.75
Zn	0.11	0.22

**Table 2.** Variation of the neutron flux parameters in the fast rabbit "B" at the BRR

Operation cycles of the BRR	$\Phi_{th}$ , (n/cm <sup>2</sup> s)	flux ratio $f = \Phi_{th}/\Phi_{epi}$
29/6	4.44 10 <sup>13</sup>	34.4
29/9	4.81 10 <sup>13</sup>	34.8
30/1	4.85 10 <sup>13</sup>	34.3
30/4	4.45 10 <sup>13</sup>	35.1
30/4	4.61 10 <sup>13</sup>	35.5
30/7	4.52 10 <sup>13</sup>	33.5

The determined values confirm the suitability of using this material. The decontamination properties of this material are also excellent and allow the use of this capsules several times during a day. The reproducibility/reliability of the irradiations was checked by irradiation of 15 different Zn foils (Goodfellow) with different irradiation times (1-3 minutes). The agreement between the resulting specific activities of these irradiations was found to be within 3% on an average.



<h1 style="margin: 0;">B N C</h1> <p style="margin: 0;"><b>Experimental Report</b></p>	<i>Experiment title</i> <b>Proficiency test on soil and botanical samples</b>	<i>Instrument</i> INAA and Gamma-spectrometry <i>Local contact</i> Ibolya Sziklai-László
	<i>Principal proposer:</i> Ibolya Sziklai-László, Centre for Energy Research, HAS <i>Experimental team:</i>	<i>Experiment Number</i> NAA-12-01-IC <i>Date</i> 25.09.2012.

## Objectives

Laboratories from different continents (Europe, Africa and Latin America) using nuclear techniques, under the IAEA Technical Cooperation (TC) projects RAF4022, RAS1018, RER4032/RER1007 and RLA0037 participated in consecutive inter-laboratory comparison rounds organized by the IAEA in conjunction with the Wageningen Evaluating Programs for Analytical Laboratories (WEPAL). The aim of this project was to test analytical performance of the laboratories in the multi-elemental analysis of various samples.

## Results

The inter-laboratory comparison rounds were related to the determination of (trace) elements in soil (ISE) and plant (IPE) samples. With the Normal Distribution Approximation (NDA) model mean and standard deviation are calculated. The results provided by the individual laboratories have been evaluated on basis of z-scores (interlaboratory difference, corrected for the spread in the results) and on the bias, relative to the mean value of the measurand and reported by the WEPAL. Satisfactory performance is attained for  $|z|$ -scores  $\leq 3$  and bias values  $\leq 20\%$ . Our NAA results, based on the  $k_0$ -standardization method, agreed very well with the reported values only a few outliers were found (i.e. Br, Sr and Zr elements). The results are shown on Figures 1 and 2.

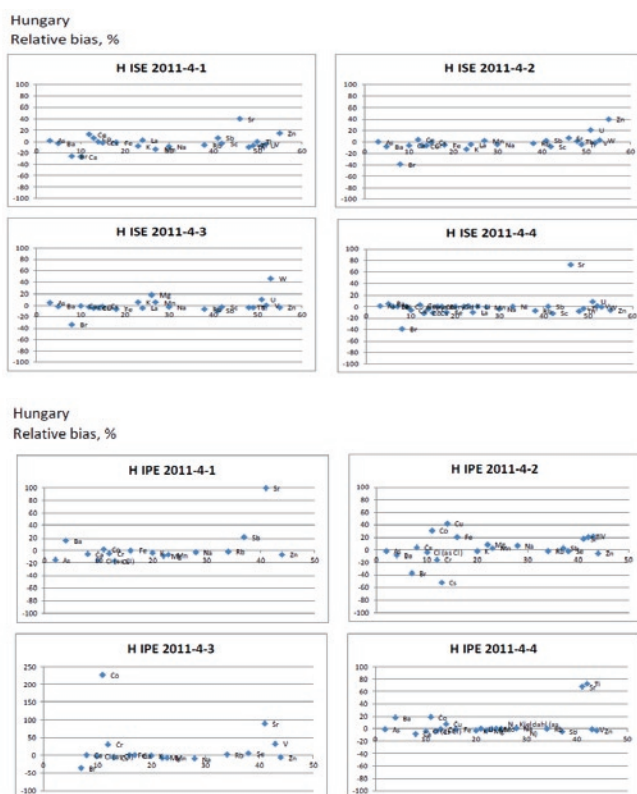


Figure 1a, b: Results of plant (IPE) and soil (ISE) samples by NAA and comparison with WEPAL data

## References

Report on the Inter-comparison feedback of Proficiency Tests performed in 2011 and 2013 for NAA and other Analytical Techniques, under regional TC projects RAF4022, RAS1018, RER1007 and RLA0037. Vienna, Austria, 27-31 May 2013.

<b>B N C</b> <b>Experimental Report</b>	<i>Experiment title</i> <b>Determination of <math>^{135}\text{Cs}</math> in nuclear power plant wastes by k0-NAA and ICP-MS</b>	<i>INAA and Gamma-spectrometry</i> <i>Local contact</i> <i>Ibolya Sziklai-László</i>
	<i>Principal proposer:</i> Ibolya Sziklai-László, Hungarian Academy of Sciences Centre for Energy Research <i>Experimental team:</i> Nóra Vajda, RadAnal Ltd., Péter Nagy, Éva Kovács-Széles, HAS Centre for Energy Research	<i>Proposal No. BRR_329</i>  <i>Date(s) of Exper.</i> 2012.03. 24.-11.20.

## Objectives

Our aim was to develop/adopt an adequate radiochemical method for the determination of  $^{135}\text{Cs}$  in nuclear waste samples that is based on the selective separation of Cs and the detection of  $^{135}\text{Cs}$  by NAA and ICP-MS methods. Since there is no  $^{135}\text{Cs}$  standard for the calibration of the methods the analytical results are comparatively evaluated by the two measuring techniques to support their goodness: accuracy and precision.

## Results

Neutron irradiations were carried out in the Budapest Research Reactor.  $^{136}\text{Cs}$  produced according to the  $^{135}\text{Cs}$  ( $n,\gamma$ ) $^{136}\text{Cs}$  reaction, was detected by gamma spectrometry, wherefrom the activity/mass of  $^{135}\text{Cs}$  was calculated according to the  $k_0$ -standardization technique. The Cs containing fractions were measured by Inductive Coupled Plasma Mass Spectrometry (ICP-MS), as well. The isobar interference due to  $^{135}\text{Ba}$  was corrected by the use of barium standard solution. Acceptable low detection limits (10-50 ng/L) and high accuracies (5-20 %) were achieved by analyzing 50-100 mL of radioactive waste samples by both techniques. Results of  $^{135}\text{Cs}$  determination in different waste samples are summarized in Table 1. Results of  $^{135}\text{Cs}$  determination by ICP-MS and NAA agreed well, a good correlation of the results is shown in Fig. 1.

**Table 1.** Measured concentration of  $^{135}\text{Cs}$  in various samples determined by ICP-MS and NAA. Uncertainties are calculated at 68% confidence level.

	ICP-MS	NAA
Sample code	Cs-135 ng/L $\pm \sigma$ (%)	Cs-135 ng/L $\pm \sigma$ (%)
H12-1	112.5 $\pm$ 2.2%*	112.5 $\pm$ 7.4%*
H12-2	67.1 $\pm$ 5.2%	56.42 $\pm$ 7.4%
H12-7	50.4 $\pm$ 6.4%	51.85 $\pm$ 19%
H12-13	17.5 $\pm$ 10%	21.32 $\pm$ 24%

\* standard deviation of parallel measurements, individual uncertainties are about 6% and 8%, respectively

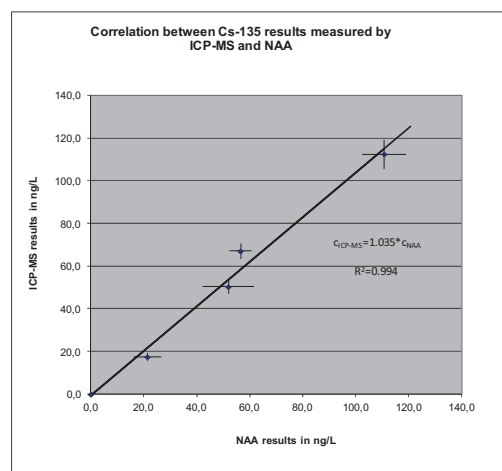


Figure 1: Comparison of ICP-MS and NAA results

## References

1.P. Nagy, N. Vajda, I. Sziklai-László, E. Kovács-Széles, A. Simonits. Determination of  $^{135}\text{Cs}$  in nuclear power plant wastes by ICP-MS and k0-NAA. 6th International k0-User, Workshop, 22-27 September 2013, Budapest, Hungary.

<b>B N C</b> <b>Experimental Report</b>	<i>Experiment title</i> <b>Implementation and test of a multi-layer control software for TAS</b>	<i>Instrument</i> TAST
	<i>Principal proposer:</i> Alex Szakál <i>Experimental team:</i> Alex Szakál, Márton Markó	<i>Local contact</i> A. Szakál
		<i>Experiment Number</i>
		<i>Date</i> 23.03.2010-14. 05.2010

### Objectives

The old VAX electronics and control system of the TAST spectrometer was renewed. The new hardware needed a new control software to drive the spectrometer. We designed a two-layer software which divides the low-level and high-level control of the spectrometer between two computers.

### Results

The Advantech motor driver cards, counter card and digital I/O card is installed on the low-level computer. This computer is running with a LINUX real-time kernel and execute the elemental commands like move or count. It is automatically turning on the air-pads and it is possible to move more motors at the same time. The computer makes sure to arrive to a given angle from the negative direction to compensate mechanical uncertainties.

The high-level control software is connecting to the low-level computer via a TCP/IP socket. The aim of the high-level program is to translate the user's commands formally given in the reciprocal space to angles of the instrument which can be sent to the low-level program. The high level program is a complete program for triple-axis measurement. It needs the crystal structure and orientation as an input and then it sends the instrument to measure at any accessible point in reciprocal space. This computer is making a log files for the scans which contain both the reciprocal coordinates and real angles of the instrument with the monitor and main detector counts. The high-level program displays the results of the current measurement and the old files can be redrawn also which is convenient for example if the user wants to review the data measured during the night.

<b>B N C</b> <b>Experimental Report</b>	<i>Experiment title</i> <b>Testing of the realigned doubly focusing monochromator</b>	<i>Instrument</i> TAST
	<i>Principal proposer:</i> Alex Szakál <i>Experimental team:</i> Alex Szakál, Márton Markó	<i>Local contact</i> A. Szakál
		<i>Experiment Number</i>
		<i>Date</i> 27.10.2010-05.11.2010

### Objectives

Realignment of the 3x7 crystals installed in the doubly focusing monochromator of TAST spectrometer was needed because due to radiation damage the plastic cogwheels moving the focus of the monochromator were broken. The cogwheels were changed to the same sized steel cogwheels. During the repair the focus of the monochromator was altered and the alignment of each crystal was needed. The alignment was done at the ATHOS cold triple-axis instrument, and the result was investigated with a neutron pin-hole camera and neutron flux measurements at the TAST instrument.

### Results

The pin-hole camera picture is shown on figure 1. The central 5 rows can be seen on the detector picture. The intensity of the spots is decreasing as we move from the centre of the monochromator. This effect is due to the small (6cm diameter) hole on the reactor and not caused by misalignment. The picture shows that there is a misalignment at the (1,-1) position from the centre.

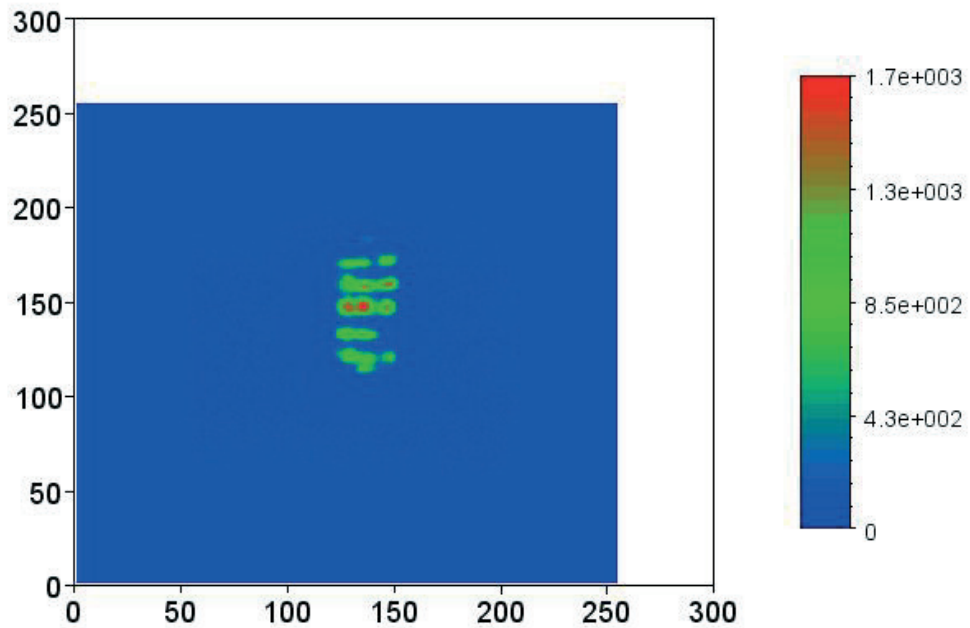


Figure 1: Pinhole camera picture of the doubly focusing monochromator.

The neutron flux was measured to be  $2 \cdot 10^6$  n/cm<sup>2</sup>/s which corresponds to our expectations.

<h1 style="margin: 0;">B N C</h1> <p style="margin: 0;"><b>Experimental Report</b></p>	<i>Experiment title</i> <b>Measurement of mosaicity and reflectivity of Heusler crystals</b>	<i>Instrument</i> TAST
	<i>Principal proposer:</i> Veress Zsolt <i>Experimental team:</i> Alex Szakál, Márton Markó	<i>Local contact</i> A. Szakál

## Objectives

Heusler crystals are used to produce polarized neutron beams. Production of these crystals with proper mosaic and reflectivity needs refinement in the technology with feedback from the neutron experiments.

## Results

We measured the mosaic and reflectivity of the crystals. The mosaicity of the crystals were good to use them as monochromator(around  $2\theta$ ), but the reflectivity was less than 15% which is not enough for that purpose. The reason of the small reflectivity could be the too big grain size, because the reflection is mainly arising from the near surface of the grains. Figure 1 shows the rocking curve of one of the crystals.

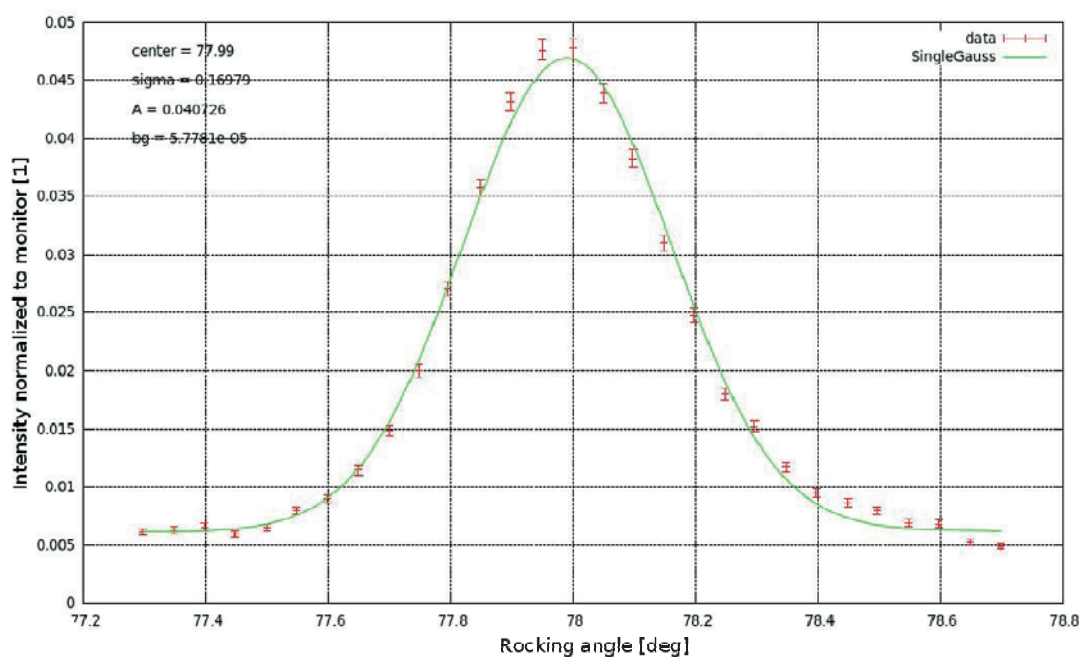


Figure 1: Rocking curve of the sample C.

<b>B N C</b> <b>Experimental Report</b>	<i>Experiment title</i> <b>Test measurements of the energy focusing properties of the TAST spectrometer</b>	<i>Instrument</i> TAST
	<i>Local contact</i> A. Szakál	<i>Experiment Number</i>
<i>Principal proposer:</i> Alex Szakál <i>Experimental team:</i> Marton Markó, Alex Szakál		<i>Date</i> 14.06.2011-24.06.2011

### Objectives

The doubly focusing monochromator and horizontally focusing monochromator was realigned and we tested the effect of focusing on the energy resolution of the instrument. Theoretically the focusing narrows the energy resolution function but broadens the Q resolution. In the present experiment we wanted to see the narrowing of the energy resolution and the intensity gain.

### Results

We measured the energy resolution of the spectrometer by using a vanadium sample. We performed energy scans at various focusing conditions.

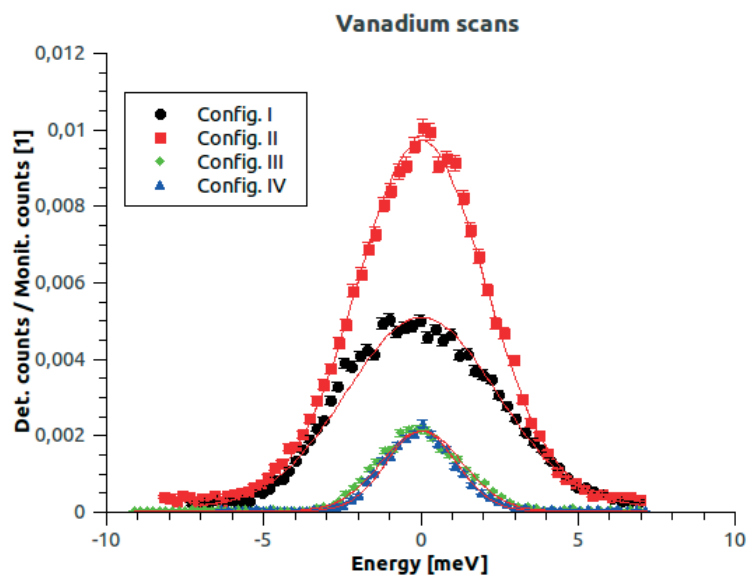
The configurations were:

Config I: Flat monochromator and analyzer

Config II: Flat monochromator, energy focusing analyzer

Config III: Flat monochromator, energy focusing analyzer, 4mm slit before detector

Config IV: Energy focusing monochromator, energy focusing analyzer, 4mm slit before detector



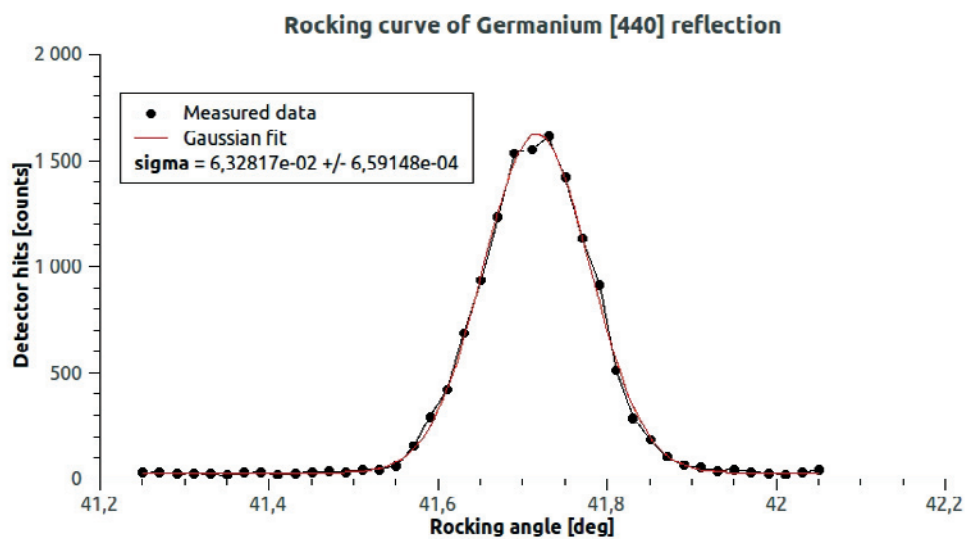
<h1 style="margin: 0;">B N C</h1> <p style="margin: 0;"><b>Experimental Report</b></p>	<i>Experiment title</i> <b>Measurement of mosaicity of Ge crystals</b>	<i>Instrument</i> TAST
	<i>Principal proposer:</i> Alex Szakál <i>Experimental team:</i> Marton Markó, Alex Szakál	<i>Local contact</i> A. Szakál

### Objectives

Germanium single crystals are widely used as neutron monochromator crystals because the favourable properties for neutrons (absorption, scattering cross section etc) and the diamond crystal structure which makes possible to eliminate the second order contamination of the beam. Production of monochromator quality crystals needs careful design of the technology. During this phase neutron measurements are needed to give feedback about the result of the technology changes.

### Results

The most challenging problem in the production is the adjustment of the mosaic of the sample without breaking it to separate crystal blocks. We measured several crystals which gave valuable information to develop the proper manufacturing technology. The rocking curve of the most promising crystal is shown on figure 1.



<b>B N C</b> <b>Experimental Report</b>	<i>Experiment title</i> <b>Transmission measurements of chopper disks</b>	<i>Instrument</i> TAST
	<i>Principal proposer:</i> Gábor Nagy <i>Experimental team:</i> Gyula Török, Márton Markó, Alex Szakál	<i>Local contact</i> Gy. Török

### Objectives

Transmission validation of chopper disks is important because a disk with too high transmission or with inhomogeneous transmission distribution can lead to spurious results on a TOF machine. The goal of the experiment was to characterize the transmission of chopper disks with neutrons.

### Results

We had to measure the transmission with high precision thus we had to take into account the existence of second order contamination of the beam. We filtered the beam with a secondary Ge monochromator which was set to an angle to reflect only the first order neutrons. Measurement of the background done also and it was subtracted. The result of one disk is shown on figure 1.

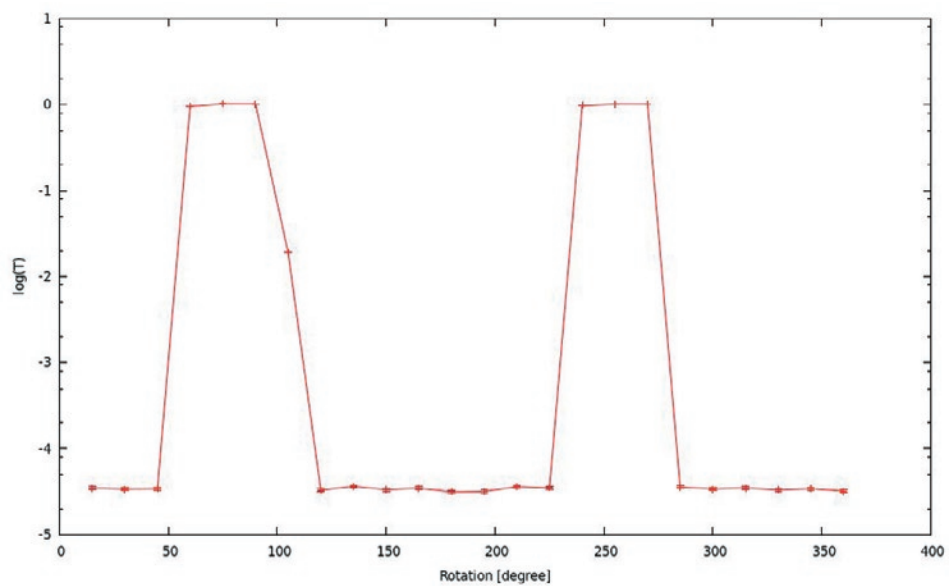


Figure 1: Transmission of a disk in the function of rotation. The  $\log(T)=0$  regions show the holes on the disks.



<b>B N C</b> <b>Experimental Report</b>	<i>Experiment title</i> <b>Measurement of H content of YH single crystal</b>	<i>Instrument</i> TAST
	<i>Principal proposer:</i> Alex Szakál <i>Experimental team:</i> Alex Szakál, Márton Markó	<i>Local contact</i> A. Szakál
		<i>Date</i> 25. 05. 2010 - 04. 06. 2010

### Objectives

We prepared an  $\text{YH}_{0.16}$  single crystal for neutron-holographic measurement at PSI. Before we started the measurement we had to make certain about the hydrogen content of the sample.

### Results

Because the hydrogen concentration is low, the phase remains the same as the Y single crystal (HCP) and the hydrogen is located at octahedral and tetrahedral interstitial places with random distribution at room temperature. These hydrogen atoms are lengthening the lattice constants linearly with the hydrogen concentration. We know from the literature the lattice constants of pure Y and  $\text{YH}_{0.25}$  (1) By measuring the lattice constants of the sample and using the linear dependence it is possible to calculate the hydrogen content. The measurement of the lattice constant has to be made with high precision because the change in lattice constant is less than 0.1%. This precision can't be reached by measuring only one reflection. We measured 11 reflections and used a self-made program which fits the orientation of the sample and the lattice parameters to the measured reflection angles using the process described in (2).

After fitting the data it turned out that the composition of the sample is really  $\text{YH}_{0.16}$  as we expected. We also checked the twinning of the crystal but we didn't find any sign of it.

### References

1. F. Beaudry, B. Spedding, Metallurgical and Materials Transactions B, 6(3):419-427, 1975
2. W.R. Busing and H.A. Levy, *Acta Cryst.* **22**, 457 (1967)

<b>B N C</b> <b>Experimental Report</b>	<i>Experiment title</i> <b>Y-polycrystalline sample measurement</b>	<i>Instrument</i> PSD
	<i>Principal proposer:</i> Alex Szakál <i>Experimental team:</i> Margit Fabian, Alex Szakál	<i>Local contact</i> Margit Fabian
		<i>Experiment Number</i>
		<i>Date</i> 2011

### Objectives

We needed a polycrystalline yttrium sample with no orientational order for a holographic demonstration experiment. We characterized our samples with neutron diffraction which gives us information about the bulk properties of the material.

### Results

The first measurements revealed that our sample has orientational order. We made powder samples by rasping the bulk one. The measurement of this sample showed no orientational order, but the peaks weakened much. This weakening is due to the defects made by rasping. These defects can be eliminated using heat treatment of the sample. We performed a 24H long heat treatment at 1500 K. The intensity of the peaks increased and there was no orientation observed in the sample. Figure 1 show the diffraction pattern before and after heat treatment.

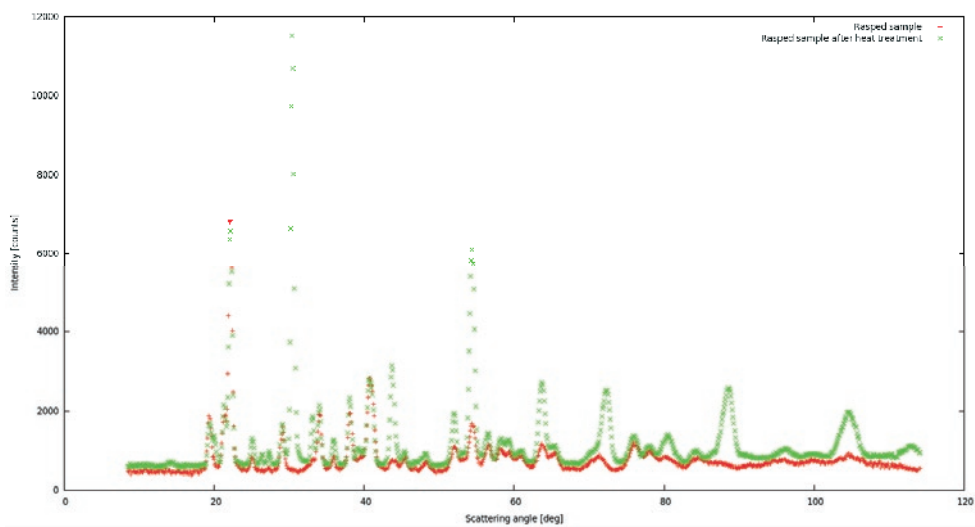


Figure 1: Diffraction pattern before and after heat treatment of rasped samples.

<b>B N C</b> <b>Experimental Report</b>	<i>Experiment title</i> <b>Experimental realization of Frame Multiplication Technique 2- NMI3</b>	<i>Instrument</i> TOF  <i>Local contact</i> György Káli
	<i>Principal proposer</i> Margarita Russina, Ferenc Mezei <i>Experimental team</i> György Káli,	<i>Experiment Number</i>  <i>Date</i> 18-22.01.2010

## Objectives

The main challenge in the instrument design at the future European Spallation Source is, to develop new kind of techniques to take full advantage of the high neutron peak flux and at the same time to take control over the other pulse parameters to best suit the instruments and individual experiments. Novel multiplexing techniques, such as Wavelength Frame Multiplication [1] and Repetition Rate Multiplication [2] allow us to create instead of one long pulse a number of mini-pulses with variable frequencies and pulse lengths but with the same peak flux as the original pulse

## Results

In our present study we have successfully tested two methods for perfect “stitching” between the different multiplexed wavelength frames. The first approach is based on asynchronous operation of the pulse shaping chopper with respect to the source pulse frequency. In addition, we have avoided accidental synchronization by selecting 199.97 Hz for the pulse shaping chopper in order to avoid 200 Hz, a simple multiple of the 8 Hz source frequenc. In this case the RRM wavelength frames are uniformly slewed over the whole spectrum, so after a sufficient number of cycles ( $10^4$  source pulses or more) the transition/overlap regions between these frames will affect every wavelength precisely the same way. The uniformity of the distribution of the chopper phases over the whole wavelength range could be easily verified in our complete event recording data set. The observed asynchronous, phase slewing diffraction pattern was observed with good statistical accuracy.

The phase slewing mode makes multiplexing WFM exactly equivalent to any TOF diffraction method operating with a single wavelength frame, both in principle and in practicalities. The normalization to the incoming neutron spectrum remains in both cases the only calibration to perform. For this purpose it suffices to determine this spectrum under identical data collection conditions, which is in practice either achieved with the help of a calibration run (e.g. with vanadium as sample) or by the use of monitor calibrated with high precision.

The other method we have tested is based on high precision and reliable normalization to the actual combined incoming neutron wavelength spectrum over all RRM wavelength frames in synchronous, fixed phase data collection mode. This approach has the advantage that it can also be used for short scans, only consisting of a few (or even a single) source pulse. In the present work this was achieved by simultaneously using a high counting rate monitor in the incoming neutron beam. This calibration/normalization also takes care of the parameter settings used in the event recording data evaluation process, e.g. TOF safety margins used in assigning the correct pulse shaping chopper pulse to each retained neutron count. Our results obtained by this method are identical within statistical error to the ones for the phase slewing data evaluation, which focuses to a wavelength domain affected by the overlap of neighboring wavelength frames.

## References

1. Mezei F and Russina M 2002 in: *Advances in Neutron Scattering Instrumentation*, , Proc. of SPIE 4785 24
2. Russina M, Mezei F 2009 *J. Nuclear Instr. and Methods*, A604 624
3. Kali Gy, Santa Zs, Bleif H.-J., Mezei F, Rosta L, Szalok M, 2007 *Z.Kristallogr. Suppl.* 26 165
4. Russina M, Kali Gy, Santa Zs and Mezei F 2011 *J. Nucl. Instr. and Methods*. A654 383
5. Russina M, Mezei F 2010 *Journal of Physics: Conference Series* 251 012079
6. M. Russina, F. Mezei , G. Kali (2011) 5th European conference on neutron scattering, Prague, Czech Republic open access Journal of Physics: Conference Series (JPCS)

<b>B N C</b> <b>Experimental Report</b>	<i>Experiment title</i> <b>Experimental realization of Frame Multiplication Technique - NMI3</b>	<i>Instrument</i> TOF  <i>Local contact</i> György Káli
	<i>Principal proposer</i> Ferenc Mezei <i>Experimental team</i> György Káli, Zs. Santa	<i>Experiment Number</i>  <i>Date</i> 18-22.01.2010

### Objectives

A key challenge in the design of pulsed sources is to provide at the same time short enough pulses to meet high neutron velocity resolution requirements in some experiments, while striving for highest beam intensity by trying to avoid making this resolution better than really needed in each experiment. Multiplexing chopper systems offer a uniquely flexible and efficient tool to accomplish this task for a broad range of neutron pulse lengths from a few  $\mu\text{s}$  to ms. Second objective to extend the wavelength band available in an experiment is to achieve a wide dynamic range in wave number  $q$ . Wavelength Frame multiplication allows us to accomplish this by using specially designed chopper system that allows the selection of a sequence of runs taken in frames with various delays after the neutron pulse. The proposed study was focused on the experimental realization of this techniques using time-of-flight diffractometer at BNC.

### Results

The Frame Multiplication has been successfully tested using TOF diffractometer at the of Budapest Neutron Center. The experimental setup, with  $LM = 10.4$  m,  $LD = 22$  m, the distances between the pulse shaping fast chopper and the two RRM frame chopper being 0.89 m and 10.4 m, respectively. The fast chopper pulse frequency was  $f_1 = 166 \frac{2}{3}$  Hz, those of the two RRM frame choppers 153.52 Hz and  $83 \frac{1}{3}$  Hz  $=f_1/2$ , respectively.  $t_m = 6$  ms, and the repetition time of the virtual source pulses 13.8888 Hz  $=f_1/12$ . With the given chopper positions designed for non-multiplexing use, the frequency ratio  $153.52 : 166.667 = 11.053 : 12$  slightly violates the RRM "quantization" rule of simple rational numbers. Therefore the 153.52 Hz chopper could not be synchronized to the others.

It was operating in an asynchronous mode, and event recording technique was used to factor in its actual time stamped phase at each revolution during data evaluation. With pulse shaping chopper systems the timing with respect to real or virtual source pulses is immaterial for determining the scattering parameters. It is "only" important in order to make sure, that the chopper system "looks" at the source when the source is "on" with the highest brightness. The results obtained on an  $\text{Al}_2\text{O}_3$  powder sample. The separation of different RRM frames is visible, since the overlap in neutron wavelength (or lattice parameter  $d$ ) between these frames included the half shadow regions and in the event recording data evaluation in these regions only neutrons were excluded that could have come from different pulse shaping chopper pulses.

**Future prospects** Experimental realization of pulse repetition technique.

### References

1. Mezei F and Russina M 2002 *in: Advances in Neutron Scattering Instrumentation, , Proc. of SPIE* 4785 24
2. Russina M, Mezei F 2009 *J. Nuclear Instr. and Methods*, A604 624
3. Kali Gy, Santa Zs, Bleif H.-J., Mezei F, Rosta L, Szalok M, 2007 *Z.Kristallogr. Suppl.* 26 165
4. Russina M, Kali Gy, Santa Zs and Mezei F 2011 *J. Nucl. Instr. and Methods*. A654 383
5. Russina M, Mezei F 2010 *Journal of Physics: Conference Series* 251 012079
6. M. Russina, F. Mezei , G. Kali (2011) 5th European conference on neutron scattering, Prague, Czech Republic open access Journal of Physics: Conference Series (JPCS)

<h1 style="margin: 0;">B N C</h1> <p style="margin: 0;">Experimental Report</p>	<i>Experiment title</i> <b>A preliminary study of medieval swords by time of flight neutron powder diffraction (TOF-NPD) method at Budapest neutron center (BNC)</b>	<i>Instrument</i>  <i>Local contact</i> György Káli
	<i>Principal proposer</i> László Rosta <i>Experimental team</i> György Káli, Zsombor Sánta	<i>Experiment Number</i>  <i>Date</i> 03.29-04.02.2010

## Objectives

The aim of the experiment was to present the applicability of the method and the instrument itself for non invasive characterization of archeological artifacts made of carbon steel. The following characteristics were planned to determine: phase composition (for steel phases as ferrite, cementite, as far as possible martensite and non-steel phases), the total carbon content, the texture and the average internal stress and dislocation density. Four medieval – or believed to be that – swords had been studied. **Sword1** strongly corroded but together with **Sword2** were visibly Damascus blades, certificated archeological objects. **Sword3** and **Sword4** were in good state but not certificated.



## Results

To gain appropriate spectra for the determination of the above mentioned characteristics of the samples in a reasonable time interval, we have collected data in high and medium resolution at one detector position fixed to 175°, but for a correct study the experiments has to be performed at extended angular range of the detectors.

Texture: To analyze the occurring preferred orientation of the crystallites in the swords they were scanned in two directions: around their longitudinal axes and around the transversal axis lying in the plane of the blade. This scans were performed at moderate resolution. Although the anisotropy in hot worked metal is much weaker than in a cold worked one, we have found that it is extremely low in the investigated objects thanks to the good manufacturing. On the other hand, the nature of the data seems to be typical for different style blades. Phase analysis: All the blades shows high, but different cementite concentration, but no other phase has been found in the applied scattering vector range expect of small amount of martensite. In forward experiments has to collect data from the lower angular range too. Stress and strain: For peak shape analysis the high resolution spectra were used. It was clearly visible, that the peak profiles shows lorentzian broadening compared to pure iron, but the parameters of the Voigt or Pseudo Voigt fits are uncertain due to the strong inelastic background and the presence of martensite. . It is interesting to note that one of the swords shows no line broadening. More accurate results can be gained using a correct model for the inelastic part, or after numerical separation of the spectra.

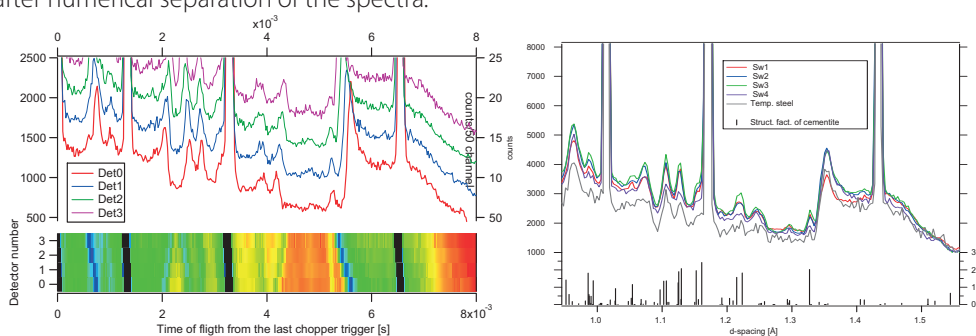


Fig 1: The angular behavior of the inelastic part of the spectra. While weak elastic peaks are parallel to the other stronger peaks (black region) the inelastic ones are inclined depending on it whether due to annihilation or emission. b: A short part of the low resolution structure spectra of the four sword with a low carbon content commercial steel (C30) after some correction, together with the calculated cementite structure factor. Sword1 shows somewhat weaker inelastic scattering, what can due to the high carbon content in the ferrite phase and the high dislocation density.

<h1 style="margin: 0;">B N C</h1> <p style="margin: 0;"><b>Experimental Report</b></p>	<i>Experiment title</i> <b>High entropy alloys</b>	<i>Instrument</i> TOF
	<i>Principal proposer</i> Lajos Károly Varga <i>Experimental team</i> György Káli	<i>Local contact</i> György Káli

## Objectives

HEA alloys consist of at least 4-5 elements in equal concentration but crystallize in 1-3 phases only. It is impossible to determine the phase composition and the chemical concentrations in all phases from one diffraction pattern – either of X-ray or neutron – numerically, but from the two practically independent (in means of scattering behavior of the atoms) spectra it sometimes can be possible, or at least one can restrict the number of parameters. Additional information as the incoherent scattering amplitude can also be used, since the expression of the isotope incoherent scattering strongly correlates to the mixing entropy, what is the key parameter of the thermodynamical behavior of these alloys. Due to the differences in the neutron and X-ray structure factors, it can even occur that one phase is invisible in the X-ray spectra but is visible with neutrons and vice-versa. It means that in this curious case even the number of the phases is difficult to determine only from one diffraction spectra. Since neutrons penetrate deep into the material and serve information about the bulk, it is more applicable for the investigation of as-cast metal samples, although a disadvantage is that neutron scattering requires larger samples. Since there is no atomic form factor for neutron scattering (i.e. it is constant), neutron diffraction is more applicable to study the short range order than commercial X-ray diffractometers. By neutron diffraction the occurrent magnetic structure can also be investigated, especially the antiferromagnetic order.

## Results

Three different alloy composition was investigated: AlNiFeCrMn, CuNiFeCrMo, CuNiFeCrMn, the later in as cast and heat-treated state in low, medium and high angular range to study the short and long range ordering. In the Cu containing alloys 1-2 disordered copper-rich and -poor solid solution phase dominates beside either weaker fcc or bcc phases or intermetallics. The Al containing alloy exhibit single phase "ordered" solution or rather CsCl-like structure, although the composition is not stoichiometric. Perfect phase analysis will be possible using X-ray diffraction pattern.

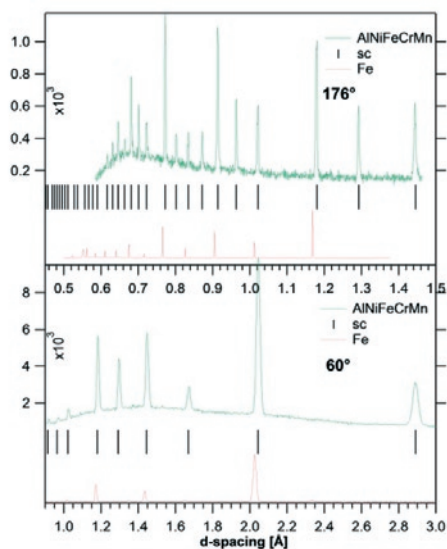


Fig 1. The as measured (not normalized) time-of-flight neutron diffraction pattern of  $Al_{20}Ni_{20}Fe_{20}Cr_{20}Mn_{20}$  HEA at two detector position (176 and 60 degree) with the corresponding simple cubic structure factor and pure Fe powder as bcc reference. (Weak peaks in the Fe spectrum corresponds to the container). - Correct structure solution can be performed taking in account the X-ray spectra.

## Future prospects

We plane in situ experiment to study the solidification process starting from the melt.

<h1 style="margin: 0;">B N C</h1> <p style="margin: 0;"><b>Experimental Report</b></p>	<i>Experiment title</i> <b>European and Indian high carbon steel blades and armours</b>	<i>Instrument</i> TOF
	<i>Principal proposer</i> A.Williams with D.Edge <i>Experimental team</i> György Káli	<i>Local contact</i> György Káli
		<i>Experiment Number</i>  <i>Date</i> 5-10.10.2011

## Objectives

A program of research into the metallurgy of medieval arms and armour has been carried out for a number of years at The Wallace Collection, London. This analysis has been carried out by the traditional methods of metallography, which are well suited to plates of armour but are much less suitable for swords and mail. This museum also houses an important collection of Indian arms and armour, whose analysis presents quite different problems. The carbon content of Indian steels is unusually high by European standards, which has led us to consider other techniques, such as neutron diffraction or gamma-activation. While the results from neutron diffraction may be compared with metallography on broken blades, problems in interpretation have arisen because the steels used historically do not correspond to modern alloys, and deductions about the heat-treatment of Indian steels, for example, have proved to be difficult. We hope that a non-invasive method of determining the carbon contents (and of equal importance, the phase contents) of swords and helmets may be developed.

## Results

Ten objects were analyzed by TOF ND, some of them on different parts. From a chosen sword blade a complete rocking curve were taken, on the others the spectra was measured at two different position to take in account the expected anisotropy. As reference pure iron powder, bulk and ground cementite and sintered alumina was used. Some object exhibited extremely high cementite content and very strong anisotropy. The high anisotropy of the three phase (including martensite) makes the determination of the total carbon content difficult, but serve very important information about manufacturing technique.

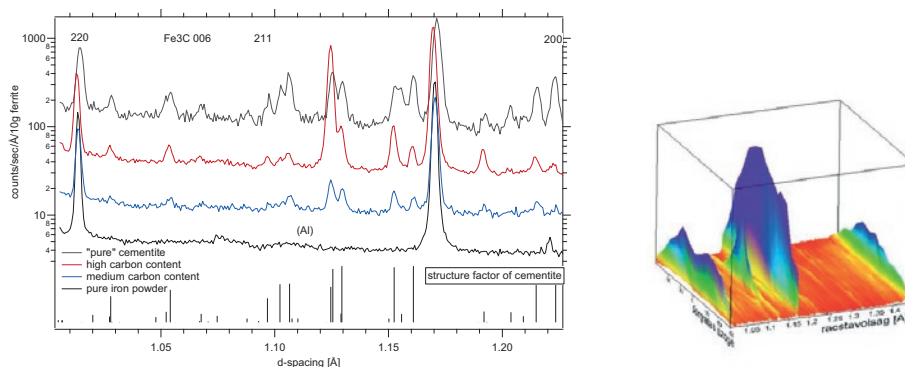


Fig 1-2. The appearance of precipitated cementite in medium and high carbon steel sword blade in the diffraction patterns and on the 2d rocking curve. The diffraction patterns are roughly normalized to 10g ferrite content (the typical weight of the illuminated volume) using the intensity of the indexed ferrite peaks. The „pure” cementite is an artificial probe, containing some ferrite, martensite and graphite. In the high carbon content blade the cementite is also present in highly oriented phases (see for example the indexed 006 peak). Note, that the scale is logarithmic and valid for the iron powder; all the others are shifted for better visibility

<b>B N C</b> <b>Experimental Report</b>	<i>Experiment title</i> <b>Investigation of periodic Ni/Ti multilayers</b>	<i>Instrument.</i> REF; GINA
	<i>Principal proposer:</i> T. Veres <i>Experimental team:</i> T. Veres	<i>Local contact</i> T. Veres; B. Nagy
		<i>Experiment Number</i> Ref 1.
		<i>Date</i>

## Objectives

Periodic multilayers of various periods and layer thicknesses were prepared as quarter wave mirrors. The properties of such Ni/Ti multilayers are crucial in neutron supermirrors. Note, these sputtered Ni layers contain Mo too, to get nonmagnetic mirrors[1]. The reflectivity properties of these systems were investigated using neutron and x-ray reflectometry. The obtained experimental results were compared with calculations. The deviation from the proposed structure and imperfectness created during sputtering process was investigated.

## Results

Samples containing 2, 4 and 8 bilayers with Ni/Ti layer thickness 66Å/59 Å, 84Å/70 Å, 115Å/87 Å were prepared at Mirrotron Ltd., using dc magnetron sputtering. The neutron reflectivity measurements were performed at constant wavelength neutron reflectometers, REF and GINA, the x-ray measurement at the instrument of Institute for Technical Physics and Materials Science. The two complementary methods revealed the same structure, and confirm each other.

In the fitting process we assumed the periodicity of the samples. The thickness of Ni and Ti layers, the real part of scattering length density, and Ni/Ti and Ti/Ni roughness were the fitting parameters. In the case of 84 Å Ni and 70 Å Ti nominal layer thicknesses, a remarkable increase in Ni and decrease in Ti thickness was observed. For the other two nominal thicknesses the deviance of thickness values was not so large. The fitted neutron scattering length density corresponds to the calculated. In some samples, the fitted x-ray scattering length density deviates from the calculated ones. The fitted roughness values on the top of Ni layers were larger than that on the top of Ti layers, in the case of every sample. It can be caused the different inter-diffusion and/or the interpenetration of crystallites of the two metals in each other.

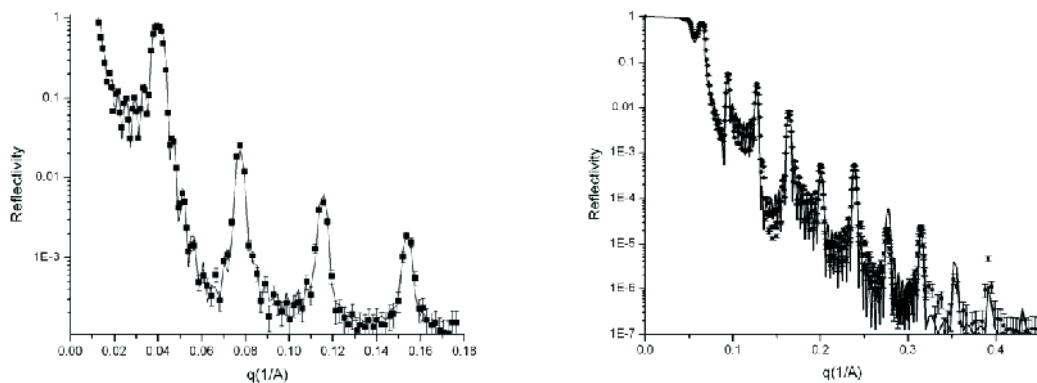


Fig. 1.: The measured and fitted neutron and x-ray reflectivity curves for sample 8x(84Å Ni/ 70Å Ti)

## References

1. R. Kovács-Mezsei, Th. Krist, Zs. Révay, Nuclear Instruments and Methods A 586 (2008) 51



<h1 style="margin: 0;">B N C</h1> <p style="margin: 0;">Experimental Report</p>	<i>Experiment title</i> <b>Neutron diffraction study of sodium borosilicate glasses from ternary up to 6-components</b>	<i>Instrument</i> PSD-1
	<i>Principal proposer:</i> E. Veress <i>Experimental team:</i> M. Fábrián, Gy. Mészáros and E. Sváb, SZFKI ; E. Veress Cluj/Romania	<i>Local contact</i> M. Fábrián

## Objectives

Multi-component borosilicate glass has been widely accepted as a host matrix for the immobilization of high-level radioactive waste [1]. We are motivated in neutron diffraction study on borosilicate glass series with 15mol% B<sub>2</sub>O<sub>3</sub> content, by adding step-by-step one additional element starting from the 3-component glass up to the 6-component uranium added multi-component borosilicate glass. We have prepared and performed structure study on 4 samples with compositions:

- 1) 60SiO<sub>2</sub>\*25Na<sub>2</sub>O\*15B<sub>2</sub>O<sub>3</sub>;
- 2) 55SiO<sub>2</sub>\*25Na<sub>2</sub>O\*15B<sub>2</sub>O<sub>3</sub>\*5BaO;
- 3) 50SiO<sub>2</sub>\*25Na<sub>2</sub>O\*15B<sub>2</sub>O<sub>3</sub>\*5BaO\*5ZrO<sub>2</sub>;
- 4) 70wt% [50SiO<sub>2</sub>\*25Na<sub>2</sub>O\*15B<sub>2</sub>O<sub>3</sub>\*5BaO\*5ZrO<sub>2</sub>]+30wt%UO<sub>3</sub>.

The specimen were melted in high temperature furnace using Pt crucible, and finally the melt was quenched by pouring it on a stainless steel plate.

## Results

We have performed neutron diffraction experiments using the BNC-PSD neutron diffractometer [2] in the momentum transfer range  $Q=0.6-10 \text{ \AA}^{-1}$ . Experiments were extended up to high  $Q$  values using the Los Alamos NL-NPDF instrument [3]. We have determined the structure factor  $S(Q)$  up to  $\approx 30 \text{ \AA}^{-1}$  exception of uranium containing glass. The reverse Monte Carlo (RMC) simulation [4] of the experimental structure factor was successfully applied to generate reliable 3-dimensional atomic configuration. The RMC simulation of the neutron diffraction data is consistent with a model for all 4-samples, see Fig. 1. The most important partial atomic pair correlation functions, like the  $g_{\text{Si-O}}(r)$ ,  $g_{\text{B-O}}(r)$  have been revealed, as they are shown in Fig. 2.

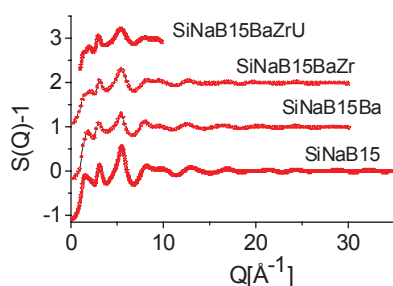


Fig.1. Neutron diffraction structure factors, experimental data (red star) and RMC simulation (line).

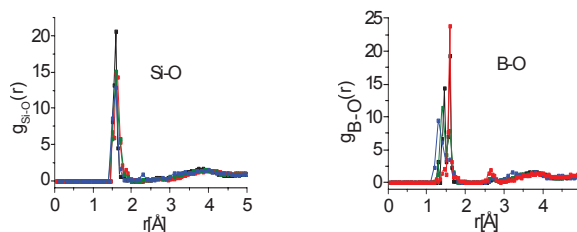


Fig. 2. The partial pair distribution functions obtained by RMC simulation, SiNaB15 (black), SiNaB15Ba (red), SiNaB15BaZr (green) and SiNaB15BaZrU (blue).

The Si-O network proved to be highly stable, it consists of slightly distorted tetrahedral SiO<sub>4</sub> units with characteristic first neighbour distances at  $r_{\text{Si-O}}=1.60 \text{ \AA}$ . For the B-O neighbourhood two characteristic first neighbour distances have been obtained at about 1.40 and 1.60 Å. The preliminary results suggest that with addition of new components, the basic network structure is stable and well defined even in the multi-component glasses.

## References

1. K.S.Chun, S.S. Kim, C.H. Kang, *Journal of Nuclear Materials* **298** (2001) 150.
2. E. Sváb, Gy. Mészáros, F. Deák, *Materials Science Forum* **228** (1996) 247.
3. Th. Proffen, S.J.L. Billinge, T. Egami, D. Louca, *Zeitschrift für Kristallographie* **18** (2003) 132.
4. R.L. McGreevy, L. Pusztai, *Molec. Simul.* **1** (1998) 359.

<b>B N C</b> <b>Experimental Report</b>	<i>Experiment title</i> <b>Uranium surrounding in sodium borosilicate glasses optimized by BaO and CaO</b>	<i>Instrument</i> PSD-2  <i>Local contact</i> M. Fábíán
	Principal proposer: E. Veress Experimental team: M. Fábíán, Gy. Mészáros and E. Sváb, SZFKI; E. Veress Cluj/Romania	<i>Proposal No.</i> BRR-223-2 <i>Date</i> 05.2010; 01. 2011.

## Objectives

Alkali borosilicate glasses are being used for vitrification of HLW generated at atomic research centers and nuclear power stations [1]. The structural aspects of these glasses have been studied in our earlier works. In the present work we have continued the neutron diffraction study on the borosilicate glasses with 10 mol% B<sub>2</sub>O<sub>3</sub> content, and CaO was added instead of BaO. The aim of the study was to investigate the effect of Ba and Ca on the of sodium-borosilicate network.

Four borosilicate glasses were prepared, with concentration (mol%):

- (1) 55SiO<sub>2</sub>\*25Na<sub>2</sub>O\*10B<sub>2</sub>O<sub>3</sub>\*5BaO\*5ZrO<sub>2</sub>
- (2) 70wt% [60SiO<sub>2</sub>\*25Na<sub>2</sub>O\*10B<sub>2</sub>O<sub>3</sub>\*5BaO]+30wt%UO<sub>3</sub>
- (3) 55SiO<sub>2</sub>\*25Na<sub>2</sub>O\*10B<sub>2</sub>O<sub>3</sub>\*5CaO\*5ZrO<sub>2</sub>
- (4) 70wt% [60SiO<sub>2</sub>\*25Na<sub>2</sub>O\*10B<sub>2</sub>O<sub>3</sub>\*5CaO]+30wt%UO<sub>3</sub>.

The samples have been prepared by conventional melt-quench technique using a high temperature electrical furnace with a platinum crucible under atmospheric conditions. All glass samples were thoroughly characterized by neutron diffraction.

## Results

Neutron diffraction measurements have been performed in  $Q=0.45-10 \text{ \AA}^{-1}$  scattering vector range, measured by the 2-axis 'PSD' diffractometer ( $\lambda_0=1.068 \text{ \AA}$ ) [2] at the 10 MW Budapest research reactor. According to the neutron diffraction pattern all specimens are fully amorphous, the change of BaO to CaO did not influenced the amorphous character. Crystalline phases were not detected, neither hydrogen was incorporated. Slight differences can be seen in the corresponding  $S(Q)$  functions, see Fig. 1, although the network structure is very similar. The experimental  $S(Q)$  data have been simulated by the reverse Monte Carlo (RMC) method [3], we obtained a good fit for all four specimens, as it is illustrated in Fig. 1.

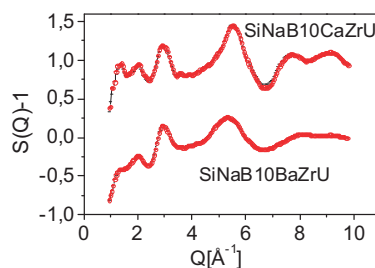


Figure 1. ND structure factors, experimental data (red circle) and RMC simulation (black line). (The curves are shifted vertically for clarity).

The results for several partial atomic pair correlation functions obtained from the RMC did show an excellent agreement within limit of error. The basic network consists of tetrahedral-SiO<sub>4</sub> and of mixed trigonal-BO<sub>3</sub> and tetrahedral-BO<sub>4</sub> units. The ND pattern shows that the specimens are fully amorphous, and no hydrogen was detected, meaning that the applied 6-component matrix glass is an effective host for embedding the large uranium ions, and they are hydrolytically stable.

## References

1. K.S.Chun, S.S. Kim, C.H. Kang, *Journal of Nuclear Materials* **298** (2001) 150.
2. E. Sváb, Gy. Mészáros, F. Deák, *Materials Science Forum* **228** (1996) 247.
3. R.L. McGreevy, L. Pusztai, *Molec. Simul.* **1** (1998) 359.

<h1 style="margin: 0;">B N C</h1> <p style="margin: 0;"><b>Experimental Report</b></p>	<i>Experiment title</i> <b>Network structure of sodium borosilicate glasses in dependence of B<sub>2</sub>O<sub>3</sub> content</b>	<i>Instrument</i> PSD-3 <i>Local contact</i> M. Fábíán
	Principal proposer: E. Veress Experimental team: M. Fábíán, Gy. Mészáros and E. Sváb, SZFKI; E. Veress Cluj/Romania	<i>Proposal No.</i> BRR-223-3 <i>Date</i> 05. 2010.

## Objectives

Borosilicate glass is the only material currently approved and being used to vitrify high level nuclear waste. In addition to immobilization of HLW, glass matrices are also being considered for isolation of many other types of hazardous materials, both radioactive as well as non-radioactive. There are many reasons why glass is preferred. Good processability allows the glass to be fabricated with relative ease and economically methods for vitrification of highly radioactive material. The most important property of the waste glass is an excellent chemical durability and corrosion resistance to a wide range of environmental conditions.

In our work we study wide range borosilicate structural. Here we have a neutron diffraction study following the possible glass network modifying influence of the increasing B<sub>2</sub>O<sub>3</sub> content in case of the 4-component glassy system: (70-x)SiO<sub>2</sub>\*xB<sub>2</sub>O<sub>3</sub>\*25Na<sub>2</sub>O\*5BaO, x=5-20 mol%.

The Si and B atoms are network formers and are located in the center of oxygen polyhedra in the configuration of tetrahedral or triangles. The advantage of the boron content is that the melting temperature significantly decreases. Most important modifiers, like Na and Ba atoms, are located within the holes of the random network structure. The glasses were melted in platinum crucible used an electric furnace at temperatures in the range from 1100 to 1350°C for 2-3h depending on the composition. The glasses were produced by rapid quenching by pouring it on a stainless steel plate.

## Results

Neutron diffraction (ND) measurements have been performed at the 10 MW Budapest research reactor using the 'PSD' neutron powder diffractometer [2]. Monochromatic wavelength of  $\lambda_0=1.068 \text{ \AA}$  was used. The diffraction spectrum was measured in the momentum transfer range of  $Q=0.45-10 \text{ \AA}^{-1}$ , see Fig. 1.

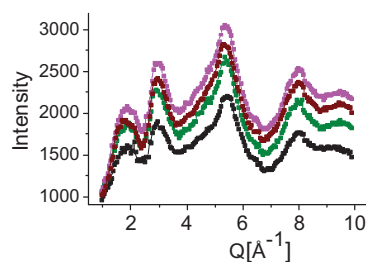


Fig. 1. Neutron diffraction pattern of glasses: Si5NaBa (black), Si10NaBa (green) Si15NaBa brown) and Si20NaBa (magenta).

The first few neutron diffraction experiments revealed their tendency to superficially adsorb H<sub>2</sub>O. In order to dry the samples, heat treatment was applied at 120°C for 4 hours under vacuum conditions, which proved to be completely sufficient to obtain neutron diffraction pattern adequate for data treatment. We have established that the gradual increase of the B<sub>2</sub>O<sub>3</sub> content did not alter the overall amorphous character, however, slight changes are observed.

## References

1. K.S. Chun, S.S. Kim, C.H. Kang, *Journal of Nuclear Materials* **298** (2001) 150.
2. E. Sváb, Gy. Mészáros, F. Deák, *Materials Science Forum* **228** (1996) 247.

<h1 style="margin: 0;">B N C</h1> <p style="margin: 0;">Experimental Report</p>	<i>Experiment title</i> <b>Structure Analysis of Selenite Glasses by Means of Neutron Diffraction</b>	<i>Instrument</i> PSD-4
	<i>Principal proposer:</i> V. Pamukchieva <i>Experimental team:</i> M. Fábíán, Gy. Mészáros and E. Sváb, SZFKI; V. Pamukchieva, Sofia/Bulgaria	<i>Local contact</i> M. Fábíán

## Objectives

Chalcogenide glasses exhibit a variety of interesting properties making them applicable in a wide range of fields. As-Se and As-Se-Te glassy compositions are very perspective for manufacturing optical fibers because of their low phonon energy, good transparency, low optical losses and good thermal and chemical stability. In this work we focused on the atomic-scale structural characterization of  $As_{40}Se_{60}$ ,  $As_{40}Se_{50}Te_{10}$  and  $As_{40}Se_{45}Te_{15}$  chalcogenide glasses using neutron diffraction method as for structure modelling reverse Monte Carlo (RMC) simulation was applied. The glassy samples with compositions were synthesized from 5N purity elements by the conventional melt-quenching method.

## Results

Neutron diffraction (ND) measurements were performed in a relatively broad momentum transfer range, combining the data measured by the 'PSD' neutron diffractometer ( $\lambda_0=1.068 \text{ \AA}$ ;  $Q=0.45-9.8 \text{ \AA}^{-1}$ ) [1] at the 10 MW Budapest research reactor and by the time-of-flight 'HIPPO' instrument at the LANSCE pulsed neutron source  $Q=0.9-50 \text{ \AA}^{-1}$  [2]. The structure factors,  $S(Q)$ 's were evaluated from the raw experimental data, using the programme packages available at these two facilities. The diffraction experimental data was treated by the reverse Monte Carlo (RMC) simulation [3] in order to get structural information about the possible atomic configurations. As a RMC starting model, for each composition a disordered atomic configuration was built up with a simulation box containing 10000 atoms. The ND patterns showed that the specimens were fully amorphous, results of the experimental structural factor  $S(Q)$  are summarized in Fig. 1. At first sight, the  $S(Q)$  spectra look similar for all three compositions, but several fine details indicate the existing differences. The partial atomic correlation functions obtained from the RMC modelling for As-Se, As-As and Se-Se atomic pairs are presented in Fig. 2.

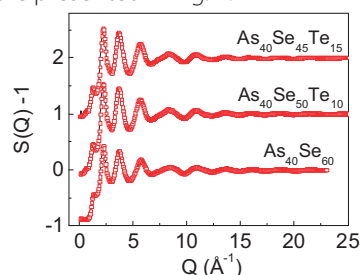


Fig. 1. Experimental structure factor data (red squares) obtained from the neutron diffraction measurements and from RMC modelling (solid line) for the studied glasses.

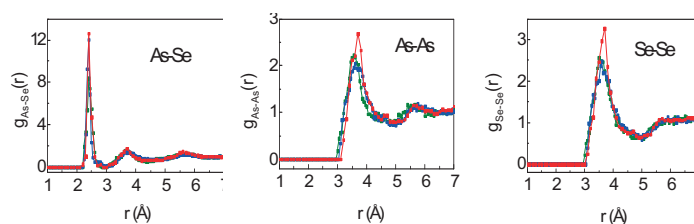


Fig. 2. Partial atomic correlation functions obtained from the RMC modelling of As-Se, As-As and Se-Se atom pairs for  $As_{40}Se_{60}$  (red),  $As_{40}Se_{50}Te_{10}$  (green) and  $As_{40}Se_{45}Te_{15}$  (blue) glasses.

The substituting a part of Se by Te atoms does not change the basic network structure within the limit of experimental and modelling errors. For all three compositions, the As-Se correlation shows a rather sharp first neighbour distance at  $2.40 \pm 0.01 \text{ \AA}$ . In the  $As_{40}Se_{50}Te_{10}$  and  $As_{40}Se_{45}Te_{15}$  glasses the possible As-As and Se-Se homopolar bonds have similar and characteristic broad peak at  $3.6 \pm 0.1 \text{ \AA}$ , while for the  $As_{40}Se_{60}$  glass the peak is shifted slightly to  $3.7 \pm 0.1 \text{ \AA}$ . Addition of Te to As-Se network has negligible effect on As-Se bonds. Therefore, in the ternary As-Se-Te system the As-Se bond distance remains the same as in the binary As-Se system. The simulations have shown a glass network building up by  $As(Se,Te)_3$  pyramids in which the Te atoms can be substitute the Se atoms.

## References

1. E. Sváb, Gy. Mészáros, F. Deák, *Materials Science Forum* 228 (1996) 247; <http://www.bnc.hu/>
2. Th. Proffen, S.J.L. Billinge, T. Egami, D. Louca, *Zeitschrift für Kristallographie* **218** (2003) 132.
3. R.L. McGreevy, L. Pusztai, *Molecular Simulation* **1** (1988) 359.

<h1 style="margin: 0;">B N C</h1> <p style="margin: 0;"><b>Experimental Report</b></p>	<i>Experiment title</i> <b>Neutron diffraction study of the structure of new molybdate glasses from the <math>\text{MoO}_3\text{-Nd}_2\text{O}_3\text{-B}_2\text{O}_3</math> system</b>	<i>Instrument.</i> PSD <i>Local contact</i> E. Sváb
	Principal proposer: Krezhov, Kiril Experimental team: M. Fábíán, E. Sváb, Gy. Mészáros, SZFKI and Kiril Krezhov Sofia/Bulgaria	<i>Experiment Number</i> BRR-235 <i>Date:</i> November 2010

## Objectives

The Mo-rare earth oxides are widely used, due to physical and chemical properties, i.e. large ion- and electron conductivity, catalytic activity, non-linear optical properties and good mechanical resistance.  $\text{MoO}_3$  is well-known as a conditional network former, it is not able to form a glass itself. The aim of this work is to get a deeper insight into the structural network characteristics of new series of molybdate glasses containing modifiers  $\text{Nd}_2\text{O}_3$  and  $\text{MgO}$ , and classical glass former  $\text{B}_2\text{O}_3$ . The  $\text{Nd}_2\text{O}_3$  is appropriate component due to its specific optical properties but it increases the melting temperature. By introducing of  $\text{B}_2\text{O}_3$  it is possible to obtain low melting materials in wider concentration range.

## Results

For this study the following amorphous samples have been prepared by rapid quench technique [1]:  $90\text{MoO}_3\text{-}10\text{Nd}_2\text{O}_3$  (Mo90Nd10),  $80\text{MoO}_3\text{-}15\text{Nd}_2\text{O}_3\text{-}5\text{MgO}$  (Mo80Nd15Mg5),  $75\text{MoO}_3\text{-}12.5\text{Nd}_2\text{O}_3\text{-}12.5\text{MgO}$  (Mo75Nd12.5Mg12.5) and  $50\text{MoO}_3\text{-}25\text{Nd}_2\text{O}_3\text{-}25\text{B}_2\text{O}_3$  (Mo50Nd25B25). The boron containing sample was prepared from  $^{11}\text{B}$ -isotope enriched to 99.6%. Neutron diffraction (ND) patterns were collected using the 'PSD' instrument ( $\lambda=1.069 \text{ \AA}$ ). The powdered specimens of about 4g/each have been filled into thin walled vanadium cans with diameter of 8mm. Also high energy X-ray diffraction (XRD) measurements have been performed in Hamburg/Hasylab Desy synchrotron at 'BW5' station [2]. For data evaluation the reverse Monte Carlo (RMC) simulation was applied to obtain a possible 3-dimensional network configuration, which is consistent with the experimental data. The RMC simulation box did contain 10000 atoms and the usual constraints were applied i.e. atomic density, cut-off distances (nearest neighbour distances for all atom pairs) and connectivity. The final RMC run gave an excellent fit both for the ND and XRD experiments, as it is illustrated in Fig. 1.

From the RMC modelling the partial atomic correlation functions  $g_{ij}(r)$  and the coordination number distributions  $\text{CN}_{ij}$  have been revealed. Formation of  $\text{MoO}_4$  units was established with  $1.80 \text{ \AA}$  Mo-O distance. For the B-O network two characteristic first neighbour distances were obtained at  $1.40 \text{ \AA}$  and  $1.60 \text{ \AA}$ , related to the trigonal  $\text{BO}_3$  and tetrahedral  $\text{BO}_4$  groups. Mixed  $\text{MoO}_4\text{-BO}_4$  and  $\text{MoO}_4\text{-BO}_3$  linkages form pronounced intermediate-range order.

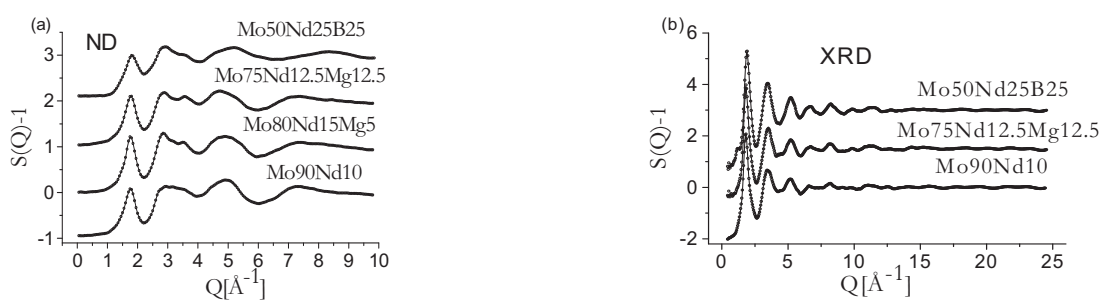


Fig. 1. Experimental data (circle) and RMC simulation (solid line): a) Neutron b) X-ray diffraction.

## References

- [1] L. Alexandrov, R. Iordanova, Y. Dimitriev J. Non-Cryst. Solids **355** (2009) 2023
- [2] H. Poulsen, J. Neuefeind, H.B. Neumann, J.R. Schneider, M.D. Zeidler, *Journal of Non-Cryst. Solids* **188** (1995) 63.

<h1 style="margin: 0;">B N C</h1> <p style="margin: 0;"><b>Experimental Report</b></p>	<i>Experiment title</i> <b>Structure study of new insulating materials</b>	<i>Instrument:</i> PSD
	<i>Principal proposer:</i> M. Fabian, BNC EKI <i>Experimental team:</i> M. Fábián, Gy. Mészáros, E. Sváb, BNC Wigner	<i>Local contact</i> M. Fábián  <i>Experiment Number</i> PSD_12_1_IH <i>Date:</i> February 2012

## Objectives

Thermilate are used for insulation, because they have good thermal efficiency, safety and easy-of-use. During the preparation is important the combination of the latest micro technology to guaranteed energy-saving and protective, decorative and functional paints and coatings for interior and external uses around the world. All thermilate products are manufactured to original formulations. We tested with neutron diffraction, to obtain the basic nature of these materials, which contain  $\text{SiO}_2$  and  $\text{Al}_2\text{O}_3$  in different percentage.

## Results

Neutron diffraction measurements were carried out at the 10MW Budapest research reactor using the PSD diffractometer[1]. The neutron structure factor,  $S(Q)$  was detected in a momentum transfer range,  $Q=0.4-10 \text{ \AA}^{-1}$ . Figure 1 show the neutron intensity measured on the thermilate sample. We obtained mixed spectra, where the amorphous character is substantially larger than the crystalline phase. Figure 2 shows an  $\text{Al}_2\text{O}_3$  standard, measured also in our PSD instrument. If we compare the two spectra, the  $\text{Al}_2\text{O}_3$  crystalline phase can be identified and also a mixed Si-Al crystalline phase is present. However, the  $\text{SiO}_2$  based amorphous phase is dominated in the thermilate spectrum.

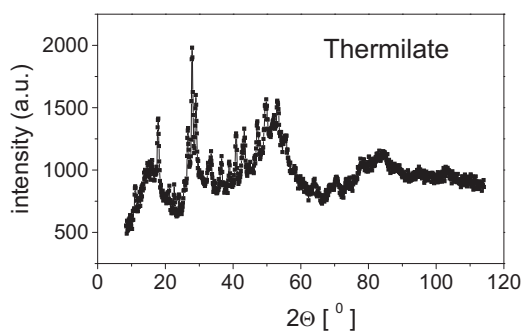


Figure 1. Neutron experimental data for thermilate.

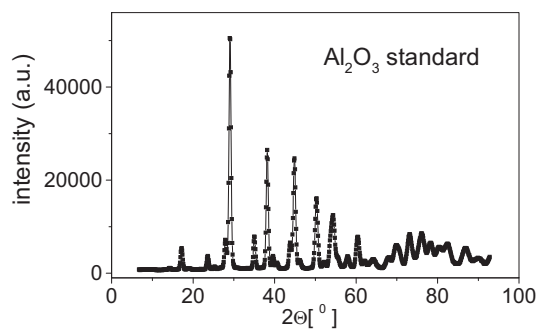


Figure 2. Neutron experimental data for  $\text{Al}_2\text{O}_3$  standard.

## Future prospects

Publication is in progress.

## References

[1] Svab E, Meszaros Gy, Deak F 1996 *Mater. Sci. Forum* **228** 247 and <http://www.bnc.hu/>

<h1 style="margin: 0;">B N C</h1> <p style="margin: 0;">Experimental Report</p>	<i>Experiment title</i> <b>Structure study of new uranium loaded borosilicate glasses</b>	<i>Instrument:</i> PSD
		<i>Local contact</i> M. Fábíán
<i>Principal proposer:</i> M. Fabian, BNC EKI <i>Experimental team:</i> M. Fábíán, Gy. Mészáros, E. Sváb, BNC Wigner		<i>Experiment Number</i> PSD_12_2_IH  <i>Date:</i> March-April 2012

## Objectives

High-level radioactive waste (HLW) produced by spent fuel reprocessing of civil nuclear reactors currently is incorporated into an inert host material. HLW contains actinides (fission and activation products), primarily U, and Pu that is the fission byproduct of the  $\text{UO}_2$  burning process. Recently, we have prepared 5-component sodium borosilicate host (matrix) glasses, which proved to be stable and capable of hosting uranium [1]. In this work we present the structure determination of a new 6-component glass system loaded with  $\text{UO}_3$  using both neutron diffraction (ND) and high-energy X-ray diffraction (XRD) experiments.

## Results

The glasses of composition  $70\text{wt.}\%[(65-x)\text{SiO}_2\cdot x\text{B}_2\text{O}_3\cdot 25\text{Na}_2\text{O}\cdot 5\text{BaO}\cdot 5\text{ZrO}_2]+30\text{wt.}\%\text{UO}_3$  with  $x=5, 10, 15, 20$  mol% (hereafter referred to as UB5, UB10, UB15, UB20) were prepared by melt-quench technique using  $^{11}\text{B}$  (99.6%) isotope. We have performed ND experiments using the 'PSD' instrument in the scattering vector range of  $Q=0.6\text{-}10\text{\AA}^{-1}$  and also high-energy XRD using the BW5/HASYLAB, DESY experimental station in the scattering vector range of  $Q=0.5\text{-}25\text{\AA}^{-1}$ . The overall run of the ND and XRD  $S(Q)$  curves is fairly different because of the different weighting factor of the two radiations, as illustrated in the overlapping  $Q$ -range for UB5 composition in Fig. 1. A simultaneous reverse Monte Carlo simulation of the two data sets was applied to generate reliable 3-dimensional atomic configurations and, to calculate several partial atomic pair correlation functions, nearest neighbour distances and coordination number distributions. For the U-O correlations two distinct first neighbour distances were determined at  $1.8\text{\AA}$  with 2 oxygen atoms and at  $2.2\text{\AA}$  with near 4 oxygen atoms. Furthermore, significant second neighbour atomic pair correlations have been established between uranium and the network former (Si, B), the modifier (Na) and the stabilizer (Zr) atoms. From these observations we may conclude that uranium ions take part in the network forming. This may be the reason of the observed good glassy stability and hydrolytic properties.

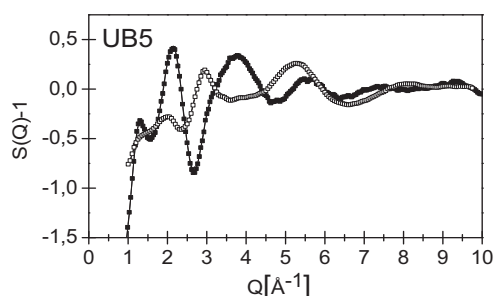


**Figure 1.** Comparison of neutron (open square) and X-ray (solid square) experimental data for UB5.

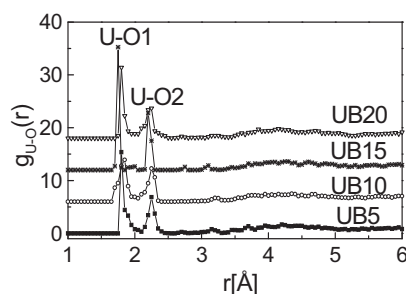


**Figure 2.** Partial U-O atomic correlation functions from RMC modelling.

## Future prospects

Publication is in progress [2].

## References

- [1] M.Fabian, Th.Proffen, U.Ruett, E.Veress, E.Svab, *J. Phys.: Condens. Matter* 22 (2010) 404206.  
[2] M.Fábíán, E.Svab, M.v.Zimmerman, *J. Non-Cryst. Solids* (2013), <http://dx.doi.org/10.1016/j.jnoncrysol.2013.09.004>

<h1 style="margin: 0;">B N C</h1> <p style="margin: 0;">Experimental Report</p>	<i>Experiment title</i> <b>Structure study of ternary Ge-Sb-Se chalcogenide glasses</b>	<i>Instrument.</i> PSD <i>Local contact</i> M. Fábíán
	<i>Principal proposer:</i> V. Pamukchieva <i>Experimental team:</i> M. Fábíán, Gy. Mészáros, E. Sváb, SZFKI; V. Pamukchieva, Sofia/Bulgaria	<i>Proposal No.</i> BRR_286 <i>Date(s) of Exp.</i> May&June 2012

## Objectives

In recent years a great deal of interest has been devoted to the structural and optical studies of chalcogenide glasses because of their wide area of applications as electrical and optical components. The physico-chemical properties of the ternary Ge-Sb-Se chalcogenide system have been studied in ref. [1]. Extending our research, in this work we focus on the atomic-scale structure characterization of the Ge<sub>40</sub>Se<sub>60</sub> and the new ternary chalcogenide family: Ge<sub>(40-x)</sub>Sb<sub>x</sub>Se<sub>60</sub> x=5, 8, 13, 20, 25 at%, compositions by neutron diffraction and RMC modeling.

## Results

Neutron diffraction measurements were carried out at the 10MW Budapest research reactor using the PSD diffractometer [2]. The neutron structure factor,  $S(Q)$  was detected in a momentum transfer range,  $Q=0.4-10 \text{ \AA}^{-1}$ . In order to get structural information on the short and intermediate range order, both, the traditional Fourier transformation technique and the reverse Monte Carlo (RMC) simulation [3] of the experimental data were applied to the data treatment.

The Ge, Sb, Se elements possess very similar neutron scattering amplitudes, which makes rather difficult to separate the atomic positions. Using reasonable cut-off distances and connectivity constraints in the RMC simulation procedure, we have obtained very good agreement between the experimental and the calculated  $S(Q)$  data, are presented in Figure 1.

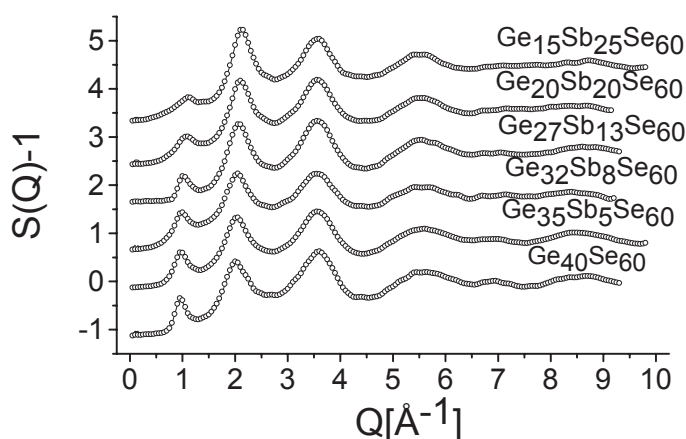


Figure 1. Structure factors for the glasses experimental (open circle) and RMC calculations (solid line)

Several first and second neighbour distances, and coordination numbers have been calculated. We have established that several first neighbour atomic distances, namely the Ge-Ge, Ge-Se, Sb-Se and Ge-Sb are centred at 2.5Å(1)-3.8Å(2), at 2.3Å, at 2.4Å and 3.75Å, respectively.

## Future prospects

The structure analysis is in progress.

## Reference

- [1] Ivanova Z G, Pamukchiva V, Vlcek M 2001 *J. Non-Cryst. Solids* **293-295** 580
- [2] Svab E, Meszaros Gy, Deak F 1996 *Mater. Sci. Forum* **228** 247 and <http://www.bnc.hu/>
- [3] McGreevy R L, Pusztai L 1988 *Mol. Simul.* **1** 359



<h1 style="margin: 0;">B N C</h1> <p style="margin: 0;">Experimental Report</p>	<i>Experiment title</i> <b>Structure Study of Ge-Sb-S(Se)-Te Glasses with Neutron Diffraction</b>	<i>Instrument</i> PSD
	Principal proposer: V. Pamukchieva Experimental team: M. Fábíán, Gy. Mészáros and E. Sváb, SZFKI; V. Pamukchieva, Sofia/Bulgaria	<i>Local contact</i> M. Fábíán

## Objectives

Chalcogenide glasses based on sulfide, selenide and telluride alloys in binary or multi-component systems are very promising materials for various optical and photonic applications in the spectral range from 0.6 to 15  $\mu\text{m}$ . These glasses are being studied mostly for applications as passive devices (lenses, windows, fibres) but they are also attractive as active elements in optical devices, such as laser fibre amplifiers and non-linear components.

Nowadays the attention is extended over telluride glasses from quaternary Ge-Sb-S(Se)-Te systems as potential candidates for integrated optics due to their high refractive index and photosensitivity as well as their transparency in the infrared spectral region. The bulk glasses with composition of  $\text{Ge}_x\text{Sb}_{40-x}\text{S}_{50}\text{Te}_{10}$  and  $\text{Ge}_x\text{Sb}_{40-x}\text{Se}_{50}\text{Te}_{10}$  ( $x=20$  and  $27$  at. %) were synthesized from 5 N purity elements by the conventional meltquenching method.

## Results

In order to get information about the structure and chemical bonding from the neutron diffraction data, two types of measurements were carried out. The neutron diffraction (ND) measurements were performed in a relatively broad momentum transfer range,  $Q=0.4\text{-}40\text{\AA}^{-1}$ , combining the data measured by the 2-axis 'PSD' monochromatic neutron diffractometer ( $\lambda_0=1.068\text{\AA}$ ;  $Q=0.45\text{-}9.8\text{\AA}^{-1}$ ) [1] at the 10 MW Budapest research reactor and by the time-of-flight 'HIPPO' instrument [2] at the LANSCE pulsed neutron source  $Q=0.9\text{-}40\text{\AA}^{-1}$ . For the two experimental instruments, the powder samples of about 3-4 g/each were placed in cylindrical vanadium containers of 8 mm diameter. The two sets of  $S(Q)$ 's were obtained in the momentum transfer range of  $Q=0.4\text{-}9.6\text{\AA}^{-1}$  and  $1.5\text{-}40\text{\AA}^{-1}$  from the 'PSD' and 'HIPPO' experiments, respectively. The coincidence of the corresponding  $S(Q)$  values was within 1 % in the overlapping  $Q$ -range. The experimental data were simulated considering each composition as three-dimensional atomic configuration to reproduce the neutron diffraction structure factors. For the RMC [3] starting model we used the density data and a 10000 atoms containing simulation box. The ND patterns showed that the specimens were fully amorphous, results of the experimental structural factor  $S(Q)$  are summarized in Figure 1.

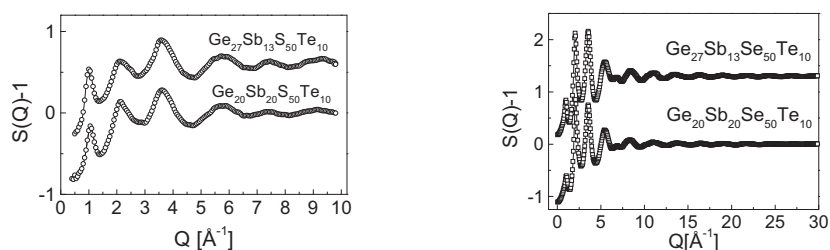


**Figure 1.** Experimental structure factor data (circles and squares) obtained from the neutron diffraction measurements and from RMC modelling (solid line) for the studied glasses.

Characteristic structural parameters, such as structure factors, partial atomic pair correlation functions, coordination numbers and bond-angle distribution functions are established. The results identify in the studied glasses Ge related tetrahedral structural units and Sb related trigonal pyramidal units, which are more defective and/or distorted in the S-containing glasses. On the basis of the density data and model simulation of the atomic glassy network for each composition, the basic physical parameters of packing density, average atomic volume and compactness are evaluated.[4]

## References

- [1] E. Sváb, Gy. Mészáros, F. Deák, *Materials Science Forum* **228** (1996) 247; <http://www.bnc.hu/>
- [2] Th. Proffen, S.J.L. Billinge, T. Egami, D. Louca, *Zeitschrift für Kristallographie* **218** (2003) 132.
- [3] R.L. McGreevy, L. Pusztai, *Molecular Simulation* **1** (1988) 359.
- [4] M. Fabian, E. Svab, V. Pamukchieva, A. Szekeres, K. Todorova, S. Vogel, U. Ruett, *Journal of Physics and Chemistry of Solids* **74** (2013) 1355

<h1 style="margin: 0;">B N C</h1> <p style="margin: 0;">Experimental Report</p>	<i>Experiment title</i> <b>Neutron diffraction study of the structure of new molybdate glasses from the MoO<sub>3</sub>-Bi<sub>2</sub>O<sub>3</sub>-WO<sub>3</sub> system</b>	<i>Instrument</i> PSD
		<i>Local contact</i> E. Sváb
Principal proposer: Krezhov, Kiril Experimental team: M. Fábrián (EKI), E. Sváb, Gy. Mészáros, (Wigner) and Kiril Krezhov Sofia/Bulgaria		<i>Experiment Number</i> BRR-309 <i>Date:</i> November 2012

## Objectives

Molybdate and tungstate glasses are among the so called non-traditional glasses. In addition to their academic importance as a suitable object for the solution of intriguing structural problems of glassy state, few compositions have proven ability for practical applications as amorphous semiconductors, electrolytes, nonlinear optical materials, reflecting windows, as well in for waste storage. The present neutron diffraction experiment aims at determination of the structural details of short range order, like atomic pair correlation functions, first neighbour distances, coordination numbers. This study would reveal the correlation between the glassy structure and composition in accordance with accumulated information including optical spectral investigations.

## Results

The glasses of composition binary 75MoO<sub>3</sub>-25Bi<sub>2</sub>O<sub>3</sub>, ternary 35MoO<sub>3</sub>-25 Bi<sub>2</sub>O<sub>3</sub>-40WO<sub>3</sub> and binary 75 WO<sub>3</sub>-25 Bi<sub>2</sub>O<sub>3</sub> (the concentrations are in mol.%) were prepared by melt-quench technique with cooling rates 10-10<sup>2</sup> K/s [1]. Neutron diffraction (ND) patterns were collected at ambient temperature using the 'PSD' instrument ( $\lambda=1.069 \text{ \AA}$ ) in the scattering vector range of  $Q=0.6-10 \text{ \AA}^{-1}$  and also high-energy XRD using the BW5/HASYLAB, DESY experimental station in the scattering vector range of  $Q=0.5-25 \text{ \AA}^{-1}$ . The overall run of the ND and XRD  $S(Q)$  curves is fairly different, as illustrated in Fig. 1, because of the different weighting factors of the two radiations.

For data evaluation the reverse Monte Carlo modelling have been applied. The Mo-O, Bi-O, W-O and O-O partial atomic correlation functions, coordination numbers and three-atom bond angle distributions have been revealed. First neighbour distances were obtained  $r_{\text{Mo-O}}=r_{\text{W-O}}=1.7 \text{ \AA}$ ,  $r_{\text{Bi-O}}=2.0 \text{ \AA}$  and  $r_{\text{O-O}}=2.6 \text{ \AA}$ . The coordination number distribution suggested that Mo and W are glass former, while Bi acts as modifier. The results, obtained so long, have shown that the basic glass forming units are MoO<sub>3</sub>, WO<sub>3</sub> and WO<sub>4</sub>.

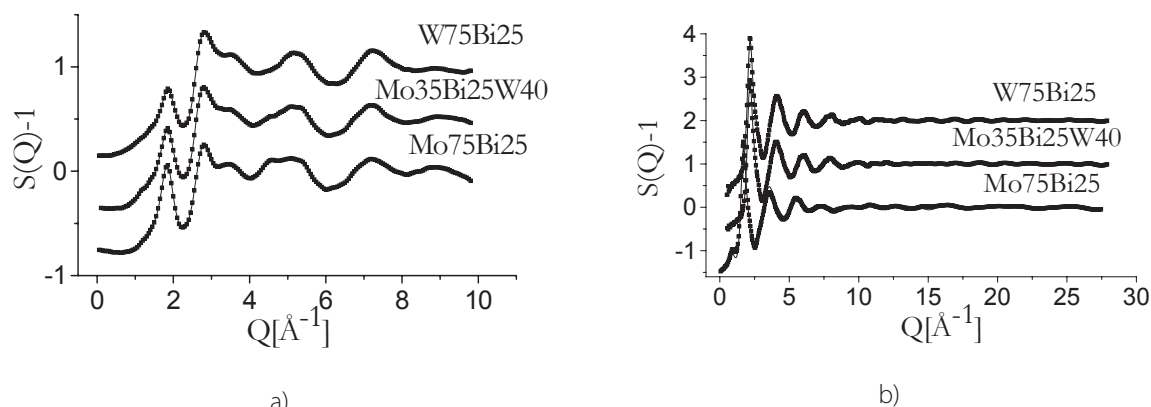


**Figure 1.** Experimental (dots) and reverse Monte Carlo simulated (line) structure factors: a) neutron diffraction and b) high energy X-ray diffraction

## Future prospects

The structure analysis is in progress.

## References

[1] Y. Dimitriev, R. Iordanova, D. Klissurski, M. Milanova, *Phys. Chem. Glasses*, **43C** (2002) 387-391.

<h1 style="margin: 0;">B N C</h1> <p style="margin: 0;"><b>Experimental Report</b></p>	<i>Experiment title</i> <b>Mesostructure of transparent porous zirconia glasses</b>	<i>Instrument:</i> SANS
	<i>Local contact</i> Laszlo Almasy	
<i>Principal proposer:</i> Vladimir Ivanov <i>Experimental team:</i> Vladimir Ivanov, Gennady Kopitsa, Olga Ivanova, Nadezda Gubanova		<i>Proposal No.:</i>  <i>Date(s) of Exper.</i> 10.07-14.07.2011

## Objectives

Transparent amorphous oxide glasses are considered to be very promising materials for photochromic devices, catalytic systems, chemical sensors, and non-linear optics devices, especially lasers. Recently we have succeeded in development of sol-gel technique of transparent zirconia glasses possessing very high surface area (up to 400 m<sup>2</sup>/g). Their structural parameters (including density, porosity, etc.) could be widely varied by changing the synthesis conditions, namely molar ratio of reactants, acidity of reaction medium etc. Thus the main goal of the proposal was to obtain information on fractal dimension, self-similarity range and mesostructure (mainly the porosity) of a series of transparent porous zirconia glasses prepared by sol-gel technique (by precipitation at different pH values) with or without ultrasonication.

## Achievements and Main Results

A common feature of all samples (control and sonicated) is the existence of two  $q$  ranges (at low and large  $q$ ) on the scattering curves where the behavior of the SANS  $d\Sigma(q)/d\Omega$  satisfies the power law  $q^{-n}$  with  $n = 3$  and  $m$ , respectively, and the medium range of  $q$  where the behavior of the SANS  $d\Sigma(q)/d\Omega$  satisfies the exponential law (the Guinier regime). The exponent  $n$  and  $m$  values found from the slope of the straight-line parts of the curves plotted in log-log scale lie in the range from 3 to 4. This corresponds to the scattering from the fractal surface with the dimension  $2 < D_s = 6 - n < 3$ .

Thus, the observed scattering patterns indicate that the all samples under investigation contain two types of scattering inhomogeneities with strongly different characteristic scales. It can be concluded that amorphous ZrO<sub>2</sub> glasses are composed of aggregates with a strongly developed surface that are formed from the initial small monomer particles which also have strongly developed surface.

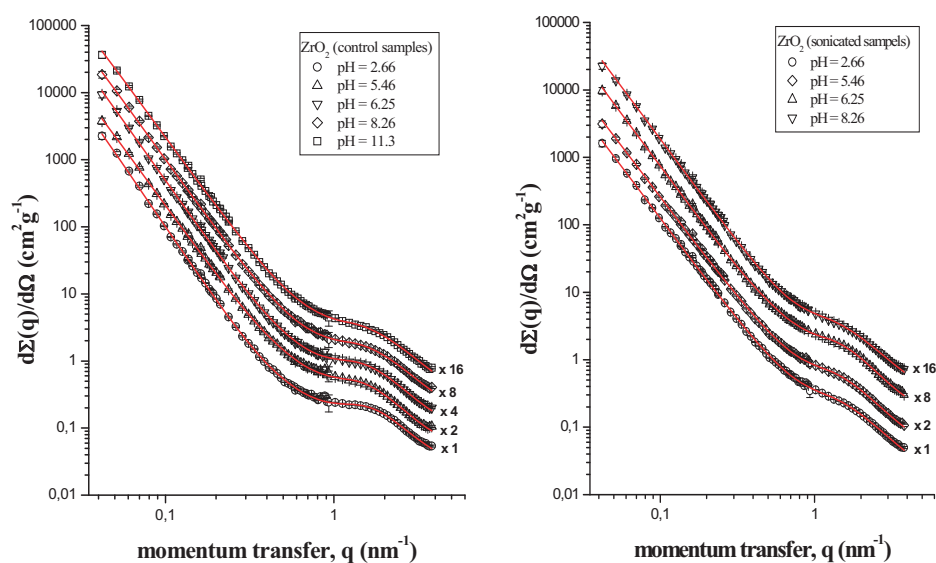


**Fig. 1** The SANS cross section  $d\Sigma(q)/d\Omega$  for the control (non-sonicated) (a) and sonicated (b) samples of the amorphous ZrO<sub>2</sub> glasses precipitated at the different pH values media.

<h1 style="margin: 0;">B N C</h1> <p style="margin: 0;"><b>Experimental Report</b></p>	<i>Experiment title</i> <b>High temperature growth mechanisms of ceria nanoparticles</b>	<i>Instrument:</i> SANS  <i>Local contact</i> Laszlo Almásy
	<i>Principal proposer:</i> Gennady Kopitsa <sup>1</sup> <i>Experimental team:</i> Vladimir Ivanov <sup>1</sup> , Olga Ivanova <sup>1</sup> , László Almásy <sup>2</sup> <sup>1</sup> PNPI Gatchina, Russia, <sup>2</sup> RISP Budapest, Hungary	<i>Proposal No.</i> BRR-271 <i>Date(s) of Exper.</i> 10.07-14.07.2011

## Objectives

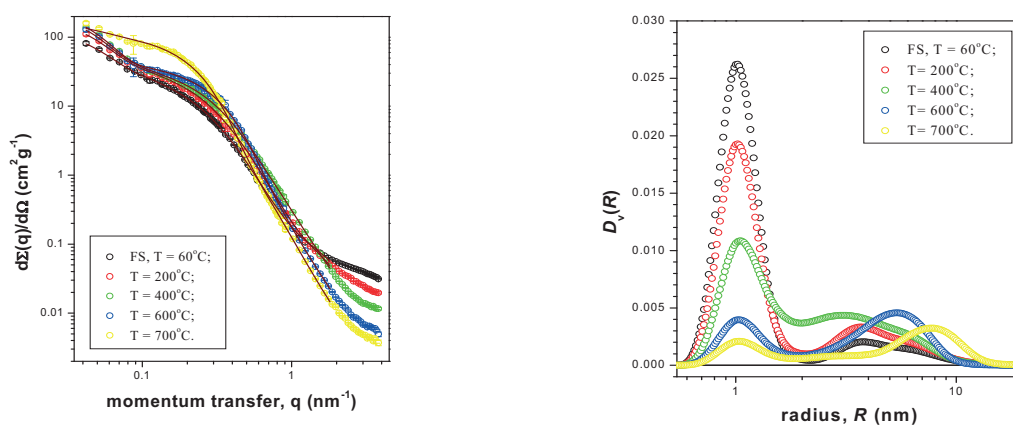
Nanocrystalline ceria is a unique multifunctional material widely used in industries. In particular, ceria is used in protective coatings, as the main component of abrasives, including those used in micro- and nanoelectronics, in catalytic systems, in trace gas sensors, in biomedical applications and in other fields.

Ceria-based materials, including oxygen sensors and car emission converters, in most cases operate at temperatures above 400–500°C because of substantially higher oxygen mobilities in ceria crystal lattice at these temperatures. Contrariwise, diffusion of cerium ions at these temperatures is nearly negligible; in particular, the volume diffusion of cerium ions is not observed even when CeO<sub>2</sub> samples are heated up to ~630°C. Nonetheless, in spite of low cation mobility, the high-temperature applications of CeO<sub>2</sub> nanomaterials are inevitably accompanied by noticeable particle coarsening and decrease in the oxygen non-stoichiometry and specific surface area of the material. Presumably, ceria particle coarsening under heating is due to cooperative mass transfer processes involving mutual movement and rotation of CeO<sub>2</sub> crystallites (i.e. due to so called “oriented attachment” of crystallites) as a whole more than due to thermally activated diffusion processes. However, the evidences of this hypothesis are still scarce. This proposal was focused on gaining information on mesostructure of a series of nanocrystalline ceria samples (3–20 nm) prepared by annealing under pre-determined conditions (60, 400, 500, 600, 700°C).

## Achievements and Main Results

The momentum dependences of the SANS cross section  $I(q)$  measured for samples of the nanocrystalline CeO<sub>2</sub> with different annealing temperatures  $T_a$  are shown in Fig.1 on log-log scale. As clearly seen, the increase of the cross sections occurs with the increasing of the annealing temperature  $T_a$ . It correspond to the behaviour of the attenuation of the incident neutron beam  $I(q=0)/I_0$ , which decreases with increasing of  $T_a$  and is inversely proportional to integral scattering cross section. It indicates that the fluctuations of the nuclear density in the xerogel CeO<sub>2</sub> increase with the increasing of  $T_a$ . This increase is visibly uneven and depends on the annealing temperature  $T_a$ . Data analysis by inverse Fourier transformation shows a bimodal particle size distribution, which evolves with changing the annealing temperature. Further data treatment and interpretation is in progress.

**Fig.1.** SANS cross section  $d(q)/d$  (left) and particle size distribution (right) for nanocrystalline CeO<sub>2</sub> samples with different annealing temperatures.



<b>B N C</b> <b>Experimental Report</b>	<i>Experiment title</i> <b>Hydrophobic interaction in aqueous solutions of methylated ureas</b>	<i>Proposal No.</i> BRR_238 <i>Local contact</i> L.Almasy
	<i>Principal proposer</i> László Almásy <i>Experimental team</i> László Almásy	<i>Date of Experiment</i> March 2010 <i>Date of Report</i> Sept 2013

## Objectives

Aqueous solutions of methylated ureas have been widely studied in the last two decades by various physico-chemical methods. These co-solvents are interesting for studying the role of hydrophobic-hydrophilic solvation of small organic molecules. All they exhibit mostly hydrophobic hydration due to their four methyl groups in case of tetramethylurea, or two methyl and an ethylene or propylene group for the closed cycle dimethylethyleneurea, and dimethylpropyleneurea. From a structural point of view, the main question of interest is the way of caging of the large hydrophobic TMU molecules into the water network, and the spatial distribution of the molecules of the two components. In some of the recent SANS studies on aqueous DMEU and DMPU were interpreted on basis of pairwise aggregation in their dilute solutions, while in other studies only the hydrogen bond network strengthening of the water surrounding the TMU has been considered to be responsible to the highly non-ideal behavior of these mixtures. The aim of the present study was to compare the strength of the hydrophobic interaction for the different systems and correlate them to the interaction forces as computed by ab initio methods.

## Results

SANS measurements were performed on solutions of TMU, DMPU, DMEU in the mole fraction range 0.02 – 0.06. The samples were filled in 2 mm thick quartz cuvettes and thermostated at temperatures 10, 25 and 40°C with an accuracy of 0.5°C. The measured raw intensities have been corrected for scattering from the empty cell and room background and scaled in absolute units using the incoherent scattering of light water. For all samples the scattering is stronger at higher temperatures. The increased scattering intensity at low angles show that all these mixtures are spatially inhomogeneous in the studied concentration range, due to an effective attractive interaction between the co-solvent molecules. The temperature dependence of this interaction suggests its hydrophobic character. The coherent scattering intensity for all solutions is rather weak, so extremely long measuring times were required to collect sufficient statistics. Finally, the initial aim of the experiment could not be achieved – to collect sufficiently precise data on the temperature dependent aggregation in order to compare and correlate with the strength of pairwise interaction energies of ab initio calculated dimers and their complexes with water molecules.

All curves for all mixtures and concentrations exhibit increased scattering at forward direction. As an illustration, a concise set of curves is shown from an earlier experiment on aqueous tetramethylurea (Fig. 1), here the average exposition time per sample was four hours, at one temperature. The scattering curves are adequately described by the Ornstein–Zernike structure factor, which corresponds to a mixture with statistical concentration fluctuations. From the experimental data, the concentration fluctuations and the Kirkwood–Buff integrals have been calculated, and the association of TMU molecules in dilute aqueous solutions have been quantitatively characterized.

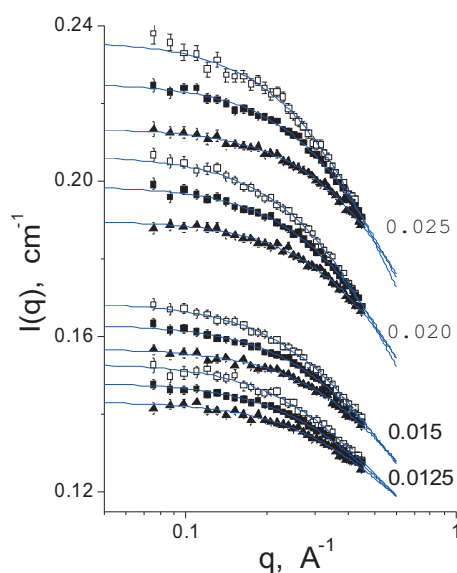


Fig. 1. SANS scattering curves for TMU – D<sub>2</sub>O mixtures at 10, 25 and 40°C. The mole fraction of TMU is indicated. The scattering intensity is higher for higher temperatures.

<b>B N C</b> <b>Experimental Report</b>	<i>Experiment title</i> <b>A SANS study of polythiophene-surfactant system</b>	<i>Proposal No.</i> BRR_246 <i>Local contact</i> N. Székely
	<i>Principal proposer</i> Matti Knaapila, Institute for Energy Technology (Norway) <i>Experimental team</i> Matti Knaapila, Noémi Székely (BNC)	<i>Date of Experiment</i> Nov 2010 <i>Date of Report</i> May 2011

## Objectives

Our original objective was to synthesise a cationic water soluble polythiophene polyelectrolyte and complex it with the surfactant sodium dodecylsulfate. The idea was to show how the surfactant can be used to control the photophysical properties in water and how this control stems from both the structure of the polymer-surfactant complexes formed and the internal organisation of the polymer within these complexes.

## Results

The experiment in Budapest was very successful. Main findings (structural interplay of polythiophene in surfactant and the subsequent optical transitions) are outlined in Fig. 1.

Poly[3-[6-(*N*-methylimidazolium)hexyl]-2,5-thiophene] bromide (P3ImiHT) was mixed with either SDS or deuterated SDS to form the P3ImiHT(SDS)<sub>x</sub> complex, where *x* is the molar ratio of surfactant to polyelectrolyte repeat unit, in D<sub>2</sub>O and studied using SANS and optical spectroscopy. At room temperature, P3ImiHT forms charged aggregates with electrostatic repulsion which is eliminated by the SDS addition. For *x* ≤ 1 P3ImiHT and SDS are molecularly mixed and form ellipsoidal (*x* = 1/5) or sheet-like (*x* = 1/2–1) P3ImiHT(SDS)<sub>x</sub> aggregates. For *x* > 1, P3ImiHT(SDS)<sub>x</sub> aggregates coexist with SDS rich micelles which turn from thick rod-like (*x* = 3/2) to non-charged (*x* = 2) and charged ellipsoidal micelles (*x* = 5), this transition driven by decreasing free ion fraction. For *x* = 5, P3ImiHT(SDS)<sub>x</sub> forms a lamellar phase with a periodicity of ~270 Å.

The structural transitions are accompanied by an initial red-shift from 422 nm (*x* = 0) to 459 nm (*x* = 1), followed by a reverse blue-shift to 400 nm (*x* = 5) of the UV/vis absorption maxima. The photoexcitation spectra follow this trend but are ~50 nm red-shifted, thus indicating energy down transfer within the density of states after photoexcitation. The photoluminescence maximum is gradually blue-shifted on increasing *x* indicating a decrease in polymer-polymer interactions.

## Future prospects

We have finished experimental work and manuscript of this work has been accepted to *Soft Matter* (2011). We have planned to extend these ideas to thermal measurements.

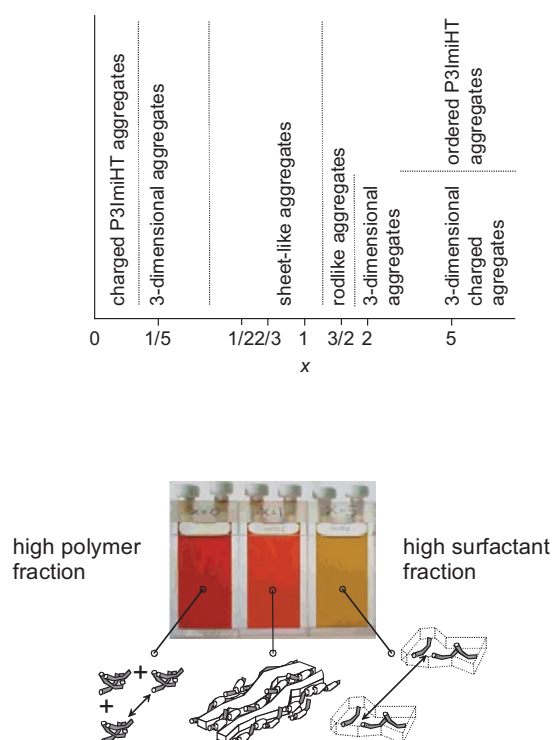


Fig.1. Above: Outlined phase diagram and structures of polymer-SDS particles. Below: Change of visual appearance with the increasing molar ratio *x*.

<b>B N C</b> <b>Experimental Report</b>	<i>Experiment title</i> <b>SANS investigation upon microstructure evolution of sol- gel derived mesoporous hybrid materials, starting from precursors of different functionalities mixtures, in presence of ionic liquids.</b>	<i>Instrument:</i> SANS  <i>Local contact</i> Noémi Székely
	<i>Principal proposer:</i> Zoltán-Imre Dudás <i>Experimental team:</i> Zoltán-Imre Dudás, Noémi Székely	<i>Proposal No.</i> BRR_259 <i>Date(s) of Exper.</i> 2011.04.26-2011.04.30.

### Objectives

The present work aims to investigate the influence of precursor nature and precursor's mol ratio and ILs content upon the nanostructure evolution of some mesoporous samples prepared in the methyltriethoxysilane/tetraethoxysilane (MT series), dimethyldiethoxy-silane/ tetraethoxysilane (DMT series), dimethyldiethoxy-silane /methyltriethoxysilane /tetraethoxy-silane (DMMT series) and tetraethoxy-silane (T) systems. The samples have been prepared by two steps sol-gel method (acid catalysed first step and NaF catalyst for the second step). The precursor's molar ratios were (1:3, 1:2, 1:1, 2:1, 3:1 for MT series); (1:3, 1:2, 2:3 for DMT series) and (1:1:4, 1:1:3 for DMMT series). The prepared hybrid materials are potential candidates as hosts within different materials, like enzymes, drugs and organic or inorganic dyes, could be immobilized.

### Main Achievements

We proposed the analysis of a series of 14 samples but given the lengthy analysis of some samples, we were able to analyze only 10. The experiments did not come across any problems, the results revealed a clear relationship between the precursor type and the structure of the final product. The data analysis revealed usual Porod and Guinier regions for some of the samples, but a part of the samples presented sign concerning a regular structures proved later by electron microscopy measurements. The result obtained from the SANS measurements are in very good concordance with the TEM images. The matrixes obtained from the precursor mixtures TEOS/VTAS 1:1 and TEOS/MTES 1:3 show particles with smooth surfaces, for the all other matrixes the structure the SEM, TEM and SANS measurements confirmed the lamellar structure.

The pore dimensions determined from the nitrogen adsorption, using BET method are consistent with the radii of gyration determined from the SANS measurements for the sample TEOS/MTES 1:1, but for the samples TEOS/DMDDES 3:2 and TEOS/MTES/DMDDES 3:1:1 2 nm difference could be observed, this difference probably due to the closed porosity.

<h1 style="margin: 0;">B N C</h1> <p style="margin: 0;">Experimental Report</p>	<i>Experiment title</i> <b>SANS study of Ormosils prepared by gamma-irradiation and sol-gel</b>	<i>Instrument:</i> SANS
		<i>Local contact</i> L. Almásy
<i>Principal proposer</i> Fernanda Margaca, Isabel Salvado, Joana Lancastre		<i>Proposal No.</i> BRR_283
<i>Experimental team</i> Fernanda Margaca, Joana Lancastre, Carlos Almeida, László Almásy		<i>Date of Experiment</i> June 2012

## Objectives

The preparation and characterization of Ormosils is currently a major field of research. These are a class of materials that enable the integration of organic and inorganic characteristics at the molecular level in a single material. In this way, unique properties make them suitable for a large variety of applications: electronic, optical, biomedical and others. Ormosils are usually prepared by sol-gel. However, polymer cross-linking can be induced by radiation. We prepared Ormosils with the same composition by the two referred methods: gamma irradiation and sol-gel. The final product is expected to have quite different porosity depending on the preparation method. The aim of the proposed experiment is to characterize and compare the porosity at the nm scale of the materials prepared by both methods of synthesis.

## Results

Two groups of hybrid material samples (A and B) were prepared by gamma irradiation from a mixture of precursors in the wt% composition 20PDMS-79TEOS-1PrZr+xCa ( $x = 0, 0.4, 1.2$  and  $3.9$ ). The calcium source used in this study was calcium phosphate with the purpose to improve their bioactivity. Calcium was added in a non-solubilized (group A) form and solubilized in small amounts of acetic acid (group B). The reference sample is the sample prepared with no calcium in the composition.

The microstructural studies of these materials at half irradiation dose (366 kGy) were performed at BNC. Figure 1a and 1b show SANS spectra obtained for the two groups of samples.

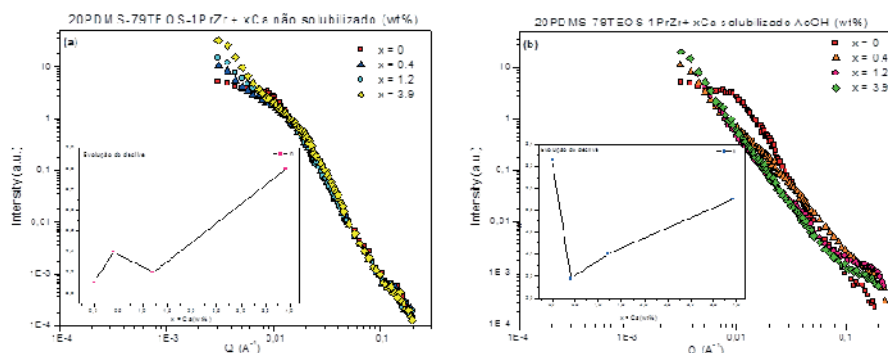


Figure 1. SANS spectra of hybrid materials with composition, in wt%, 20PDMS-79TEOS-1PrZr+xCa ( $x = 0, 0.4, 1.2$  and  $3.9$ ). 1a: Ca non-solubilized; 1b: Ca solubilized in acetic acid (AcOH).

From these results we conclude that the method of adding calcium in the composition of the hybrids (non-solubilized and solubilized) affects the microstructure of the materials: in group A the microstructure of the samples, at the nanoscale, is of the surface fractal type, while in group B it is of the mass fractal type. In addition, as the calcium content increases the nature of the oxide network is different: in group A the surface of the oxide regions become slightly smoother, while in group B the mass fractal density of the oxide network increases.



<h1 style="margin: 0;">B N C</h1> <p style="margin: 0;">Experimental Report</p>	<p><i>Experiment title</i></p> <p><b>Interaction of lipopeptide surfactin with Betaine type surfactants in solution</b></p>	<p><i>Instrument:</i> SANS</p> <p><i>Local contact</i> L. Almásy</p>
	<p><i>Principal proposer</i> Aihua Zou, Vasyl Haramus, Fang Liu</p> <p><i>Experimental team</i> Aihua Zou, Vasyl Haramus, Fang Liu, and László Almásy</p>	<p><i>Proposal No.</i> BRR_314</p> <p><i>Date of Experiment</i> August 2012</p>

## Objectives

Surfactin, which is secreted by various strains of *Bacillus subtilis*, is one of the most powerful biosurfactants so far known. It consists of a peptide loop of seven amino acid residues and a C13-15  $\beta$ -hydroxy hydrophobic fatty acid chain. Due to its amphiphilic structure, surfactin exhibits significant surface and biological activities. It is known that surfactant mixtures, always provide a synergistic enhancement of many aspects of performance and functionalities. In the immediate future, there is a strong and urgent need to understand the fundamental properties of surfactin mixed with conventional surfactants, and that is the focus of our research.

Surface tension measurements indicate an obvious synergistic enhancement of the mixtures of betaine type surfactant with surfactin and this synergistic effect is related with the structure of betaine type surfactant. We intend to obtain the structure of the complexes by SANS.

## Results

To take Surfactin, Surfactin/STDAB and Surfactin/C<sub>12</sub>BE mixtures as examples, the SANS scattering curves and  $P(r)$  functions are shown in Figure 1. Scattering data show that for the two equimolar mixtures, compared with pure Surfactin solutions, the intensity of Surfactin/STDAB is higher, while for Surfactin/C<sub>12</sub>BE, it is reduced. This reveals the interaction strength between Surfactin and two betaines to follow the order of Surfactin/STDAB > Surfactin/C<sub>12</sub>BE.

The distance distribution function  $P(r)$  is nearly symmetric for pure Surfactin in PBS buffer, indicating a nearly spherical shape of the micelle. For mixtures, the  $P(r)$  functions suggest that there are almost homogeneous sphere-like aggregates in Surfactin/STDAB system and ellipsoidal aggregates in Surfactin/C<sub>12</sub>BE system.

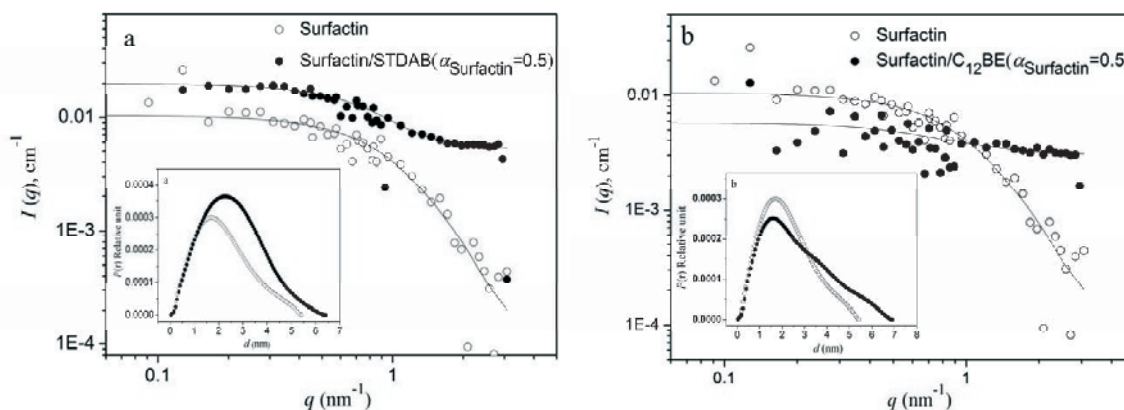


Figure 1. Small-angle neutron scattering data and  $P(r)$  functions for solutions of 0.24mM pure Surfactin, 0.24mM equimolar Surfactin/STDAB and Surfactin/C<sub>12</sub>BE mixtures in buffered D<sub>2</sub>O solutions at 25

## References

Liu, F.; Xiao, J. W.; Haramus, V. M.; Almasy, L.; Willumeit, R.; Mu, B. Z.; Zou, A. H. Interaction of the Biosurfactant, Surfactin with Betaines in Aqueous Solution. *Langmuir* 6, 18 (2013)

<h1 style="margin: 0;">B N C</h1> <p style="margin: 0;">Experimental Report</p>	<i>Experiment title</i> <b>Arrays of iron-nickel nanowires under magnetic field</b>	<i>Instrument:</i> SANS
	<i>Principal proposer:</i> Andrey Chumakov <i>Experimental team:</i> Iliya Roslyakov, Gennady Kopitsa, Laszlo Almasy	<i>Local contact</i> Laszlo Almasy

## Objectives

Investigation of magnetic properties of nanowire arrays is of interest in connection with concept of miniaturization of the electronic elemental base. Application of small-angle diffraction of neutrons allows one to get sometimes unexpected results which are inaccessible for conventional (such as SQUID) techniques. Analyzing magnetic and interference (nuclear-magnetic - NM) contributions to the scattering one can find that the NM contribution increases upon increase of the magnetic field and reaches saturation at  $H=H_s$ . The NM contribution (proportional to average magnetization) does not exhibit any hysteresis. On the contrary, the pure magnetic contribution shows the hysteretic behaviour upon magnetic field reversal and forms the "butterfly"-like field dependence of intensity, which is symmetric with respect to  $H = 0$  (S.V.Grigoriev et al., JETP Letters, **94**, 2011, p.635). Thus the main goal of the proposal was investigation of remagnetization process of the different compounds of  $Fe_{1-x}Ni_x$  nanowires embedded into the pores of anodic alumina membranes. We expected to observe the "butterfly"-like field dependence of magnetic Bragg intensity that should be different for different compounds of  $Fe_{1-x}Ni_x$ .

## Achievements and Main Results

Two samples with different compounds of nanowires  $Fe_{42}Ni_{58}$  (length of nanowires  $L=54 \mu m$ ) and  $Fe_{19}Ni_{81}$  ( $L=40 \mu m$ ) were studied. The SANS from nanowire array was measured upon magnetic field reversal at perpendicular orientation of the magnetic field to the neutron beam (and longitudinal axes of nanowires). We observed an enhancement of a coherence of the magnetization in the neighbouring wires in array upon field reversal at  $H \sim H_s$ . We believe that the observed coherent effects can be a result of the competition between the external field and dipol-dipol interaction, however the exact mechanism is still under discussion.

The chosen geometry of the experiment allows the observation of the diffraction pattern from the ordered structure of the porous matrix, as well as from the superstructure of magnetic nanowires, in the small-angle scattering range. We obtained the magnetic contribution of the scattering, obtained as  $I_H(Q) = I(Q,H) - I(Q,0)$ . The remagnetization in the external field for both measured samples is shown in Fig.1 within the field range from  $H = 0$  to  $H_{max} > H_s$ , where  $H_s \approx 100$  mT is the saturation field (from SQUID data). Here for the first time was shown graphically the attainment of saturation  $I_H$  at the external fields  $H > H_s$ . The intensity of the magnetic contribution to the neutron scattering has no hysteresis (Fig. 1) for both permalloy compounds. This differs from the similar behaviour for the arrays of Ni-nanowires and is rather like for arrays of Co-nanowires. We expect that the obtained data will give a key for understanding the nature of the "butterfly"-like field dependence of intensity under study.

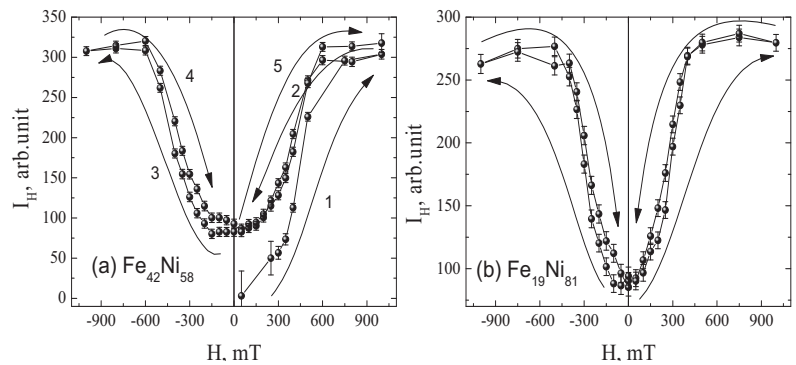


Fig. 1. Field dependence of the intensities of the magnetic coherent contribution  $I_H(Q_{10})$  of the samples (a)  $Fe_{42}Ni_{58}$  and (b)  $Fe_{19}Ni_{81}$ .

<h1 style="margin: 0;">B N C</h1> <p style="margin: 0;">Experimental Report</p>	<p><i>Experiment title</i></p> <p><b>Small-Angle Neutron Scattering of Phenylene-modified Bolaamphiphiles</b></p>	<p><i>Instrument:</i></p> <p>SANS</p>
	<p><i>Local contact</i></p> <p>L. Almásy</p>	<p><i>Proposal No.</i></p> <p>BRR_332</p> <p><i>Date of Experiment</i></p> <p>November 2012</p>
<p><i>Principal proposer</i></p> <p>Simon Drescher, Institute of Pharmacy, Martin-Luther-Universitaet Halle-Wittenberg, Germany</p> <p><i>Experimental team</i></p> <p>Simon Drescher and László Almásy</p>		

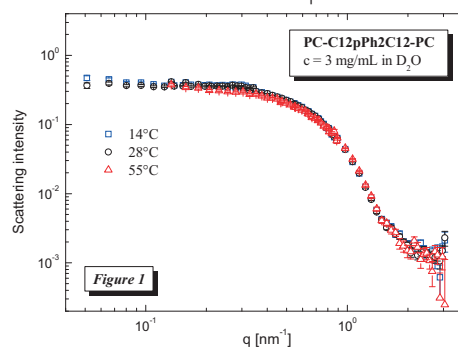
## Objectives

Single-chain bolaamphiphiles (BAs), which are composed of a long alkyl chain of 22 to 32 carbon atoms and two polar phosphocholine headgroups attached at both ends, usually form a dense network of nanofibres in aqueous suspension – already at concentrations of 1 mg/mL. These nanofibres are built up by single BA molecules that are arranged side by side but twisted relative to each other due to the bulky headgroup. Since the self-assembly into nanofibres is exclusively driven by hydrophobic interactions between the alkyl chains, we were interested in the consequences of perturbations within the alkyl chain with regard to self-assembly and aggregate formation. Therefore, we synthesized three new BAs containing a phenylene, a biphenylene, and two methyl branches, respectively, within the alkyl chain – and we investigate aqueous suspensions of these novel BAs by means of SANS at different temperatures in order to provide information about aggregate structure.

## Results

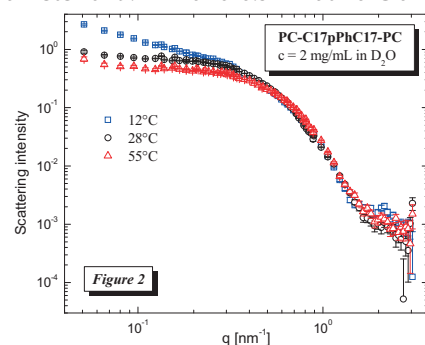
Unmodified BAs built up a fibrous network if suspended in water. During heating these nanofibres reversibly transform into small aggregates such as spherical micelles. This transformation occurs at a distinct temperature (investigated with DSC) that is sensitive to perturbations within the alkyl chain as well as headgroup structure. Hence, it is comprehensible that the insertion of a phenylene, a biphenylene, and two methyl branches, respectively, led to a drastic decrease of the fibre-micelle-transformation temperature.

Aqueous suspensions of both BAs (with a biphenylene moiety, *PC-C12pPh2C12-PC*, and with two methyl groups, respectively, within the alkyl chain) showed no DSC transition between 2 and 95°C. SANS measurements (Fig. 1) showed the formation of spherical micelles at 28°C, with a diameter of 6.9nm and an aggregation number ( $N_{agg}$ ) of 55 bola molecules per micelle for the biphenylene-BA, and a diameter of 6.8nm and  $N_{agg} = 39$  molecules for the methyl-branched BA. A temperature increase led only to small changes in the size of the micelles, e.g., for the biphenylene-BA we found at 55°C a diameter of 6.5nm and  $N_{agg} = 47$ .



Another situation is found for the phenylene-modified BA (*PC-C17pPhC17-PC*): An aqueous suspension of this BA showed a distinct endothermic transition in the DSC at 22.8°C that is probably linked with a fibre-micelle-transformation. Above this transition we observed micelles with a diameter of 9.7nm and 8.5nm at 28°C and 55°C, respectively (Fig. 2).  $N_{agg}$  ranged from 79 (28°C) to 56 (55°C).

Both values are comparable with measurements of unmodified BAs. Below the transition we observed the formation of nanofibres with a diameter of 5.7nm, which roughly corresponds to the length of the phenylene-modified BA, and a  $N_{agg}$  of 6 molecules per 1nm of the nanofibre. The last value ( $N_{agg}$ ) is slightly smaller compared to unmodified BAs reflecting the disordered self-assembly due to the insertion of a phenyl ring within the alkyl chain. It is noteworthy that for the re-formation of the fibres the samples has to be stored for 12h at 4°C indicating a kinetically hindered process.



<h1 style="margin: 0;">B N C</h1> <p style="margin: 0;"><b>Experimental Report</b></p>	<i>Experiment title</i> <b>Small-angle neutron scattering investigation of polyurethane aged in dry and wet air</b>	<i>Proposal No.</i> BRR_ <i>Local contact</i> L. Almásy
	<i>Principal proposer</i> Bo Chen, Guangai Sun, and Qiang Tian, Institute of Nuclear Physics and Chemistry, Mianyang, China <i>Experimental team</i> Qiang Tian, Guanyun Yan, and László Almásy	<i>Date of Experiment</i> June 2012 <i>Date of Report</i> Sept 2013

## Objectives

Polyurethanes are usually intended for long-term use. It is essential to know how the material changes with time at various environmental conditions. Our motivation is to reveal the influence of aging on the microstructures of Estane 5703 by SANS.

## Results

Microstructures of Estane swollen after aging at 70°C in dry air and at 100% relative humidity have been studied by SANS technique. The contrast between the hard and soft domains had been enhanced by swelling with deuterated toluene. The scattering shows the domain structure of the materials characteristic of polyurethanes consisting of soft and hard segments (SSs and HSs). Domains consisting of HSs are modeled by Debye-Anderson-Brumberger shape factor, and their spatial distribution is described by the Percus-Yevick structure factor. The fitted results are shown in Figure 1. The domain sizes, described by the correlation length ( $a_{cor}$ ), which increases from 2.3 nm to 2.5 nm and the interdomain distance increases from 8.4 nm to 8.8 nm for the sample aged at 70°C for 2 months in dry air, while  $a_{cor}$  increases from 2.3 nm to 3.8 nm and their distance increases from 8.4 nm to 10.6 nm for the sample aged at 70°C for 1 month in wet air. The hydrolysis at 70°C is suggested to be the main reason for these changes. This study contributes to understanding the structure-property correlations of polyurethanes in different environments.

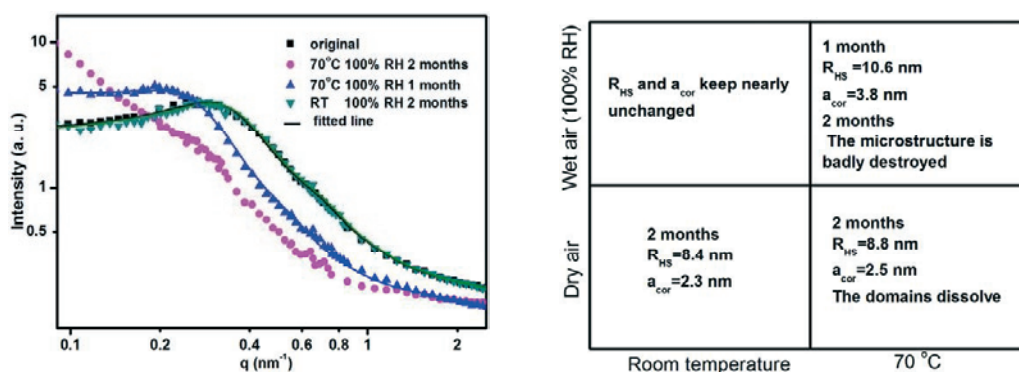


Figure 1 (left) SANS data of Estane aged at 70°C in wet air for 1 and 2 months, as well as at RT in wet air for 2 months  
 Figure 2 (right) Microstructural changes of Estane 5703 at various aging conditions

## References

Q. Tian et al. "Small-angle neutron scattering investigation of polyurethane aged in dry and wet air" *paper submitted to Polymer Express Letters*

<b>B N C</b> <b>Experimental Report</b>	<i>Experiment title</i> <b>Comparing the thylakoid membrane system in intact leaves and isolated membranes from them</b>	<i>Instrument</i> SANS
	<i>Principal proposer</i> Renáta Ünnepep <i>Experimental team</i> Tünde Tóth, László Kovács, Győző Garab, Gergely Nagy	<i>Local contact</i> R. Ünnepep

## Objectives

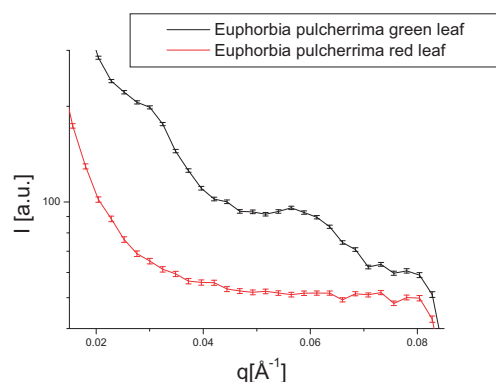
In order to obtain information on the ultrastructure and structural flexibility of the thylakoid membranes in intact leaves non-invasive techniques are of great importance. To this end, we carried out SANS measurements on intact leaves under physiologically relevant conditions.

Our aim was to compare the scattering profiles of several kind of leaves of plants (*Hedera helix*, corn (*Zea mays*), spinach (*Spinacia oleracea*), *Arabidopsis thaliana*, *Euphorbia pulcherrima*) with each other and some of their isolated thylakoid membranes.

## Results

We have performed several SANS experiments on thylakoid membranes isolated from spinach and pea. We found that the thylakoid membrane system of granal chloroplasts displays two characteristic peaks. The first peak has been proposed to originate from the stroma membrane and we suppose that the second peak relate the form factor of the paired membrane. We found a characteristic peak around  $0.027 \text{ \AA}^{-1}$  in the scattering profile of leaves in a previous measurement at ILL during a pilot experiment.

All of measured leaves have got a peak around  $0.027 \text{ \AA}^{-1}$  which suggest a membrane periodicity of around  $230 \text{ \AA}$  and isolated thylakoid membranes have got a peak around  $0.02 \text{ \AA}^{-1}$  ( $310 \text{ \AA}$ ). Our experiments performed on a plant with variegation (*Schefflera arboricola*) showed that the peaks are missing in non-green parts of the leaves, which lose the ability to produce chloroplasts. *Euphorbia pulcherrima* (poinsettia) have got green leaves and red leaves on the top. The peaks are also missing in these red leaves Fig 1. The neutron flux at the BNC and the sensitivity of Yellow Submarine do not allow the monitoring of light induced changes in leaves, which can be observed at the ILL. These data clearly show that the observed peak is related to the thylakoid membrane system. Optimization of the measurements on leaves was achieved by infiltration with D<sub>2</sub>O.



1. Fig Scattering profiles of *Euphorbia pulcherrima*

<b>B N C</b> <b>Experimental Report</b>	<i>Experiment title</i> <b>SANS studies of temperature-induced phase separation of PVCL in aqueous media.</b>	<i>Instrument:</i> SANS  <i>Local contact</i> Renáta Ünnepe
	<i>Principal proposer:</i> Alexander Jigounov <i>Experimental team:</i> Alexander Jigounov	<i>Proposal No.</i> BRR-248 <i>Date(s) of Exper.</i> 13-23.09.2011

### Objectives

Poly(N-vinylcaprolactam) (PVCL) is one of the amphiphilic water-soluble polymers which show a thermoresponsive behavior. It exhibits a lower critical solution temperature (LCST) close to physiological values (303-311 K, depending on the molecular weight). Temperature-induced phase separation of aqueous solution of PVCL samples of varying concentrations were proposed to be investigated by SANS. Stable particles are formed above the phase transition temperature (lower critical solution temperature). With polymer concentrations > 1 wt% macroscopically visible milk-white turbidity of the solution is observed. Small-angle neutron scattering (SANS) measurements should provide important information on the size and shape of PVCL mesoglobules, polymer concentration in mesoglobules, and etc.

### Results

Samples PVCL in D2O of different concentrations were measured at two sample-detector distances (1.3m and 5.6m) with velocity selector 6000 RPM (wavelength 3.9 Å). Six temperature points, 10 °C, 20 °C, 30 °C, 35 °C, 40 °C, 60 °C, which corresponds to the states before and after LCST, were measured. For each given concentration the slope of the scattering curve is changed, indicating the coil-globule transition. Unfortunately, due to the relatively large temperature step, it is impossible to determine the temperature shift in LCST for different concentrations. In the middle-q range the slope of the scattering curve is rising up to -1.6. According to power-law it corresponds to the transition from stiff rods to swollen Gaussian-coil in a good solvent. The Giration radius also increases. For example, for the sample with concentration of 5 wt.% Giration radius increases from 3.89 nm at 10 °C up to 4.74 nm at 35 °C. With higher temperatures more compact particles are formed. Unfortunately, after the coil-globule transition part of the dissolved sample segregates and concentration in a measured window decreases. This leads to a dramatic intensity decrease. The periodic peaks on the scattering curve after 40C can suggest that spherical particles are formed. But it is not possible to make a good fit over the whole q-range and estimate form factor parameters. Several concentrations were measured to estimate scattering contrast. These calculations are sensitive to the intensity values in small q-range, which are not very good resolved.

<b>B N C</b> <b>Experimental Report</b>	<i>Experiment title</i> <b>SANS structural studies of the stability of PMAA-PEO nanoparticles in ionic solution</b>	<i>Instrument:</i> SANS  <i>Local contact</i> Renáta Ünnepe
	<i>Principal proposer:</i> Borislav Angelov <i>Experimental team:</i> Borislav Angelov	<i>Proposal No.</i> BRR-247 <i>Date(s) of Exper.</i> 13-23.09.2011

### Objectives

The main objective of the project was a small angle neutron scattering (SANS) investigation of the structure and stability of self-assembled polymer/surfactant complexes. These complexes are formed by hydrophilic block copolymers poly(methacrylic acid) and poly(ethylene oxide) (PMAA-PEO) in solution with a charged ionic surfactant based on sodium dodecyl sulphate. Different concentration ratios between the polymer and the surfactant were measured which revealed the steps toward the formation of the investigated complexes. In a broader framework, these polymers are important in drug delivery, because they have an ability to form nanoparticles with a controllable size and relatively low polydispersity compared to other polymer systems.

### Results

The SANS measurements were performed at the SANS diffractometer Yellow Submarine. The wave vector covered a  $q$ -range from  $0.015 \text{ \AA}^{-1}$  to  $0.4 \text{ \AA}^{-1}$ . The utilized neutron beam had a wavelength  $4.12 \text{ \AA}$  at 6000 rpm of the velocity selector. The detector was 2D gas filled with an area divided  $64 \times 64$  pixels. The samples were liquid solutions in deuterated water ( $D_2O$ ) with  $0.05M$   $Na_2B_4O_7$  buffer. Quartz cuvettes (2cm wide and 2mm thick) were used as a sample container. All measurements were at room temperature. The concentration ratios between the polymer PMAA-PEO and the surfactant were 0, 10, 20, 30 and 40 %. Pure surfactant, and calibration samples from cadmium were also measured. After the conventional procedures for data acquisition, radial integration and background subtraction, the obtained 1d scattering curves from SANS were compared with the corresponding small angle X-ray scattering curves. The SANS measurements were very useful for structural model building and validation. The pure polymer could be fitted with a polydisperse Gaussian coil, while the gradual addition of the surfactant caused the appearance of micellar-like aggregates on the polymer backbone and formation of complexes.

It was our first experiment at Budapest Neutron Reactor and it passed without notable difficulties. The polymer did not scatter too much, and the exposure time was increased to 6 hours per sample. This improved the signal to noise ratio. In a future experiment, a longer time could be desirable in order to measure more samples.

<b>B N C</b> <b>Experimental Report</b>	<i>Experiment title</i> <b>Thylakoid membranes of algae and higher plants</b>	<i>Instrument:</i> SANS  <i>Local contact</i> Renáta Ünnep
	<i>Principal proposer:</i> Dorthe Posselt <i>Experimental team:</i> Prof. Győző Garab, Ottó Zsiros, Petar Lambrev	<i>Proposal No.</i> BRR_313 <i>Date(s) of Exper.</i> 17.09.2012- 21.09.2012

## Objectives

Photosynthetic organisms have evolved multilamellar membrane systems, the thylakoid membranes, closed flattened membrane vesicles. In plants, the thylakoid membranes are differentiated into granum and stroma regions, also called stacked or appressed and unstacked or non-appressed regions. The minimum repeat distances (RD) of membrane system are different in stroma membranes (~270 Å) and the granum (~160 Å) according to literature electron microscopy (EM) data. Our earlier SANS experiments on leaves and thylakoid membranes isolated from the same leaves revealed that the most commonly used isolation methods (using sorbitol as osmoticum) does not retain the native structure of thylakoids. In order to conform this, we have carried out additional measurements on leaves and isolated thylakoids at the Yellow Submarine.

## Results

At the PSI (Villigen, Switzerland) we compared the repeat distances (RD) of thylakoid membranes in leaves and in suspensions of isolated thylakoid membranes, obtained from the same leaves. It was found that upon isolation of the membranes and suspending in media containing sorbitol as osmoticum led to the swelling of membranes, as shown by a substantial increase of the RD values compared to those obtained in leaves. This increase was observed not only under isotonic conditions (0.4 M sorbitol) in the presence of 10 mM MgCl<sub>2</sub> (RD values between 280 and 300 Å) but also under hypertonic conditions (up to 2 M sorbitol) which somewhat reduced the RD (~260 Å) compared to the isotonic conditions. In contrast, in the presence of NaCl under isotonic and hypertonic conditions the thylakoid membranes appeared to retain their in vivo states and exhibited RD values (~220-230 Å) very similar to those in leaves (~210-220 Å). Our electron microscopy measurements basically confirmed these observations, but with EM, on essentially the same materials, we found somewhat smaller RD values (~190-200 Å). Results at Yellow submarine

This discrepancy between the EM and SANS data might be explained by the fixation procedure, in particular, by the effect of glutaraldehyde - the peak which originates from the periodicity of granum thylakoid moved from  $q=0.024$  (260Å) Å<sup>-1</sup> to  $0.027$  (230Å) Å<sup>-1</sup>. Nevertheless, a bias of SANS toward larger RD values, i.e. toward thylakoid membranes containing wider aqueous phases, cannot be ruled out. With biological samples repetitions are needed, so during this Yellow Submarine SANS measurement we repeated these isolation methods and confirmed our findings on different plant materials. Photosynthesis is functional in unripe avocado fruits, which contains, in a thin layer under the skin, mature granal thylakoid membranes. When measuring this outmost green layer of the fruit, very wide and small peak was received around  $0.027$  Å<sup>-1</sup>.

## References (Published or accepted papers, research reports, conference lectures, seminars etc.)

R Ünnep, O Zsiros, K Solymosi, L Kovács, P Lambrev, T Tóth, L Rosta, G Nagy and G Garab. The ultrastructure and flexibility of thylakoid membranes in intact leaves and isolated chloroplasts as revealed by small angle neutron scattering, ICNS, 2013 (poster)



<h1 style="font-size: 2em; margin: 0;">B N C</h1> <p style="margin: 0;">Experimental Report</p>	<i>Experiment title</i> <b>SANS investigation of the structure and flexibility of the multilamellar organization of the thylakoid membranes of higher plants and in intact cells of the diatom <i>Phaeodactylum tricornutum</i></b>	<i>Instrument</i> SANS
	<i>Principal proposer</i> Renáta Ünnepe <i>Experimental team</i> M. Szabó, Gy. Káli, Gy. Garab, P. Lambrev, Y. Miloslavina, G. Nagy	<i>Local contact</i> R. Ünnepe, Gy. Káli

## Objectives

The major goal was to identify the origin of SANS signal originating from diatom cells. To this end, we measured the algal cells suspended in buffers with different osmolarities and at different temperatures. We also planned to study isolated granal membranes and PSII-enriched particles (BBY) to identify the  $\sim 0.07 \text{ \AA}^{-1}$  SANS signal tentatively assigned to originate from membrane pairs.

## Results

In diatoms the membrane system is organized into groups of three loosely stacked thylakoid membranes. The Bragg peak originates from repeat distance of this membrane system; an additional peak is found at around  $0.07 \text{ \AA}^{-1}$ . Treatment with increasing concentrations of sorbitol caused significant changes in the shape and position of both characteristic peaks, suggesting a decrease of RD of the thylakoid membranes and a shrinkage of the stacked adjacent membrane pairs in a sorbitol concentration-dependent manner. The characteristic peak at  $Q \sim 0.037 \text{ \AA}^{-1}$  gradually diminished in the presence of increasing concentrations of sorbitol, which indicates loss of periodicity of the thylakoid membranes. When the same cells were resuspended in sorbitol-free ASP2 medium again, the peak position and intensity of the two characteristic peaks recovered almost fully, indicating that the original state of the thylakoids could be restored (Fig. 1).

Heat treatment also affected the lamellar order of the thylakoid membranes, as reflected by the substantial diminishment of the Bragg peak between  $0.03$  and  $0.04 \text{ \AA}^{-1}$ . Since this band is assigned to originate from the long-range lamellar order of the thylakoids it can be concluded that the membrane system is disorganized following the heat treatment at  $40 \text{ }^\circ\text{C}$ . At the same time, the second peak, between  $0.07 \text{ \AA}^{-1}$  and  $0.08 \text{ \AA}^{-1}$ , is largely retained. Its shift to larger  $Q$  values nevertheless indicates that the reorganizations also affect the membrane pairs. CD and SANS results were found to be correlated with each other (Fig. 2). Our data are consistent with the tentative assignment of the SANS signal of diatoms at  $q \sim 0.07 \text{ \AA}^{-1}$  however its identification requires further experiments.

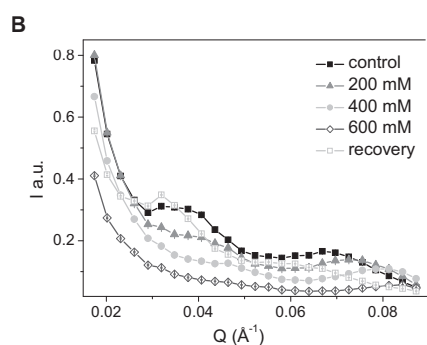


Fig 1. Sorbitol effect on diatom.

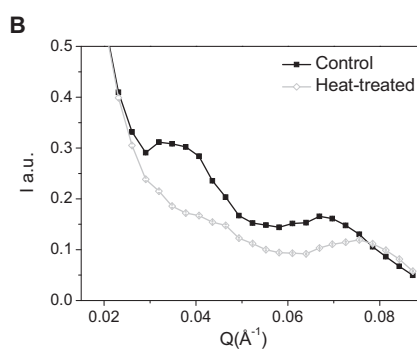


Fig 2. Temperature effect on diatom.

## Future prospects

We would like to find the origin of the signal at  $q \sim 0.07 \text{ \AA}^{-1}$  with the aid of several kinds of species and their mutants.

## References

1. Nagy, G et al. Photosynth. Res. 111(1-2):71-79

<b>B N C</b> <b>Experimental Report</b>	<i>Experiment title</i> <b>Test SANS measurements of isolated thylakoid membranes, algae and cyanobacteria</b>	<i>Instrument</i> SANS <i>Local contact</i> R. Ünnepe Gy. Káli
	<i>Principal proposer</i> Renáta Ünnepe <i>Experimental team</i> L. Kovács, M. Szabó, Gy. Káli, Gy. Garab, G. Nagy	<i>Experiment Number</i>  <i>Date</i> 27-30.10.2010

We have carried out test experiments on photosynthetic living organisms in vivo for further SANS investigations.

Detector-sample distance: 5.6 m

Selector speed: 6000 rpm

Temperature: 20 °C

Magnetic field: 0.7 T

1. *Phaeodactylum tricornutum* is a type of diatom. They were measured in ASP2 heavy water medium, high concentration of sorbitol (600 mM), and finally in ASP2 heavy water medium again to study the reversible process. They were grown under low light and high light conditions.

2. *Synechocystis* cyanobacterial cells were grown in 50 %, 75 %, 95 % D<sub>2</sub>O and they were measured in 100% D<sub>2</sub>O for contrast variation method.

3. One of our aims was to study the changes of state transitions in *Chlamydomonas reinhardtii*; hence, they were measured under

- dark adaption
- illuminated with blue light
- illuminated with far red light

to induce state transition.

4. Thylakoid membranes and subchloroplast fractions were isolated with different isolation techniques (digitonin, sonication) and were measured in different q-ranges (at 6000, 4000, 3000 rpm).

<h1 style="margin: 0;">B N C</h1> <p style="margin: 0;">Experimental Report</p>	<i>Experiment title</i> <b>Understanding the structure of epoxy-silicate and epoxy-titanate hybrids</b>	<i>Instrument:</i> SANS
	<i>Local contact</i> László Almásy	<i>Proposal No.</i> BRR 288 <i>Date(s) of Exper.</i> 30.11-04.11.2011
<i>Principal proposer:</i> Gennady Kopitsa <sup>1</sup> <i>Experimental team:</i> Tamara Khamova <sup>1</sup> , László Almásy <sup>2</sup> <sup>1</sup> PNPI Gatchina, Russia, <sup>2</sup> RISP Budapest, Hungary		

## Objectives

Search of effective measures for counteraction to microbial destruction (fungi, lichens, algae and bacteria) of the stone monuments of the cultural heritage is one of the important scientific and practical tasks in the modern world. Chemical biocides (compounds of quaternary ammonium, organotin, organosilicon etc.) are used against the bio-destruction processes most often. Application of toxic chemical biocides may be dangerous for the applicator, environment and the stone material. In the last years “soft” biocides (photocatalysts, nanodiamonds, etc.) were used actively for protection of building materials against bio-damages. The advantage of soft biocides is that they are ecological, their inhibiting effect on microbial community can be long-term and they can be applied in small concentrations. Preliminary data indicate that the nanodiamond changes the fractal structure of sol-gel-derived materials. Under influence of ND the type of fractal aggregation and the aggregate size essentially varied at nanoscale. Thus the main goal of the proposal was to obtain information on the structure of a series of epoxy-silicate and epoxy-titanate bulk samples, on their fractal characteristics, aggregate structure, etc.

## Achievements and Main Results

Fig.1. shows the experimental curves of the differential cross section  $I(q)$  for the epoxy-silicate hybrids prepared with different concentrations of the epoxy and tetra-ethoxy-silane (TEOS) components. According to this figure, the observed scattering decreases with the increasing of the concentration of TEOS component. Moreover, all data sets display three regimes where the behaviors of the SANS cross section  $I(q)$  are significantly different. In particular, in the intermediate range  $q$  the scattering cross section for all the samples satisfies the power law  $q^{-n}$ . The exponent  $n$  values found from the slope of the straight-line parts of the curves plotted in log-log scale lie in the range from 1.35 to 1.93, pointing to volume fractal structure. Deviations from the power law are observed for all the samples both at lower and high  $q$  values. For large  $q$  values the scattering fades into the incoherent background.

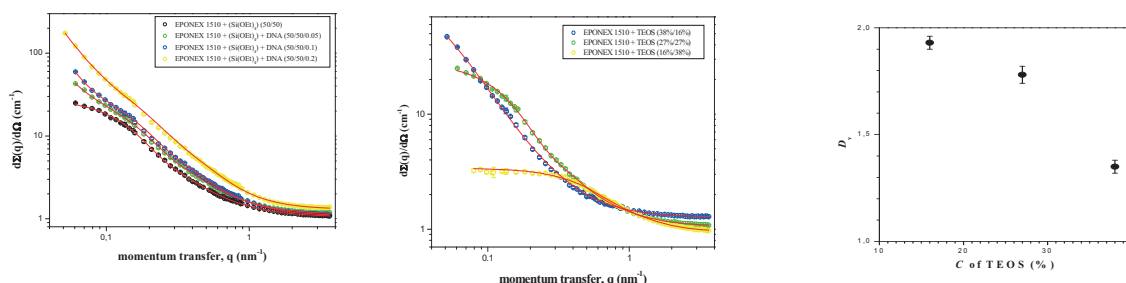


**Fig. 1** SANS cross section  $I(q)$  for the epoxy-silicate hybrids prepared with different concentrations of the epoxy and TEOS components (left), and epoxy-silicate hybrids doped by nano-diamonds (middle). Volume fractal dimension  $D_v$  of the epoxy-silicate hybrids versus the concentration of the TEOS components.

<h1 style="margin: 0;">B N C</h1> <p style="margin: 0;"><b>Experimental Report</b></p>	<i>Experiment title</i> <b>Structure of the primary component of large sintered artificial opals</b>	<i>Instrument:</i> SANS
	<i>Local contact</i> László Almásy	<i>Proposal No.:</i> 
<i>Principal proposer:</i> Grigoryeva Natalia <sup>1</sup> <i>Experimental team:</i> Voronina Ksenia <sup>1</sup> , Gubanova Nadezda <sup>1</sup> , Gennady Kopitsa <sup>1</sup> , László Almásy <sup>2</sup> <sup>1</sup> PNPI Gatchina, Russia, <sup>2</sup> RISP Budapest, Hungary		<i>Date(s) of Exper.</i> 27.06-01.07.2012

## Objectives

Nowadays spherical particles of silicon dioxide are actively used in different areas such as information and communication technologies. Submicron and nanometer spherical particles of amorphous SiO<sub>2</sub> are obtained by sol-gel method with hydrolysis tetraethoxysilane reaction in aqueous-alcoholic medium in the presence ammonium hydroxide, called multistage Stober-Fink-Bohn method. These particles possess complicated inner structure of fractal type. It was suggested that the large-scale spherical particles of silica (with diameter about 1 μm) have tertiary formations and consist of smaller spherical particles (secondary formations). Secondary formations, in its turn, consist of even smallest primary spherical particles with diameter of about 5-10 nm. These suggestions were made on the base of analysis of the dependence of opal matrix apparent density on the size of the constituent SiO<sub>2</sub> particles.

This experiment aims the structural characterization of new material made on the base of porous silicon oxide spheres synthesized by modified Stöber method. The goal of the experiment is to perform a systematic study of structural parameters of the spheres and the influence of porosity (size of pores, structure and its periodicity as well as presence of guest material inside the pores) on the structural properties of photonic medium.

## Achievements and Main Results

Silica particles were prepared using the modified Stöber method by the tetraethyl-ortho-silicate (TEOS) hydrolysis reaction in aqueous-alcoholic solution in the presence of ammonium hydroxide (50% vol. ethanol, 1.0 M ammonium). The scattering curves in double logarithmic scale on the Figure 1. For regions  $Q < 0.2 \text{ nm}^{-1}$  and  $Q > 1 \text{ nm}^{-1}$  behavior of scattering curve obeys a power law  $Q^{-n}$ . The characteristic feature at intermediate range  $0.2 < Q < 1 \text{ nm}^{-1}$  is the presence of a broad peak of scattering intensity. Additionally, one can distinguish a smeared maximum near  $Q \sim 0.41 \text{ nm}^{-1}$ . Moreover, there is a deviation from power law at  $Q < 0.09 \text{ nm}^{-1}$  which can be related to multiple scattering.

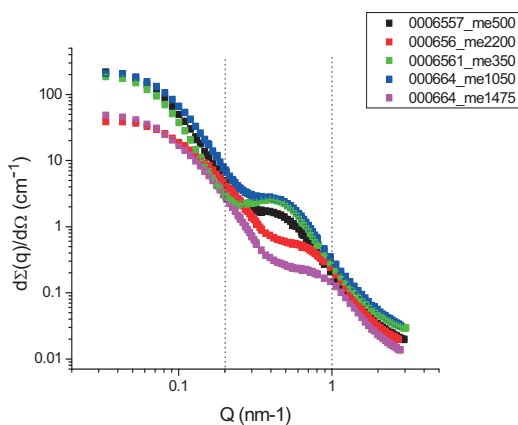


**Fig.1.** The SANS cross section  $d\Sigma(q)/d\Omega$  for the samples of silica particles with different diameters (■ - 350, ■ - 500, ■ - 1050, ■ - 1475, ■ - 2200 nm)

**Conclusion.** On the basis of SANS data the following features of the internal structure of SiO<sub>2</sub> microspheres were established:

- 1) Silica particles with sphere diameters of 500 – 1800 nm consist of primary particles near 7 – 10 nm in size.
- 2) Spatial arrangement of primary particles has a short-range order.
- 3) Degree of fractality is from 2.1 to 2.9 for primary particles.

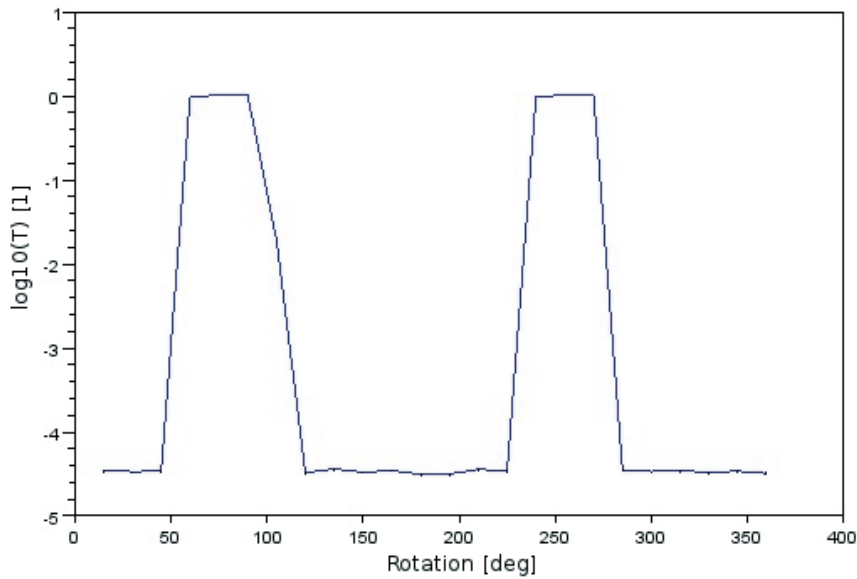
These SANS results agree with the hierarchical model of internal structure of SiO<sub>2</sub> particles.

<b>B N C</b> <b>Experimental Report</b>	<i>Experiment title</i> <b>Transmission measurement of chopper disks</b>	<i>Instrument.</i> TAST
	<i>Principal proposer:</i> Alex Szakál <i>Experimental team:</i> Marton Markó, Alex Szakál	<i>Local contact</i> Alex Szakál
		<i>Experiment Number</i> TAST_12_01CW <i>Date</i> 29. Feb 2012 – 6 March 2012

### Objectives

Chopper disks are key elements in the modern Time-of-flight neutron devices. One of the most important property of these disks is the neutron transmission. The transmission measurement requires a well monochromatized beam with low second order contamination and good signal to noise ratio because of the low transmission of the disks. To suppress the second order we used a germanium sample which reflects only the first order radiation, and used some additional shielding to lower the instrumental background. We placed the disk between the germanium sample and the detector and measured the detected intensity with the chopper at points shifted by 15 degrees.

### Results



Transmission one of the chopper disks in the function of rotation angle.

<b>B N C</b> <b>Experimental Report</b>	<i>Experiment title</i> <b>Measurement of the mosaicity and reflectivity of HOPG samples</b>	<i>Instrument.</i> TAST <i>Local contact</i> Alex Szakál
	<i>Principal proposer:</i> Alex Szakál <i>Experimental team:</i> Alex Szakál	<i>Experiment Number</i> TAST_12_02CW <i>Date</i> 30. Aug 2012 – 04 Sept. 2012

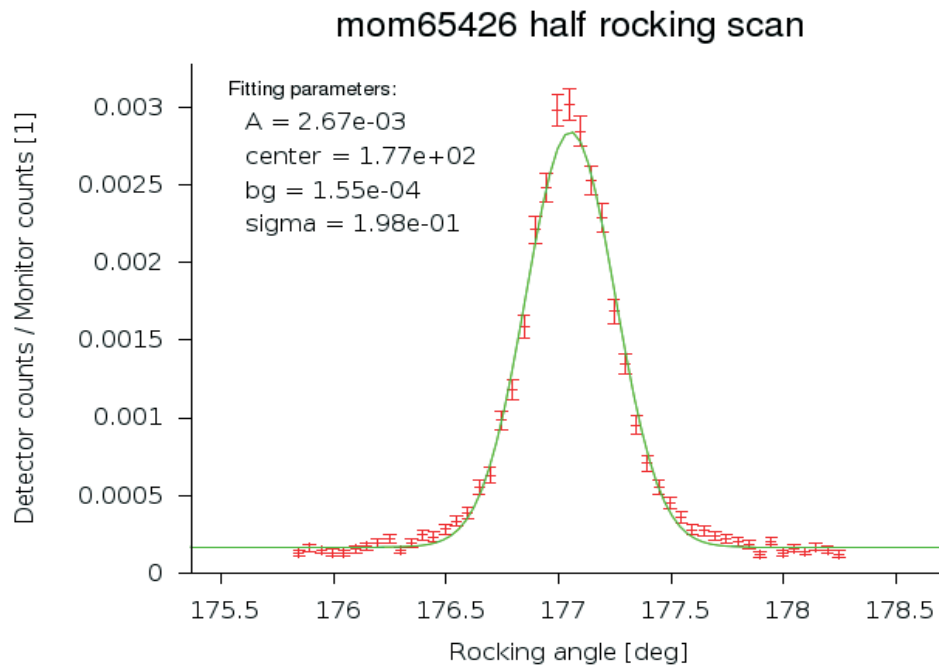
### Objectives

Highly oriented pyrographite is the most widely used neutron monochromator crystal. The production of these crystal is difficult and the quality of the samples are fluctuating. In order to maximize the performance of a monochromator each crystal should be measured independently and the position on the monochromator should be chosen on the basis of the measurement results.

The mosaic of the crystals are typically in the range between 0.3-0.5 degrees. Better collimation and monochromatization is needed for this experiment than what is available with the copper monochromator. We used a Si wafer on the place of the sample to produce a monochromatic and less divergent beam. We put the sample into the analyzer drum and use a slit between the sample and the Si wafer. The slit is set in such a way that the beam is smaller than the sample so there are no neutrons which go around the sample. We measured the rocking curve and the peak intensity of the samples.

### Results

We measured and reported the mosaicity and reflectivity of 20 HOPG slabs from different producers. There were significant differences in mosaicity and reflectivity depending on the manufacturer of the sample.

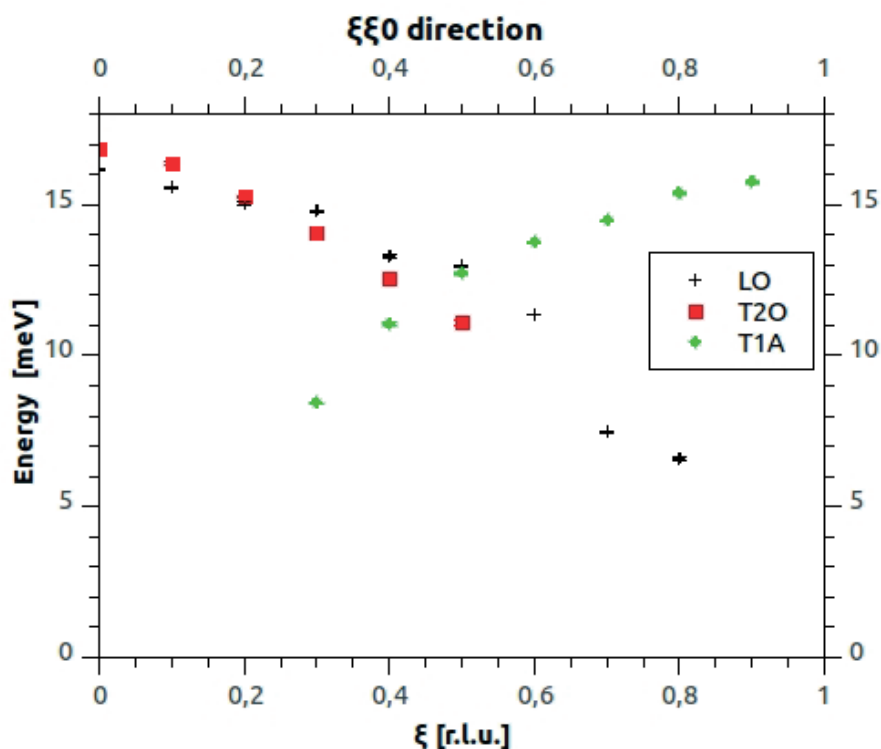


<h1 style="margin: 0;">B N C</h1> <p style="margin: 0;"><b>Experimental Report</b></p>	<i>Experiment title</i> <b>Investigation of the phonon spectra in beta-Sn</b>	<i>Instrument</i> TAST
	<i>Principal proposer:</i> Alexander Ivanov <i>Experimental team:</i> Alexander Ivanov, Alex Szakál	<i>Local contact</i> Alex Szakál

### Objectives

Phonon spectra of beta-Sn has been already measured by several authors but there are still not measured branches in it. We want to compare the effect of the first order phase transition (beta  $\rightarrow$  gamma) on the phonon branches. In order to do that, first we wanted to get information about the unknown branches. We measured two optic and one acoustic branch at high energy transfers.

### Results



Dispersion curves after fitting the const-Q scans.

<b>B N C</b> <b>Experimental Report</b>	<i>Experiment title</i> <b>Investigation of periodic Ni/Ti multilayers</b>	<i>Instrument.</i> REF; GINA
	<i>Principal proposer:</i> T. Veres <i>Experimental team:</i> T. Veres	<i>Local contact</i> T. Veres; B. Nagy
		<i>Experiment Number</i> Ref 1.
		<i>Date</i>

### Objectives

Periodic multilayers of various periods and layer thicknesses were prepared as quarter wave mirrors. The properties of such Ni/Ti multilayers are crucial in neutron supermirrors. Note, these sputtered Ni layers contain Mo too, to get nonmagnetic mirrors[1]. The reflectivity properties of these systems were investigated using neutron and x-ray reflectometry. The obtained experimental results were compared with calculations. The deviation from the proposed structure and imperfectness created during sputtering process was investigated.

### Results

Samples containing 2, 4 and 8 bilayers with Ni/Ti layer thickness 66Å/59 Å, 84Å/70 Å, 115Å/87 Å were prepared at Mirrotron Ltd., using dc magnetron sputtering. The neutron reflectivity measurements were performed at constant wavelength neutron reflectometers, REF and GINA, the x-ray measurement at the instrument of Institute for Technical Physics and Materials Science. The two complementary methods revealed the same structure, and confirm each other.

In the fitting process we assumed the periodicity of the samples. The thickness of Ni and Ti layers, the real part of scattering length density, and Ni/Ti and Ti/Ni roughness were the fitting parameters. In the case of 84 Å Ni and 70 Å Ti nominal layer thicknesses, a remarkable increase in Ni and decrease in Ti thickness was observed. For the other two nominal thicknesses the deviance of thickness values was not so large. The fitted neutron scattering length density corresponds to the calculated. In some samples, the fitted x-ray scattering length density deviates from the calculated ones. The fitted roughness values on the top of Ni layers were larger than that on the top of Ti layers, in the case of every sample. It can be caused the different inter-diffusion and/or the interpenetration of crystallites of the two metals in each other.

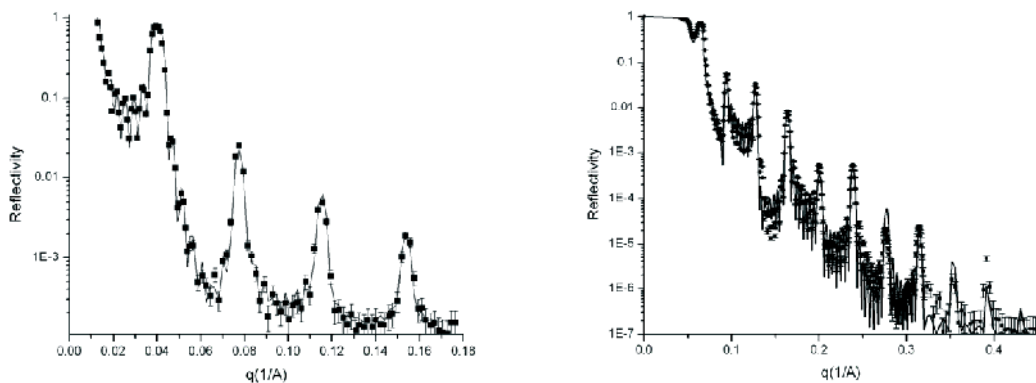


Fig. 1.: The measured and fitted neutron and x-ray reflectivity curves for sample 8x(84Å Ni/ 70Å Ti)

### References

1. R. Kovács-Mezsei, Th. Krist, Zs. Révay, Nuclear Instruments and Methods A 586 (2008) 51



<h1 style="margin: 0;">B N C</h1> <p style="margin: 0;"><b>Experimental Report</b></p>	<i>Experiment title</i> <b>High critical angle supermirror developments</b>	<i>Instrument.</i> REF
	<i>Principal proposer:</i> R. Kovács-Mezei <i>Experimental team:</i> T. Veres; L. Riecsánszky	<i>Local contact</i> T. Veres

**Results**

M5 supermirrors (critical angle 5 times larger, than that of pure Ni) were made at Mirrotron Ltd. The reflectivity was measured at REF constant wavelength reflectometer.

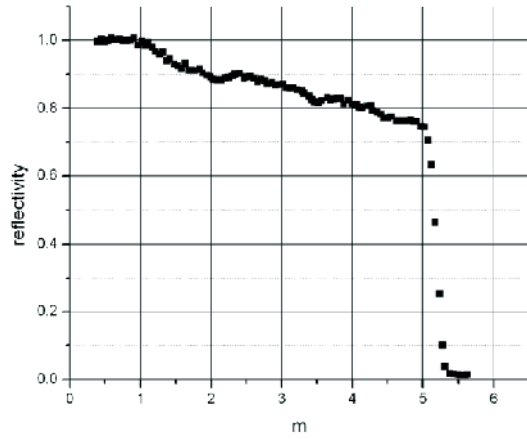


Fig. 1.: Measured reflectivity of an m5 supermirror. The unit of x axis is the critical q of pure Ni.

The reflectivity of the mirrors at the critical is 75%, which is a quite high value.

<h1 style="margin: 0;">B N C</h1> <p style="margin: 0;">Experimental Report</p>	<i>Experiment title</i> <b>Comparative structure analysis of aggregates in water-based magnetic fluids with sterical and electrostatic stabilization by SANS</b>	<i>Instrument</i> SANS
	<i>Local contact</i> N.Szekely	<i>Experiment Number</i>
<i>Principal proposer:</i> M. Avdeev <i>Experimental team:</i> A.Feoktystov, E. Tombacz		<i>Date</i> March 2011

## Objectives

The aim of the experiment was to compare the aggregate structure in magnetic fluids (MFs) with different (electrostatic and steric) stabilization of magnetite dispersed in water. This study was a continuation of our experiments on the SANS contrast variation with water-based magnetic fluids stabilized with citric (CA) and polyacrylic (PAA) acids (electrostatic stabilization), which revealed similar developed aggregates in the solution under physiological conditions. Now we have concentrated on MF sterically stabilized by means of double coating of magnetite nanoparticles (mean size below 10 nm) with oleic acid (OA). All of the studied fluids are considered as biocompatible sources of magnetic nanoparticles in medical applications [e.g. 1-4].

## Results

The comparison of the contrast variation data for MFs with PAA and OA stabilization is presented in Fig.1. A principal difference in the change of the scattering for the two samples can be distinguished and related to the different organization of the stabilizing shell around magnetite nanoparticles composing the aggregates. In the PAA sample the aggregates have a developed character and can be characterized by the close-to-fractal structure. The found match point (104%) corresponds well to the crystalline magnetite, which is consistent with the developed structure of aggregates providing full access of water to magnetite surface. In the case of the OA sample the aggregates are more compact; their characteristic size is about 50 nm. The appearance of the band in the scattering at large  $q$ -values when increasing the volume fraction of D<sub>2</sub>O in the solvent proves the surfactant presence in the closed aggregate structure. The latter is confirmed by the found match point of about 47%, whose shift towards lower values in comparison with the PAA sample is determined by the light hydrogen-containing component in the aggregates.

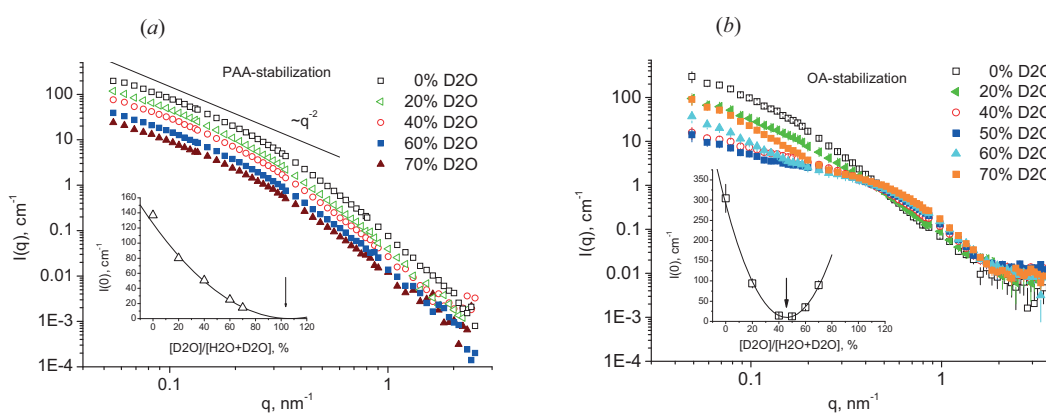


Fig.1. Contrast variation for 0.5% MFs stabilized with PAA- (a) and OA- (b). Solid line in (a) show power-law dependence corresponding to the scattering from developed cluster with fractal dimension of 2. Insets show dependences of experimental  $I(0)$  (points) on the D<sub>2</sub>O volume fraction in solvent with parabolic fits (lines). Arrows there indicate experimental match points.

The current study proves a specific shell structure in electrostatically stabilized MFs. One can hardly speak about the shell in this case; presumably, the charged molecules (independent on their size such in the cases of CA and PAA stabilization) are discretely distributed over the magnetite nanoparticles, which explains the observed access of water to their surface. In the case of sterically stabilized MFs such as the OA stabilized fluid the shell shows rather well-distinguished structure.

<h1 style="margin: 0;">B N C</h1> <p style="margin: 0;"><b>Experimental Report</b></p>	<i>Experiment title</i> <b>Four point bending device test</b>	<i>Instrument</i> ATHOS
	<i>Principal proposer:</i> Gy. Török <i>Experimental team:</i> Gy. Török	<i>Local contact</i> Gy Török
		<i>Date</i>

**Objectives**

According to the IAEA Residual Stress Technical Doc.1575 We tested a four point bending device in the residual stress setup on ATHOS (Fig 1.)

**Results**

Four point bending test

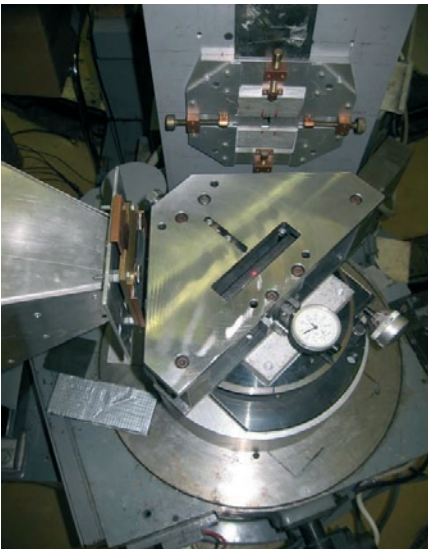


Fig1. The bending device in test position.



*According to the collaboration with JRC we have received the drawing for a 4 point device, what we manufactured and tested on a 10mm thick 20x200 mm steel plate. That was an additional proof of instrument setup and bending device. The serial of results are displayed on Fig.2. The results fit well to the expected line.*

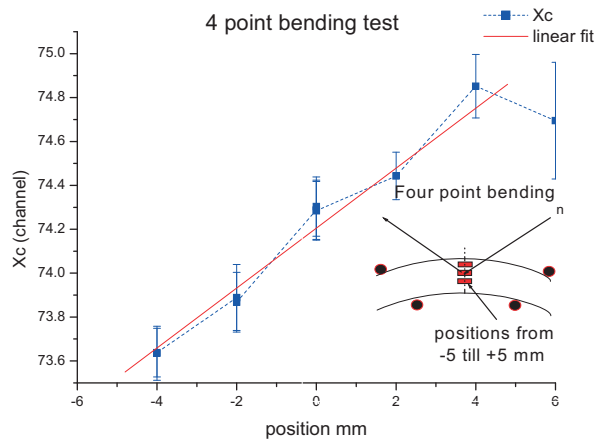


Fig.2., The peak position shift of bent flat 10mm thick plate

<h1 style="margin: 0;">B N C</h1> <p style="margin: 0;"><b>Experimental Report</b></p>	<i>Experiment title</i> <b>Validation of WAMAS type residual stress sample at Budapest Neutron Centre</b>	<i>Instrument</i> ATHOS
	<i>Principal proposer:</i> Chen Bo, China Nuclear Institute of Physics and Chemistry Mianyang <i>Experimental team:</i> Gy. Torok	<i>Local contact</i> Gy. Torok

## Objectives

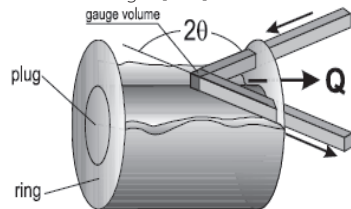
The penetration of thermal neutrons makes the neutron diffraction a powerful tool for the residual strains measurement in depth of poly-crystalline materials. The technique has developed on the last 15 years such that residual strains can be measured routinely to  $10^{-4}$  strain to depths in excess of 25mm in steel and 50-100mm in aluminium [1]. The measurement and validation of residual stress by neutron scattering plays an important role in the engineering science. For the test of new Round Robin type sample we used the cold neutron triple axis spectrometer ATHOS in order to check the followed procedure and instrumental setup.

## Results

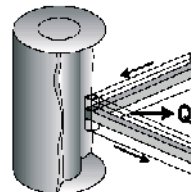
The instrument where the measurement was carried out was the cold neutron triple axis spectrometer ATHOS, because this instrument has a high flexibility and a relatively big sample table (~400 mm diam.) for investigation industrial samples. This spectrometer has a vertically focussing PG monochromator and continuously changeable wavelength what can give a chance for comfortable setup for measurement of industrial samples. However the monochromator-sample distance is relatively high (~1600 mm) at this distance is easy to carry out the necessary beam focussing. In order to avoid a big parallax's error we tried to minimize the incident slit to reference point distance (ISD) (actually was 170mm) The detector slit to reference point distance is changeable actually was 100mm. The 200x200 mm position sensitive delay line type detector [3] was placed from 850m mm from the reference point. This distance can be shifted when the sample size requires or better the resolution is needed. The sample was provided by CIAE similar to VAMAS Aluminium Ring & Plug Aluminium Ring.

Measurement Settings:

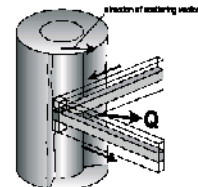
Measurement Direction:	Hoop	Radial	Axial
Reflection [hkl]:	200	200	200
Nominal Wavelength [Å]:	2.86	2.86	2.86
Incident Slit Width [mm]:	3	3	3
Detector Slit Width [mm]:	3	3	3
Incident Slit Height [mm]:	20	20	6
Detector Slit Height [mm]:	20	20	6



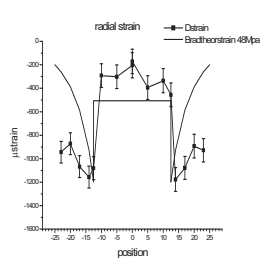
The measurement arrangement of axial strain



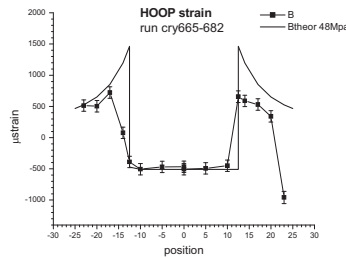
and radial strain



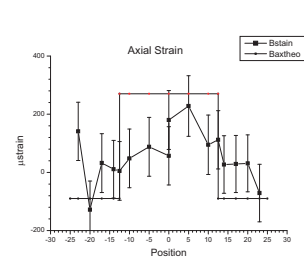
The measurement of hoop (tangential) strain.



The measured and calculated radial strain



The measured and calculated hoop strain



The measured and calculated axial strain

<h1 style="margin: 0;">B N C</h1> <p style="margin: 0;"><b>Experimental Report</b></p>	<i>Experiment title</i> <b>Residual stress measurement of Wamas Round Robin sample in BNC</b>	<i>Instrument</i> ATHOS
	<i>Principal proposer:</i> Gy. Torok <i>Experimental team:</i> Gy. Torok	<i>Local contact</i> Gy Torok

**Objectives**

The strain analysis by neutron beam is a most direct investigation strains and stresses in the material science due to a good penetration features and enough intensity for proper resolution. Because of this feature of neutrons the unique method of investigation of strains and stresses in 3 direction. For the preparation of a standard, it was agreed a series of 'round-robin' experiments should be undertaken. The standard samples examined, were an aluminium alloy shrink-fit 'ring and plug' assembly. It was demonstrated that, provided the recommended procedures are followed, with a positional tolerance of  $\pm 0.1\text{mm}$  can be achieved an accuracy in strain of  $\sim 10^{-4}$ , giving a resolution in 7 to 20MPa in most materials of practical interest.

**Results** VAMAS Aluminium Ring & Plug Aluminium Ring & Plug Set No.:2

Measurement Settings:

Measurement Direction:		Hoop	Radial	Axial
Reflection [hkl]:		111	111	111
Absolute or Nominal Wavelength [Å]:	3.3	3.3		
Calibration Procedure:	No			
Incident Slit Width [mm]:		3	3	
Detector Slit Width [mm]:		3	3	
Incident Slit Height [mm]:		20	20	
Detector Slit Height [mm]:		20	20	

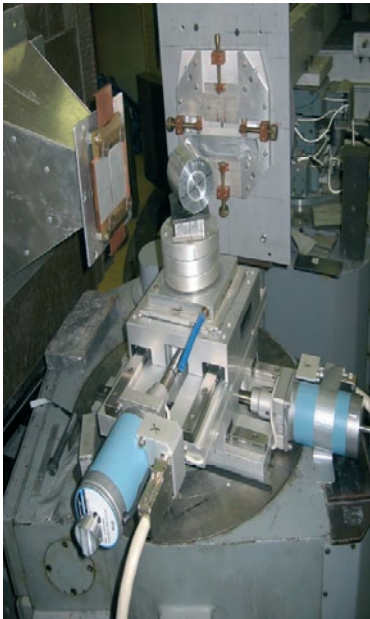


Fig 1 a, The experimental setup.

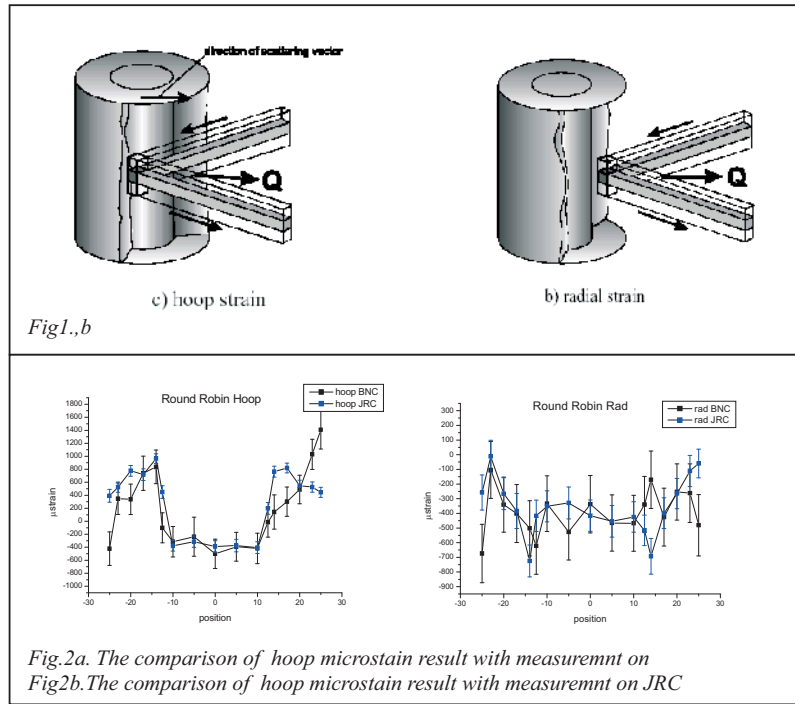


Fig.2a. The comparison of hoop microstrain result with measurement on JRC.  
 Fig.2b. The comparison of hoop microstrain result with measurement on BNC

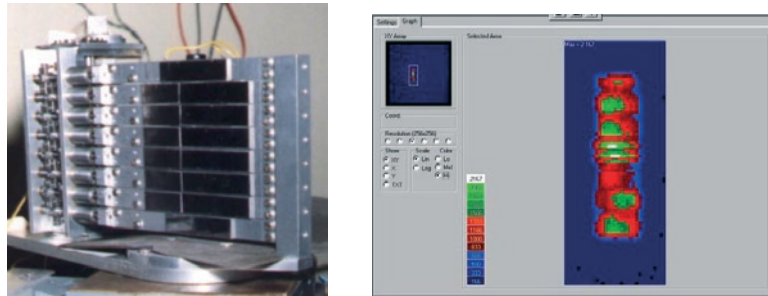
We have carried out the measurement on the wavelength. We could not measure the axial stress due to very high preferred orientation of sample in direction 111. Fig.2a. The comparison of hoop microstrain result with measurement on JRC. Here a detectable difference is seen in position region +10-25 mm. The reason is the high preferred orientation at direction 111 and multiple scattering in the depth of sample. The JRC measurement was carried out at different wavelength. Fig.2b. The comparison of hoop microstrain result with measurement on BNC. We have to mention that, after the calibration measurement of D0, an unwanted slip of detector's physical position has been occurred, what we detected after the procedure of measurement. So we needed to correct the scattering angle of 0.05 deg in comparison with earlier report.

<h1 style="margin: 0;">B N C</h1> <p style="margin: 0;"><b>Experimental Report</b></p>	<i>Experiment title</i> <b>Monochromator characterisation measurement using 2D detector</b>	<i>Instrument</i> ATHOS
	<i>Principal proposer:</i> Gy. Torok <i>Experimental team:</i> Gy. Torok	<i>Local contact</i> Gy Torok

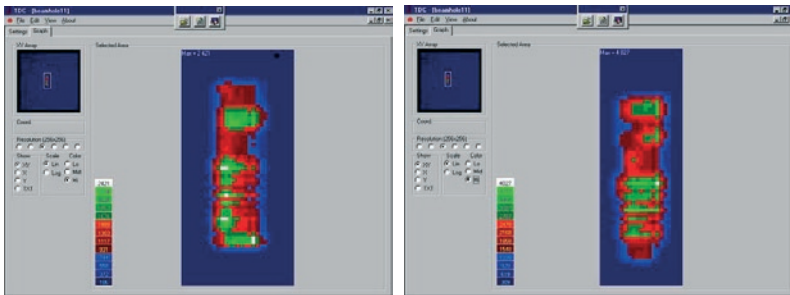
## Objectives

A method for monochromator quality were tested. We used a "Camera Obscura "arrangement for displaying the element of monochromator lamellae.

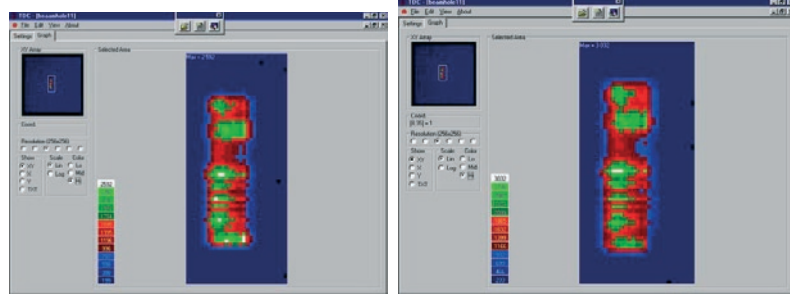
## Results



The monochromator and the first picture (cry085)



The picture changes after the Z axis tuning of monochromator. (cry088 cry089)



Final optimization process (cry90 and cry91) slight tuning of vertical focussing.

Here well seen that the brightness of lamellae is different. The overall intensity is grown for 50% however well seen that a new arrangement can give some extra intensity gain.

The picture reflects the sum of two effects what we could not decouple, the intensity distribution of beama in te neutron guide I and the misorientation and quality of each crystal elements.

<h1 style="margin: 0;">B N C</h1> <p style="margin: 0;"><b>Experimental Report</b></p>	<i>Experiment title</i> <b>Arrangement of setup on the reflection of Si ingot.          (demo of quantum mechanics effects.)</b>	<i>Instrument</i> ATHOS
	<i>Principal proposer:</i> Gy. Torok J. T.Grosz <i>Experimental team:</i> Gy. Torok	<i>Local contact</i> Gy Torok

**Objectives**

For the fabrication on bent crystal monochromator the check of crystal orientation is the first step. In order to check the Si single crystal ingot we used the Athos spectrometer.

**Results**

The pictures what we received clearly demonstrates the dynamical theory of diffraction. We did the following arrangements:

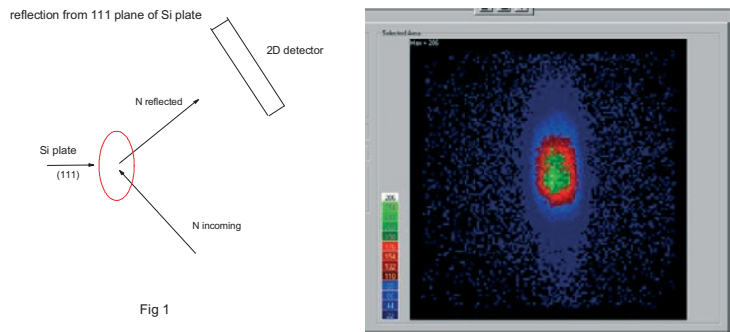
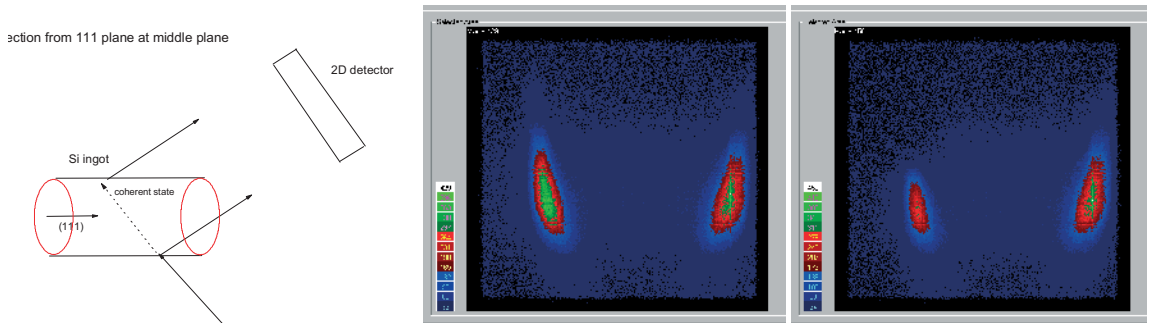


Fig 1  
The arrangement of reflection on the Si plate



The arrangement of reflection inside the crystal. The picture, and when outgoing side closed with Cd ) At these pictures the beam is going through at the bottom 1/3 part of Si ingot. (that cause the kidney form) The scattering from coherent state is seen after the reflection.

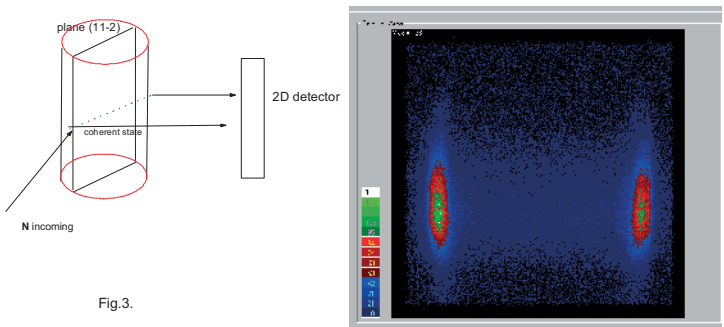


Fig.3.

The Fig3 shows the scattering from (2 2-4) plane on pic cry107 The scattering from coherent state is seen between reflections.

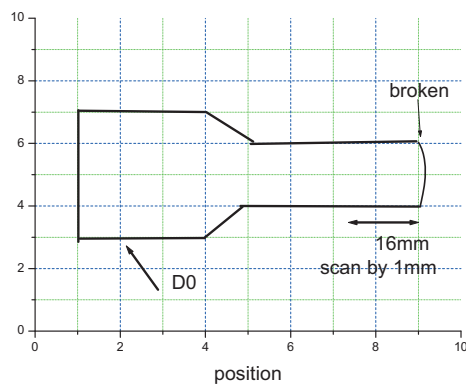
<h1 style="margin: 0;">B N C</h1> <p style="margin: 0;"><b>Experimental Report</b></p>	<i>Experiment title</i> <b>Residual stress scan on broken Ferrite steel</b>	<i>Instrument</i> ATHOS
	<i>Principal proposer:</i> L.Sun Mianyang CIPC <i>Experimental team:</i> Gy. Torok J.Sun Mianyang CIPC	<i>Local contact</i> Gy Torok

### Objectives

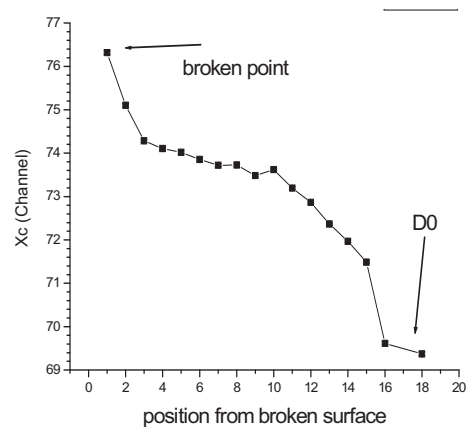
The mechanism of destruction of given sample was investigated. This process is strongly affected of crystalline structure of material. The residual stress along the broken sample indicates the history of breaking process.

### Results

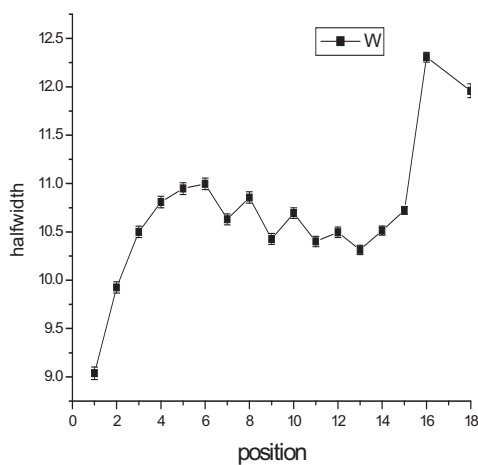
The investigated sample was a standard mechanical probe after mechanical destruction.



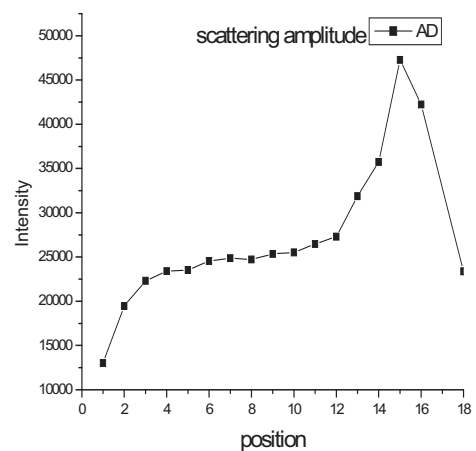
The form of probe



The microstrain along the sample arb un.



The changing of diffraction peak halfwidth and the scattering amplitude



The used wavelength was 2,86Å the measured strain direction was perpendicular to the sample long axis. We detected a 10-12mm long deformed zone near by the brake point. Also the changing of scattering intensity and the halfwidth indicates the substantial modification of average orientation of crystalline structure

### Future prospects

Investigation of breaking mechanism is an important engineering task and should be carried out for the construction element.



<h1 style="margin: 0;">B N C</h1> <p style="margin: 0;"><b>Experimental Report</b></p>	<i>Experiment title</i> <b>Total scattering experiments on different phases of C<sub>2</sub>Cl<sub>6</sub></b>	Instrument: MTEST
	<i>Principal proposer:</i> L. Temleitner (Wigner RCP)	Local contact L. Temleitner
<i>Experimental team:</i> L. Temleitner		

## Objectives

The hexachloroethane (C<sub>2</sub>Cl<sub>6</sub>) is an orthorhombic molecular crystal at room temperature, which undergoes several phase transitions until it sublimates [1]. The first transition occurs at 316 K, where it transforms to a monoclinic intermediate phase, whose structure resolved very recently [2]. The next phase is stable between 344 K and 458 K, where it sublimates. The former phase is a body-centered cubic phase.

The main aim of the present study is to understand the structural phase transitions more deeply, especially its effect on the local order. The so-called total scattering analysis is able to provide this kind of information. It consists of Bragg and diffuse scattering contributions. The former one is the result of the scattering on the average structure and the latter one is the consequence of short-range order between atoms.

## Results

The sample has been placed into the beamline furnace in a 8 mm diameter vanadium can. To prevent evaporation of the volatile sample counter-screw sealing with Viton O-rings has been constructed, allowing to resist pressure up to 2 bars.

The measurement has been carried out using 1.44 Å wavelength neutrons, with 30' collimator. First, the measurement on the bcc phase at 370 K was done, then a liquid phase was observed and measured at 458 K due to non-ambient conditions. Moreover, the corresponding empty instrument measurement has been done. Because of the lower symmetry of the ordered and the intermediate phases, the receiving side collimator was replaced by a tight one. This made the resolution better, but increased the time of measurement to a full reactor cycle for each (2 samples and one empty can). The empty cell corrected pattern can be seen in Figure 1.

The similarity of the bcc and liquid phase is remarkable in Fig. 1. This indicates a similar short-range order in both phases. This is significant for the change to the monoclinic phase, which has been interpreted as a substitution disorder by Bragg analysis [2]. Between the ordered and monoclinic phase, the diffuse scattering signal slightly changed.

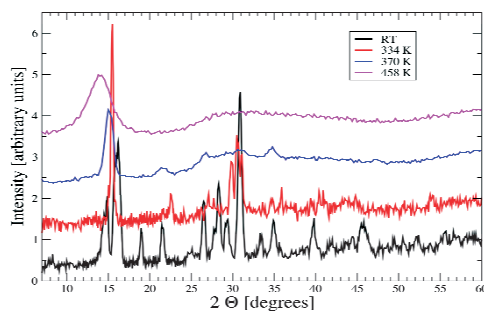


Figure 1. Diffraction pattern of hexachloroethane on different phases

## Future prospects

The result of the measurement will be combined with already measured X-ray data by Reverse Monte Carlo simulations and will be published.

## References

- [1] P. Gerlach, W. Prandl, Acta Cryst. A44 128 (1988).
- [2] P. Negrier, et al., Cryst. Growth & Des. 13 782 (2013).

<b>B N C</b> <b>Experimental Report</b>	<i>Experiment title</i> <b>Total scattering experiments on aqueous electrolyte solutions</b>	<i>Instrument:</i> MTEST
		<i>Local contact</i> L. Temleitner
<i>Principal proposer:</i> L. Temleitner (Wigner RCP) <i>Experimental team:</i> V. Mile, I. Harsányi (Wigner RCP)		<i>Proposal No.</i> MTEST_12_2_IH <i>Date(s) of Exp.</i> 17-26 Apr 2012

## Objectives

Aqueous electrolyte solutions are in the centre of scientific interest from long time and their structure is still not known in details. Other salts solutions have been examined by the research group before [1], some samples were measured before successfully here, at Budapest Neutron Centre [2]. The size of ion shells and the number of water molecules in them are responsible for the ion's behavior in the solution. Biologically, one of the most important cation is calcium. It has key role in muscular movements and it is one of the basic components of the bone tissues. Its hydration has special feature, bones must be solid, but the ion has to be in solution on the way to bones and in muscles. Besides its biological importance, calcium ion itself is very good model for diffraction experiments, because of its relative big size and the high solubility of its simple salts in water the ion has significant weight in both X-ray and neutron diffraction experiments.

The measured samples were heavy water solutions of two calcium salts:  $\text{CaBr}_2$  at 10, 6 and 1 mol% and  $\text{CaI}_2$  at 3 and 1 mol% concentrations. The aims of these measurements at first were to see whether MTEST is appropriate for collecting data on aqueous solutions. Second goal was to see if any structural differences could be detected between measured data on MTEST of different anions and concentrations.

Over the calcium containing samples, we attempted to measure a 4.3 mol% aqueous nickel sulphate solution, as a step towards more complicated hydrated ions and also connected to phosphoric acid solutions examined before [3].

## Results

The measurement has been carried out with 1.43 Å wavelength. During the measurements the samples were contained in a 6 mm vanadium can. For these measurements wide range data were collected at  $7-144^\circ$  range ( $0.6-8.3 \text{ \AA}^{-1}$  in Q).

Resulting normalized curves show the typical shape of water and aqueous salt solutions, one main peak at ca  $2 \text{ \AA}^{-1}$ , and following smaller ones. The position of the first peak is shifted with concentration. The quality of the data are according to the reachable statistics of the given neutron source, detailed analysis has to be applied, but the main features can be observed easily.

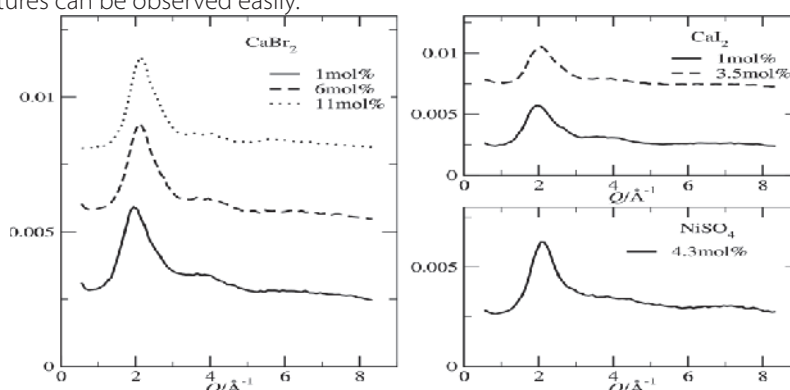


Figure 1. a) Normalized experimental neutron diffraction data of  $\text{CaI}_2$  and  $\text{CaBr}_2$  solutions at 5 concentrations. b) Normalised experimental neutron diffraction data of 4.3 mol%  $\text{NiSO}_4$  solution (/home/ildi/niso4/niso4\_q.dat)

## Future prospects

The result of the measurement will be combined with X-ray data by Reverse Monte Carlo simulations, possibly will be compared with molecular dynamics simulations and the will be published.

## References

- [1] Harsanyi et al. J Chem Phys 122 124512 (2005)
- [2] Harsanyi et al. J Mol Liq 131-132 60 (2007)
- [3] Harsanyi et al. J Phys Cond Matt accepted (2013)

<h1 style="margin: 0;">B N C</h1> <p style="margin: 0;"><b>Experimental Report</b></p>	<i>Experiment title</i> <b>Trial measurement of the linear position sensitive detector of the MTEST diffractometer</b>	<i>Instrument:</i> MTEST
	<i>Principal proposer:</i> L. Temleitner (Wigner RCP)	<i>Local contact</i> L. Temleitner
<i>Experimental team:</i> L. Kószegi, L. Temleitner		<i>Date(s) of Exp.</i> 26-27 Apr 2012

## Objectives

The MTEST instrument with single detector setup is able to study internal stress and texture of alloys in a small volume by measuring the shift of Bragg-peak(s) and spots (single crystal). The installation of the high-temperature vanadium furnace (RT..1000°C, which is unique in BNC) extended its abilities not only on its original domain, but melts and high-temperature phases of crystals. The medium-low level of background makes possible to record the so-called total scattering diffraction pattern. This pattern consists of the Bragg and diffuse scattering, which are related to the average crystal structure (Bragg) and short/medium range order between the atoms (diffuse). As we showed on MTEST\_12\_1\_IH report, the required time to record 4 phases with the corresponding calibration and empty can measurement took 4 reactor cycles with single detector. To record the diffraction pattern on reasonable time in the future, an ORDELA 1200N type one-dimensional linear position sensitive detector has been started to install. For signal processing, an ORDELA AIM-206 encoder and a 2k Ortec Trump-PCI multichannel analyzer used.

The purpose of the present measurement after the setup of electronics is to check the detector efficiency, its applicability to measurement of liquid and amorphous materials and get some suggestion for the design of the shielding of the detector.

## Results

The measurement has been carried out with 1.44 Å wavelength, without any collimators of the monochromatic beam. During the measurement of aqueous solution (MTEST\_12\_2\_IH), the detector has been placed about 2 meters from the sample, without any shielding (not disturbing the another measurement). So, the incoming neutrons from the sample and the background provided almost direction independent pattern. Thus, the relative efficiency of the detector has been recorded over a night (see Fig. 1). When measurement on solutions has been finished, the detector placed about 30 cm from the sample, approximately 38° degrees of 2θ of its centre. To reduce the background both side cadmium foils has been used. Empty instrument, 6 mm (wall thickness: 0.05 mm) vanadium can, and 99 mol% D2O measured over 15 minutes.

We concluded that the efficiency of the detector makes possible to measure liquid samples. Also, the slope of the detector efficiency is almost flat, but the observed background is high.

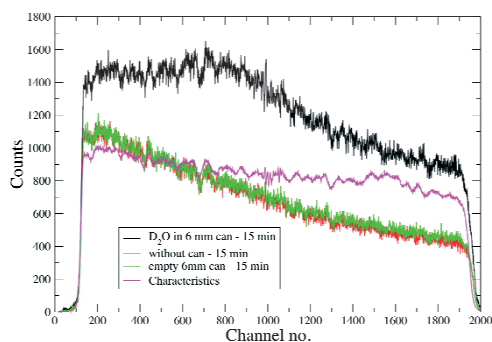


Figure 1. a) Measured raw pattern by the linear position-sensitive detector. Black solid line: D2O in 6 mm can; red solid line: empty instrument; green solid line: 6 mm vanadium can; magenta solid line: rescaled detector characteristics.

## Future prospects

The level of background should be suppressed by proper shielding. At the time of writing, it has been designed and the current level of it equals to the difference between red and green curves (approx. 25 counts) on Figure 1.

<h1 style="margin: 0;">B N C</h1> <p style="margin: 0;"><b>Experimental Report</b></p>	<i>Experiment title</i> <b>Commissioning the triple monochromator-changer</b>	<i>Instrument:</i> MTEST  <i>Local contact</i> L. Temleitner
	<i>Principal proposer:</i> L. Temleitner (Wigner RCP) <i>Experimental team:</i> L. Kőszegi (Wigner RCP), L. Temleitner	<i>Proposal No.</i> MTEST_12_4_IH <i>Date(s) of Exp.</i> 10-12 Oct 2012 16-18 Oct 2012

## Objectives

The MTEST diffractometer obtains five single crystal monochromators, which allows performing various studies on this machine. However, changing them is a laborious (requires to remove about 10 tons of biological shield) and time-consuming (waiting until radiation reaches an acceptable level) task. To save time and make possible to tailor the resolution and range of impulse transfer on demand even in one reactor cycle, a triple monochromator-changer (Figure 1) has been created as in-house development (idea: László Kőszegi, design: Péter Schlosser, construction: Technical Base of Wigner RCP).

## Results

During the 2012 summer shutdown period of the reactor, the shielding of the monochromator removed and the changer installed mechanically. On the time of the integration into the control system figured out, that the resolution of the encoder belonging to the horizontal axis is insufficient (1 step=22'). Thus, this part has been redesigned to allow 5' accuracy.

Within the available crystals, the Cu (111) (most intense), Cu (220) (high Q-range), Ge (111) (good resolution) has been selected and placed into the changer. At the same take-off angle (40°) with 30' collimator of the monochromatic beam, the pattern of nickel powder in 6 mm diameter of vanadium can has been recorded to determine the wavelength for each (see Table 1).

To test the reproducibility of the mechanics (with slightly different beam compared the previous paragraph) after the recording of nickel pattern, three of the four motors are removed far away from their original positions and set them again. Then, the pattern recorded and wavelength has been determined (see Table 2). Only very small inaccuracy has been found.

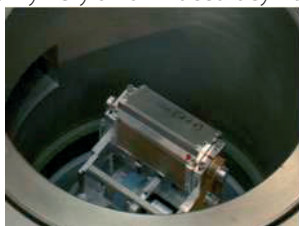


**Figure 1.** The installed monochromator-changer

Crystal	Wavelength [Å]	cps
Ge (111), 15'	2.251(2)	155
Cu (111), 30'	1.4399(3)	2240
Cu (220), 30'	0.8816(3)	330

**Table 1.** Wavelength and beam intensity (monitor counter) at 40° take-off angle of the monochromator with 30' collimator

Run	1 <sup>st</sup>	2 <sup>nd</sup>
Wavelength (Å)	1.4403(7)	1.4393(6)
zero error (°)	-0.56(2)	-0.55(2)

**Table 2.** Result of the reproducibility test

## Future prospects

Using the monochromator changer made possible to change wavelength on demand within 5 minutes (this can be decreased by improving of the control software). Based on the results of the test of reproducibility, the measurement of amorphous materials (where usually requires higher Q-range) can be done much more economical by recording Cu (111) and the remaining part in Q (with some overlapping) by Cu (220). Another application in the case of crystalline materials is to increase resolution by changing to Ge (111). The advantage of this development is enjoyed not only at room, but until 1000°C using the installed vanadium furnace.

<h1 style="margin: 0;">B N C</h1> <p style="margin: 0;">Experimental Report</p>	<i>Experiment title</i> <b>Oriental correlations in the liquid phase of 1,1-dibromo-1-chloro-2,2,2-trifluoroethane (C<sub>2</sub>F<sub>3</sub>Br<sub>2</sub>Cl)</b>	<i>Instrument:</i> MTEST
	<i>Principal proposer:</i> Sz. Pothoczki (Wigner RCP)	<i>Local contact</i> L. Temleitner
<i>Experimental team:</i> Sz. Pothoczki, L. Temleitner (Wigner RCP)	<i>Proposal No.</i> MTEST_12_5_IH	<i>Date(s) of Exp.</i> 18-26 Oct 2012

## Objectives

Phase transitions and phase stabilities under different thermodynamic conditions are important for both physics and material science. To understand them deeply it is necessary to follow with attention the local, intermediate and long range ordering. A total scattering experiment is able to provide this information. Analysis of the total scattering type diffraction pattern gives information about the average structure and the differences from it, as well: Bragg scattering provides knowledge on average structure and the diffuse part is characteristic to the local order. Molecular crystalline materials are rich in crystalline phases (under different thermodynamic conditions). Within these materials — beyond the average structure — local ordering (and its changes within the same crystal phase) can play a significant role during transitions from one phase to another. This proposal aimed to determine the total scattering structure factor of crystalline C<sub>2</sub>F<sub>3</sub>Br<sub>2</sub>Cl and answer two main questions: What kind of mutual arrangements of molecules are preferred? What is the role of dipolar interactions?

## Results

The measurement has been carried out with 1.4380(5) Å neutrons at room temperature using a 0.7 cm<sup>3</sup> gel-like sample. During the measurements the sample (C<sub>2</sub>F<sub>3</sub>Br<sub>2</sub>Cl) was contained in a 6 mm vanadium can, which is rotated along its cylindrical axis to prevent preferred orientation. The observed diffraction pattern (Figure 1) shows the usual features of plastic crystals: the great part of the observed signal is originated from the diffuse scattering and there are only few Bragg-peaks, whose intensities are significant in comparison with diffuse scattering. This shows increasing disorder, where even the material is crystalline, the mutual orientation of the molecules have a determined role in short range.

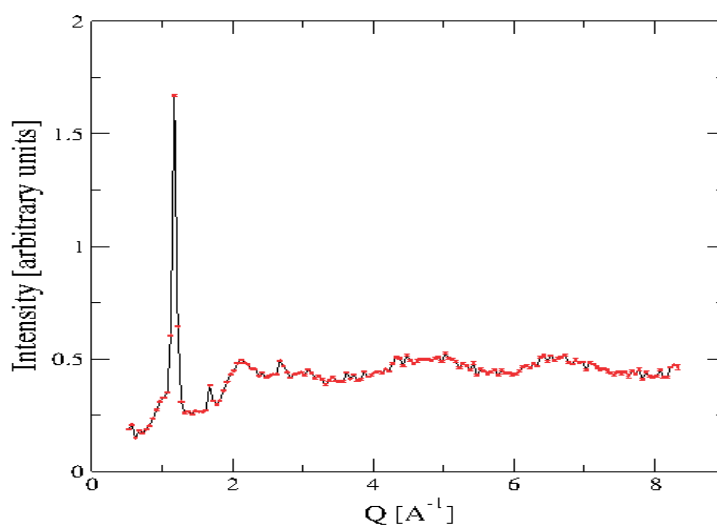


**Figure 1.** Corrected neutron powder diffraction pattern of C<sub>2</sub>F<sub>3</sub>Br<sub>2</sub>Cl

## Future prospects

We have already undertaken a series of experiments using X-ray diffraction experiments to study the liquid and crystalline phase of C<sub>2</sub>F<sub>3</sub>Br<sub>2</sub>Cl. All of neutron diffraction structure factors are to be used in combination with our SPring-8 experimental results to be analysed simultaneously by means of the Reverse Monte Carlo (RMC) structural modeling method. Additionally, classical molecular dynamics simulations will be carried out on the same systems, using standard software and potential models (see, e.g., Gromos). This is a unique combination, leading to a much deeper understanding of the structure than it would be possible to gain on the sole basis of either technique. Actually, these simulations on progress.

<h1 style="margin: 0;">B N C</h1> <p style="margin: 0;">Experimental Report</p>	<i>Experiment title</i> <b>Neutron diffraction study on molten aluminosilicates and mixed non-ferrous oxide systems</b>	<i>Instrument:</i> MTEST
	<i>Principal proposer:</i> G. S. E. Antipas (National Technical University of Athens)	<i>Local contact</i> L. Temleitner
<i>Experimental team:</i> G. S. E. Antipas, K. Karalis (National Technical University of Athens)		<i>Date(s) of Exp.</i> 12-16 Nov 2012

## Objectives

The short-range order of aluminosilicates and mixed oxides in the liquid state (1500 °C) and in the glass state [2] during aerodynamic levitation was studied by high-energy X-ray diffraction [1]. In order to extend the above analysis was necessary the use of neutron diffraction (ND). A superposition of the ND dataset promotes an RMC supercell with a higher fraction of uncoordinated oxygens, more pronounced Fe-Al cluster interconnections and a markedly reduced Fe-Si-Mg cluster bridging, as compared to the RMC-generated environment restricted solely by XRD total scattering.

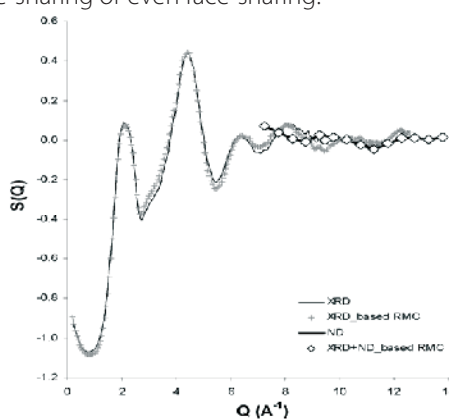
## Results

Because of we would like to get information about the local structure, we chose short wavelength (with the help of Cu (220) crystal 0.881 Å was used). The sample placed in a 8 mm-diameter vanadium can with a wall thickness of 0.15 mm and was then measured via a single BF<sub>3</sub> proportional counter. During the measurement, the scan range was from 60 to 144 degrees, thus allowing Q-range between 7.2 and 13.5 Å<sup>-1</sup>. The interpretation of the ND high-Q spectrum in a multi component system such as the one treated in the current study is an ambitious task. The simulation using high resolution XRD, ND and RMC is considered to enhance reliability. Fig. 1 is a comparison of the RMC-estimated vs. the experimental total structure factor for both simulations. The XRD offered satisfactory resolution up to approximately 12 Å<sup>-1</sup>; the material's S(Q) shape below 0.7 Å<sup>-1</sup> is suggestive of long-range ordering, while short-range order is flagged by the fluctuations between 5.5 and 11.5 Å<sup>-1</sup>. Similarly the ND offered satisfactory resolution between 7-14 Å<sup>-1</sup>.

## Conclusions

The additional RMC restriction by the ND dataset had a mixed effect on different partials; overall, however, the additional ND dataset led to an increase of the oxygen coordination of both network forming as well as network modifying cations. Atomic environments indicated the higher fraction of non-bonded oxygens at approximately 2%; introduction of the ND-constraint in RMC fitting also promoted Fe-Al cluster interconnections and reduced the frequency of corner-linked bridged Fe-Si-Mg clusters via oxygen bridges in favor of other linkage types as edge-sharing or even face-sharing.

Figure 1. Glass experimental (lines) and RMC-generated (points) total structure factors.



## References

- [1] G.S.E. Antipas et al., Journal of Molecular Structure, 1019 (2012) 151-158.
- [2] G.S.E. Antipas et al., Journal of Physics: Condensed Matter, 2013.

<h1 style="margin: 0;">B N C</h1> <p style="margin: 0;"><b>Experimental Report</b></p>	<i>Experiment title</i> SANS study of the structure of biogenic ferrihydrite dispersion in aqueous solution using the contrast variation technique.	<i>Proposal No.</i> BRR_233 <i>Local contact</i> A. Meiszterics
	<i>Principal proposer:</i> Maria Balasoiu <sup>1,4</sup> <i>Experimental team:</i> Lidia Ishchenko <sup>2</sup> , Serghei Stolyar <sup>2</sup> , Rauf Iskhakov <sup>2</sup> , Alexander Kuklin <sup>1</sup> , Yuriy Raikher <sup>3</sup> , Aniko Meiszterics <sup>1</sup> FLNPh, JINR, 114980, Dubna, Russia <sup>2</sup> Siberian Federal University, 660041, Krasnoyarsk, Russia <sup>3</sup> Institute of Continuum Media Mechanics, Ural Branch of RAS, Perm, Russia <sup>4</sup> IFIN-HH, PO Box MG-6, Bucharest, Romania	<i>Date(s) of Exper.</i>  2010-02-24  <i>Date of Report</i> 2013-10-05

## Objectives

Intense research interest to nanoparticles is motivated by their unique physical properties, important both from fundamental and technological points of view, for example in high density magnetic recording media, permanent magnets, magnetic refrigeration, magnetic sensing, etc. Biogenic iron oxides particles make a separate class of magnetic nanoparticles that is of special interest for biomedical applications. In the given experiment water dispersions of biogenic iron oxides particles metabolized by *Klebsiella Oxytoca* bacteria are probed by small-angle neutron scattering to reveal features of the nanoparticles system and compared with similar results of ferritine standard (Sigma-Aldrich) sample.

## Results

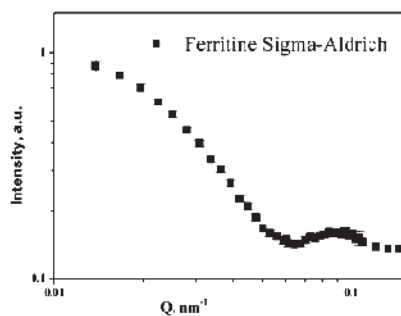


**Fig.1** Experimental SANS curve of a 10% ferritine Sigma-Aldrich sample.

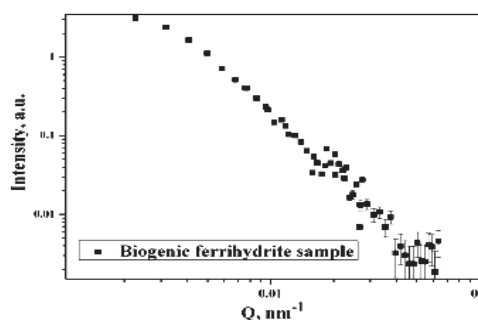


**Fig.2** Experimental SANS curve of a biogenic ferrihydrite sample.

We have investigated a 10% ferritine standard Sigma-Aldrich dispersion in D-water, in Fig.1 is presented the obtained experimental SANS curve. In Fig.2 are represented the experimental SANS curve of the biogenic ferrihydrite dispersion.

Using the FITTER program it was found for ferrihydrite sample a form factor for cylinder having diameter  $2R$  and height  $L$ , described with the expression

$$P(Q) = 4 \int_0^{\frac{\pi}{2}} \frac{\sin^2(QH \cos \alpha)}{(QH \cos \alpha)^2} \frac{J_1(QR \sin \alpha)}{(QR \sin \alpha)^2} \sin \alpha d\alpha$$

where,  $J_1$  is the cylindrical Bessel function of order 1, best represents the experimental data.

## Future prospects

We plan the continuation of the investigation using ultrasonic treatment for improving the long-term stability in aqueous solution of biogenic ferrihydrite nanoparticles samples under ambient conditions in experiments with improved statistics and contrast variation matching.

<b>B N C</b> <b>Experimental Report</b>	<i>Experiment title</i> <b>SANS study of lysozyme amyloid aggregate disassembly caused by magnetite nanoparticles</b>	<i>Proposal No.</i> BRR 245 <i>Local contact</i> N.Szekely
	<i>Principal proposer:</i> Peter Kopčanský <i>Experimental team:</i> Gábor Lancz, Peter Kopčanský, Milan Timko, Mikhail Avdeev, Artem Feoktystov,	<i>Date(s) of Exper.</i> Dec 2010 <i>Date of Report</i> Feb 2011

## Objectives

Amyloid aggregates of proteins are related to several diseases. Some nanoparticles are able to change this pathological state of proteins. In this study, the effect of magnetic nanoparticles on amyloid fibrils of the protein lysozyme was studied by small angle neutron scattering (SANS). Mixtures of electrostatically stabilised magnetite ( $\text{Fe}_3\text{O}_4$ ) nanoparticles with hen egg white lysozyme (HEWL) amyloid fibrils were prepared and measured. Time dependence of the structures in such mixtures was investigated. Also, the structure of pure amyloid fibrils was of interest. Electrostatically stabilized magnetic fluids (MFs) containing sodium oleate and dextran, which were probed prior in mixtures with amyloid fibrils, were studied as well.

## Results

The amyloid HEWL fibrils were in diluted hydrochloric acid providing an acidic environment compatible with the  $\text{Fe}_3\text{O}_4$  particles stabilised with perchloric acid. The obtained SANS curves from mixtures of fibrils and magnetite particles with different content of  $\text{D}_2\text{O}$  (Fig.1a) were compared with previous measurements (PSI, Villigen) performed about two months earlier. These mixtures declared practically the same SANS curves. In MIX 12 with nearly pure  $\text{D}_2\text{O}$  the scattering length density of the magnetite particles of the ionic ferrofluid was almost the same as of  $\text{D}_2\text{O}$ , thus the scattering came practically solely from the protein structure.

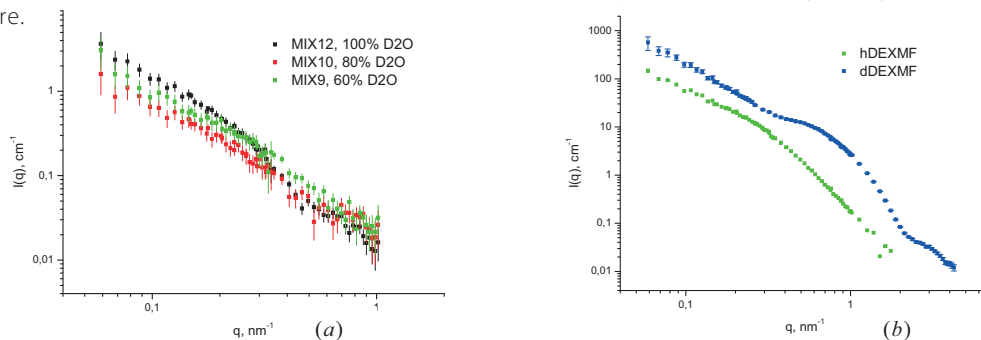


Fig.1. Experimental SANS curves ( $T = 37^\circ\text{C}$ ) from (a) fibril+MF mixtures (concentration of amyloid 1.5 mg/ml) and (b) dextran containing MFs with  $\text{H}_2\text{O}$  (hDEXMF) and  $\text{D}_2\text{O}$  (dDEXMF).

No significant change in the behaviour of the curves for pure amyloid fibrils ( $\text{HCl}+\text{D}_2\text{O}$ ) with low (1.5 mg/ml) and high (10 mg/ml) concentration was detected. Beside HEWL fibrils in diluted  $\text{HCl}$ , systems close to  $\text{pH } 7$  were tried as well. Both amyloid and native protein solutions in phosphate buffer were unstable. The residual scattering (non-precipitated particles) in the case of native protein could be related to lysozyme. The experimental radius of gyration of the registered Guinier region coincided rather well with the theoretical value of 1.53 nm calculated from the protein crystal structure.

The scattering from ionic ferrofluid with dextran (Fig.1b) was treated by the indirect Fourier transform showing that single particles of magnetite were partially aggregated before the coating with surfactant with characteristic aggregate size of about 20 nm. It is seen from the absolute values of the scattering intensity at two contrasts (Fig.1b) that the match point of the system is shifted towards H-solvent, thus reflecting the formation of quite extended surfactant shell around these aggregates taking more than 50 vol. % in the complex particles. The secondary aggregation (size above 120 nm) is also reflected in the scattering curves.

## Future prospects

The lack of difference of SANS curves between the mixtures and pure amyloid fibrils, and also the lack of change in time, was contrary to the expectation. A fluorescence study of MIX 12 showed a structural alteration of fibrils. A suggested mechanism is that upon binding of magnetite particles to the fibrils a change of secondary structure of the protein molecules took place without the disassembly of fibrils on the size level of below 100 nm, which is detectable in SANS measurement. By following data analysis a model of (helical) fibril structure is foreseen. To make further growth in this field, mixtures at physiological conditions and mixtures of more progressed disassembly should be studied.



# *Instruments* | **6.**

## 6.1. PSD – NEUTRON POWDER DIFFRACTOMETER WITH POSITION SENSITIVE DETECTORS

*Instrument scientists: Margit Fábrián<sup>1,2</sup> and Erzsébet Sváb<sup>2</sup>*

- <sup>1</sup> Centre for Energy Research, Hungarian Academy of Sciences, H-1525 Budapest P.O.B. 49, Hungary
- <sup>2</sup> Institute for Solid State Physics and Optics, Wigner Research Centre for Physics, Hungarian Academy of Sciences

The PSD neutron diffractometer is suitable for atomic structure investigations of amorphous materials, liquids and crystalline materials where the resolution requirements are not high. It is a 2-axis diffractometer equipped with a linear position sensitive detector system. The detector assembly is mounted on the diffractometer arm and it spans a scattering angle range of 25° at a given detector position. The entire diffraction spectrum can be measured in five steps. During the year of 2002, the detector system of the PSD has been upgraded: instead of the original analogue design, a new system has been purchased from Studsvik NFL (Sweden) with a digital electronics technology. The

detector system is based on three <sup>3</sup>He filled linear position sensitive Reuter-Stokes detectors (610 mm in length, 25 mm diameter), similarly as the previous ones, but a more novel type (P4-0824208). Three detectors are placed in the scattering plane above each other. Data transfer and instrument control has been done by PC-AT (Master PC) with Eagle I/O card. A Windows based - user friendly - instrument software program package has been developed. Recently the interface electronics has been fully upgraded. A new dedicated electronic device has been constructed, which serves for the electronic control of the movements and data transfer of the diffractometer.

**Table 1.** ▶  
Characteristic features of the PSD diffractometer for two actual arrangements

Channel	thermal, 9T tangential	
Primary collimation	Soller-type : 20'	
Take-off monochromator angle facility	$-5^\circ < 2\Theta_M < 45^\circ$	
Monochromator and mosaicity	Cu(111), 16'	Cu(220), 20'
Monochromatic wavelength	1.069 Å	0.66 Å
Resolution, $\Delta d/d$	$1.2 \cdot 10^{-2}$	$2.4 \cdot 10^{-2}$
Flux at the sample position	$10^6 \text{ ncm}^{-2}\text{s}^{-1}$	$10^5 \text{ ncm}^{-2}\text{s}^{-1}$
Beam size at the specimen	10 mm×50 mm	
Scattering angle, $2\theta$	$5^\circ < 2\theta < 110^\circ$	
Momentum transfer interval, Q	0.6-9.2 Å <sup>-1</sup>	0.8-15.8 Å <sup>-1</sup>
Monitor counter	fission chamber	
Detector system	3 linear position sensitive <sup>3</sup> He detectors the detector assembly spans 25° scattering angle at a given position	
Data collection	Xilinx preprogrammed unit	
Data transfer and control	PC-AT with Eagle I/O card and a dedicated electronic device	
Remote control and file transfer	Windows programme package	

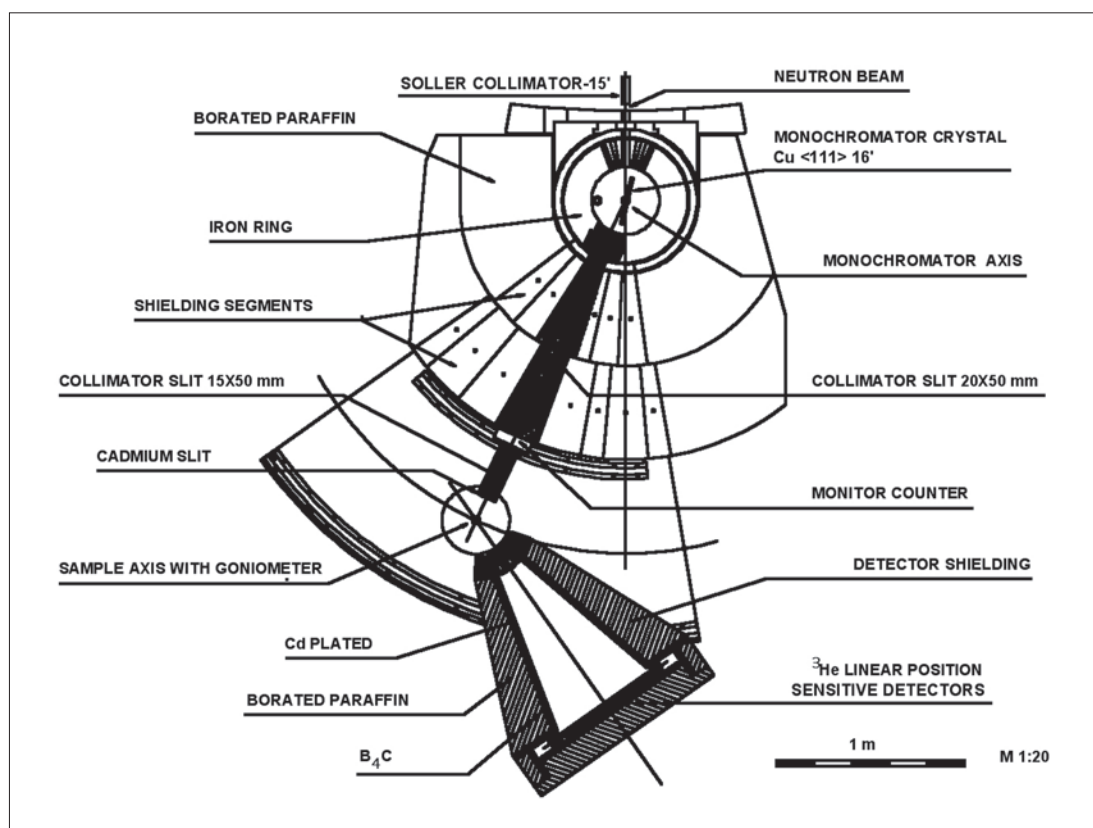


Figure 1. Schematic arrangement of the PSD neutron diffractometer



Figure 2. Photographs taken from the PSD neutron diffractometer

## 6.2. MTEST DIFFRACTOMETER

*Instrument scientists: László Temleitner, László Kőszegi*

Institute for Solid State Physics and Optics, Wigner Research Centre for Physics

The M(aterial)TEST neutron diffractometer was originally designed for studying internal stresses in alloys. Recently, the diffractometer has been upgraded by a position sensitive detector and by a monochromator changer; this way, a more efficient use of the available beamtime, with various sample environments, can be achieved. At the present status, the instrument allows for performing total (Bragg and diffuse) scattering measurements on powder, liquid and amorphous materials. The four-circle goniometer maintains also the chance for texture measurements.

The MTEST diffractometer is installed on the 6th axial thermal channel of the reactor. The maximum flux can be obtained at a wavelength of 0.144 nm. A sapphire single crystal is used, deep inside the beam shutter, to filter out epithermal neutrons. The neutron flux at the sample table is  $2 \cdot 10^6$  neutron/(cm<sup>2</sup>·sec) at a wavelength of 0.133 nm.

In order to produce monochromatic beams, various single crystals are available (Table 1.). Changing the wavelength is easy and doable in 5 minutes, by using the newly designed monochromator changer that can use 3 crystals: (Ge(111), Cu(111) and Cu (220)). The diffractometer is equipped with air cushions to achieve the necessary flexibility for a continuously variable wavelength. Thus, monochromator take-off angles between 28° and 54° may be set, without removing any elements of the current setup (the upper limit increases to 90° if some elements are removed). This allows to obtain neutron beams of wavelengths between 0.065 nm and 0.35 nm.

From the monochromator to the sample various Soller-type collimators can be installed (1°, 40', 30' and 12').

A low efficiency fission chamber monitor and an Ordela position sensitive detector (with two sample/detector positions) serve data collections. For high resolution measurements, a BF3 point-detector (with various receiving collimators) is available. The diffraction spectra can be measured up to 144° by a single detector, up to 141° by using "near position" and up to 151° by "far position" of the position sensitive detector. The whole angular range can be covered by 6 ("near") or 10 ("far") angular positions of this detector. The current level of background in "near" position equals to the scattered intensity from a 6 mm diameter, 0.05 mm thick, 40 mm long vanadium sample holder.

At the sample stage, the following options are available by the four-circle goniometer:

Automatic X, Y sample displacements, manual Z displacement.

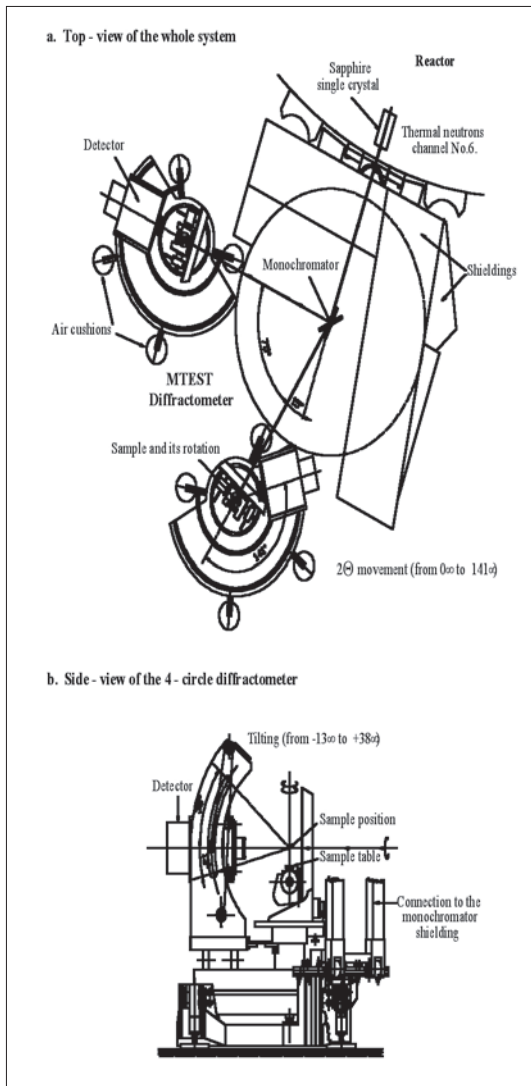
Automatic sample changer is available for 4 samples (only with four-circle goniometer).

Sample environment: vacuum-furnace (RT to 1000°C); liquid N<sub>2</sub> cryostat (scheduled to be installed in 2013 and commissioned in the first half of 2014).

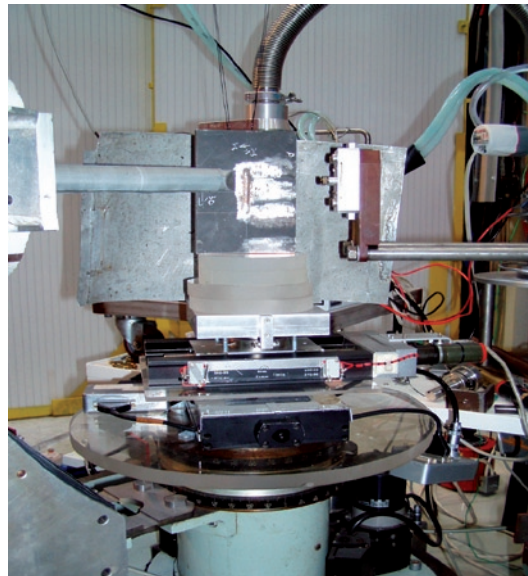
Our group is ready to help users, starting from measurements, through data evaluation, simulation and publication.

**Table 1.** Available monochromators

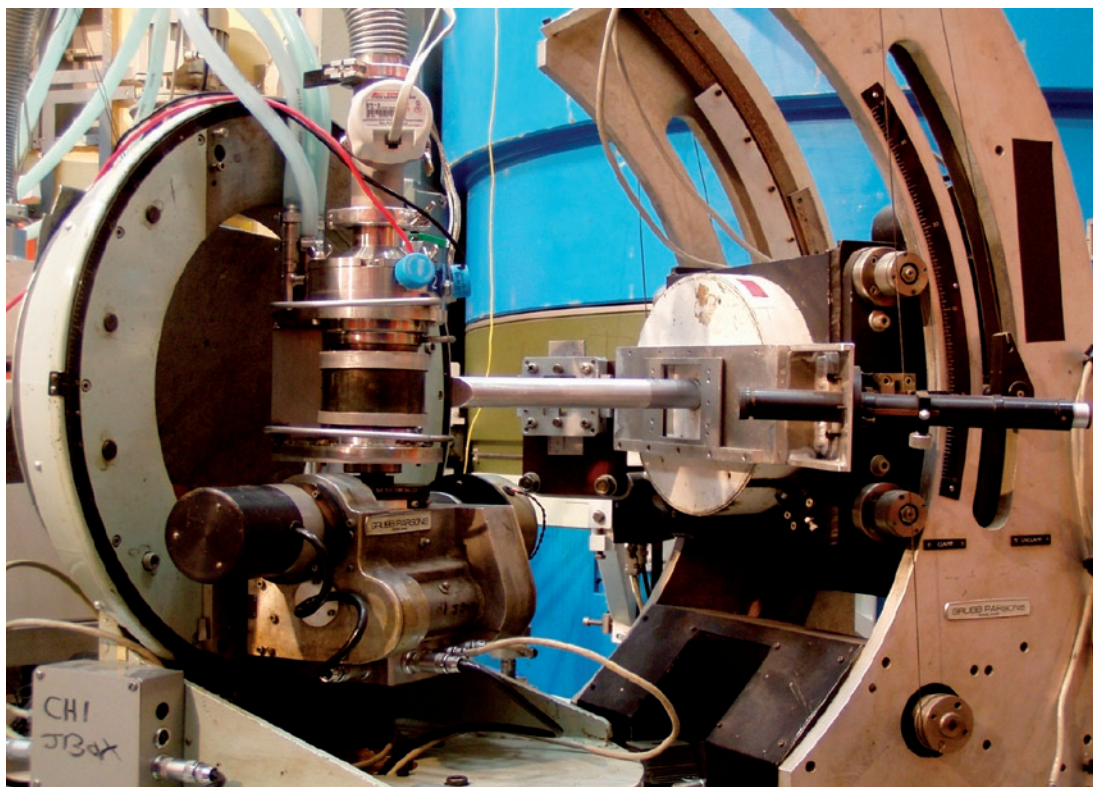
Monochromator	Ge(111)	Cu(111)	Ge(220)	Cu(220)
Wavelength at 40° take-off angle (nm)	0.223	0.143	0.137	0.087
The corresponding Q-range (Å <sup>-1</sup> )	0.25~5.35	0.4~8.35	0.4~8.7	0.65~13.7



◀ **Figure 1.**



◀ **Figure 3.**  
MTEST diffractometer with the automatic X, Ysample displacements



◀ **Figure 2.**  
MTEST diffractometer with the point detector and goniometer option together with the vacuum-furnace (RT-1000°C)

## 6.3. TOF – HIGH RESOLUTION TIME-OF-FLIGHT POWDER DIFFRACTOMETER

**Instrument scientists:** György Káli

**Instrument team:** Gy. Káli, G. Eszenyi

Institute for Solid State Physics and Optics, Wigner Research Centre for Physics

The high resolution time-of-flight powder diffractometer (TOF) at BNC has been installed to a radial thermal neutron beam in a new guide-hall in collaboration with the Hahn-Meitner-Institut. According to Monte-Carlo simulation results [2-3] it was expected that this type of instrument can outperform a conventional crystal monochromator powder diffractometer at continuous reactor source in the resolution range of  $\Delta d/d = 1-5 \times 10^{-3}$ . The other advantage to apply TOF monochromatisation to neutron diffractometry on a continuous source is the variable resolution and intensity. A full diffraction spectrum can be gained within a variable bandwidth with ultrahigh resolution or with high intensity at conventional resolutions.

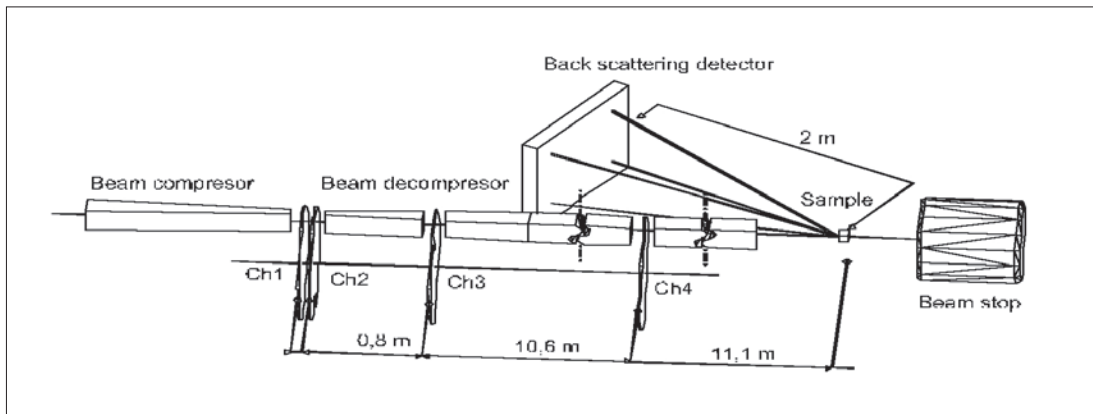
The monochromator system consists of a fast double and the two single choppers and a straight neutron guide with  $2.5 \times 10 \text{ cm}^2$  cross section at the end. The double chopper is designed for a maximum speed of 12000 rpm. While in high resolution mode the very short -  $10 \mu\text{s}$  - neutron pulse and the 25m total flight path allows us to obtain a diffractogram with an accuracy of  $10^{-3} \text{ \AA}$  (at back scattering mode) in a single measurement on polycrystalline materials, in low resolution mode liquid diffraction can be performed at good neutron intensity up to  $15 \text{ \AA}^{-1}$  scattering vector. As it was expected, the beam was contaminated with epithermal and fast neutrons because the straight guide is directed on the centre of the zone and the gadolinium coated chopper disks are transparent for them. Temporary silicon filters

was applied with which the signal-noise ratio had been increased by a factor of 5-10. The double disk chopper (Ch1 and Ch2) has two windows: a  $1.5^\circ$  opening for short pulses ( $10 \mu\text{s}$ ) and a  $15^\circ$  window for long variable pulses ( $20-200 \mu\text{s}$ ), and can be operated in parallel or counter rotating mode. The latter option is used to produce very short pulses at high speed. To minimize the opening time the neutron beam is reduced from 25 to 10 mm width at the position of the pulse choppers using a 4.5m compressor neutron guide section before and a same decompressor after them (see Figure1). Ch3 limits crosstalk between different pulses and Ch4 prevents frame overlap.

The instrument is working in back scattering mode to reach the best possible resolution. Until the planned detector (a  $60 \times 100 \text{ cm}^2$  2D detector) reach completion, a box of four  $^3\text{He}$  tube is used with a 2.5MHz event recording board. Because of the much smaller surface, the box is placed closer (2m) to the sample opposite to the designed (3m). To achieve the maximum resolution the 2D position sensitive detector will be applied in combination with a banks of 400 pieces 6 mm thick pressed  $^3\text{He}$  tubes to cover the whole available angular range. The data are acquired in so called list or time stamping mode: all the event on the detector, the chopper signs and optionally changes in the sample environment are registered with the time passed since the starting of the experiment. In this mode many uncertainties can be filtered out during the treatment and re-treatments.

### References:

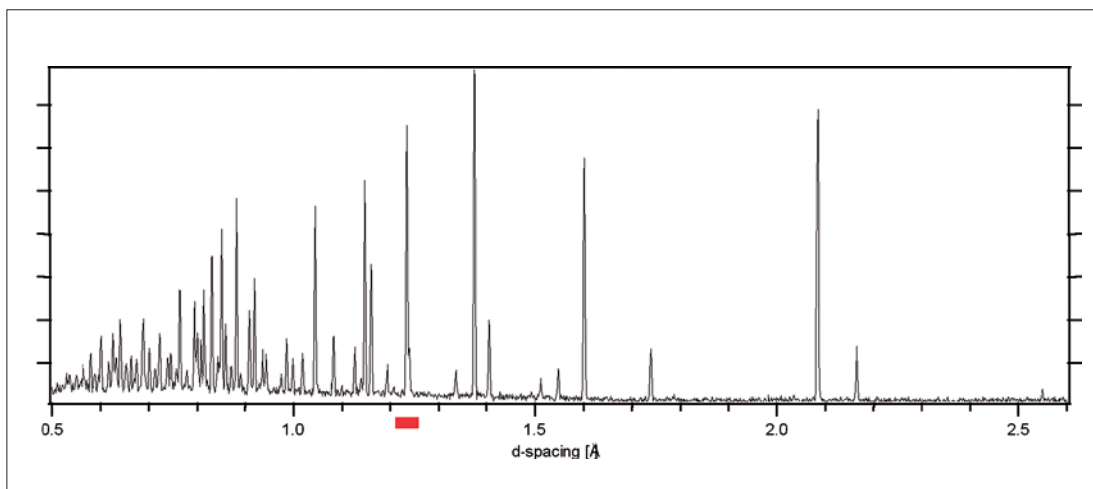
1. H. J. Bleif, D. Wechsler and F. Mezei, 2000, *Physica B*; V276-278, p 181-182
2. J. A. Stride, F. Mezei, H. -J. Bleif and C. Guy., 1997 *Physica B*; V 234-236, p. 1157-1159,.
3. J. Peters, H.-J. Bleif, Gy. Káli, L. Rosta and F. Mezei, 2006, *Physica B*; 385-86 1019-1021
4. Káli Gy., Sánta Zs., et al. 2006 *Proceedings of EPDIC10 Zeitschrift für Kristallographie*;



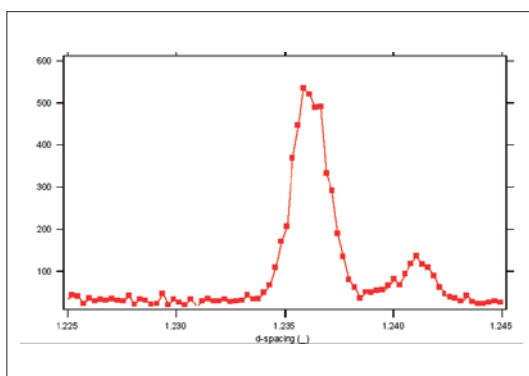
◀ **Figure 1.**  
Instrument Layout

Total flight path from chopper 1	$L=25$ m
Wavelength range	0.08-0.5 nm
Bandwidth in single experiment $\Delta\lambda$	from 0.4 nm to 0.08 nm (200 Hz)
Resolution $\Delta d/d$	$1 \times 10^{-3}$ at $d=0.15$ nm
Straight neutron guide cross section	$25 \times 100$ mm <sup>2</sup>
Coating	Supermirror NiTi, $m=2$
Beam flux at opened windows	$4 \times 10^7$ neutron/s/cm <sup>2</sup>
Pulse length	10-1000 $\mu$ s
Max. speed for the double chopper	12000 rpm

◀ **Table 1.**  
Main parameters



◀ **Figure 2.**  
The medium resolution wide-band spectra from sintered alumina illustrates the  $d$ -spacing range available for high resolution at back scattering.



◀ **Figure 3.**  
The (1 1 9) and (1 0 10) peaks from a high resolution spectra.

## 6.4. YS-SANS – SMALL ANGLE NEUTRON SCATTERING INSTRUMENT YELLOW SUBMARINE

*Instrument scientists: László Almásy, Adél Len, Renáta Ünne*

Wigner Research Centre for Physics, Neutron Spectroscopy Department

The SANS diffractometer *Yellow Submarine* covers a Q-range from 0.003 to 0.7 Å<sup>-1</sup> allowing to probe structures at length scales from 5 Å to 1500 Å. It has a wide range of applications from studies of defects and precipitates in materials, surfactant and colloid solutions, ferromagnetics, magnetic correlations, alloy segregation, polymers, proteins, biological membranes. The instrument is installed on the curved neutron guide No.2, with 4x4 cm<sup>2</sup> cross-section, made of (1.5 θ<sub>c</sub>) supermirrors. The beam is monochromatized by a multidisc type velocity selector, (L. Rosta: Physica B 174 (1991) 562) the rotation speed can be tuned between 700 and 7000 rot/min (wavelengths between 3.5 and 25 Å). The width Δλ/λ of the transmitted wavelength distribution can be varied between 12% and 30% by changing the tilt angle between the selector axis and the direction of the neutron beam. 5 m and 1m collimation distances allow the optimization of flux and resolution for different sample-to-detector distances.

### Sample environment

In most of the experiments an automatic sample changer with 6 positions is used. It can be thermostated from an external bath between -10 and 100°C. A 11 position sample changer can be used for ambient temperature experiments. Liquid nitrogen cryostat, or closed cycle refrigerator can be used (from 10K-300K). Electromagnets can also be mounted on the sample table (field 1.4T in the gap 25mm)

### Detector

The scattered neutrons are detected by a 64 x 64 pixels (1cm x 1cm pixel size) two dimensional position sensitive LETI (Grenoble, France) detector filled with BF<sub>3</sub> gas.

### Data acquisition

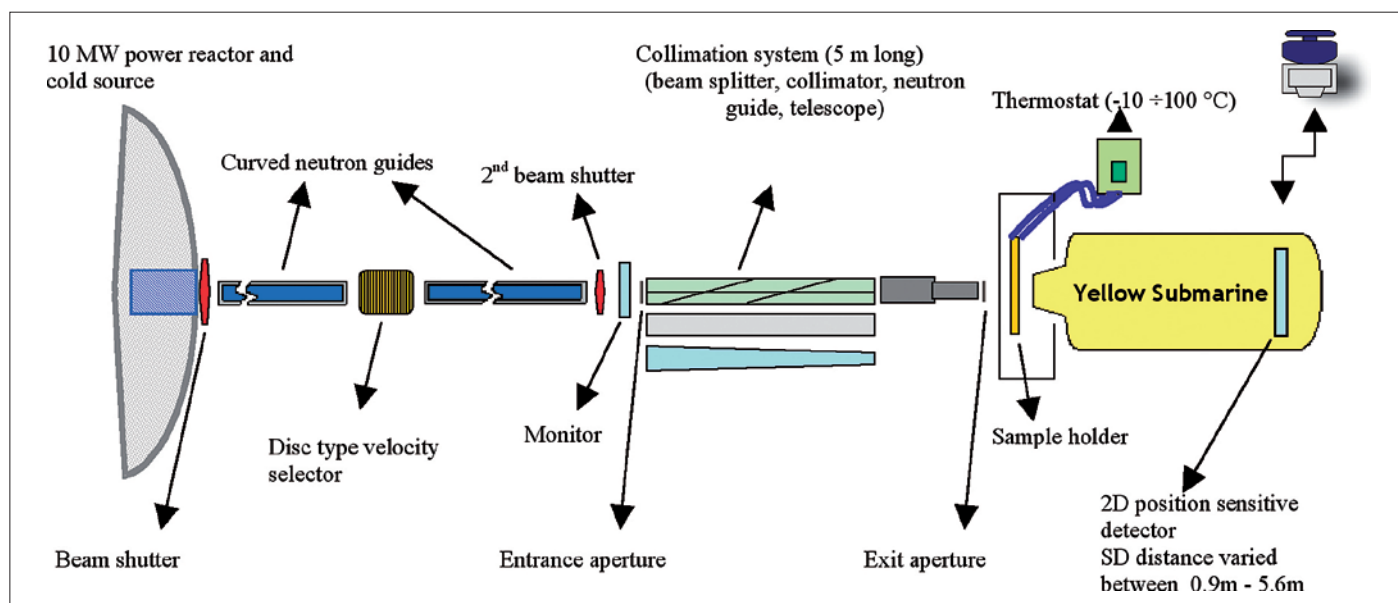
The control and data acquisition electronics and software have been made by Laboratoire Léon Brillouin, Saclay, France, and ANTE Ltd., Budapest, Hungary.

**Table 1.** ▶  
Main characteristics

Beam tube :	Cold neutron guide No.2/1
Monochromator :	Multidisk velocity selector
Detector:	2D position sensitive, 64 x 64 cm <sup>2</sup> , filled with BF <sub>3</sub> gas
Collimations :	1 m or 5m
Flux at the guide exit :	5x10 <sup>7</sup> n/cm <sup>2</sup> /sec
Sample-to-detector distance:	Continuously adjustable between 0.92 and 5.6 m
Incident wavelength:	3 – 25 Å
Wavelength spread:	Adjustable between 12 – 30%



**Scheme of the SANS diffractometer Yellow Submarine**



## 6.5. REF – COLD NEUTRON REFLECTOMETER

*Instrument scientists: Tamás Veres, László Cser*

Wigner Research Centre for Physics, Neutron Spectroscopy Department

The schematic view of the reflectometer is shown in the Figure 1 below. The original position of REF was the guide No. 3. This scheme illustrates the configuration of the reflectometer after relocation to the guide No. 1. Due to the geometrical restrictions in the guide hall the neutron path had to be aligned parallel with the guide No.1. This solution could be realised by introduction of a double monochromator system with pyrolytic graphite (PG). The slit system, the sample holder table and the control electronics remained as it

was in the previous position. The main technical novelty is the installation of a 2D position sensitive detector.

The reflectometer operates at wavelength:  $\lambda = 4.28 \text{ \AA}$   
Maximal scattering angle:  $\Theta_{\text{scatt}} = 5^\circ$   
Angular resolution is variable by changing of the slit widths using micrometer screws down to 0.0055 grad.  
Flux of the neutrons:  $200 \text{ n/cm}^2 \text{ sec}$   
Background for the whole detector:  $5 \text{ n/sec}$

### Utilization of the reflectometer

- quality control of supermirror multilayers;
- thin layer studies for a PhD work.

In the current configuration with the relatively low

flux and increased background the applicability of the reflectometer is mostly limited to the investigation of large area industrial samples. An example is shown in Fig.2.

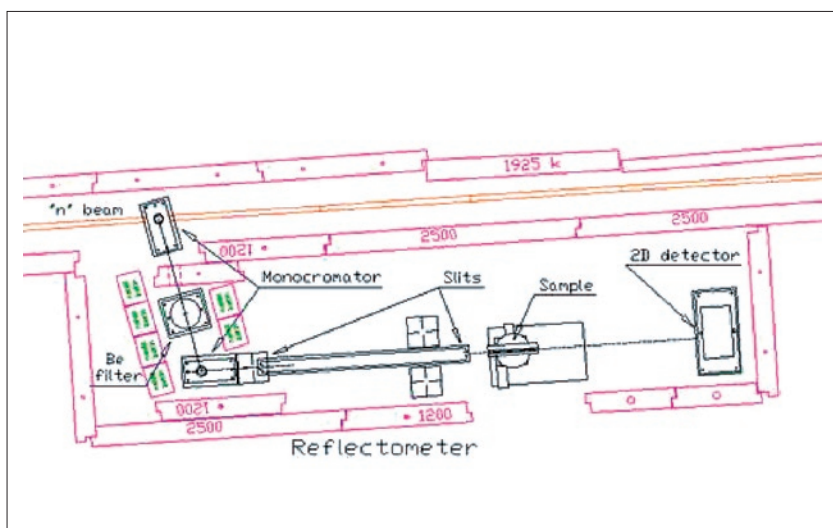


**Figure 1.**  
The schematic view of the reflectometer (REF) at the guide No.1.

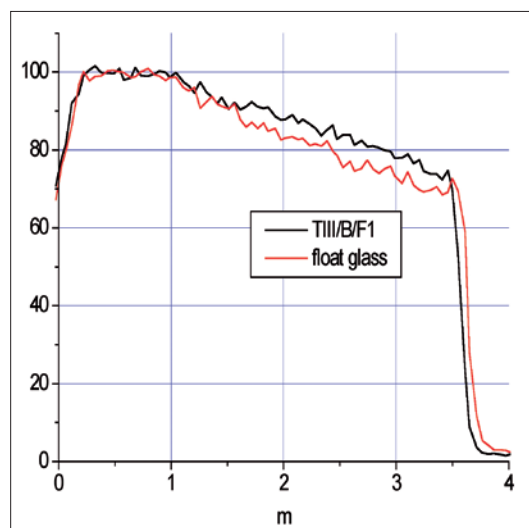


**Figure 2.**  
Tests of  $m=3,5$  supermirror coating on polished borokrone glass (RMS surface roughness:  $4 \text{ \AA}$ ) measured by neutron reflectometry, compared to float test glass.

### Improvements in progress

The double monochromator system is being replaced by a focusing phase space compressing geometry using high quality PG crystals. Due to the improvement in the mosaicity and focusing geometry, according to Monte-Carlo simulations,

a tenfold increase of beam intensity is expected to be achieved at the sample position. The PSD detector is also to be upgraded for the 2D analysis by a new data acquisition system. It is also essential to get rid of the epithermal neutrons

causing the dominant part of the background. For that both the shielding of the guide No.1 and that of the reflectometer will be improved. In this way the reflectometer will be again attractive for the users by offering an intensity/background ratio much better than at the earlier position at the guide No.3.

Potential use after upgrading:

- Fast quality check of supermirrors;
- continuation of the standing-wave observation;
- application for nanometer thickness measurements;
- application for biological investigations (e.g. bio-membranes).

**Typical papers for REF:**

- Veres T, Cser L: Study of the reflectivity of neutron super mirrors influenced by surface oil layers; Rev Sci Instr; 81, 063303, 2010
- Bodnarchuk V, Cser L, Ignatovich V, Veres T, Yaradaykin S: Investigation of periodic multilayers; JINR Comm; E14, 127, 2009
- T. Veres , L. Cser, V. Bodnarchuk, V. Ignatovich, Z.E. Horváth, B. Nagy: Investigation of periodic

## 6.6. GINA - NEUTRON REFLECTOMETER WITH POLARIZATION OPTION

*Instrument scientists: L. Bottyán, D.G. Merket, B. Nagy*

Wigner Research Centre for Physics

### **CHARACTERIZATION OF THIN FILMS AND MULTILAYERS**

The GINA reflectometer is a constant-energy angle-dispersive, vertical-sample instrument [1,2]. The setup is displayed in Figure 1 and the operation parameters are summarized in Table 1. The focusing graphite monochromator MONO provides neutrons with wavelength 4.6 Å and  $\approx 1\%$ . The polarized neutron beam is produced by using a magnetized supermirror (P1) and an adiabatic radio-frequency (RF) spin flipper [3] (SF1). The beam scattered on the sample may undergo spin analysis by an identical setup of a spin flipper and a spin analyzer (P2), and finally it is detected by a two-dimensional position sensitive neutron detector (DET). The incident intensity is monitored by a low efficiency ( $\sim 0.1\%$  at  $\lambda = 4.6$  Å) beam intensity monitor (IM). The components of the reflectometer are mounted on two heavy-load optical benches. The first one supports the beam shutter (BS), the IM, the beryllium filter (BF), the slit (S1) and the SM polarizer (P1), the adiabatic RF spin flipper (SF1) and the slit (S2). The downstream end of the bench is fixed to the central sample tower ST and supports the various sample environment components (electromagnet, cryostat, etc.). The incident angle on the sample surface is set by the major ( $\theta$ ) goniometer of ST. The second bench – the  $2\theta$ -arm of the reflectometer – supports the slit S3, the spin flipper SF2, the spin analyzer P2, and the detector along with its electronics and dedicated control PC mounted underneath. The slit S4 in front of the detector is optionally used when data collection is restricted to specularly scattered neutrons. The  $2\theta$ -motion is driven by a wheel running on the marble surface while the corresponding air pads are activated.

### **SAMPLE ENVIRONMENT**

GINA is dedicated to reflectometry of magnetic heterostructures, for studies requiring different environmental parameters, such as (low) temperature and (occasionally high) external magnetic fields. A closed-cycle cryostat (12 to 300 K range) can be

The monochromator MONO is situated behind a concrete biological shielding (SH) and comprises five highly oriented pyrolytic graphite crystals on small motorized 2-circle cradles for horizontal alignment and vertical focusing. Higher harmonics intensity is efficiently filtered by a Be block. The transmission of the filter is 87% for  $\lambda = 4.6$  Å, with liquid nitrogen cooling.

The polarized neutrons are produced by an Fe-Co/Si magnetic SM placed in an in-plane vertical magnetic field of 30 mT in transmission geometry (P1 in Figure 1). Spin analysis of the specularly reflected beam is performed by a single magnetic SM analyzer (P2) of identical construction with P1. In order to decrease the scattering of neutrons by the beam-line components, adiabatic RF spin flippers are installed. The flipper coil is placed in a longitudinal gradient field with a center field of 5.6 mT. The flipper coil is part of a resonant circuit, with typical values of effective RF current and bandwidth of 4 A and 4.5 kHz at the resonance frequency of 166 kHz

Fine definition of the beam is maintained by the four slits with cadmium blades. The blades are operated with a precision of 0.05 mm. With these optical elements the setup exhibits a relative Q-resolution of 10% to 2% for the available Q-range of 0.005 to  $\sim 0.25$  Å<sup>-1</sup>.

Scattered neutrons are registered by a delay line type multi-wire proportional chamber with active area of 200x200 mm<sup>2</sup> and spatial resolution of 1.6 mm (FWHM). The detector is filled with a <sup>3</sup>He / CF<sub>4</sub> gas mixture of 2.5/3 bar partial pressures and is encased in a boron-containing shielding for background suppression.

mounted on the sample tower ST with or without the electromagnet. At GINA an air-cooled electromagnet is available, which generates magnetic fields up to 550 mT. The optional water-cooled air core coil pair provides fields up to approx. 35 mT.

## EXAMPLE REFLECTOGRAM

Our example in Figure 2 highlights the polarized specular reflectivity performance of GINA on a sample of a  $20 \times 20 \text{ mm}^2$  isotope-periodic multilayer prepared with a  $\text{MgO}(001)/[{}^{\text{nat}}\text{Ni}(15\text{nm})/{}^{62}\text{Ni}(5\text{nm})]_5$  nominal layer structure by molecular beam epitaxy (MBE) [4]. Spin-dependent neutron reflectivities were recorded at room temperature. The sample was magnetized from the initial nonmagnetized (as prepared) state by 50 mT in-plane external magnetic field. The total data collection time was 56 hours. The measured  $R^+$ ,  $R^-$  and the spin asymmetry are displayed in Figure 2. The *simultaneous* fit using FitSuite program [5] to the measured  $R^+$  and  $R^-$  (solid lines in Figure 2) reveals  $(17.5 \pm 0.5) \text{ nm}$  and  $(5.35 \pm 0.5) \text{ nm}$  thickness for  ${}^{\text{nat}}\text{Ni}$  and  ${}^{62}\text{Ni}$  layers, respectively. The

magnitude of the fitted scattering length densities ( ${}^{\text{nat}}\text{SLD} = (9.13 \pm 0.5) \times 10^{-6} \text{ \AA}^{-2}$  and  ${}^{62}\text{SLD} = (-7.01 \pm 1) \times 10^{-6} \text{ \AA}^{-2}$ ) show only minor deviations from their known bulk values. The magnetizations of the  ${}^{\text{nat}}\text{Ni}$  and  ${}^{62}\text{Ni}$  layers were constrained identical and the fit provided  $0.44 \pm 0.12 T$ . This value amounts 66% of the known room temperature saturation magnetization  $M_s$  of the bulk Ni. According to the magneto-optical Kerr-loops the magnetization at 50 mT (the value of external field in the reflectivity measurement) is 74% of the saturation magnetization of the same sample. The lower value of 66% given by the reflectivity fit can be explained by a somewhat lower magnetization in the virgin magnetization state of the sample during the reflectivity experiment.

## References:

1. L. Bottyán, D.G. Merkel, B. Nagy, J. Major, Neutron News, 23, 21 (2012)
2. L. Bottyán, D.G. Merkel, B. Nagy, Sz. Sajti, L. Deák, G. Endrőczy, J. Füzi, A.V. Petrenko, J. Major, submitted to Review of Scientific Instruments
3. S.V. Grigoriev, A.I. Okorokov and V.V. Runov, Nucl. Instrum. and Meth. A 384, 451 (1997)
4. The sample was prepared in the MBE laboratory of the KFKI Research Institute for Particle and Nuclear Physics Budapest. This laboratory provides growth and characterization services of metallic multilayers – including deposition of various stable isotopes ( ${}^{57}\text{Fe}$ ,  ${}^{62}\text{Ni}$ , etc.) also for external users.
5. Sz. Sajti: FitSuite data fitting and simulation program code available from [www.fs.kfki.hu](http://www.fs.kfki.hu)

Wavelength	$3.9 \div 5.1 \text{ \AA}$ in five steps
Present wavelength	$4.6 \text{ \AA}$
Max. scattering angle	$\geq \theta = 35^\circ$
Angular resolution ( $\Delta\theta$ )	$0.003^\circ$
$\Delta\lambda/\lambda$	$\sim 1\%$
Background level	$0.01 \text{ cps cm}^{-2}$
Detector	2D PSD, $200 \times 200 \text{ mm}^2$
Detector spatial resolution	$1.6 \times 1.6 \text{ mm}^2$
Neutron flux at the monochromator position	$4 \times 10^5 \text{ n} \times \text{cm}^{-2} \times \text{s}^{-1}$
Background reflectivity	$< 7 \times 10^{-6}$
Overall polarization efficiency	0.9

Table 1.

Operation parameters of GINA

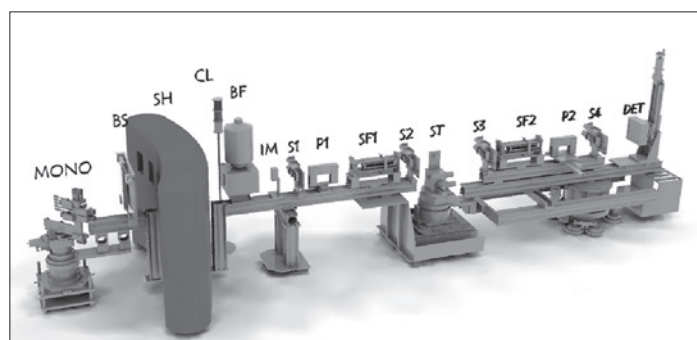


Figure 1.

The layout of the GINA neutron reflectometer.

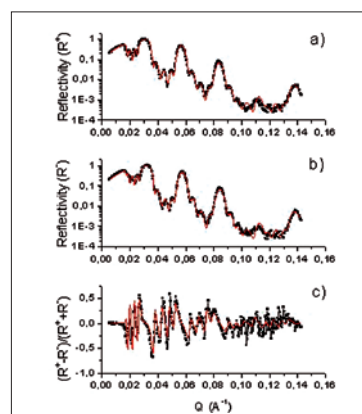


Figure 2.

Measured  $R^+$ ,  $R^-$  specular polarized reflectivities and the derived spin asymmetry,  $(R^+ - R^-)/(R^+ + R^-)$  on  $\text{MgO}(001)/[{}^{\text{nat}}\text{Ni}(15\text{nm})/{}^{62}\text{Ni}(5\text{nm})]_5$ . The statistical errors for most data points are smaller than the symbol size.

## 6.7. ATHOS - COLD NEUTRON TREE-AXIS SPECTROMETER

*Instrument scientists: Gyula Török, Alex Szakál*

Wigner Research Centre for Physics, Neutron Spectroscopy Department

The cold neutron three-axis spectrometer (TAS) at BNC is installed on the 17 m position of the first neutron guide (NG1). The beamline is a borofloat glass substrate NiTi coated supermirror ( $m=2$ ) guide. This instrument was in extensive use on a thermal beam in the period of 1972-86. Since the reactor reconstruction and the cold source installation this instrument – with a major upgrade – has been relocated on this cold neutron guide and it was named ATHOS.

The ATHOS instrument provides moderate resolution (0.01-1.0 meV) with sufficient intensity for use in a wide range of problems. It is ideally suited for the study of phonon dispersion curves in single crystals, tunneling modes of energies greater than  $\approx 0.025$  meV, quasielastic scattering studies of rotational and non-local diffusion in the time regime of picoseconds, vibrations of surfaces or molecules adsorbed on surfaces and phonon density of states for that large class of materials which contain hydrogen. Specific mention of the applicability of neutron scattering to the study of hydrogenous materials should be emphasized here. The hydrogen nucleus has the largest cross section (scattering interaction) for neutron scattering and is predominantly incoherent. Hydrogen vibrations have been detected in samples containing as little as 0.01 mol. of total hydrogen in the sample. Because the instrument is energy sensitive, it can also be used to measure purely elastic scattering whether it be due to coherent (nuclear or magnetic) or incoherent events. Information on the time-averaged structure of the atomic and molecular constituents of the sample is therefore accessible. Finally, the ability of producing and analyzing polarized neutrons allows more detailed measurement of the magnetic properties of the sample. These magnetic properties can be static, i.e., a structural description of the magnetic moments, or dynamic such as magnons.

The range of energies (0.025-14 meV) of excitations accessible to this instruments is substantially larger (although with poorer resolution) than available with the spin-echo and backscattering spectrometers. Independent control of the momentum ( $Q$ ) and energy transfer ( $E$ ) is routine if required as opposed to the time of flight spectrometer in which  $Q$  and  $E$  are related by the instrumental configuration. The monochromatic beam is provided by a 90mm high focusing multi-blade ZYA grade pyrolytic graphite monochromator.

The movable part of the monochromatic shielding has a chain type construction. Changing the incident wavelength the whole chain is driven by the monochromator-sample arm. This construction automatically provides the most effective shielding near the detector area (see Fig.1). This enables very low background conditions (1 neutron/300s).

For higher order filtering in the incident monochromatic beam a multidisc neutron velocity selector can be installed in front of the sample goniometer, or Ge analyzer used. The beam divergence is determined by thin film Soller-type Mylar collimators coated with gadolinium-oxide paint. A 200x200 mm<sup>2</sup> two dimensional position sensitive <sup>3</sup>He detector in medium resolution mode was installed in 1999. Using this detector the efficiency of data collection has been raised 40 times in quasielastic mode.

Although this tree-axis spectrometer has been designed for structural and dynamical studies of condensed matter – because of the limited number of other operational equipment – the instrument is extensively used in a multi purpose regime, e.g. for high-resolution diffractometry, strain analysis, reflectometry, quasielastic and inelastic scattering. This spectrometer has been served also for testing polarization setups, detectors, monitors, any other neutron beam components developed in our

Laboratory. For example a neutron spin-echo setup was also realized on this instrument (Fig.1). This "mini-spin-echo" can be used for training and

methodical development purposes (Török Gy, Lebedev VT, Nagy A, Gordeev GP, Zsigmond G, *Physica Status Solidi C* **1**, No 11, 3182 (2004).

Beam tube :	Cold neutron guide No.1/1
Monochromator :	pyrolitic graphite 90x80 mm (24min mosaicity)
Analyser :	pyrolitic graphite 50x90 mm (24min mosaicity), or Ge monocrystal (15min mosaicity)
Collimations :	interchangeable 45', 30', 15'
Range of monochromator angle:	$36^\circ < 2\theta < 126^\circ$
Range of scattering angle :	$-120^\circ < 2\theta < 70^\circ$
Range of analyser angle :	$-40^\circ < 2\theta < 120^\circ$
Range of crystal orientation :	$0^\circ < 2\theta < 360^\circ$
Angular resolution :	0.01°
Flux at specimen :	$2 \times 10^6$ n/cm <sup>2</sup> /.sec
Beam size :	25x90 mm <sup>2</sup>
Momentum transfer :	0 – 2.7 Å <sup>-1</sup>
Energy transfer :	0 - 9 meV
Characteristic resolution at 3.3 Å	120-150 µeV
Sample enviroment :	Thermostate (-20°C - 100°C), cryostat (15 K) , magnet up to 2T (max scattering angle 100 deg) furnace up to 1000°C

◀ **Table 1.**  
Main parameters  
of the spectrometer



◀ **Figure 1.**  
Neutron spin-echo setup  
installed on the TAS

## 6.8. TAST/HOLO - THERMAL NEUTRON TREE-AXIS SPECTROMETER AND NEUTRON HOLOGRAPHIC INSTRUMENT

*Instrument scientists: Alex Szakál, Gyula Török*

Wigner Research Centre for Physics, Neutron Spectroscopy Department


The thermal neutron three-axis spectrometer (TAST) at BNC is installed on the thermal neutron channel No.8 at the Budapest Research Reactor. The instrument provides moderate resolution (~1.0 meV) with sufficient intensity for use in a wide range of problems. It is ideally suited for the study of phonon and magnon dispersion curves in single crystals, phonon density of states for that large class of materials which contain hydrogen. Independent control of the momentum ( $Q$ ) and energy transfer ( $E$ ) is routine if required as opposed to the time of flight spectrometer in which  $Q$  and  $E$  are related by the instrumental configuration. This triple axis spectrometer can also be used in a multipurpose regime, e.g. for high-resolution diffractometry, strain analysis, quasielastic and inelastic scattering as well as for thermal beam irradiation and transmission tests.

The monochromatic beam is provided by a 90mm high doubly focusing multi-blade Cu monochromator. In order to suppress the intensity of fast neutrons 15 cm long sapphire single crystal

is inserted in the primary shutter. For higher order filtering in the incident monochromatic beam a Ge analyzer can be used. The beam divergence is determined by thin film Soller-type Mylar collimators coated with  $Gd_2O_3$ .

A highly efficient (90% at 1 Å)  $^3He$  single counter of 1" diameter is applied as detector. A two dimensional position sensitive detector in medium resolution mode is also available. Using this detector the efficiency of data collection can be raised about 40 times in quasielastic mode. For energy analyzing a focusing pyrolytic graphite crystal assembly is used.

The spectrometer can be equipped by an Eulerian Cradle, or a goniometer that can hold various sample environment devices up to a weight of 100 kp. Since 2005 TAST can be used also as a dedicated instrument for atomic resolution neutron holography measurements both in neutron or gamma ray detection modes.

**Table 1.**   
Main parameters  
of the spectrometer

Beam tube :	Channel No.8 (radial - sapphire single crystal filter)
Monochromator :	Cu 200 (doubly focusing)
Analyzer :	pyrolytic graphite 002 (horizontally focusing)
Detector	$^3He$ single
Range of monochromator angle:	$14^\circ < 2\theta < 90^\circ$
Range of analyzer angle :	$-100^\circ < 2\theta < 120^\circ$
Range of crystal orientation :	$0^\circ < 2\theta < 360^\circ$
Angular resolution :	$0.01^\circ$
Flux at specimen at 1 Å:	$2 \times 10^6$ n/cm <sup>2</sup> /.sec
Beam size :	50x50/10x15 mm <sup>2</sup> (depends on focusing)
Momentum transfer :	$0.2 - 10 \text{ \AA}^{-1}$
Energy transfer :	1 - 60 meV



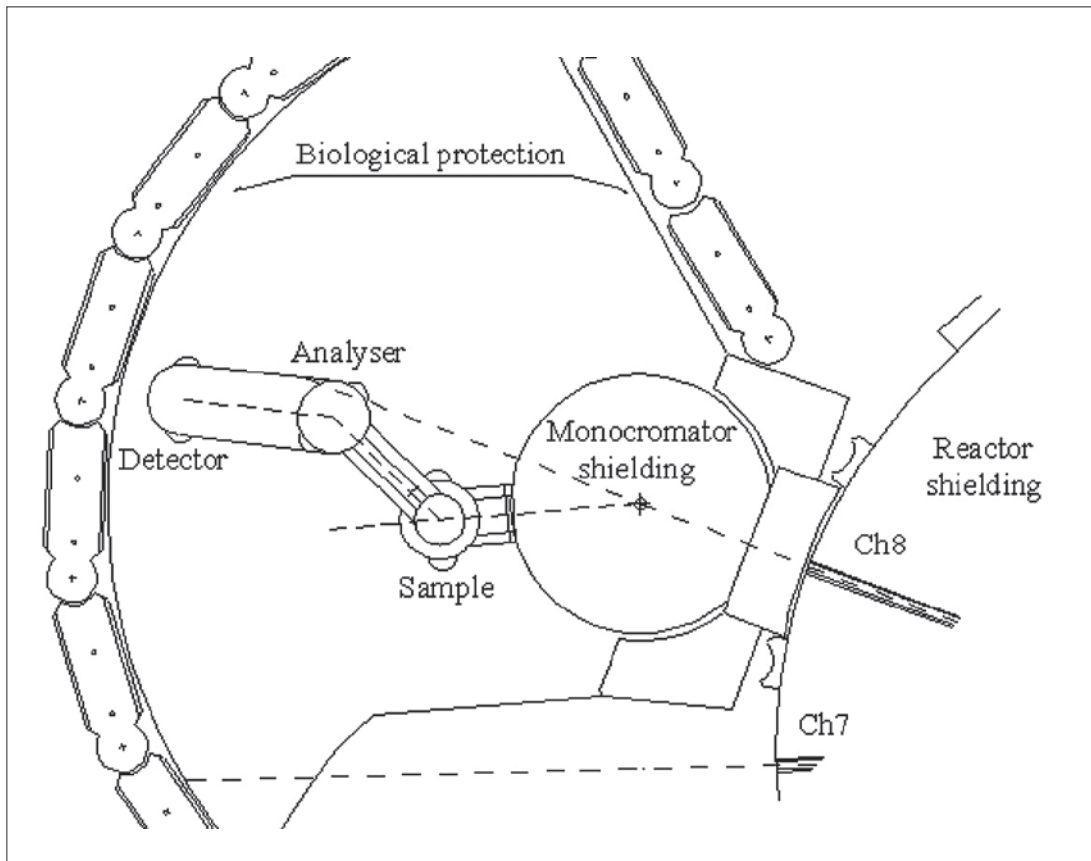
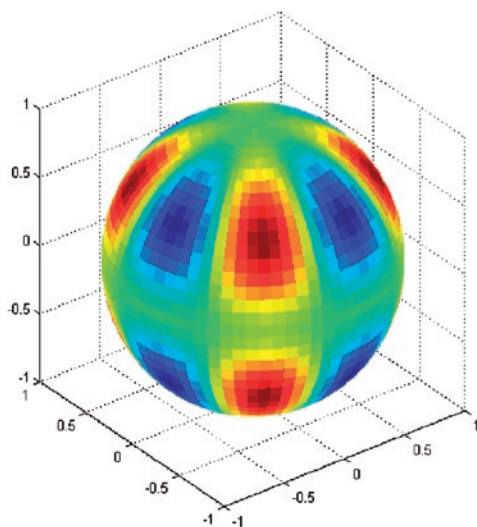


Figure 1. Layout of the thermal neutron three-axis spectrometer

## New facility in our research activity: neutron holography setup

The principle and two ways of experimental realisation of atomic resolution neutron holography was proposed by Lószly CSER (BNC). An international team lead by L. Cser has performed the first successful experiment proving the feasibility of the so called internal detector on a Pb-Cd single crystal. Neutron holography is a unique method for direct measurement of local lattice distortions with sub-picometer accuracy. On the TAST instrument a dedicated holography setup was installed at the Budapest Reactor (Figure on the right). The first holographic spectra were recorded on an  $\text{NH}_4\text{Cl}$  single crystal.



## 6.9. DYNAMIC RADIOGRAPHY STATION

*Instrument responsible: Horváth László, Márton Balaskó*

Centre for Energy Research, Hungarian Academy for Sciences

Neutron radiography utilizes transmission to obtain information on the structure and/or inner processes of a given object. It is used for various non-destructive test measurements. A dynamic

radiography station has been built out visualize and analyse the flow of fluids, the evaporation and the condensation processes in closed metal objects, tube systems and other types of dynamic events.

### **Main parameters of the dynamic radiography station:**

- Thermal channel: No. 2

#### **„A” In the conventional arrangement:**

- Complex pin-hole type collimator for neutron and gamma radiation with a collimation ratio of  $L/D = 170$
- Neutron flux at the objects position:  $6 \cdot 10^7 \text{ n} \times \text{cm}^{-2} \times \text{sec}^{-1}$ , behind of CD an In filter:  $3 \times 10^6 \text{ n} \times \text{cm}^{-2} \times \text{sec}^{-1}$
- Gamma intensity:  $\sim 8,5 \text{ Gy/h}$
- X-ray energy: 50-300 keV; 5 mA
- Variable beam diameter, with a maximum of 150 mm at the object position.

Maximum surface for investigation:  
 $700 \times 1000 \text{ mm}^2$

- Maximum weight of the investigated object: 250 kg

#### **„B” In the extended inspection area (for study of helicopter rotor blades)**

- Maximum beam diameter: 185 mm
- Maximum surface: for investigation  $9750 \times 700 \text{ mm}^2$
- Maximum weight of the investigated object: 200 kg

- Practicable to study, the efficiency of the moisture condition of the inspected objects, by a Moistening module is driven by a High pressure water pump
- Converters (radiation into light): for neutron radiography NE 426 scintillation screen with resolution of  $100 \mu\text{m}$ ; for gamma and X-ray radiography NaCs single crystal with resolution of  $200 \mu\text{m}$ , or ZnS screen with resolution of  $100 \mu\text{m}$
- Variable filters: Cd, In
- Detection of the radiography image: low-light-level TV camera with a light sensitivity of  $10^{-4} \text{ lux}$ , imaging cycle is 40 msec, and a double cooled CCD camera ( $756 \times 580 \text{ pixel}$ ), 10 bit.
- Radiography image is visualised on monitor, stored by S-VHS video recorder and DVD recorder and for further quantitative analysis a Quantel image processing system is used with Sapphire V.0.5 software, and an Iman  $\beta$  version software.
- Photo-luminescent Imaging Plates technique used by X-ray radiation or by neutron radiation with transfer method BAS IP-SR 20x25 and IP-SR 20x40 [In and Dy ( $100 \mu\text{m}$ ) foils]. The evaluation of exposed IP-s are by BAS 2500 reader unit used an AIDA picture reconstruction software.

***Unique feature of the dynamic radiography station :***

Our radiation sources give a possibility to study semi-simultaneously or simultaneously the investigated objects by neutron-, gamma- and X-ray radiography to use the all advantages of the

complementary features of the different radiations. Simultaneously, other non-destructive inspection as vibration diagnostics and acoustic emission can be used.

## 6.10. NORMA - NEUTRON OPTICS AND RADIOGRAPHY FOR MATERIAL ANALYSIS

*Instrument scientists: Zoltán Kis, László Szentmiklósi*

Centre for Energy Research, Hungarian Academy for Sciences

The NORMA facility is located at the end position of the neutron guide NG1 as a complementary part of the NIPS facility. It has been designed for neutron radiography (NR) and tomography (NT), and as a position feedback for imaging-driven Prompt Gamma Activation Imaging (PGAI). In latter mode, the combination with the element information obtained with NIPS gamma spectroscopy detector makes well localized element analysis possible.

The beam arrives through a flight tube of 5×5 cm<sup>2</sup> cross section into a sample chamber with dimensions of 20×20×20 cm<sup>3</sup> for imaging and position-sensitive applications. It is made of AlMgSi alloy, and lined from inside with <sup>6</sup>Li-enriched polymer. By removing one or more side panels, larger objects (or at least parts of those) up to 5 kg weight could also be imaged (such as a sword, vase, stones, etc.). Samples can be loaded manually from the top, or placed onto an XYZw motorized sample stage with a travel distance of 200 mm and a guaranteed precision of 15 μm, which is introduced to the sample chamber from the bottom.

The imaging system of the NORMA setup consists of a 100 μm thick <sup>6</sup>Li/ZnS scintillator, an Al coated quartz mirror and a cooled, black-and-white, back illuminated Andor iKon-M CCD camera with 1024×1024 pixels and 16-bit pixel depth, mounted

in a light tight aluminum housing. The custom optics projects a 48.6×48.6 mm<sup>2</sup> field of view (in which the beam spot is about 40×40 mm<sup>2</sup>) onto the 13.3×13.3 mm<sup>2</sup> sensitive surface of the CCD chip. The spatial resolution of the imaging system changes linearly between 230-660 μm, proportional to the 1.5-100.5 mm distance from the scintillator screen. The measured L/D ratio, characteristic to the neutron beam's divergence, was found to be 233. The specifications of the facility are listed in Table 1. The spatial distribution of the beam is illustrated in Figure 1a; whereas the energy distribution of the neutrons, measured by time-of-flight technique, is shown in Figure 1b.

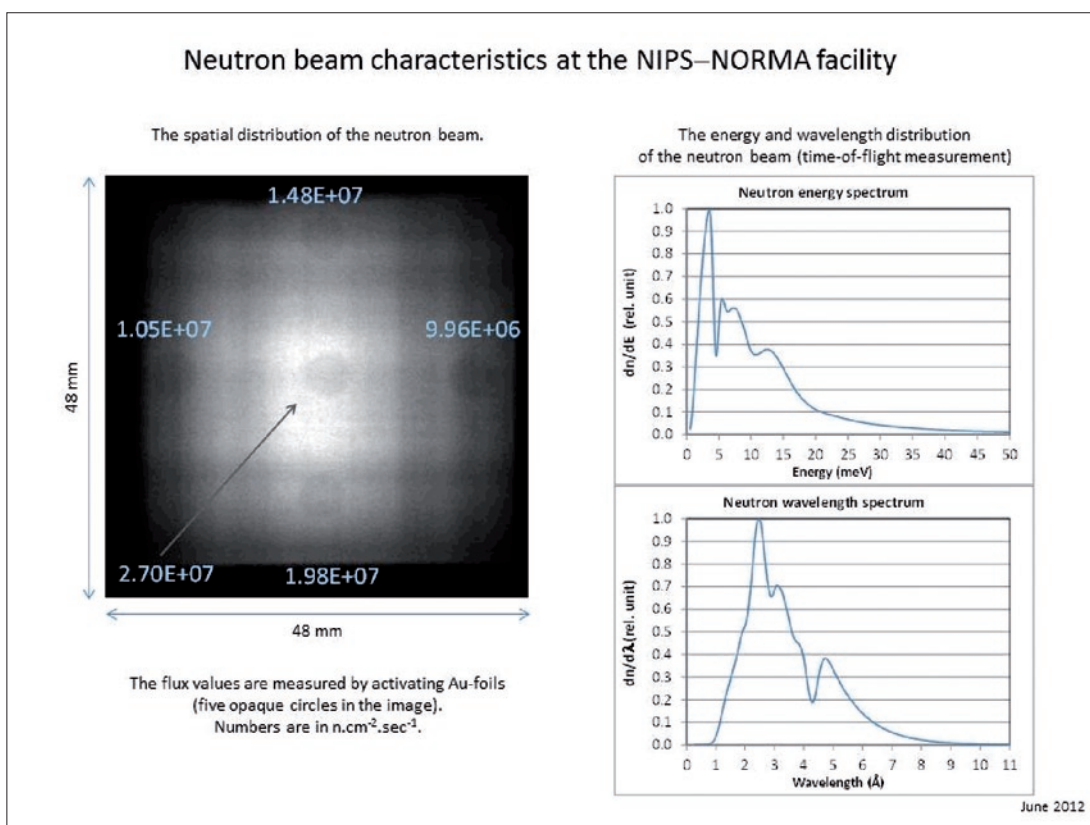
The radiography images taken at NORMA require several steps of data treatment. The spatial inhomogeneity of the beam and the thermal noise of the camera should be removed. These are called 'beam image correction' and 'dark image correction', respectively. In tomography, the goal is to determine a measure of the interaction probability between the material and the neutron as a function of spatial coordinates. This quantity delivers the structural information about the interior of the sample. The reconstruction codes, such as the OCTOPUS reconstruction software, apply the inverse Radon-transformation and filtered back projection algorithms. The visualization of the dataset in 3D space (volume rendering) is carried out using VGStudio 2.1.

---

*NORMA - Neutron Optics and Radiography for Material Analysis >*

Beam size for imaging:	up to 40×40 mm <sup>2</sup>
Beam cross section for PGAA/PGA:	2×2cm <sup>2</sup> , 1.4×1.4cm <sup>2</sup> , 1×1cm <sup>2</sup> , 42mm <sup>2</sup> , 23mm <sup>2</sup> , 10mm <sup>2</sup> , 5mm <sup>2</sup> , 1×20 mm <sup>2</sup> slit
Collimation ratio (L/D) :	233
Beam energy distribution:	Cold beam
Thermal-equivalent flux at target:	≈2.7×10 <sup>7</sup> ×cm <sup>-2</sup> s <sup>-1</sup>
Scintillator screen :	100 μm thick <sup>6</sup> Li/ZnS scintillator on an Al plate
Mirror:	Al coated quartz mirror set in 45 degree to the neutron beam
Lens:	Canon EF 85mm f1.2 L II USM
Standard imaging detector :	Back-illuminated Andor iKon-M 934 CCD camera with 1024×1024 pixels and 16-bit pixel depth
Spatial resolution:	230-660 μm according to the 1.5-100.5 mm distance from the scintillator screen
Sample stage:	XYZw motorized sample stage with a travel distance of 200 mm and a guaranteed precision of 15 μm
Sample chamber dimensions:	20×20×20 cm <sup>3</sup>
Sample environment:	Ambient pressure and temperature

Table 1. Specifications of the NORMA facility



Figures 1a. and 1b. a) The spatial distribution of the neutron beam at the sample position of the NIPS/NORMA facility and some flux values measured by gold foils; and b) the energy and wavelength distribution of the neutron beam.

## 6.11. BIO – BIOLOGICAL IRRADIATION CHANNEL

*Instrument responsible: Balazs Zabori*

Centre for Energy Research, Hungarian Academy of Sciences

An irradiation facility existed at the BRR from 1968 for 18 years. During the reconstruction of the reactor a new system for biology and dosimetry research was designed and completed in 1995. The final tests and the investigation of the beam quality were performed in early 1996. Since that time the system is in continuous operation and improvement.

The channel lock consists of 3 steel and heavy-concrete segments turnable by an excentrical axis to open and close the channel. There is an internal remotely controlled filter holder at a distance of 262 cm from the core which has six windows with the following materials: four Bi disks of 5, 10, 15 and 20 cm thick and one Pb disk of 20 cm, the 6<sup>th</sup> one is an open hole. At the orifice of the beam tube two cylindrical tanks were constructed of alumina to serve as a water shutter and its emergency water storage, respectively. The water can be pumped up from and released to a larger buffer tank located outside of the reactor shielding block by pressurized air. A micro-processor controlled electronic unit connected to a PC operates the two shutters and the internal filter systems. The construction materials inside the beam tube work as internal, not removable filters with total thickness of 18 mm Pb and 15 mm Al.

The irradiation cavity is situated outside of the shielding block of the reactor in a distance of 1400 mm, thus its surface-to-reactor core distance is 3100 mm including the exchangeable core window (65 mm) made either of beryllium (rolling as the fast neutron reflector, too) or of aluminum. This window can be changed only during the maintenance or refueling period. The

use of the aluminum window results in a hard neutron spectrum. Between the shielding surface of the reactor and the cavity there is a borated water shielded collimator with a useful diameter of 10 cm. It is possible to use this collimator as a holder for outer filters of about 800 mm length. Presently, filters of plexi-glass, polyethylene, iron, aluminum and lead are available to decrease the gamma and neutron intensity or to modify the neutron spectrum and the neutron-to-gamma ratio. There are two changeable filter disks of boron-carbide working as thermal and epithermal absorbers. The collimator is movable on a rail. The samples to be irradiated can be rotated to achieve a uniform, homogeneous irradiation. Cadmium or Boron carbide filters are used, if required, for decreasing the thermal neutron contribution. A large variety of irradiation geometry can be configured inside or outside of the collimator depending on the state, shape, weight of the material to be exposed.

The cavity is surrounded by a borated water shield which can be moved on a rail, as well. The whole construction is covered and surrounded by shielding elements, like a bunker, made of borated water and paraffin wax, heavy concrete and lead.

Three levels of the dosimetry system were developed: real time, active beam monitors; passive activation, track-etch and TL detectors and computer codes for spectrum and dose calculations. Each exposure is individually planned and continuously monitored during the procedure. Some typical dose and flux values are presented in 1. Table and the schematic view of the system is presented in 1. Figure.

Quantity	Energy range	Min	Max
Neutron dose rate (mGy/s)	$E > 0.5 \text{ eV}$	0.023	14
Gamma dose rate ( $\mu\text{Gy/s}$ )	-	1.5	2570
Fast neutron flux ( $\text{cm}^{-2}\text{s}^{-1}$ )	$E > 100 \text{ keV}$	$2 \times 10^6$	$2 \times 10^9$
Intermedier neutron flux ( $\text{cm}^{-2}\text{s}^{-1}$ )	$100 \text{ keV} > E > 0.5 \text{ eV}$	$8 \times 10^3$	$2 \times 10^6$
Thermal neutron flux ( $\text{cm}^{-2}\text{s}^{-1}$ )	$E < 0.5 \text{ eV}$	$5 \times 10^4$	$3 \times 10^8$

Table 1. Presently existing minimum and maximum dose and flux values.

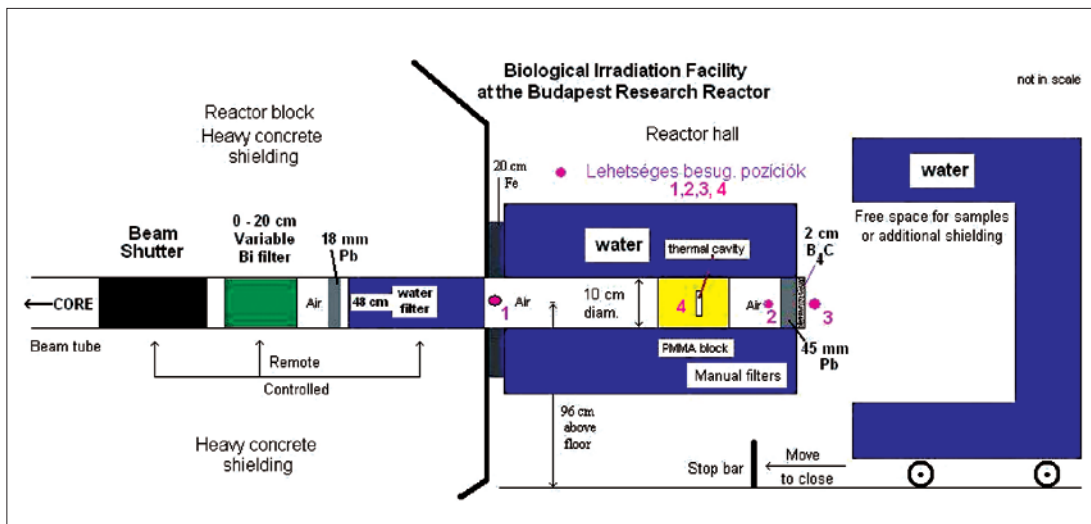


Figure 1. Schematic view of the Biological Irradiation Facility

## 6.12. PGAA – PROMPT GAMMA ACTIVATION ANALYSIS

*Instrument scientists: Zsolt Kasztovszky, László Szentmiklósi, Boglárka Maróti*

Centre for Energy Research, Hungarian Academy for Sciences

When a nucleus captures a neutron, the binding energy of the neutron is promptly emitted in the form of gamma radiation. The energies of the gamma photons are specific to the nucleus, while their numbers are proportional to the quantity of that nuclide. By analyzing the energy spectrum of these gamma rays, the isotopic and elemental contents of the irradiated sample can be determined. This is the principle of the prompt gamma activation analysis method.

The PGAA facility is located near the end position of the neutron guide No. 1. It is used for non-destructive elemental analysis of samples by observing neutron-capture prompt gamma rays. From the cold neutron-source of the Budapest Research Reactor, the neutrons are guided to the experimental positions by a curved neutron guide to decrease the background coming from the reactor core. Before the beam enters to the experimental area, the beam is divided into two sub-beams (upper and lower) by suitable collimators, and the upper beam operates the PGAA facility. The neutron guide has been recently upgraded with  $2\Theta_c$  supermirror guides that improved the thermal-equivalent neutron flux at the PGAA sample positions to  $9.6 \times 10^7 \text{ cm}^{-2} \text{ s}^{-1}$ . The beam could be collimated to a maximum cross-section of  $2 \times 2 \text{ cm}^2$ . The intensity of the incoming neutron flux is monitored and recorded with an ORDELA Model 4511 N neutron detector throughout the whole reactor campaign.

For special experiments, a pulsed beam can also be used. Modulation in the order of milliseconds can be done by a revolving chopper blade, while longer on-off periods can be achieved with a fast beam shutter.

The experimental area is a  $3 \times 6.5 \text{ m}^2$  space at the rear end of the guide hall (see Figure 1). The neutrons enter the cabin and fly along a 3 m long evacuated aluminum flight-tube across the experimental area, to the beam stop placed at the

wall of the guide hall. A pneumatically actuated instrument shutter is used to control the entry of the neutron beam into the cabin while two computer-controlled secondary shutters are in place to allow independent operation of the PGAA and NIPS/NORMA facilities. Sections of the modular aluminum flight tube can easily be removed and reinstalled as needed. Collimators of appropriate sizes are used for the two beams. At present, the upper beam is used for PGAA measurements while the lower beam is used for NIPS/NORMA experiments.

The PGAA target chamber is at 1.5 m distance from the end of the guide. The sample chamber can be evacuated or filled up with gases to decrease beam-induced background. To prevent scattering of neutrons to the PGAA sample from the lower beam, a layer of neutron absorber is placed below the sample. The targets are mounted on thin Al frames by Teflon strings. Optionally, an automated sample changer with a capacity of 16 samples can be used. A neutron absorber after the PGAA target chamber stops the upper beam.

The detector system of the PGAA facility consists of an n-type high-purity germanium (Canberra HPGe 2720/S) main detector with closed-end coaxial geometry, and a BGO Compton-suppressor surrounded by a 10 cm thick lead shielding. The sample-to-detector distance is adjustable, but it is typically 230 mm. By removing the front detector shielding the HPGe main detector can be placed as close as 12 cm to the target.

The BGO annulus and catchers around the HPGe detect most of the scattered gamma photons. If the events from the HPGe and the BGO are collected in anticoincidence mode, Compton-suppressed spectra can be acquired. An analogue spectroscopy amplifier combined with an ADC and an Ethernet-based multichannel analyzer (Canberra AIM 556A) collects the counts.



Beam tube:	NG1 guide, end position
Distance from guide end:	1.5 m
Beam cross section (computer selectable):	2×2cm <sup>2</sup> , 1.4×1.4cm <sup>2</sup> , 1×1cm <sup>2</sup> , 42mm <sup>2</sup> , 23mm <sup>2</sup> , 10mm <sup>2</sup> , 5mm <sup>2</sup> , 1/30 attenuator
Thermal-equivalent flux at target:	≈9.6×10 <sup>7</sup> cm <sup>-2</sup> s <sup>-1</sup> (in air)
Vacuum in target chamber (optional):	≈1 mbar
Target chamber Al-window thickness	0.5 mm
Form of target at room temperature:	Solid, powder, liquid; gas in a pressurized container
Target packing at atmospheric pressure:	sealed FEP Teflon bag or vial
Sample chamber dimensions:	4×4×10 cm <sup>3</sup>
γ-ray detector	n-type coax. HPGe, with BGO shield
Distance from target to detector window:	230 mm
HPGe window:	Carbon epoxy, 0.5 mm
Relative efficiency:	27% at 1332 keV ( <sup>60</sup> Co)
FWHM:	2.1 keV at 1332 keV ( <sup>60</sup> Co)
Compton suppression factor:	≈5 (1332 keV) to ≈40 (7000 keV)

**Table 1.**  
Specifications of the PGAA facility

A schematic drawing of the experimental area, the sample chambers and the HPGe-BGO detector

assembly is shown in Figure 1. The main parameters of the PGAA system are collected in Table 1.

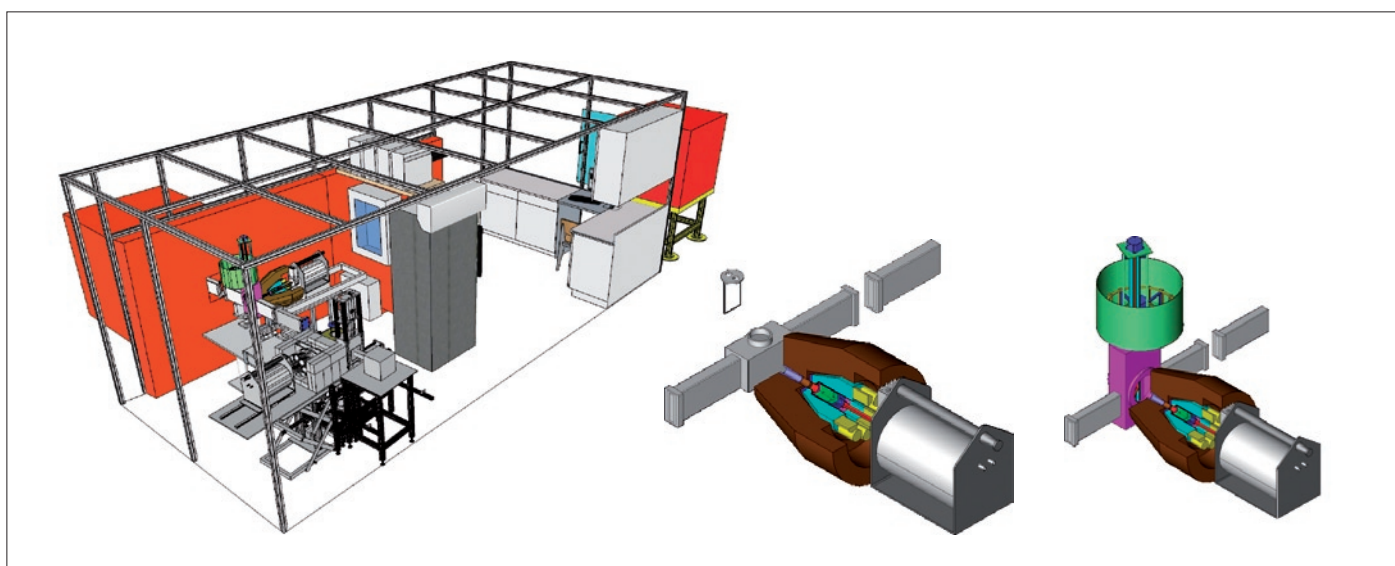


**Figure 1.**

Layout of the PGAA-NIPS experimental area (left). The PGAA facility, with the standard sample chamber (middle) and with the automated sample changer (right)

## 6.13. NIPS - NEUTRON-INDUCED PROMPT GAMMA-RAY SPECTROSCOPY

**Instrument scientists: László Szentmiklósi, Zoltán Kis, Katalin Gméling**

Centre for Energy Research, Hungarian Academy for Sciences

Operated by: Centre for Energy Research, Nuclear Analysis and Radiography Department

Instrument responsible: László SZENTMIKLÓSI, +36-1-3922222/3153,

szentmiklosi.laszlo@energia.mta.hu

Instrument scientist(s): Zoltán KIS, Katalin GMÉLING

Location: Cold neutron guide No.1/4

The NIPS facility is located at the end position of the neutron guide No.1. It is designed for a wide range of experiments that involve nuclear reaction-induced prompt and delayed gamma radiations,  $\gamma$ - $\gamma$ -coincidences, large-sample PGAA, Prompt-Gamma Activation Imaging (PGAI).

From the cold neutron-source of the Budapest Research Reactor, the neutrons are guided to the experimental positions by the same curved neutron guides as for the PGAA facility. Before the beam enters to the experimental area, the beam is divided into two sub-beams (upper and lower) by suitable collimators, and the lower one operates the NIPS facility. The thermal-equivalent neutron flux at the NIPS sample positions is  $2.7 \times 10^7 \text{ cm}^{-2} \text{ s}^{-1}$ . The beam could be collimated to a maximum cross-section of  $4 \times 4 \text{ cm}^2$ . The intensity of the incoming neutron flux is monitored and recorded with an ORDELA Model 4511 N neutron detector throughout the whole reactor campaign.

The beam arrives through a flight tube of  $5 \times 5 \text{ cm}^2$  cross section. If multiple detectors are to be placed close to the sample, a narrow aluminum tube with a  $5 \times 5 \times 5 \text{ cm}^3$  sample chamber is available. Alternatively a sample chamber with dimensions of  $20 \times 20 \times 20 \text{ cm}^3$  is available for large-sample PGAA and position-sensitive applications. It is made of AlMgSi alloy, and lined from inside with  $^6\text{Li}$ -enriched polymer. By removing one or more side panels, larger objects up to 5 kg weight could also be analyzed (such as a sword, vase, stones, etc.). Samples can be loaded manually from the top, or placed onto an XYZ $\omega$  motorized sample stage with a travel distance of 200 mm and a guaranteed

precision of 15  $\mu\text{m}$ , which is introduced from the bottom. If custom devices are to be built into the beam, a short flight tube without a sample chamber is the proper choice.

An n-type coaxial HPGe detector (Canberra GR 2318/S) equipped with a Scionix BGO Compton suppressor is used for the routine prompt gamma measurements. This latter can accommodate HPGe detectors with larger crystals (up to end cap diameter of 76 mm). The passive shielding is made of standard lead bricks in a thickness of 10 cm for each direction. A changeable gamma collimator system is available for PGAI measurements consisting of three different lead collimators with an opening of 30 mm in diameter, a  $2 \times 20 \text{ mm}^2$  slit and a  $5 \times 5 \text{ mm}^2$ , respectively. The gamma detector systems are regularly calibrated for counting efficiency and non-linearity. This procedure results in a precision of about 0.5% for the relative efficiency curve, 1% for the absolute efficiency curve and a precision of 0.005-0.1 keV for energy determination of peaks. The complex  $\gamma$ -ray spectra are evaluated with the spectroscopy program Hypermet-PC.

A digital signal processor combined with an Ethernet-based multichannel analyzer module (Canberra AIM 556B) collects the counts. Alternatively, a four-channel, all-digital XIA Pixie 4 spectrometer can also be used. A user-friendly facility control program, "Budapest PGAA-NIPS Data Acquisition Software", has been written for manual, semi-automatic, and unattended automatic batch measurements. It controls the beam shutters, the motorized sample stage and the gamma acquisition.

Table 1.  
Specifications of NIPS facility

Beam tube:	NG1 guide, end position
Distance from guide end:	2.6 m
Beam cross section for PGAA/PGAI:	2×2cm <sup>2</sup> , 1.4×1.4cm <sup>2</sup> , 1×1cm <sup>2</sup> , 42mm <sup>2</sup> , 23mm <sup>2</sup> , 10mm <sup>2</sup> , 5mm <sup>2</sup> , 1×20mm <sup>2</sup> slit
Beam cross section for imaging:	up to 40×40 mm <sup>2</sup>
Thermal-equivalent flux at target:	≈2.7×10 <sup>7</sup> ×cm <sup>-2</sup> s <sup>-1</sup>
Vacuum in target chamber:	Not available
Form of target at room temperature:	Solid, powder, liquid; gas in a pressurized container
Target packing at atmospheric pressure:	sealed FEP Teflon bag or vial
Sample chamber dimensions:	5×5×5 cm <sup>3</sup> /20×20×20 cm <sup>3</sup>
Distance from target to detector window:	minimum 25 mm, typical 280 mm
γ-ray detector	n-type coax. HPGe, with BGO shield
HPGe window:	Al, 0.5 mm
Relative efficiency:	23% at 1332 keV ( <sup>60</sup> Co)
FWHM:	2.2 keV at 1332 keV ( <sup>60</sup> Co)
Compton-suppression factor	≈3.5 (1332 keV) to ≈30 (7000 keV)

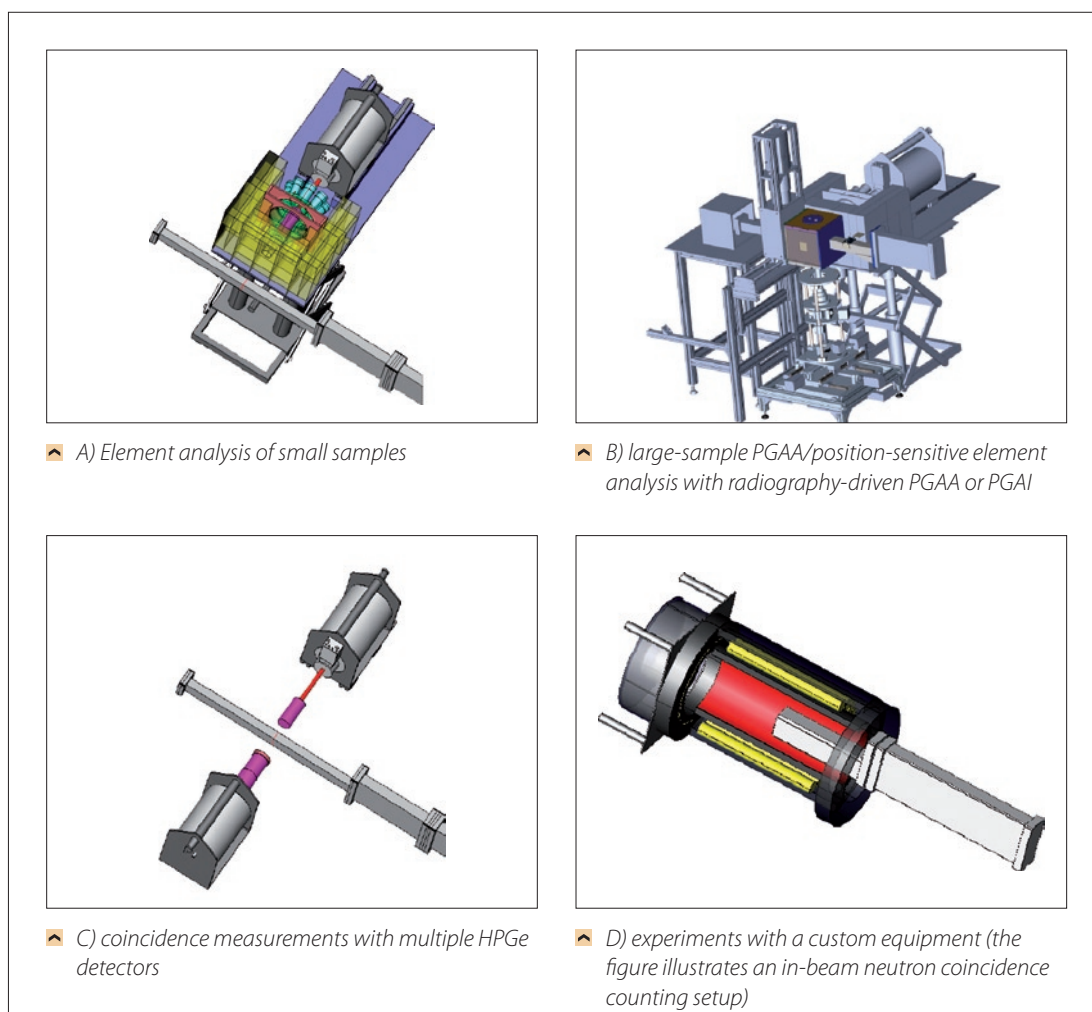


Figure 1.  
Possible configurations of the NIPS experimental station. The beam arrives from the lower-right corner of the images.

## 6.14. BAGIRA3 – REACTOR IRRADIATION LOOP

*Instrument scientists: Attila Kovács, Ferenc Gillemot, Ákos Horváth*

Centre for Energy Research, Hungarian Academy for Sciences

At the Budapest Research Reactor, two gas cooled irradiation rigs (BAGIRA 1 and 2) have been operated since 1998. Twenty four different irradiation researches have been performed, testing irradiation ageing of reactor and fusion devices, structural materials, as low alloyed and stainless steels, Al, Ti and W alloys, ceramics etc. The devices served more than 12 years. The material aged by irradiation and corrosion, and their capacity cannot satisfy the up-to date requirements of the newly developing materials.

Presently the main interest of the nuclear industry is the development of fusion reactors and Generation IV reactors. To increase the efficiency

and decrease the impact on the environment, high operation temperature will be used. Consequently high temperature irradiation combined with in pile creep and fatigue testing are the future tasks of the irradiation devices.

Nowadays, there are only a few research reactors in Europe. With the new device in connection with the hot laboratory and with the existing know-how, we are capable of participating in international research projects, as well as customized irradiation and post irradiation examination in cooperation with several institutes and nuclear power industries worldwide.

### **Description of the new device**

The new device is called Budapest Advanced Gas-cooled Irradiation Rig with Aluminium structure 3, BAGIRA3.

The main features of it are:

- The rig capacity is 36 Charpy size specimen (appr. 1200 gr steel) or similar. The specimen sizes and shape can be varied according to the requirements, since only the target simple holder has to be changed.
- At each of the new six zones, the electric heating can be separately controlled, ensuring to keep

the required irradiation temperature within  $\pm 5^\circ\text{C}$ . Irradiation temperature can be controlled between  $150^\circ\text{--}650^\circ\text{C}$  with gamma and electric heating and helium-nitrogen gas mix cooling.

- The maximum fluence rate is  $1\text{--}5 \cdot 10^{13}$  n/cm<sup>2</sup> E>1MeV (approximately 0,5 dpa/year). The irradiation rig is shielded with boron carbide, to filter the thermal neutrons, reducing the activity of the irradiated specimens and the nuclear heating. Reduced target activity decreases the cost of the test or transportation of the irradiated specimens.

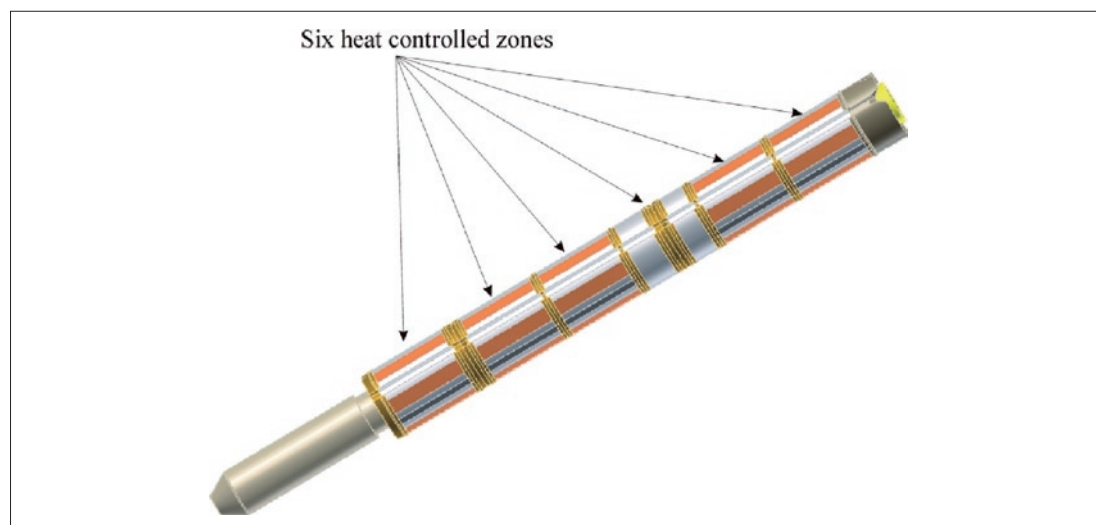


**Figure 1.** Target holder, filled with specimens

- The target holder is separated from the thermocouples and electric heating system. This way the cost of the heating elements and thermocouples decreasing, and only minor quantity of aluminium or titanium heat removal material goes into the radioactive waste
- The new target pick up and eject system allows the quick target change during the operation brake of the reactor , and active target also can be used (e.g. irradiated and annealed material can be reirradiated)
- The target can be rotated during irradiation to ensure the same irradiation of the specimens located on the same level.
- The rig design allows irradiation creep or irradiation-low cycle fatigue study too.
- The device is designed for automatic operation, programmable, and it has several safety features, (including emergency passive cooling system, automatic reset in case of any malfunction of the control system, etc.)



◀ **Figure 2.**  
Assembled Bagira3 in the reactor channel with the view of the rotating engine

### ***The present situation and the remaining work***

The equipment is ready and the control software is tested several hundred hours. Twelve different safety tests performed successfully, and the Hungarian National Safety Authority

permitted the installation into the reactor. The test run in 2012 august was also successful. The rig operates from January 2013 in several research projects.

### ***References:***

- Gillemot Ferenc: „Study of Irradiation Effects at the Research Reactor” Strenghths of materials, Vol 42. No 1. 2010, Springer Science pp.78-83

## 6.15. RNAA – REACTOR-NEUTRON ACTIVATION ANALYSIS

*Instrument scientists: Ibilya Sziklai-László, Dénes Párkányi*

Centre for Energy Research, Hungarian Academy for Sciences

Combined with computerized high resolution gamma-ray spectrometry, RNAA offers mostly non-destructive, multi-element routine analysis needed in such areas as environmental monitoring, geochemistry, nutrition, archaeology and material

science. Among its favourable characteristics negligible matrix effects, excellent selectivity and high sensitivity are worth mentioning, for about 75 elements less than 0.01 µg can be determined.

### Instrumentation



**Figures 1a. and 1b. >**

*The multi-purpose pneumatic transfer system  
The Field Point modular based I/O of the multi-purpose pneumatic transfer system*

Besides more than 40 vertical channels, a pneumatic sample transfer system is also available at the BRR (Figures 1 and 2). The control and data acquisition electronics and software of the fast rabbit system of the BRR has been upgraded recently. In the new system Field Point modular based I/O was implemented (National Instruments, USA). In order to extend the irradiation period (up to 20 minutes) a new sample holder capsule made from a high purity polymer (DuPont™ Vespel® SP-1) was used. The cleanliness of this new material was measured by INAA as well as the surface contamination of

the capsule during irradiations and the sample temperature inside the capsule. The concentrations of the Al, As, Cu, Mg, Mn, and Na producing short half - life isotopes with impurities <0.7 ppm, have no limiting effects on the usage of these capsules in several irradiation cycles per day.

In the “B” vertical pneumatic tube, thermal neutron flux variation along the axis of the irradiation capsule is less than 5 %. Neutron flux parameters have been measured with the “Bare Triple- Monitor” method using Zr, Al-0.1%Au and Fe foils (Table 1).

**Table 1. >**

*Main specifications for channel “B” and rotating channel No17*

Inner dimensions of the polyethylene rabbit	14 mm dia. x 42 mm
Thermal neutron flux	$4.45 \times 10^{13} \text{ n/cm}^2\text{s}$
f (thermal to epithermal flux ratio)	34.8
$\alpha$ (representing the epithermal flux with $1/E^{1+\alpha}$ )	0.029

For long cycle irradiations, samples together with flux monitors are irradiated in one of the vertical, rotating irradiation channels (N°17) of the reactor

at a thermal neutron flux density of  $1.86 \cdot 10^{13} \text{ n} \cdot \text{cm}^{-2} \cdot \text{s}^{-1}$ , a thermal to epithermal flux ratio ( $f$ ) of 42 and  $\alpha = 0.031$ .

### Gamma-ray spectrometry

High resolution gamma-ray spectrometric measurements are performed with a Canberra HPGe detector (energy resolution of 1.82 keV and rel. efficiency of 36% for the 1332.5 keV  $^{60}\text{Co}$  line) and TRP preamplifier,

Cl 2026 amplifier (4  $\mu\text{s}$  shaping); ACCUSPEC/B MCA (2x 8K), 8715 8K/800 ns ADC and Genie 2000 program for data acquisition. Counting losses are corrected with a Loss-Free Counting module (Figure 2).

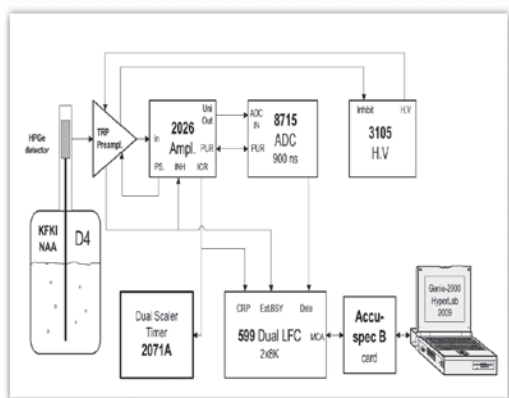


**Figure 2.**  
A gamma-ray spectrometer equipped with Dual Spectrum LFC module

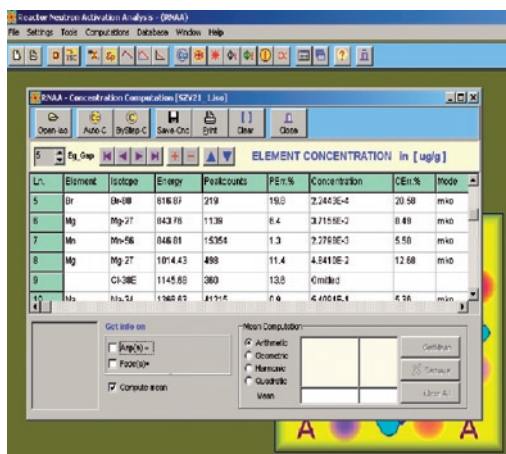


**Figure 3.**  
Screen shot of the RNAACNC program

### Gamma spectra evaluations and calculation of element concentrations

For gamma-ray spectrum evaluation, the Hypermet-PC (ver. 5.) is applied involving automatic peak search, energy calibration, net peak counts computation with the NonLin and Dual Spectrum Loss-Free Counting (LFC) Option. For the quantitative evaluation, an in-house program RNAACNC, based

on the  $k_0$  standardization, is used. This program supports the following features: absolute activity, alpha value, element concentration, detector efficiency, isotope identification, thermal and fast neutron flux and flux ratio ( $f$ ), nuclear data library, specific activity computation (Figure 3).

### Developments and applications

Selenium and other trace element levels were measured in basic food ingredients, human milk and formula milk from Hungary. Se intake, blood status and urinary Se excretion of healthy, diabetic and asthmatic children were also measured.

The activity concentrations of characteristic fission and corrosion products (Cr, Mn, Co, Cu, Fe, etc.) in the primary cooling water and the chemical concentrations of different impurity components in various water systems of the BRR are measured to monitor the water quality.

Epithermal neutron activation analysis (ENAA) was developed, boron activation ratios (RB) and improvement factors (IFB) for 23 nuclides were determined. Using the boron shield a very effective suppression of strongly

activating  $1/v$  and low resonance target isotopes (i.e.  $^{24}\text{Na}$ ,  $^{42}\text{K}$ ,  $^{38}\text{Cl}$ ,  $^{46}\text{Sc}$ ,...) can be achieved and number of important nuclides ( $^{75}\text{As}$ ,  $^{197}\text{Au}$ ,  $^{111}\text{Cd}$ ,  $^{121}\text{Sb}$ ,  $^{124}\text{Sn}$ ,  $^{238}\text{U}$ ) can be determined in geological and biological samples with minimum delay.

A radiochemical method for the selective separation of Cs has been adopted and tested. NAA and ICP-MS were applied parallel for the accurate determination of  $^{135}\text{Cs}$  in nuclear power plant wastes. Acceptable low detection limits (10-50 ng/L) and high accuracies (5-20 %) were achieved by both techniques. Results of  $^{135}\text{Cs}$  determination by ICP-MS and NAA agreed well.

Using NAA complementing with PGAA in the fields of materials material science, archaeometry and geology.

## 7. *Education*



## **GRADUATE AND POSTGRADUATE COURSES**

Computer Aided Engineering (L. Zoltan SZIE)

Control theory (J. Füzi, PTE) 2010-2011

Digital Control (J. Füzi, PTE-PMMK) 2011

Disorder in condensed phases (L. Pusztai) 2010-2011

Electronics (J. Füzi, PTE-PMMK) 2011

Introduction to the neutron scattering for the microscopic investigation of matter, with applications in Physics, Chemistry, Biology and Geology (G. Nagy, Grenoble, France) 2010

Machine elements I. (L. Zoltan SZIE)

Machine elements II. (L. Zoltan SZIE)

Neutron beam methods in materials science, (L. Rosta, BME) 2010

Research of materials structures by neutron scattering (L. Rosta, ELTE) 2010

## **LABORATORY PRACTICE AND SEMINARS**

Control theory practice (J. Füzi, PTE-PMMK) 2010-2011

Electronics laboratory practice (J. Füzi, PTE-PMMK)

Laboratory practice in neutron diffraction (L. Pusztai, ELTE) 2010-2011

Neutron detectors (J. Orbán, BME-NTI) 2011

Practice course in experimental physics for engineer-physicists (A. Szakál, BME) 2010-2011

Practice course in electrodynamics for energy-engineers (A. Szakál, BME) 2010- 2011

Introduction of the PGAA and NIPS facilities, (Z.Kis, L. Szentmiklósi, Zs. Kasztovszky, T. Belgya, Zs. Révay: AEKI Open University, 21 November 2011

## **PH.D. STUDENTS**

László Z (SZIE) Magnetic bearings for neutron beam phase space tailoring (Supervisors: J. Nagy, J. Füzi)

Merkel DG (ELTE) Modification and study of magnetic thin films (Supervisor: Bottyán L)

Nagy B (BME): Superconductor-ferromagnet proximity effects in thin films revealed by neutron reflectometry (Supervisor: Bottyán L)

Orbán J (BME): Investigation and development of signal processing electronics for position sensitive particle counters (Supervisor: Rosta L and Sükösd Cs\*)

Szakál A (BME); Investigation of the structure and dynamics of metal-hydrogen systems with neutron scattering (Supervisor: Cser L)

Ünnep R (ELTE); Study of self-assembly functional nano particles by neutron scattering (Supervisor: Mezei F)

### ***DISSERTATIONS***

Gméling K (PhD, ELTE) A Kárpát-Pannon térség miocén-kvarter mészkáli vulkáni kőzeteinek bór geokémiai összetétele és kapcsolata a szubdukciós folyamatokkal: prompt-gamma aktivációs analitikai vizsgálatok (Supervisor:

Len A (PhD, ELTE) Tungsten Wires Studied by Small Angle Neutron Scattering (Supervisor: Rosta L)

Markó M (BME) Atomic resolution neutron holography (Supervisor: Cser L)

Meiszterics A (ELTE): Calcium containing bioceramics prepared by sol-gel method and their (Supervisor: Rosta L and Sinkó K\*)

Nagy G (ELTE, Université de Grenoble) Analysis of lamellar systems related to the photosynthesis with the use of neutron scattering (Supervisor: Rosta L, Peters J, Timmins P, Garab Gy)

Mile V (ELTE) Structural studies of aqueous cesium-halide solution (Supervisor: L. Pusztai)

Székely NK (PhD, ELTE) Small angle neutron scattering study on aqueous solutions of various diols and methylurea derivatives (Supervisor: Rosta L)

Szilágyi V (PhD ELTE) Inka kori kerámiák archeometriai vizsgálata (Paria, Bolívia): nyersanyageredet és technológia (Supervisor: )

Tanczikó Ferenc (PhD, ELTE) Determination of the direction of magnetization by elliptically polarized resonant photons (Supervisor: Bottyán L)

# *Events* | **8.**

## CONFERENCES

The **5<sup>th</sup> Central European Training School on Neutron Scattering (CETS 2010)** has been held between May 31 - June 04, 2010. The school was organized by the Neutron Spectroscopy Department and the Budapest Neutron Centre. The course provided an introduction to neutron scattering with special emphasis to hands-on-training at the BRR facilities. The training consisted of five days of tutorial lectures given by renowned lecturers from Europe including also major neutron centers like Dubna, FRM II, HZ-Berlin, ILL. The lectures were followed by experimental works at the instruments to demonstrate to the students the art of utilization of instruments at a large-scale facility giving insight in sample preparation, experiment planning and running as well as data processing and interpretation of results. The participants were divided into groups of maximum 5-6 students in order to facilitate individual involvement in the performance of the experiment. The school brought together young physicists, chemists, biologists, actual or potential neutron users. Most of the attendees (23 non-Hungarian students) came from our neighbour countries. We enjoyed, in particular, the last day poster session including the student's flash oral presentations: most of the work they presented had witnessed of serious effort - and their excitement of presenting was a nice moment of the school.

**CHARISMA** - (Cultural Heritage Advanced Research Infrastructures: Synergy for a Multidisciplinary Approach to Conservation/Restoration) is an EU-funded integrating activity project carried out in the FP7 Capacities Specific Programme "Research Infrastructures". CHARISMA aims to target the lack of support currently offered to researchers on cultural heritage, as museums curators, conservators and conservation scientists. Central objective of the technical plan is the development of a coherent powerful platform to offer access directly to the widest number of scientific techniques available in large scale facilities and small/medium installations and tools, supporting the most promising and innovative experimental research, helping EU researchers to carry out advanced characterisation of heritage materials and exploiting advanced instrumentation capable to meet specific interests and to provide cross-subject solutions.

CHARISMA 2nd Interim Meeting was held in Budapest at the Hungarian Academy of Sciences on March 3 to 4, 2011 with the participation of more than 60 experts from the the European Union partner institutes. It has been an honor to organise the event at Budapest, after the serial meetings of CHARISMA, located at the Louvre, Prado and the di Belle Arti in Florence. Hungarian platform is a part of a support service, which offers to transnational users from Europe and associated countries, in order to let them carry out at best their research, exploiting the most advanced instrumentation and to multi-techniques available in medium and large scale facilities in Europe. For applying to techniques for non-destructive examination of objects and samples the FIXLAB access is planned to two strongly integrated platforms, where Large Scale Facilities are coupled to a set of medium scale instrumentations, completed when needed with more conventional examination and analysis tools. One platform in France (Synchrotron SOLEIL, AGLAE Ion-beam - CNRS) is devoted to ion-beam and synchrotron radiation investigations and the other one, in Hungary (Budapest Neutron Centre and ATOMKI), is devoted to neutron and micro-PIXE investigations. Neutron facility open to the national and international community, recognized component of the European network of neutron centers, joining institutes of RISP, IKI and RMKI. The activity – including 21 European partner institutes – provides transnational access to most advanced scientific instrumentations and knowledge allowing scientists, conservators-restorers and curators to enhance their research at the field forefront. The three research institutes of Hungarian Academy of Sciences are put together to form the neutron platform in CHARISMA. The infrastructure offers for access to neutron techniques and non-destructive neutron experiments at the Budapest Research Reactor. The 2nd Interim Meeting was welcomed by Prof. Norber Kroó, Vice-president of the Hungarian Academy of Sciences. On the first day the scientific results of the first 18 months of the project were introduced and evaluated along with the discussion of future plans of the activity. On the second day the project related financial and other administrative tasks had been negotiated by the participants.

**NMI3** - To mark the Hungarian Presidency of the European Union the annual Board meeting of the Neutron Muon Integrated Infrastructure Initiative (NMI3) project in FP7 was held on the 12th of May 2011 in Budapest, it was hosted by BNC, and organised by the contribution of the Neutron Spectroscopy Department. This project gathers the 10 major European neutron source facilities and another 10 adjoining institutions to provide access and research opportunities for a wide community of researchers. Nearly 50 delegates of the project partners discussed the next 4 years plans: the great news at this occasion was that the European Commission has awarded a 13 M€ grant to this project. Having recognized the last few year's developments at our facility, BNC was the only to increase its share among the project partners.

**ENSA** – The European Neutron Scattering Association (ENSA) held its first annual Committee meeting on the 13th of May 2011 in Budapest, it was hosted by the Budapest Neutron Centre, and organised by the Neutron Spectroscopy Department. ENSA groups 24 countries as member organizations and it has recently performed a thorough survey on the European user community establishing that neutron science and the utilization of neutron beam facilities at neutron source centres have a healthy growth to reach by now a community as large as 6000 users in Europe. During this meeting it was also considered that over the past two decades Hungary became an important part of the European neutron scattering landscape. As Prof. M. Steiner (HZ-Berlin) formulated: "The Budapest Neutron Center is one of the international user centers financially supported by the European Union, many research results of Hungarian scientists are highly recognized and in 2005 Hungary became one of the 14 member countries of ILL in Grenoble, the world leader in

neutron research. This multifaceted presence in an area of European leadership in science largely contributes to the reputation of Hungary as a most valuable partner." This ENSA meeting was attended by ~40 delegates and observers.

**IAEA** - A symposium "Concerted Actions in Research and Applications with Neutron Beams in Europe" was organized by the International Atomic Energy Agency (IAEA) in collaboration with the Government of the Republic of Hungary through the Budapest Neutron Centre on 1-3 June 2011 in Budapest. The IAEA promotes networking, coalitions and regional collaboration to improve the efficient and sustainable utilization of Research Reactors (RRs). This workshop aimed to strengthen the cooperative efforts of the member institutions in the field of neutron beam research and applications. The event covered the main neutron beam methods, examined the current status of neutron beam facilities and discussed the future trends in neutron science and applications in Europe. The role of smaller neutron beam facilities was evaluated in particular. The workshop also intended to provide a forum for sharing of information and good practices among developed and developing countries in the region, including leading neutron research centres. The meeting was attended by 39 participants from 14 Member States in Europe. The workshop covered several topics as research and industrial applications using various neutron beam techniques, recent modernization/upgrade projects related to neutron beam facilities, education and training using neutron beams. Brief summaries of individual presentations are given in the Book of Abstracts. Technical tour to the Budapest Neutron Centre (BNC), including Budapest Research Reactor and its neutron beam facilities was organized as part of the meeting agenda.

## **WORKSHOPS**

**Spallation target workshop** has been held on the 2<sup>nd</sup> July 2010 at the KFKI site hosted by the Atomic Energy Research Institute with participation of the Research Institute for Solid State Physics, Mirrotron Co, Japan Proton Accelerator Research

Complex (JPARC) and the Rogante Engineering Co. Lectures were focused on spallation neutron source development, considering different target options and industrial aspects of some target related issues.

## **PROFESSIONAL TRAINING**

**Professional training in neutron research and instrumentation** was provided by the Neutron Spectroscopy Department (SZFKI), Nuclear Solid State Physics Department (RMKI) and the Mirrotron Co. for visiting scientists of the Institute of Nuclear Physics and Chemistry, Mianyang, China. The event has been held on July 10- August 26, 2010 at the MTA KFKI Research Campus in Budapest, consisting training in neutron scattering with specific orientation on neutron reflectometry, delivering lectures by leading scientists of the Budapest Neutron Centre (BNC) and hands-on-training using BNC neutron facilities. The training performed on the cold and thermal neutron beam instruments of BNC included the following items: introduction to neutron techniques and instruments at BNC, training in Monte Carlo simulation for spectrometer components and neutron spectrometer function utilization, assistance in performance of real and simulated experiments at BNC reflectometers and training in data treatment.

The Neutron Spectroscopy Department in cooperation with MIRROTRON Co. organized a training course in Neutron Research and Instrumentation with the specific purpose of training in Residual Strain Neutron Diffraction for a group of scientists and engineers of the Institute of Nuclear Physics and Chemistry, Mianyang, China in the period of June 19 - July 16, 2011 (4 weeks).

The training consisted of education in neutron scattering with specific orientation on neutron diffraction and strain scanning, including lectures given by leading scientists of the Budapest Neutron Centre (BNC) and renowned European experts invited by BNC as well as hands-on training using BNC neutron facilities. The training has included the following items: Introduction to neutron techniques and instruments at BNC, training in MC simulation for spectrometer components, training in neutron spectrometer function utilizations, assistance in performing real experiments at BNC diffractometers, training in data treatment

Mini-symposium "Modern nuclear and other analytical methods for the application in research of microelements in health, agriculture and the environment" was organized in Budapest, 18 October, 2011 by the KFKI Atomic Energy Research Institute of HAS and the Microelement Committee of HAS.

### **Experimental Methods in Material Science**

Polarized neutron reflectometry is part of the course "Experimental Methods in Material Science" at the University of Technology and Economics Budapest (BME) for Master students in physics. The one day session is divided into two lectures and two hands-on laboratory practices on neutron reflectometry and on small angle neutron scattering.

*Publications* | **9.**

## ARTICLES

1. Kulvelis\* YV, Trunov\* VA., Lebedev\* VT, Orlova\* DN, Török Gy, Gelfond\* ML; Complexes of ferromagnetic fluids with photoditazin and their promising applications in photodynamic therapy; *Journal of Structural Chemistry*; **150**, 949-953, 2009
2. Lebedev\* VT, Vinogradova\* LV, Török Gy; Structural features of star shaped fullerene (C<sub>60</sub>) Containing Polystyrenes, Neutron Scattering Experiments; *Polymer Science Ser A*, **50**, 1090-1097, 2009
3. Aksenov\* VL, Tropin\* TV, Kyzyma OA, Avdeev\* MV, Korobov\* MV, Rosta L; Formation of C<sub>60</sub> fullerene clusters in nitrogen-containing solvents, Chemistry and physics of polymers and fullerenes, biology, and pharmacology; *Physics of the Solid State*; **52**, 1059-1062, 2010
4. Aksenov\* VL, Avdeev\* MV, Shulenina\* AV, Zubavichus\* YV, Veligzhanin\* AA, Rosta L, Garamus\* VM, Vekas\* L, Neutron and synchrotron radiation scattering by nonpolar magnetic fluids, *Crystallography Reports*; **56**, 5, 792-801, 2011
5. Almásy L, Bende\* A; Ab initio structures of interacting methylene chloride molecules with comparison to the liquid phase; *J Mol Liq*; **158**, 205-207, 2011
6. Avdeev\* MV, Tropin\* TV, Bodnarchuk\* IA, Yaradaikin\* SP, Rosta L, Aksenov\* VL, Bulavin\* LA; On structural features of fullerene C<sub>60</sub> dissolved in carbon disulfide: Complementary study by small-angle neutron scattering and molecular dynamic simulations; *The Journal of Chemical Physics*; **132**, 164515, 2010
7. Balasoiu\* M, Bica\* I, Raikher\* YL, Dokukin\* EB, Almasy L, Vatzulik\* B, Kuklin\* AI; Particle concentration effects on the ferrofluids based elastomers microstructure, *Optoelectronics and Adv Mat*; **5**, 514-517, 2011
8. Bende\* A, Almásy L; AB initio study of mixed clusters of water and N,N'-dimethylethyleneurea; *Ukrainian J Phys*; **56**, 796-800, 2011
9. Bende\* A, Almásy L; Weakly bonded cluster structures of N,N'- dimethylethyleneurea and water; *J Mol Liq*; **162**, 45-49 2011
10. Borella, A., et al., Determination of the 209Bi (n,γ)210Bi and 209Bi (n,γ)210m,gBi reaction cross sections in a cold neutron beam; *Nuclear Physics A*, 2011. **850** (1): p. 1-21.
11. Cornelius\* TW, Schiedt B, Severin\* D, Pepy G, Toulemonde\* M, Apel\* PYu, Boesecke\* P and Trautmann\* C; Nanopores in track-etched polymer membranes characterized by small-angle X-ray scattering, *Nanotechnology*; **21**, 155702-155709, 2010
12. Füzi J, Rosta L; Neutron beam conditioning for focusing SANS spectrometers; *J Phys Conf Ser*; **241**, 012075, 2010
13. Gallová\* J, Uhríková\* D, Kučerka\* N, Svorková\* M, Funari\* SS, Murugova\* TN, Almásy L, Mazúr\* M, Balgavý\* P; Influence of cholesterol and beta-sitosterol on the structure of EYPC bilayers; *J Membrane Biol*; **43**, 1-13, 2011
14. Gunsing F, et al., Neutron Capture on (209)Bi: Determination of the Production Ratio of (210m)Bi/(210g)Bi.; *Journal of the Korean Physical Society*, 2011. **59**(2): p. 1670-1675.
15. Heaton\* ME, Rogante\* M, Len A, Denieffe\* D; Investigation of the processing effects of UV, heat and laser ablation on SU-8 microturbines; A first approach by small angle neutron scattering; *Multidiscipline Modeling in Materials and Structures*; **6**, 364-372, 2010
16. Hurst, A., et al., Gamma Spectrum from Neutron Capture on Tungsten Isotopes. *Journal of the Korean Physical Society*, 2011. **59**(2): p. 1491-1494.
17. Justino\* LGG, Ramos\* ML, Knaapila\* M, Marques\* AT, Kulda\* CJ, Scherf\* U, Almásy L, Schweins\* R, Burrows\* HD, Monkman\* AP; Article Gel formation and interpolymer alkyl chain interactions with Poly(9,9-dioctylfluorene-2,7-diyl) (PFO) in toluene solution: results from NMR, SANS, DFT, and semiempirical calculations and their implications for PFO β-phase formation; *Macromolecule*; **44**, 334-343, 2011
18. Khaydukov Yu.N, Aksenov VL, Nikitenko YuV, Zhernenkov KN, Nagy B, Teichert A., Steitz R, Rühm A, Bottyán L; Magnetic Proximity Effects in V/Fe Superconductor / Ferromagnet Single Bilayer Revealed by Waveguide-Enhanced Polarized Neutron Reflectometry; *J. Supercond. Nov. Magn.* **24** (2011) 961 - 968.
19. Khaydukov YuN, Nikitenko YuV, Bottyán L, Rühm A, Aksenov VL; Feasibility of Study Magnetic Proximity Effects in Bilayer "Superconductor / Ferromagnet" Using Waveguide Enhanced Polarized Neutron Reflectometry; *Crystall. Rep.* **55** (2010) 1235 - 1241.



20. Kis, Z., T. Belgya, and L. Szentmiklosi, Monte Carlo simulations towards semi-quantitative prompt gamma activation imaging; *Nucl Instr. and Method*, **638**(1): p. 143-146. 2011
21. Kis Z., et al., Műtárgyak roncsolásmentes vizsgálata neutronokkal – az EU-Ancient Charm project; *Fizikai Szemle*; **7-8**: p. 235-239. 2011
22. Knaapila\* M, Evans\* RC, Vasil\* M, Garamus\* VM, Almásy L, Székely NK, Gutacker\* A, Scherf\* U, Burrows\* DH; Structure and "Surfactochromic" Properties of Conjugated Polyelectrolyte (CPE): Surfactant Complexes between a Cationic Polythiophene and SDS in Water; *Langmuir*; **26(19)**, 15634-15643, 2010
23. Knaapila\* M, Bright\* DW, Nehls\* BS, Garamus\* VM, Almásy L, Schweins\* R, Scherf\* U, Monkman\* AP; Development of intermolecular structure and beta-phase of random poly[9,9-bis(2-ethylhexyl)fluorene]-co-(9,9-dioctylfluorene) in methylcyclohexane; *Macromolecules*; **44**, 6453-6460, 2011
24. Knaapila\* M, Bright\* DW, Stepanyan\* R, Torkkeli\* M, Almásy L, Schweins\* R, Vainio\* U, Preis\* E, Galbrecht\* F, Scherf\* U, Monkman\* AP; Network structure of polyfluorene sheets as a function of alkyl side chain length; *Phys Rev E*; **83**, 051803, 2011
25. Knaapila\* M, Evans\* RC, Gutacker\* A, Garamus\* VM, Szekely NK, Scherf\* U, Burrows\* HD; Conjugated polyelectrolyte (CPE) poly[3-[6-(N-methylimidazolium)hexyl]-2,5-thiophene] complexed with aqueous sodium dodecylsulfate amphiphile: synthesis, solution structure and "surfactochromic" properties; *Soft Matter* **7, 15**, 6863-6872, 2011
26. Kornilov N., et al., The U-235(n, f) Prompt Fission Neutron Spectrum at 100 K Input Neutron Energy; *Nuclear Science and Engineering*; **165**(1): p. 117-127. 2010
27. Krakovsky\* I, Székely NK; Small-angle neutron scattering study of nanophase separated epoxy hydrogels; *Journal of Non-Crystalline Solids*; **356**, 368-373, 2010
28. Krakovsky\* I, Székely NK; SANS and DSC study of water distribution in epoxy-based hydrogels; *European Polymer Journal* **47**, 2177-2188, 2011
29. Kulvelis\* YU, Lebedev\* VT, Trunov\* VA., Ivanova\* IN, Török Gy; Building of complexes of sulphonated tetraphenylporphyrine with Poly-N-vinylpyrrolidone by the data of small angle neutron scattering; *Journal Poverhnost – X-ray – synchrotron and neutron investigation*; **2**, 14–20, 2011
30. Kulvelis\* YV, Trunov VA, Lebedev\* VT, Orlova DN, Török Gy, Gelfond ML; Structure of magnetically guided nanocarriers of the photodithazine sensitizer from small-angle neutron scattering data; *Physics of the Solid State*; **52**, 1040-1044, 2010
31. Lebedev\* VT, Kulvelis\* YV, Török Gy; Dynamics of water in binary and ternary solutions of DNA and porphyrins; *Physics of the Solid State*; **52**, 1074-1079, 2010
32. Lebedev\* VT, Orlova\* DN, Lebedev\* VM., Török Gy, Melnikov\* AB, Vinogradova\* LV, Selforganisation of sulpho-polystyrene ionomers with ionogenic groups of SO<sub>3</sub>Li in carbon tetrachloride; *Russian Journal of Applied Chemistry*, **83**, 864-868, 2010
33. Lebedev\* VM, Lebedev\* VT, Orlov\* SP, Pevzner\* BZ, Tolstichin\* IN, Török Gy; Supra atomic structure of radiation defects in synthetic quartz by the data of small angle neutron scattering; *Physics of the Solid State*, **52**, 1000-1005, 2010
34. Lebedev\* VT, Mel'nikov\* AB, Török Gy, Vinogradova\* LV; Self organization of sulfopolystyrene ionomers in solutions: dependence on the polarity of the solution and the content of ionogenic groups in chains 1, 2; *Vysokomolekulyarnye Soedineniya, Ser A*; **53, 8**, 1362-1375, 2011
35. Lebedev\* VT, Török Gy, Vinogradova\* LV; Internal organization and conformational characteristics of star shaped polystyrene with fullerene C<sub>60</sub> as a branching center in deuterotoluene; *Polymer Science, Ser A*; **53**, 7, 537–545, 2011
36. Lebedev\* VT, Török Gy, Vinogradova\* LV, Mechanisms of the self organization of star shaped polymers with a varied structure of branching center based on fullerene C60 in solutions; *Crystallography Reports*; **56, 7**, 1118–1122, 2011
37. Marczak\* W, Czech\* B, Almásy L, Lairez\* D; Molecular clusters in aqueous solutions of pyridine and its methyl derivatives; *Phy Chem, Chem Phys*; **13**, 6260-6269, 2011
38. Markó M, Krexner\* G, Schefer\* J, Szakál A, Cser L; Atomic resolution holography using advanced reconstruction techniques for 2D detectors; *New Journal of Physics*; **12**, 063036, 2010

39. Merkel DG, Bottyán L, Tanczikó F, Zolnai Z, Nagy N, Vértesy G, Waizinger J, Bommer L; Magnetic patterning perpendicular anisotropy FePd alloy films by masked ion irradiation; *J. Appl. Phys.* **109** (2011) 124302.
40. Merkel DG, Sajti Sz, Fetzer Cs, Major M, Ruffer R, Rühm A, Stankov S, Tanczikó F, Bottyán L: Isotope-periodic multilayer method for short self-diffusion paths – a comparative neutron and synchrotron Mössbauer reflectometric study of FePd alloys; *J. Phys. Conf. Ser.* **211** (2010) 012029.
41. Merkel DG, Horváth ZE, Szócs DE, Kovács-Mezei R, Kertész GGy, Bottyán L: Stress relaxation in Fe/Si neutron supermirrors by He<sup>+</sup> irradiation; *Physica B* **406** (2011) 3228 - 3242.
42. Meiszterics A, Rosta L, Peterlik H, Rohonczy J, Kubuki S, Hentis P, Sinkó K, Structural characterization of gel-derived calcium silicate systems; *Journal of Physical Chemistry A*; **114**, 10403-10411, 2010
43. Nagy G, Posselt D, Kovács L, Holm JK, Szabó M, Ughy B, Rosta L, Peters J., Timmins P, Garab Gy; Reversible membrane-reorganizations during photosynthesis in vivo - revealed by small-angle neutron scattering; *Biochem J.*; **436**, 225-30, 2011
44. Nikitin AM, Borisov MM, Mukhamedzanov EK, Sajti S, Tanczikó F, Deák L, Bottyán L, Khaydukov Yu.N., Aksenov VL; Precision Structural Diagnostics of Layered Superconductor/Ferromagnet Nanosystems V/Fe by Reflectometry and Diffuse Scattering of Synchrotron Radiation; *Crystal. Rep.* **56** (2011) 858 - 865.
45. Orbán J, Cser L, Rosta L, Török Gy, Nagy A; Design and experimental results of a large, position sensitive, multi-wire prototype detector developed at BNC Review Article; *Nuclear Instruments and Methods in Physics Research Section A: Accelerators, Spectrometers, Detectors and Associated Equipment*; **632**, 124-127, 2011
46. Petrenko VI, Avdeeva MV, Garamus VM, Bulavin LA, Aksenov VL, Rosta L; Colloids and surfaces A: Physicochemical and engineering aspects; *An International Journal of Colloids and Surfaces A*; **369**, 160-164, 2010
47. Petrenko VI, Aksenov VL, Avdeev MV, Bulavin LA, Rosta L, Vekas L, Garamus VM, Willumeit R; Analysis of the structure of aqueous ferrofluids by the small-angle neutron scattering method; Non-Crystalline materials, nanostructures and liquids; *Physics of the Solid State*; **52**, 974-978, 2010
48. Revay Zs., Szentmiklosi L, Kis Z; Determination of new k(0) values for prompt gamma activation analysis at Budapest; *Nuclear Instruments & Methods in Physics Research Section a-Accelerators Spectrometers Detectors and Associated Equipment*, **622**(2): p. 464-467. 2010
49. Rogante M, Pasquini U, Rosta L, Lebedev V; Feasibility study for the investigation of Nitinol self-expanding stents by neutron techniques; *Physica B: Condensed Matter*; **406**, 527-532, 2011
50. Rogante M, Rosta L; Forged components and possibilities of their investigation by neutron techniques; *Croatian Society for Mechanical Technologies*; **69-81**, 2010
51. Rogante, M., Z. Kasztovszky, and A. Manni, Prompt Gamma Activation Analysis of bronze fragments from archaeological artifacts; *Notizario Neutroni e Luce di Sincrotrone*; **15**(1): p. 12-23. 2010
52. Rosta L, Baranyai R, Budapest Research Reactor 20 years of international user operation, *Neutron News*; **22**, 31-36, 2011
53. Rosta L, Len A, Pépy G, Harmat P, Nano-scale morphology of inclusions in tungsten wires a complex SANS study, *Neutron News*; **23**, 2011
54. Russina M, Káli Gy, Sánta Zs, Mezei F; First experimental implementation of pulse shaping for neutron diffraction on pulsed sources; *Nuclear Instruments and Methods in Physics Research Section A: Accelerators, Spectrometers, Detectors and Associated Equipment*; **654**, 383-389, 2011
55. Schulze R; et al., New neutron based imaging methods for cultural heritage studies. *Archeologia e Calcolatori*, **21**: p. 281-299. 2010
56. Seghedi I; et al., Note on the evolution of a Miocene composite volcano in an extensional setting, Zărand Basin (Apuseni Mts., Romania); *Central European Journal of Geosciences*; **2**(3): p. 321-328; 2010
57. Sleaford, B., et al., *Capture Gamma-ray Libraries for Nuclear Applications*. *Journal of the Korean Physical Society*; **59**(2): p. 1473-1478; 2011
58. Szakál A, Czifrus Sz, Markó M, Füzi J, Rosta L, Cser L; Optimization of focusing supermirror neutron guides for low gamma background; *Nuclear Instruments and Methods in Physics Research A*; **06**, 007, 2010

59. Szakmány, G., et al., Discrimination of prehistoric polished stone tools from Hungary with non-destructive chemical Prompt Gamma Activation Analyses (PGAA); *Eur. J. Mineral*; **23**: p. 883-893; 2011
60. Szentmiklósi L; et al, Upgrade of the Prompt-Gamma Activation Analysis (PGAA) and the Neutron Induced Prompt-gamma Spectroscopy (NIPS) facilities at the Budapest Research Reactor; *J. Radioanal. Nucl. Chem*; **286**: p. 501-505; 2010
61. Szentmiklósi L, Révay Zs, Belgya T; Measurement of partial gamma-ray production cross-sections and k(0)-factors for radionuclides with chopped-beam PGAA-Part II. *Nuclear Instruments & Methods in Physics Research Section a-Accelerators Spectrometers Detectors and Associated Equipment*; **622**(2): p. 468-472; 2010
62. Péterdi B., et al., Bazalt anyagú csiszolt kőszeközök közettani és geokémiai vizsgálata (Balatonöszöd - temetői dűlő lelőhely); *Archaeometriai Műhely*; 1: p. **33-68**. 2011
63. Tanczikó F, Sajti Sz, Deák L, Merkel DG, Endrőczy G, Nagy DL, Bottyán L., Olszewski W, Szymanski K; Neutron proportional gas counter for linear and elliptical Mössbauer polarimetry; *Rev. Sci. Instrum.* **81** (2010) 023302.
64. Tapasztó\* O, Tapasztó\* L; Markó M; Kern\* F; Gadow\* R; Balácsi\* C; Dispersion patterns of graphene and carbon nanotubes in ceramic matrix composites; *Chemical Physics Letters*; **511**, 340-343, 2011
65. Teschner D., et al., *Role of Hydrogen Species in Palladium-Catalyzed Alkyne Hydrogenation*. *Journal of Physical Chemistry C*, **114**(5): p. 2293-2299. 2010
66. Török Gy, Lebedev\* VT, Vinogradova\* LV, Orlova\* DN, Shamanin\*VV; Molecular correlations in bulk star-shaped polystyrene with fullerene C<sub>60</sub> center; *Fullerenes, Nanotubes and Carbon Nanostructures*, **18**, 431-436, 2010
67. Veres T, Cser L; Study of the reflectivity of neutron super mirrors influenced by surface oil layers; *Review of Scientific Instruments*; **81**, 063303, 2010
68. Wallner, A., et al., *Neutron-capture Studies on (235)U and (238)U via AMS*. *Journal of the Korean Physical Society*, **59**(2): p. 1410-1413; 2011
69. Zamponi\* M, Pyckhout-Hintzen\* W, Wischnewski\* A, Monkenbusch\* M, Willner\* L, Kali Gy, Richter\* D; Molecular Observation of Branch Point Motion in Star Polymer Melt; *Macromolecules*; **43**, 518-524, 2010
70. Nagy G, Pieper J, Krumova SB, Kovács L, Trapp M, Garab G, Peters J; Dynamic properties of photosystem II membranes at physiological temperatures characterized by elastic incoherent neutron scattering. Increased flexibility associated with the inactivation of the oxygen evolving complex; *Photosynth Res*; **111**, 113-124, 2011
71. Rosta L, Len A, Pépy G, Harmat P, Nano-scale morphology of inclusions in tungsten wires – a complex SANS study; *Neutron News*; **23**, 13-16, 2011
72. Szakál A, Czifrus S, Markó M, Füzi J, Rosta L, Cser, L; Optimization of focusing supermirror neutron guides for low gamma-background; *Nucl Instr Meth A*; **634**, S130-S133, 2011
73. Cser L, Krexner G, Markó M, Szakál A; Neutron holography – a brief history and overview; *Neutron News*; **23**, 17-20, 2012
74. Fábrián M, Sváb E; Uranium surrounding in borosilicate glasses from neutron- and X-ray diffraction and reverse Monte Carlo modeling; *Neutron News*; **23**, 9-12, 2012
75. Kasztovszky Zs, Rosta L; How can neutrons contribute to Cultural Heritage Research; *Neutron News*; **23**, 25-28, 2012
76. Mezei F, Russina M, Káli Gy; Neutron diffraction for long pulse neutron sources; *Neutron News*; **23**, 29-31, 2012
77. Nagy G, Szabó M, Ünnep R, Káli Gy, Miloslavina Y, Lambrev PH, Zsiros O, Porcar L, Rosta L, Garab G; Modulation of the multilamellar membrane organization and of the chiral macrodomains in the diatom *Phaeodactylum tricorutum* revealed by small-angle neutron scattering and circular dichroism spectroscopy; *Photosynth Res*; **110**, 71-79, 2012
78. Posselt D, Nagy G, Kirkensgaard JJK, Holm JK, Aagaard TH, Timmins P, Rétfalvi E, Rosta L, Kovács L, Garab Gy; Small-angle neutron scattering study of the ultrastructure of chloroplast thylakoid membranes – periodicity and structural flexibility of the stroma lamellae; *Biochim Biophys Acta – Bioenergetics*; **8**, 1220-1228, 2012

79. Saerbeck T, Klose F, Le Brun AP, Füzi J, Brule A, Nelson A, Holt SA, James M; Polarization "Down Under": The polarized time-of-flight neutron reflectometer PLATYPUS; *Rev Sci Instr*; 83, 081301/1-12, 2012
80. Török Gy, Lebedev V, Vinogradova L; Structural and conformational properties of polymeric stars with fullerene centre in solutions by SANS; *Procedia Chemistry*; 4, 154-163, 2012
81. Rosta L, Nyolcvan éves a neutron; *Nukleon*; 5(4), 1-5, 2012
82. Rosta L, Neutronkutatók Magyarországon; *Nukleon*; 5(5), 1-5, 2012
83. Franklyn CB, Török Gy; Use of small angle neutron scattering to study various properties of wool and mohair fibres; In: *Proc. Applications of Nuclear Techniques Eleventh International Conference (12–18 June 2011 Crete, Greece)*; AIP Conf Proc; 1412, 93-97, 2011
84. Russina M, Mezei F, Kali Gy; First implementation of novel multiplexing techniques for advanced instruments at pulsed neutron sources; *J Phys Conf Ser*; 340, 2012
85. Vrhovšek\* A, Gereben O, Jamnik\* A, Pusztai L; Hydrogen bonding and molecular aggregates in liquid methanol, ethanol and propanol; *J Phys Chem B*; 115, 13473-13488, 2011
86. Harsányi I, Bopp\* PA, Vrhovšek\* A, Pusztai L; On the hydration structure of LiCl aqueous solutions: a Reverse Monte Carlo based combination of diffraction data and Molecular Dynamics simulations; *J Mol Liq*; 158, 61-67, 2011
87. 104. Fábrián\* M, Sváb E, Pamukchieva\* V, Szekeres\* A, Vogel\* S, Ruett\* U; Study of As–Se–Te glasses by neutron-, X-ray diffraction and optical spectroscopic methods; *J Non-Cryst Solids*; 358, 860-868, 2012
88. Temleitner L, Pusztai L, Rubio-Arroyo\* MF, Aguilar-Lopez\* S, Klimova\* T, Pizio\* O; Microscopic and mesoscopic structural features of an activated carbon sample, prepared from sorghum via activation by phosphoric acid; *Materials Research Bulletin*; 47, 4409-4413, 2012
89. Sváb E, Beregi\* E, Fábrián\* M, Mészáros Gy; Neutron diffraction structure study of Er and Yb doped YAl<sub>3</sub>(BO<sub>3</sub>)<sub>4</sub>; *Optical Materials*; 34, 1473–1476, 2012
90. Harsányi I, Temleitner L, Beuneu\* B, Pusztai L; Neutron and X-ray diffraction measurements on highly concentrated aqueous LiCl solutions; *J Mol Liq*; 165, 94-100, 2012
91. Ohara\* K, Temleitner L, Sugimoto\* K, Kohara\* S, Matsunaga\* T, Pusztai L, Itou\* M, Ohsumi\* H, Kojima\* R, Yamada\* N, Usuki\* T, Fujiwara\* A, Takata\* M; The roles of the Ge–Te core network and the Sb–Te pseudo network during rapid nucleation-dominated crystallization of amorphous Ge<sub>2</sub>Sb<sub>2</sub>Te<sub>5</sub>; *Advanced Functional Materials*; 22, 2251-2257, 2012
92. Gereben O, Kohara\* S, Pusztai L; The liquid structure of some food aromas: joint X-ray diffraction, all-atom Molecular Dynamics and Reverse Monte Carlo investigations of dimethyl sulfide, dimethyl disulfide and dimethyl trisulfide; *J Mol Liq*; 169, 63-73, 2012
93. Pothoczki Sz, Temleitner L, Pusztai L; Determination of molecular orientational correlations in disordered systems from diffraction data; *Advances in Chemical Physics*; 150, 143-168, 2012
94. Antipas\* GSE, Temleitner L, Karalis\* K, Kohara\* S, Pusztai L, Xenidis\* A; A containerless study of short-range order in high-temperature Fe–Si–Al–Ca–Mg–Cr–Cu–Ni oxide systems; *J Mol Struct*; 1019, 151-158, 2012
95. Steinczinger\* Zs, Pusztai L; An independent, general method for checking consistency between diffraction data and partial radial distribution functions derived from them: the example of liquid water; *Condensed Matter Physics*; 15, 23606/1-6, 2012
96. Gereben O, Pusztai L; Molecular conformations and the liquid structure in bis(methylthio)methane and diethyl sulfide: diffraction experiments vs molecular dynamics simulations; *J Phys Chem B*; 116, 9114-9121, 2012
97. Mile V, Gereben O, Kohara\* S, Pusztai L; On the structure of aqueous cesium fluoride and cesium iodide solutions: Diffraction experiments, Molecular Dynamics simulations and Reverse Monte Carlo modeling; *J Phys Chem B*; 116, 9758-9767, 2012
98. Gereben O, Pusztai L; RMC\_POT, a computer code for Reverse Monte Carlo modeling the structure of disordered systems containing molecules of arbitrary complexity; *Journal of Computational Chemistry*; 33, 2285–2291, 2012

99. Voleska\* I, Akola\* J, Jóvári P, Gutwirth\* J, Wagner\* T, Yannopoulos\* SN, Jones\* RO; Structure, electronic, and vibrational properties of glassy Ga<sub>11</sub>Ge<sub>11</sub>Te<sub>78</sub>: Experimentally constrained density functional study; *Phys Rev B*; 86, 094108/1-9, 2012
100. Kaban\* I, Jóvári P, Wang\* R-P, Luther-Davies\* B, Mattern\* N, Eckert\* J; Structural investigations of Ge<sub>5</sub>As<sub>x</sub>Se<sub>95-x</sub> and Ge<sub>15</sub>As<sub>x</sub>Se<sub>85-x</sub> glasses using x-ray diffraction and extended x-ray fine structure spectroscopy; *J Phys: Condensed Matter*; 24, 385802:1-7, 2012
101. Chrissanthopoulos\* A, Jóvári P, Kaban\* I, Gruner\* S, Kavetsky\* T, Borc\* J, Wang\* W, Ren\* J, Chen\* G, Yannopoulos\* SN; Structure of AgI-doped Ge–In–S glasses: Experiment, reverse Monte Carlo modelling, and density functional calculations; *J Solid State Chem*; 192, 7-15, 2012
102. Fábián\* M, Sváb E; Uranium surrounding in borosilicate glasses from neutron- and X-ray diffraction and reverse Monte Carlo modeling; *Neutron News*; 23, 9-12, 2012
103. Fábián\* M., Sváb E; Boroszilikát üvegek szerkezetvizsgálata neutrodiffrakcióval (Neutron diffraction study of borosilicate glasses, in Hungarian); *Nukleon*; V(119), 1-6, 2012
104. L. Bottyán, D.G. Merkel, B. Nagy, J. Major: Neutron Reflectometer with Polarization Option at the Budapest Neutron Centre *Neutron News* 23 (2012) 21 - 24.
105. L. Deák, T Fülöp: Reciprocity in quantum, electromagnetic and other wave scattering *Ann. Phys. - New York* 327 (2012) 1050 - 1077.
106. L. Deák, L. Bottyán, T. Fülöp, G. Kertész, D.L. Nagy, R. Rüffer, H. Spiering, F. Tanczikó, G. Vankó: Switching reciprocity on and off in a magneto-optical X-ray scattering experiment using nuclear resonance of a-<sup>57</sup>Fe foils *Phys. Rev. Lett.* 109 (2012) 237402.
107. D.E. Walker, M. Major, M.B. Yazdi, A. Klyszcz, M. Haeming, K. Bonrad, C. Melzer, W. Donner, H. von Seggern: High mobility indium zinc oxide thin film field-effect transistors by semiconductor layer engineering *ACS Appl. Mater. Inter.* 4 (2012) 6835 - 6841.
108. Gy. Török , V. Lebedev, L. Vinogradova Structural and Conformational Properties of Polymeric Stars with Fullerene Centre in Solutions by SANS *Procedia Chemistry* 4 ( 2012 ) 154 – 163
109. Yu. V. Kul'velis, V. T. Lebedev, V. A. Trunov, O. N. Primachenko, S. Ya. Khaikin, D. Torok, and S. S. Ivanchev Effect of Preparation Conditions on Nanostructural Features of the NAFION® Type Perfluorinated Proton Conducting Membranes ISSN 0965\_5441, *Petroleum Chemistry*, 2012, Vol. 52, No. 8, pp. 565–570. © Pleiades Publishing, Ltd., 2012. Original Russian Text © Yu.V. Kul'velis, V.T. Lebedev, V.A. Trunov, O.N. Primachenko, S.Ya. Khaikin, D. Torok, S.S. Ivanchev, 2012, published in *Membrany i membrannye tekhnologii*, 2012, Vol. 2, No. 3, pp. 179–185. ВЛИЯНИЕ УСЛОВИЙ ПОЛУЧЕНИЯ НА НАНОСТРУКТУРНЫЕ ОСОБЕННОСТИ ПЕРФТОРИРОВАННЫХ ПРОТОНОПРОВОДЯЩИХ МЕМБРАН ТИПА NAFION Ю. В. Кульвелис, В. Т. Лебедев, В. А. Трунов, О. Н. Примаченко, С. Я. Хайкин, Д. Торок, С. С. Иванчев *МЕМБРАНЫ И МЕМБРАННЫЕ ТЕХНОЛОГИИ*, 2012, том 2, № 3, с. 179–185
110. Fábián M, Sváb E. Boroszilikát üvegek szerkezetvizsgálata neutrodiffrakcióval, *Nukleon* V. 119 1 (6pp) (2012)
111. E. Sváb, E. Beregi, M. Fábián, Gy. Mészáros, Neutron diffraction structure study of Er and Yb doped YAl<sub>3</sub>(BO<sub>3</sub>)<sub>4</sub>, *Optical Materials* 34 1473 (4pp) (2012)
112. M. Fábián, E. Sváb, Uranium Surrounding in Borosilicate Glasses from Neutron- and X-ray Diffraction and Reverse Monte Carlo Modelling, *Neutron News* 23 9 (4pp) (2012)
113. M. Fabian, E. Svab, V. Pamukchieva, A. Szekeres, P. Petrik, S. Vogel, U. Ruett, Study of As-Se-Te glasses by neutron-, X-ray diffraction and optical spectroscopic methods, *J. Non-Cryst Solids* 358: pp. 860-868 (2012)
114. Lancastre\* JJH, Margaça\* FMA, Ferreira\* LM, Falcão\* AN, Miranda Salvado\* IM, Nabiça\* MSMS, Fernandes\* MHV, Almásy L; Thermal analysis and SANS characterization of hybrid materials for biomedical applications; *J Therm Anal*; 109:(1) pp. 413-418. (2012)
115. Füzi J, Rosta L; Neutron Beam Conditioning for Focusing SANS Spectrometers, *J Phys Conf Ser*, accepted for publication
116. Kulvelis\* YV, Lebedev\* VT, Trunov\* VA, Ivanova\* IN, Török Gy; Building of complexes of sulphonated tetraphenylpophyrine with Poly-N- vinylpyrrolidone by the data of small angle neutron scattering; *Journal Poverhnost-X-ray-synchrotron and neutron investigation*; accepted for publication

117. Lebedev\* VT, Török Gy, Vinogradova\* LV; Effect of center of branch for the selforganisation of fullerene containing star-shape polystyrenes in deuterated toluene; *Journal of Applied Chemistry*; accepted for publication
118. Lebedev\* VT, Török Gy, Vinogradova\* LV; Structure and supramolecular formations of fullerene containing polymers with heteroarms in deuterated toluene; *Vysokomolekulyarnye Soedineniya A*; accepted for publication
119. Lebedev\* VT, Török Gy, Vinogradova\* LV, The internal organisation and conformation features of star-shape polystyrene with C<sub>60</sub> center of junction; *Vysokomolekulyarnye Soedineniya, Ser*; accepted for publication
120. Markó M, Szakál A, Török Gy, Cser L; Construction and testing of an instrument for neutron holographic study at the Budapest research Reactor; *Review of Scientific Instruments*; 81, 105110, accepted for publication
121. Nagy G, Szabó\* M, Ünneper R, Káli Gy, Miloslavina\* Y, Lambrev\* PH, Zsiros\* O, Porcar\* L, Timmins\* P, Rosta L, Garab\* Gy; Modulation of the multilamellar membrane organization and of the chiral macrodomains in the diatom *Phaeodactylum tricornutum* revealed by small-angle neutron scattering and circular dichroism spectroscopy; *Photosynthesis research*; 110, accepted for publication
122. Meiszterics A, Sinkó K, Study of bioactive calcium silicate ceramic systems for biomedical applications; IFMBE Proceedings, accepted for publications
123. Petrenko\* VI, Avdeev\* MV, Turcu\* R, Vekas\* L, Aksenov\* VL, Rosta L, Bulavin\* LA, Structure of powders of magnetic nanoparticles with polymer coating based on substituted pyrroles by small-angle neutron scattering; *Surface Investigations. X-ray, Synchrotron and Neutron Technique*; accepted for publication
124. Tropin\* TV, Kyrey\* TA, Kyzyma\* EA, Feoktystov\* AV, Avdeev\* MV, Bulavin\* LA, Rosta L, Aksenov\* VL, Study of mixed solutions C<sub>60</sub>/NMP/toluene by means of UV-Vis spectroscopy and small-angle neutron scattering, *Surface Investigations X-ray, Synchrotron and Neutron Techniques*; accepted for publication
125. Pépy\* G; Practice of 2D data treatment in SAS, *Journal of Physics*, accepted for publication
126. Rogante\* M, Pasquini\* U, Rosta L, Lebedev\* V; Feasibility study for the investigation of Nitinol self-expanding stents by neutron techniques, *Physica B*, in press.
127. Russina\* M, Káli Gy, Sánta Zs, Mezei F; First Experimental implementation of pulse shaping for neutron diffraction on pulsed sources; Accepted to Nucl.Instr.& Methods A.

### CONFERENCE PROCEEDINGS

1. Belgya, T, Kasztovszky Z, Szilágyi V; Provenance Studies of Archaeological Artifacts using PGNAA; *4th International Symposium on Nuclear Analytical Chemistry (NAC-IV)*, R. Acharya, Reddy, A.V.R., Chatt, A., Venugopal, V., Editor; BARC, Dept. of Atomic Energy, Trombay, Mumbai, 400085 Bhabha Atomic Research Center, Mumbai, India. p. 88-92; 2010
2. Belgya T, Kis Z; PGAA analysis of isotopically enriched samples; *Proceedings of the Final Scientific EFNUDAT Workshop*, E. CHIAVERI, Editor; European Laboratory for Particle Physics, CERN, Geneva, Switzerland, 30 August – 2 September p. 1-7. 2010
3. Belgya T, Szentimiklosi L, Kis Z; Cold neutron source spectra at the Budapest PGAA-NIPS facilities; *Report on Consultance meeting, IAEA NDC(NDS)-0590 Vienna*. p. 17-20. 2010
4. Meiszterics, K. Sinkó; „Study of bioactive calcium silicate ceramic systems for biomedical applications“ *EUROPEAN IFMBE MBEC 2011 - 5th European Conference of the International Federation for Medical and Biological Engineering*, Proceedings
5. Franklyn\* C, Gyula Török; SANS observations of the efficacy of different wool cleaning agents; *5th European conference on neutron scattering, Prague, Czech Republic, 17-22 July, 2011*, Proceedings

6. Franklyn\* C, Gy Török; The use of small angle neutron scattering to study the effect of the wetting process in wool and mohair fibres; *5<sup>th</sup> European conference on neutron scattering, Prague, Czech Republic, 17-22 July, 2011*, Proceedings
7. Hlavathy, Z., et al., *Urán kimutatása aktív, pulzáló hidegneutronos gerjesztéssel, a késő neutronok mérésével*. 2010, Országos Atomenergia Hivatal: Budapest. p. 1-23.
8. Hlavathy Z., et al., *Urán kimutatása hidegneutronos gerjesztéssel, nagy hatásfokú koincidencia-berendezéssel és a késő neutronok mérésével különböző időtartományokban*; OAH-ÁNI-ABA-04/11. 2011
9. Hurst AM., et al., *Data evaluation methods and improvements to the neutron-capture g-ray spectrum*; *Second International Ulaanbaatar Conference on Nuclear Physics and Applications*; AIP Conf. Proc. 2011: Ulaanbaatar, Mongolia 2010. p. 24-31. 2011
10. Kasztovszky Zs., et al., *New Developments in Neutron Radiography*; *IAEA Radiation Technology Series No. 2: Nuclear Techniques for Cultural Heritage Research*, M. Rossbach, International Atomic Energy Agency: Vienna. p. 121-129. 2011
11. Kasztovszky Zs; et al., *Archaeometry Applications of Cold Neutron Based Prompt Gamma Neutron Activation Analysis*, *IAEA Radiation Technology Series No. 2: Nuclear Techniques for Cultural Heritage Research*, M. Rossbach, International Atomic Energy Agency: Vienna. p. 165-178. 2011
12. Kasztovszky Zs, Sajó SV; *Neolitikus rézgyöngyök vizsgálata Polgár-Csőszhalom lelőhelyről – előzetes eredmények*; *Archeometria Műhely, elektronikus journal*, 137-140. 2010
13. Lebedev\* VT, Mel'nikov\* AB, Török Gy, Vinogradova\* LV: *Hydrodynamic features of polystyrene ionomers with ionogen groups SO<sub>3</sub>Li in weakly polar solvents*; In: *Proc. V-th Russian Kargin's conference (Moscow, Russia, 21 June, 2010)*; Poster P5-129 Thesis p. 68, Proceedings
14. Mezei F, *Multiplexing neutron chopper systems and pulsed neutron source design*; *ICANS XIX. March 8-12, 2010; Grinwald, Switzerland*, in press
15. Rogante\* M, Rosta L; *Forged components and possibilities of their investigation by neutron techniques*; *Proc. 1st Int. Conf. Mechanical Technologies and Structural Materials, Split, Croatia, 21-22 October 2010*, Ed.: D. Zivkovic, Croatian, Society for Mechanical Technologies, Split, Croatia, p. 69-81, 2010
16. Rosta L; *Multipurpose Utilisation of a Medium Flux Research Reactor – Benefit for the Society*, *International Conference on Research Reactors: Safe Management and Effective Utilization, 4-18 November 2011, Rabat, Morocco, IAEA-CN-188*, Proceedings, accepted for publication
17. Száraz\* Z, Török Gy, Vladimir\* K, Hähner\* P, Ohms\* C; *Microstructure evolution of high Cr-content ODS steels during thermal ageing*; *DIANA I: 1st International Workshop on Dispersion Strengthened Steels for Advanced Nuclear Applications, Aussois, France, April 4-8, 2011*, Proceedings
14. Száraz\* Z, Török Gy, Ohms C, Hahner P; *SANS investigation of microstructure evolution in high Cr-content oxide*, *5<sup>th</sup> European conference on neutron scattering, Prague, Czech Republic, 17-22 July, 2011*, Proceedings
15. Lebedev\* VT, Vinogradova\* LV, Török Gy; *Neutron scattering studies structures and self-assembly of star-shaped polymers with fullerene centres in solutions*, *Macromolecular Symposia; Wiley-Vch Verlag GmbH & Co KgaA (Wiley –VCH) 2010*, accepted for publication
16. Chris Franklyn, Gyula Török *The Use of Small-angle Scattering to Study Wool and Mohair Fibres* International Proceeding of the Innovation in Polymer Science and Technology 2011 (IPST2011), ISBN 978-602-18820-0-9. and *Procedia Chemistry of Elsevier vol. 4*, the Proceeding of the IPST2011, *Indonesian Polymer Journal (MPI) of Indonesian Polymer Association (HPI) vol. 13(2) 2011, vol. 14(1-2) 2012*.

## **BOOKS, BOOK CHAPTERS**

1. L.Cser: *Kondenzált közegek vizsgálata neutronszórással (Investigation of condensed agents with neutron scattering, in Hungarian)*, Typotex kiadó, 2010

## WORKSHOP

1. Belgya, T., *Target preparation for in-beam thermal neutron capture experiments*, in *EFNUDAT Fast Neutrons, Scientific Workshop on Neutron Measurements, Theory and Applications Nuclear Data for Sustainable Nuclear Energy*, F.-J. Hamsch, Editor. 2010, European Commission: Geel, Belgium, 28 – 30 April, 2009. p. 21-26.
2. Belgya, T., *Determination of thermal radiative capture cross section*, in *EFNUDAT Slow and Resonance Neutrons, a Scientific Workshop on Nuclear Data Measurements, Theory and Applications, 23-25 September 2009* T. Belgya, Editor. 2010, II-HAS: Budapest, Hungary. p. 115-120.
3. Belgya, T. *EFNUDAT – Slow and Resonance Neutrons*. in *The 2nd EFNUDAT workshop on Neutron Measurements, Theory and Applications, 23-25 September 2009*. 2010. Budapest, Hungary: Institute of Isotope, Hungarian Academy of Sciences.
4. Käppeler F., et al., *EFNUDAT synergies in astrophysics*, in *Proceedings of the Final Scientific EFNUDAT Workshop*, E. CHIAVERI, Editor. 2011, European Laboratory for Particle Physics (CERN): CERN, Geneva, Switzerland, 30 August – 2 September 2010. p. 9-15
5. Kis Z., et al., *Determination of the total neutron capture cross section for  $^{58}\text{Ni}(n,\gamma)^{59}\text{Ni}$  reaction*; *EFNUDAT Slow and Resonance Neutrons, a Scientific Workshop on Nuclear Data Measurements, Theory and Applications, 23-25 September 2009* T. Belgya, Editor. 2010, II-HAS: Budapest, Hungary. p. 121-126.
6. Massarczyk R., et al., *Photon strength function deduced from photon scattering and neutron capture*; *EFNUDAT User and Collaboration workshop; Measurements and Models of Nuclear Reactions, 25-27 May 2010*. 2010: Paris, France. p. EPJ Web of Conferences 8, 07008.
7. Oberstedt, A., et al., *Measurement of prompt fission  $\gamma$ -rays with lanthanum halide scintillation detectors*, in *Proceedings of the Final Scientific EFNUDAT Workshop*, E. CHIAVERI, Editor. 2011, European Laboratory for Particle Physics (CERN): CERN, Geneva, Switzerland, 30 August – 2 September 2010. p. 85-89.
8. Oberstedt, S., et al., *Correlation measurements of fission-fragment properties*, in *EFNUDAT User and Collaboration workshop: Measurements and Models of Nuclear Reactions, 25-27 May 2010*, EPJ Web of Conferences 8. 2010: Paris, France. p. 03005.
9. Oberstedt, S., et al., *VERDI – a double fission-fragment time-of flight spectrometer*, in *Proceedings of the Final Scientific EFNUDAT Workshop*, E. CHIAVERI, Editor. 2011, European Laboratory for Particle Physics (CERN): CERN, Geneva, Switzerland, 30 August – 2 September 2010. p. 91-97.
10. Pécskay, Z. and K. Gméling, *Role of the intrusive processes within the evolution of the Neogene-Quaternary calc-alkaline volcanism of the Carpathians. New Advances in Maar-Diatreme Research in Hungary, Germany and New Zealand*, in *Results and Perspectives International Maar Workshop 13-15 August 2010*, B. Károly Németh, Editor. 2010: Tapolca, Hungary.
11. Ferenc Gillemot<sup>1</sup>, Norbert Kresz<sup>2</sup>, Ferenc Oszwald<sup>2</sup>, Andreas Ulbricht<sup>3</sup>, Mercedes Hernández Mayoral<sup>4</sup>, Gyula Török<sup>5</sup>, Bertrand Radiguet<sup>6</sup>, Sylvain Chambrelaud<sup>6</sup>, Ákos Horváth<sup>1</sup>, Márta Horváth<sup>1</sup>, Attila Kovács<sup>1</sup>  
Paper Title: Microstructural changes in highly irradiated 15H2MFA steel  
Symposium: 26th Symposium on the Effects of Radiation on Nuclear Materialsx

## BOOKS, BOOK CHAPTERS

1. Jóvári P, Kaban I\*; *Structural study of multicomponent glasses by the reverse Monte Carlo simulation technique; Nanostructured Materials for Advanced Technological Applications*; Ed. J. P. Reithmaier, P. Petkov, W. Kulisch, C. Popov; in press, 2008





## EXPERIMENTAL STATIONS AT BNC

Acronym	Instrument	Current status	Responsible person phone: +361 392 2222 /EXT, e-mail
PSD	Powder diffractometer, Thermal beam No.9	scheduled, FP7	Margit FÁBIÁN/1965 fabian.margit@bnc.hu
MTEST	Materials test diffractometer, Thermal beam No.6	scheduled, FP7	László TEIMLEITNER /1469 temleitner.laszlo@bnc.hu
TOF	Time-of-flight diffractometer, Thermal beam No.1	scheduled, FP7	György KÁLI/1439 kali.gyorgy@bnc.hu
YS-SANS	Small angle scattering spectrometer (Yellow Submarine), Cold guide No.2	scheduled, FP7	Laszlo ALMÁSY/1447 almasy.laszlo@bnc.hu
F-SANS	Focusing small angle scattering spectrometer, Cold guide No.3/2	Under commissioning	Adél LEN/ 1447 len.adel@bnc.hu
REFL	Neutron reflectometer, Cold guide No.1/2	scheduled, FP7	Tamás VERES /1738 veres@szfki.hu
GINA	Polarised neutron reflectometer, Cold guide No.3/1	scheduled, FP7	Laszlo Bottyan/2761 bottyan.laszlo@bnc.hu
ATHOS	Three-axis spectrometer, Cold guide No.1/1	scheduled, FP7	Gyula TÖRÖK/1439 torok.gyula@bnc.hu
TAST	Three-axis spectrometer on a thermal beam, Thermal beam No.8	scheduled, FP7	Alex SZAKAL/1416 szakal.alex@bnc.hu
DNR/SNR	Dynamic/static radiography, Thermal beam No.2/3	scheduled, FP7	László HORVÁTH/1434 horvath.laszlo.z@energia.mta.hu
NORMA	Neutron Tomography, Cold guide No.1/4	scheduled, FP7	Zoltán KISS/ 3311 kis.zoltan@bnc.hu
BIO	Biological irradiations, Thermal beam No.5	scheduled, FP7	Balázs ZÁBORI/1341 zabori.balazs@bnc.hu
PGAA	Prompt gamma activation analysis, Cold guide No.1/3	scheduled, FP7	László SZENTMIKLÓSI /3143 szentmiklosi.laszlo@bnc.hu
NIPS	Neutron Induced Prompt- Gamma Spectroscopy, Cold guide No.1/4	scheduled, FP7	Zsolt KASZTOVSZKY /3234 kasztovszky.zsolt@bnc.hu
BAGIRA	Controlled temperature irradiation rig, Reactor tank	scheduled, FP7	Attila KOVÁCS/1420 kovacs.attila@energia.mta.hu
RNAA	Fast-rabbit system and activation analysis, Reactor tank	scheduled, FP7	Ibolya SZIKLAI /1411 sziklai.ibolya@bnc.hu